Cell wall morphogenesis in *Bacillus subtilis*

James Brown

Thesis submitted in partial fulfilment of the requirements of the regulation for the degree of Doctor of Philosophy Newcastle University Faculty of Medical Sciences

Institute of Cell and Molecular Biosciences

27th June 2016

Abstract

Almost all bacteria are surrounded by a peptidoglycan cell wall. This cell wall imposes the shape of the bacterial cell and enables the cell to resist turgor pressure, localise proteins and coordinate cell division. Despite being 'essential', bacteria can grow and divide indefinitely in a wall-less state known as the L-form. Conventionally, L-form bacteria in the laboratory are grown at high concentrations of osmoprotectant such as salt or sucrose due to their sensitivity to turgor. However, L-forms have been isolated from various environments, including from persistent infections where such isotonic conditions may not be relevant.

Here I show that L-forms derived from the Gram-positive model organism *Bacillus subtilis* can be readily adapted to media containing very low concentrations of osmoprotectant (sucrose or salt), lending support to theories regarding the natural role of L-forms. Regeneration of the wall of the adapted strains revealed a raft of phenotypic changes including, but not limited to: cell branching, misplaced septa and increased cell length. Whole genome sequencing of these mutant strains revealed several mutations. Among the mutations identified was a partial deletion of the gene coding for the actin homologue, MreB. In the walled state, MreB directs and coordinates the peptidoglycan synthesis machinery as a means to control the morphology of the cell. Characterisation of the mutation in *mreB* revealed that loss of this important protein is sufficient to enable the growth of L-forms in low osmolarites.

The cell wall of Gram-positive bacteria also contains teichoic acids (TA). TAs linked to the lipids in the cell membrane (Lipoteichoic acids; LTA) are essential for the viability of the pathogen *Staphylococcus aureus*. In contrast, LTA is dispensable in *B. subtilis*, where loss of the primary synthase, LtaS, acts as a suppressor mutation in strains that lack the MreB homologue, Mbl.

Based on the observation that loss of *ltaS* improved the growth of a *Δmbl* mutant in *B. subtilis* a screening method was previously developed from which 5 candidate actinomycete strains producing potential inhibitors of LtaS were identified. Preliminary experiments narrowed the focus to one strain that reproducibly produced an active compound, which was purified and characterised. Various properties of the compound

were consistent with it acting as an inhibitor of LtaS. Mass spectrometry (MS) and MS-MS data suggested a potential identity for the inhibitor that could plausibly represent a substrate analogue. Treatment with the compound impaired the growth of *S. aureus*.

Acknowledgements

I would like to take this opportunity to thank my supervisors, Jeff Errington and Ling Juan Wu for helping me develop as an independent and competent (I think!) scientist. I am particularly grateful to Ling for putting up with me in the day-to-day management of my projects.

I would like to thank all my friends and colleagues in the CBCB who have helped me either in the lab, or made my experience of my PhD enjoyable.

My thanks extend to Nick Allenby and the all the staff at Demuris for all the help in the natural product screening featured in chapter 5. In particular I would like to thank Kaveh Emami for the help growing the *Streptomyces* and Ryan Sweet for growing my *Streptomyces* strain in the 20 L biofermenter.

I would like to thank Lucy Eland, Wendy Smith and Ian Selmes for performing the whole genome sequencing featured in this work. In addition to the sequencing I would like to thank Ian for always ensuring I had all the necessary equipment for performing the experiments featured in this thesis.

Most of all I would like to thank Nadia Rostami, without whose unflinching support I would not have been able to complete this PhD.

Finally, I would like to thank my family; without them I would not have reached this far.

Table of contents

Contents

List of figures

List of tables

Abbreviations

Å	Ångström (0.1 nm)
ABC-transporter	ATP-binding cassette transporter
ACP	Acyl transfer protein
Amp	ampicillin
ATP	Adenosine triphosphate
BCFA	Branched chain fatty acids
B. subtilis	*Bacillus subtilis*
C_{55}-PP	Undecaprenyl-pyrophosphate/bactoprenol
CAA	Casamino acids
Cm	chloramphenicol
CBB	Coomassie Brilliant Blue
CDP	Cytidine diphosphate
CL	Cardiolipin
CM	Cell membrane
CoA	Coenzyme A
CS	Compatible solute
CW	Cell wall
DAG	Diacylglycerol
DAPI	4,6-diamidino-2-phenylindole
dH_2O	Deionised water
DNA	Deoxyribonucleic acid
E. coli	*Escherichia coli*
e.g.	*Exempli gratia* (for example)
EDTA	Ethylenediaminetetraacetic acid
Erm	Erythromycin
Et al.	*Et alii* (and others)
FAS II	Type II fatty acid synthesis pathway
GalNAc	N-acetylgalactosamine
GDP	Guanosine diphosphate

GTP	Guanosine triphosphate
GFP	Green fluorescent protein
Glc_2-DAG	Diglycosyldiacylglycerol
GlcNAc	N-acetylglucosamine
Glu	Glucose
GroP	Glycerol phosphate
GTP	Guanosine triphosphate
h	Hour/hours
HPP	Heptaprenyl diphosphate
IM	Inner membrane
IPTG	Isopropyl β-D-1-thiogalactopyranoside
Kan	Kanamycin
LB	Luria-Bertani broth
LTA	Lipoteichoic acid
ManNAc	N-acetylmannosamine
min	Minute/minutes
MM	Minimal media
MNM	$MgCl_2$ / NaCl / Maleic acid
MOPS	3-(N-morpholino)-2-hydroxypropanesulphonic acid
MRSA	Methicillin resistant *Staphylococcus aureus*
MS channels	Mechanosensitive channels
MS	Mass spectroscopy
MSM	$MgCl_2$ / Sucrose / Maleic acid
MurNAc	N-acetyl muramic acid
NA	Nutrient agar
NAG	N-acetylglucosamine
NAM	N-acetyl muramic acid
NB	Nutrient broth
no.	Number
OD_{600} / OD_{450}	Optical density measured at a wavelength of 600nm or 450nm respectively

OM	Outer membrane
PAB	Penassay broth
PAGE	Polyacrylamide gel electrophoresis
PAMPs	Pathogen associated molecular patterns
PBP	Penicillin binding protein
PBS	Phosphate buffered saline solution
PC	Precursor
PCR	Polymerase chain reaction
PDB	Protein database
PEG	Polyethylene glycol
PG	Peptidoglycan
PhG	Phosphotidylglycerol
Phl	Phleomycin
P_i	Inorganic phosphate
Poly (GroP)	Polyglycerolphosphate
PVDF	Polyvinylidene fluoride
rpm	Revolutions per minute
RNA	Ribonucleic acid
ROS	Reactive oxygen species
S. aureus	*Staphylococcus aureus*
S. coelicolor	*Streptomyces coelicolor*
SCFA	Straight chain fatty acid
SD	Standard deviation
SDS	Sodium lauryl sulphate
SMM	Spizizen minimal media
Spc	Spectinomycin
spp.	Species
SSC	Sodium chloride – sodium citrate solution
TA	Teichoic acid
TAE	Tris – acetate – EDTA
TE	Tris – EDTA

TES	Tris – EDTA – sodium chloride
Tet	Tetracycline
UDP	Uridine diphosphate
vs	versus
WTA	Wall teichoic acid
Zeo	Zeocin

Amino acids are represented by one or three letter codes; chemicals by elemental symbols

1. Introduction

1.1 The cell envelope

1.1.1   Overview

The bacterial cell envelope acts as the interface between the external environment and the internal bacterial environment. It both protects the cell from the hazardous external environments and allows the cell to interact with its surroundings. In addition it provides a framework that enables positioning and ordering of the cellular contents.

This envelope is a complex structure that consists of two main elements: the cell wall and the cell membrane. In Gram negative organisms, an additional external cell membrane is present. Gram positive bacteria lack this external cell membrane, though their cell envelope is further enriched by the presence of teichoic acids (TAs). The differences between the two envelopes is depicted in figure 1.1.

These various components will be discussed, largely in the context of the Gram positive, soil dwelling, model organism *Bacillus subtilis*, and the roles they play in allowing bacteria to respond to dynamic and challenging environments. Further, the effect loss of some of these components play on bacterial physiology and the unique insights they provide will also be addressed.
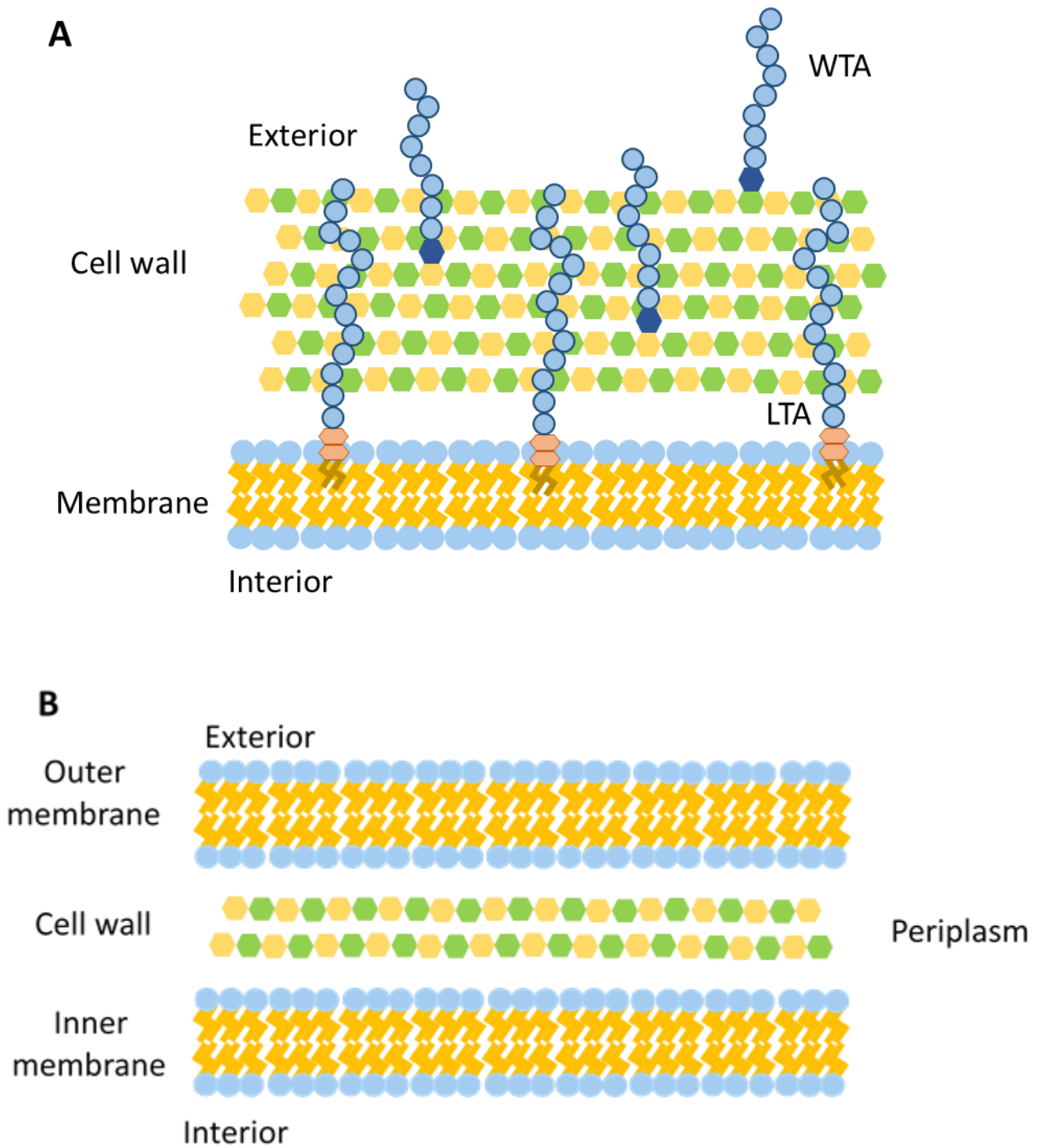
Figure 1.1. Schematic representation of the cell envelope of Gram-positive (A) and Gram-negative (B) bacteria. Diagram omits the presence of the various proteins associated with the cell envelope for the purposes of simplification.

1.1.2 Peptidoglycan

The peptidoglycan is a semi-rigid structure that surrounds and constrains the cell membrane. Whilst the basic composition of the peptidoglycan is shared between most bacteria, the structure varies. The variation in structure was first identified in 1884 by Hans Christian Gram, who found that staining could separate bacteria into two groups; those that stained negatively (Gram-negatives) and those that stained positively (Gram-positives). Bacteria that are Gram positive have a single membrane that is surrounded by a thick cell wall. By contrast, Gram-negative organisms have a thin cell wall that is sandwiched between an inner and an outer cell membrane (Madigan et al., 2009).

1.1.2.1 Composition

Peptidoglycan is a polymer composed of glycan strands containing alternating subunits of the aminosugars β-(1-4) N-acetylglucosamine (GlcNAc [NAG]) and β-(1-4) acetyl muramic acid (MurNAc [NAM]). These are linked by glycosidic bonds that are catalysed by transglycosylases. The glycan strands are linked together through the crosslinking of peptide residues found on the MurNAc subunits by the transpeptidase activity of the Penicillin-binding-proteins (PBPs). The pentapeptide residues on MurNAc consist of L-alanine, D-isoglutamine, meso-diaminopimelic acid and two D-alanine residues. It is between the penultimate D-alanine residue and the ε-amino group of the meso-diaminopimelic acid that the crosslinking reaction takes place. It is through this reaction that the terminal D-alanine is lost (Vollmer and Bertsche, 2008). Exactly how the glycan strands are arranged is unknown. The most common view is that the glycan strands lie parallel to the cell surface, with the main body of glycan strands running along the transverse of the longitudinal axis (Turner et al., 2014). The alternative possibility is that the glycan strands are perpendicular to the cell surface (Dmitriev et al., 1999, Dmitriev et al., 2003, Meroueh et al., 2006). However, at least in *E. coli,* there is insufficient peptidoglycan present to fully cover the cell in this fashion. In addition, the average length of the glycan strands is too great to fit within the periplasm (Vollmer and Holtje, 2004, Harz et al., 1990).

The synthesis of peptidoglycan has been extensively studied for many decades, with many comprehensive reviews available (Vollmer and Bertsche, 2008, Typas et al., 2012, Scheffers and Pinho, 2005, Barreteau et al., 2008). For this work the synthesis of

peptidoglycan in *B. subtilis* will be used as an example. It can be thought that peptidoglycan synthesis pathway can be divided broadly into two steps: synthesis of the precursors within the cell and the assembly of the polymer outside the cell. GlcNAc is synthesised within the cell from fructose-6-phosphate in a series of reactions by the enzymes GlmM and GlmU. In turn, GlcNAc acts as the precursor for the synthesis of the UDP-MurNAc pentapeptide by enzymes encoded by the *murA-F* and *murZ* genes. The resulting products are then linked to undecaprenyl-pyrophosphate (C_{55}-PP/bactoprenol), a carrier molecule that is embedded within the membrane. Upon linkage, the resulting molecule is called lipid I. The addition of UDP-GlcNAc to lipid I by MurG results in the creation of a Lipid II molecule. So far, all these steps have taken place inside the cell. Lipid II is flipped across the membrane to the exterior of the cell in a process thought to be mediated by MurJ (Ruiz, 2008, Meeske et al., 2015), though other candidates have been implicated in the past (Ehlert and Holtje, 1996). That *B. subtilis* remains viable following the loss of *murJ,* suggests the other candidates, such as *rodA* and *ftsW* also possess flippase activity(Fay and Dworkin, 2009, Scheffers and Tol, 2015). Once outside the cell, the precursors are incorporated into the pre-existing cell wall by the PBPs. The PBPs are responsible for both the transglycosylation and transpeptidation reactions. Different PBPs have varying roles in the synthesis of the cell wall, as reflects their varying localisation patterns. For example, PBP2B localises to the division septa, whereas PBP2A localises to the sites of cell elongation. It is thought that their interaction partners, as well as substrate availability help to regulate the activity of these enzymes (Rowland et al., 2010, Lages et al., 2013, Garner et al., 2011).

The peptidoglycan (PG) cell wall is not a static structure, and must be constantly remodelled and sculptured for a number of reasons, the least of which are cell elongation and division. In rod-shaped bacteria such as *B. subtilis* or *E. coli* new PG material is inserted in helices along the lateral cell wall (Vollmer and Bertsche, 2008). The process of elongation alternates with division. Unlike elongation which involves the addition of new glycan strands and peptide crosslinking, PG synthesis during division creates a plate of new PG that is part of the division septum. The presence of the new wall material leads to the separation of the cell membranes, resulting in the creation of the daughter cells. It is currently unclear whether the Z-ring constriction at the septum

provides the force necessary for the separation of the membranes, or whether it instead acts as scaffold, directing the synthesis of the peptidoglycan, with the newly synthesised PG causing the scission of the two cells (Meier and Goley, 2014, Osawa et al., 2008, Lan et al., 2009). Complete separation of the two daughter cells requires the actions of autolytic enzymes which degrade the material connecting the two cells. In addition, autolytic enzymes are distributed across the cell surface where they play specific roles in cell morphogenesis. Regulation of autolysins and PBPs in Gram-positive bacteria is thought to involve many different components (Goehring and Beckwith, 2005, Smith et al., 2000, Stewart, 2005). Two of these are the teichoic acids and the actin-homologue, MreB. These two components will be discussed later.
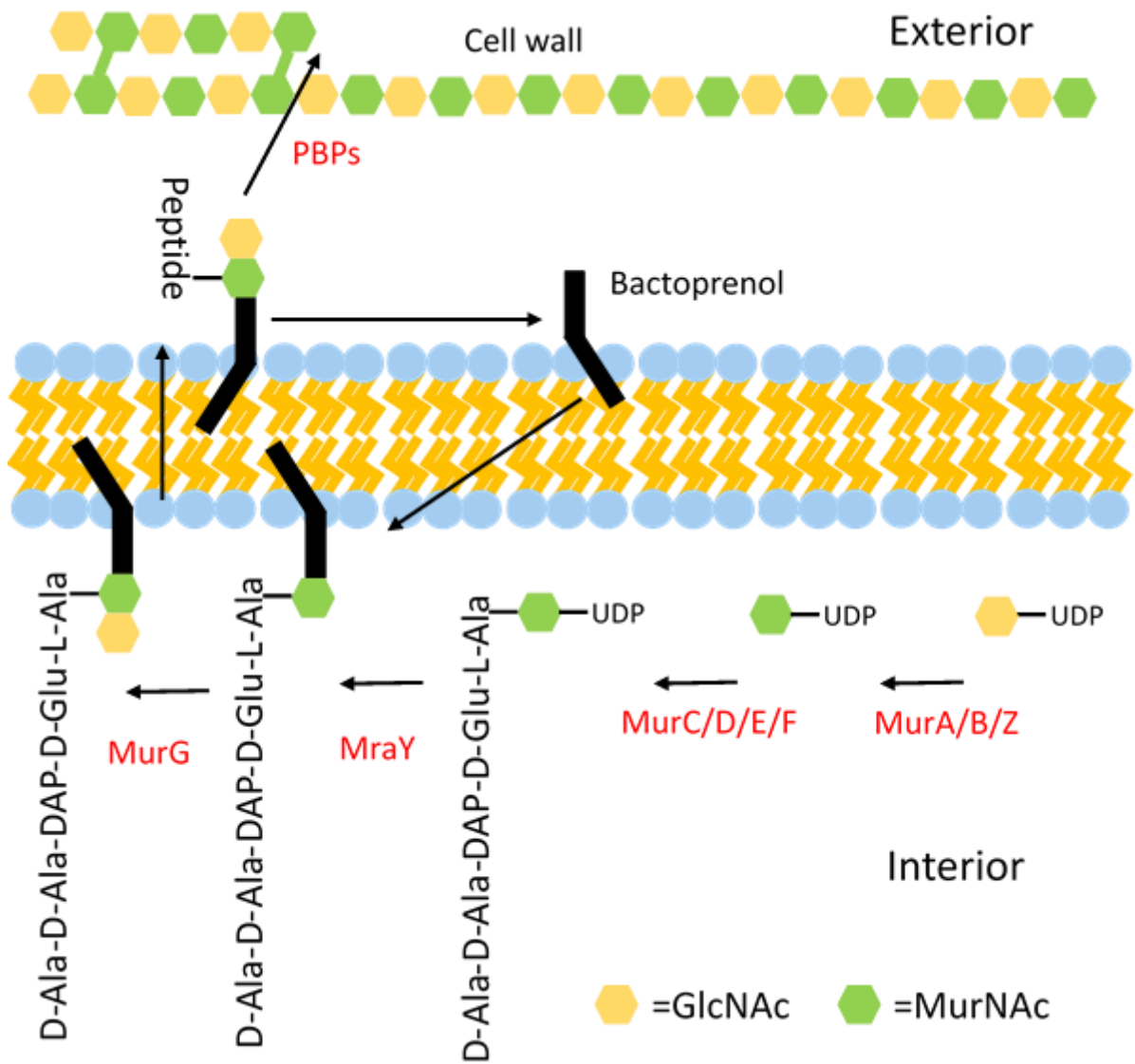
Figure 1.2. Cartoon schematic of peptidoglycan synthesis pathway in *B. subtilis*. Enzymes in the pathway are highlighted in red.

1.1.2.2 Roles

As touched on previously, the peptidoglycan plays a number of key roles in the survival of the bacterial cell. To this end, the cell wall is often regarded as essential, with some level of peptidoglycan found in almost all bacteria, with the exception being a few genera of bacteria such as *Mycoplasma*. However, under certain conditions bacteria can grow and divide in a wall-less state known as L-forms. These L-forms will be discussed later. Its importance is highlighted by the fact that it is the main target for antibiotics as well as a primary antigen for the immune system.

In addition to the direct roles that will be discussed below, the peptidoglycan mediates many secondary roles as it is frequently a binding site for the surface proteins of Gram-positive bacteria (in Gram-negative bacteria the proteins tend to be embedded in the outer membrane). This anchoring of proteins to the cell wall is mediated by a class of enzymes known as sortases (Perry et al., 2002, Ruzin et al., 2002). The surface proteins play a myriad number of roles, including mediating the interactions between the cell and its surroundings. For instance, many of the surface proteins are directly involved in colonisation of the appropriate environmental niche; many pathogens and commensals possess proteins that bind to specific eukaryotic molecules. Similarly, other proteins in these organisms act to shield and hide the antigens of the cell surface from the immune system of the host.

Many of the attached proteins act to sense changes in their external environments. This could involve changes in nutrient availability, solute concentrations, or the presence of other bacteria as is the case with quorum sensing.

1.1.2.2.1   Turgor

One of the key roles of the cell wall is to resist turgor pressure, preventing lysis of the cell in hypotonic conditions. Turgor pressure arises due to the difference between the internal solute concentrations and the external osmolarity. Unlike the *Eukaryotes*, bacteria lack systems for active water transport; instead the cellular water content is governed by osmosis. Soil bacteria such as *B. subtilis* face constant changes in their external osmolarity due to precipitation and evaporation. After rainfall, the external osmotic pressure is likely to drop, resulting in the influx of water into the cell as a result of osmosis. Bacteria have adopted ways to cope with such changes, and these will be

described later. However, the first line of defence is the PG wall; it possesses sufficient strength and elasticity to resist the turgor pressure long enough for additional coping mechanisms to come into play.

1.1.2.2.2 Shape

A wide array of bacterial shapes exist - from rods and spirals to cocci (Leeuwenhoek, 1695). These shapes are thought to be selectable features that affect nutrient uptake, motility and predation, amongst others. All of the morphologies arise from the cell wall, and how it is sculpted. Upon removal of the cell wall in isotonic conditions, the bacteria lose their characteristic morphologies and instead become spherical protoplasts. Similarly, the prepared sacculi of bacteria retain the same shapes from which it was originally isolated (Vollmer et al., 2008). The shapes of daughter cells formed by the peptidoglycan are identical to the cell shape of the parent, an indication for involvement of a genetic component. In species with complex cell shapes the cell shape is governed by the cytoskeleton protein MreB. MreB and its role in cell shape regulation and peptidoglycan synthesis will be discussed at length later.

1.1.2.2.3 Protein localisation

The cell shape imposed by the peptidoglycan enables the correct localisation of many proteins. Some of these proteins specifically bind to regions of the membrane with certain curvatures; the membrane curvature is imposed by the peptidoglycan cell wall. For instance, the Min system localises to the cell pole and prevents septal formation at sites away from the midcell. Localisation of MinCD to these sites is dependent on the presence of DivIVA. It has been demonstrated that the localisation of DivIVA to the cell poles is not dependent on the presence of any other proteins. Instead DivIVA recognises the negative curvature of the membrane at the poles (Lenarcic et al., 2009). In comparison, the *B. subtilis* spore coat assembly protein SpoVM preferentially binds to membrane with positive curvature. This ensures the protein accumulates on the membrane of the spore, rather than on the mother cell (van Ooij and Losick, 2003, Ramamurthi et al., 2009, Gill et al., 2015).

1.1.3 Cell membrane

In Gram-positive organisms a single cell membrane lies beneath the cell wall. This contrasts with Gram-negative bacteria, which sandwich their cell wall between an inner cell membrane and an outer cell membrane. At its simplest, the membrane can be considered to consist of a phospolipid bilayer that is studded with proteins. This semi-permeable membrane acts to separate the internal environment of the cell from the external environment, yet at the same time allows the cell to sense and interact with its surroundings. The membrane is a highly complex and ordered system. This complexity and how it allows the cells to structure its internal composition and react to external stimuli will be discussed below.

In *B. subtilis* the phospholipids that make up the cell membrane are synthesised by the type II fatty acid synthesis pathway (FAS II). Unlike the FAS I system in higher eukaryotes which consists of a polypeptide expressed from a single gene, the FAS II system is composed of many different gene products. Whilst the pathway is best elucidated for *E.coli*, the following description of the pathway will be discussed in the context of *B. subtilis* as there are significant differences in the fatty acid composition of the two species. In bacteria, the substrate for fatty acid synthesis is acetyl Co enzyme A (acetyl-CoA), itself a product of glucose metabolism. Conversion of acetyl-CoA into the intermediate, malonyl-CoA is catalysed by the coordinate functions of the acetyl-CoA carboxylase proteins (Acc). There are four of these proteins in *B. subtilis*; AccA, AccB, AccC and AccD. In bacteria it is not thought that malonyl-CoA has any other use outside of the FAS II pathway, therefore this is the step that commits the bacteria into producing fatty acids (Cronan and Waldrop, 2002). The malonyl group is then removed from the CoA subunit and transferred onto the acyl transfer protein (ACP) by the transacylase, FabD. It is onto the ACP that all subsequent intermediate molecules are attached to during fatty acid synthesis. In the next stage, FabH catalyses the first condensation reaction in which acetyl-CoA is used as the primer and the malonyl-ACP is the acceptor. FabH is the primary regulator of fatty acid diversity due to the substrate specificity of the enzyme (Choi et al., 2000). Replacement of the endogenous FabH with that from another species results in fatty acids with a different structure (Li et al., 2005). To produce branched chain fatty acids α-keto acids are used as the primers instead of

acetyl-CoA. The α-keto acids arise following the deamination and decarboxylation of the amino acids proline, leucine and isoleucine. Outside of the use of the α-keto acids, the synthesis of branched chain fatty acids proceeds in the same way as the straight chain fatty acids. After the first condensation reaction, the fatty acid precursor then enters the elongation cycle. The first step of the cycle involves the β-Ketoacyl-ACP reductase, FabG. The action of FabG is dependent on the presence of NADP (Toomey and Wakil, 1966). The intermediate produced by the actions of FabG is then dehydrated by either FabZ or FabA. The cycle is then completed by the actions of the reductase FabI/K/L/V, depending on the species (Heath et al., 2000). New rounds of elongation are then initiated by the actions of FabB. Some of the intermediate products are used for additional functions in bacteria, such as the production of the cofactor, biotin (Lin et al., 2010). The properties of the fatty acids affects the fluidity of the membrane. The properties of the fatty acids affects the fluidity of the membrane. The fluidity refers to the viscosity of the membrane; the level of viscosity is important for the motility, mobility and function of membrane embedded proteins. The level of membrane fluidity is affected by the temperature of the environment in which the bacterial cell is found - the warmer the environment, the more fluid a membrane will become. The fluidity of the membrane is also affected by the composition of the membrane. As alluded to earlier, the bacterial cell can produce different types of fatty acids, which will affect the fluidity of the cell. For example, branched chain fatty acids are more fluid than those with a straight chain; this arises because the branching limits the number of intermolecular interactions. The same phenomena occurs in regards to the other properties of the fatty acid such as the chain length, where longer chains result in an increased number of intermolecular interactions, and therefore a decrease in the fluidity (Parsons and Rock, 2013). In response to changes in temperature, the membrane fluidity will be altered to maintain a constant level of viscosity in a process called homeoviscous adaptation.

The products of the elongation cycle are intercepted by glycerol-3-phosphate acyltransferases that transfer the acyl-group from ACP to glycerol-3-phosphate, resulting in the production of phosphatidic acid. This stage represents the interface between fatty acid synthesis and membrane expansion. Phosphatidic acid is converted into CDP-

diacylglycerol (CDP-DAG) by CdsA. CDP-DAG acts as the branch point between the generation of zwitterionic phospholipids and acidic phospholipids. The diversity of head groups and the electrostatic charges they possess has been shown to be necessary for integral membrane proteins to adopt the correct topology (Zhang et al., 2005, Xie et al., 2006).

A

BCFA

Amino acids

SCFA

Metabolism

B-Ketoacyl-ACP → Elongation

Isovaleryl-CoA → FabH

Malonyl-ACP

FabD

Acetyl-CoA → Malonyl-CoA

AccABCD

B

Phosphatidic acid

CTP

CdsA

PP_i

L-serine

CMP

CDP-DAG

Glycerol-3-P

CMP

PssA

PgsA

Phosphatidylserine

Phosphatidylglyerolphosphate

Psd

YgpQ?
YutG?

CO_2

P_i

Phosphatidylethanolamine

Phosphatidylglycerol

Glycerol

Lysine

ClsA

MprF

Cardiolipin

lysyl-phosphatidylglycerol

Figure 1.3. Pathways of the phospholipid synthesis pathways. **(A)** The initiation of fatty acid synthesis. Enzymes involved are displayed in red. BCFA: branch chained fatty acids, derived from amino acids; SCFA: straight chain fatty acids, derived from metabolism. **(B)** Schematic of phospholipid head group synthesis. Enzymes involved are displayed in red; putative enzymes are indicated with a question mark. CMP = cytidine monophosphate; Glycerol-3-P = Glycerol-3-phosphate. For brevity, the schematic of fatty acid elongation was omitted.

1.1.3.1 Composition and organisation

Historically, the membrane was predicted to have a homogeneous distribution of the lipids and proteins, as predicted by the fluid mosaic model (Singer and Nicolson, 1972). Recent work instead suggests a new model in which the lipid and protein components of the membrane are distributed in a laterally heterogeneous manner. The heterogeneity of the membrane allows for the orchestration of many cellular events including cell division, chromosome segregation and osmosensing (Fishov and Norris, 2012). As mentioned, a primary component of the membrane are the phospholipids. The phospholipids contained in the membrane bilayer are not identical. They may have different head groups, which may vary in size and charge, and tails may differ, with varying lengths, saturation and branching. All these differences will contribute towards how the phospholipid interacts with other lipids, but also with the membrane associated proteins, which would in turn influence the formation of discrete lipid domains within the membrane.

This segregation of lipids has been demonstrated in both *E. coli* and *B. subtilis*, and almost certainly extends to other species. The relative quantities of the lipids does vary between *E. coli* and *B. subtilis,* with the membrane of *B. subtilis* comprising of roughly 20% phosphatidylethanolamine (PE), 40% phosphatidylglycerol (PG), 25% cardiolipin (CL) and 15 % lysyl-phosphatidylglycerol.

The first domains discovered were those involving the segregation of the anionic phospholipid, cardiolipin. CL in *B. subtilis* is synthesised by ClsA at the septum (Nishibori et al., 2005). In addition to its presence at the septum CL is observed to localise at the cell poles (Mileykovskaya and Dowhan, 2009). One hypothesis for the segregation of CL to the poles concerns the shape of the lipid. The hydrophobic tail of CL has a wider cross-section than the hydrophilic head, resulting in a cone shape. Due to this shape the most energetically stable environment tends to be the pole, where the membrane is pinned to the cell wall due to osmosis pressure resulting in a negative curvature (Huang et al., 2006).

As mentioned, CL is not the only species whose distribution is coordinated in the bacterial membrane. It has been demonstrated using fluorescent cationic styryl dyes that preferentially associate with PG or CL that PG assembles into helical domains along

the long axis of the cell. Evidence suggests that these helical domains are linked to the helices formed by the peptidoglycan synthesis machinery, with MinD, FtsA and SecA using the presence of PG as a cue for localisation (Barak et al., 2008).

In addition to the various distributions of the PG and CL, there is evidence suggesting the presence of lipid rafts within the bacterial membrane. These rafts had been previously identified in eukaryotes, where they help organise signal transduction proteins, amongst others. It was observed that proteins similar to the eukaryotic proteins were present in bacteria and that these proteins were not homogeneously distributed within the cell membrane. Further, these proteins do not colocalise with PG or CL, instead localising with polyisoprenoids. As with PG and CL, the rafts enable the colocalisation of proteins with similar, or shared pathways, such as the signal transduction proteins (Lopez and Kolter, 2010).

Perhaps one of the key roles the membrane plays is in the regulation of osmosis. The membrane acts as a partially permeable membrane that generally restricts the movement of most solutes, but permits the movement of water. Therefore, when a cell encounters hypotonic or hypertonic conditions water will rapidly cross the membrane in an attempt to diffuse or concentrate the cell contents. As the cell swells or contracts the distribution and coordination of the lipids will change. These changes are recognised by osmosensing proteins which act to normalise the cellular osmolarity. In *E. coli*, one of these osmosensing proteins is ProP, which responds to hypertonic conditions. ProP localises to the cell poles (Romantsov et al., 2007). Here, it associates with CL, with the phospholipid affecting the response of the protein to changes in osmolarity (Tsatskis et al., 2005).

CL was used as an example to demonstrate the multiplicity of roles individual phospholipids may play and the complexity of the membrane. Other phospholipids play important roles in structuring the cell through interacting with each other, with proteins and with small molecules.

1.1.4 Teichoic acids

The simplest diagrams of the Gram positive cell envelope will only feature a cell membrane surrounded by a PG cell wall. This is not the case, with anionic polymers called teichoic acids making up 30-60% of the cell wall. The TAs come in two types: those linked to the PG (Wall teichoic acids; WTA) and those linked to the lipid head groups of the membrane (Lipoteichoic acids; LTA). Not all Gram positive organisms have conventional LTA or WTA, though they generally possess functionally similar anionic structures instead. Interestingly, the replacement of LTA is associated with high GC content of the genome. In many species such as *B. subtilis* and *S. aureus*, the teichoic acids are polymers of polyglycerol phosphate (Gro-P). However, Gro-P is not the only substrate for TA synthesis, with subunits of ribitol phosphate and galactose not uncommon among different species (Neuhaus and Baddiley, 2003).

Whilst structurally similar in most bacteria, LTA and WTA are synthesised in distinct, separate pathways. This is even the case in bacteria such as *B. subtilis* where the repeat units are exactly the same. After synthesis the teichoic acid may be further modified through d-alanylation of the Gro-P subunits, a process carried out by enyzmes encoded by the *dlt* operon. Levels of d-alanylation vary across species and between WTA and LTAs. D-alanylation is further modulated in response to changes in pH, temperature and changes in the external osmolarity.

TAs have been implicated in a number of roles, though the functions remain somewhat unclear despite decades of research. TAs have been proposed to be involved in the cation homeostasis (Archibald et al., 1961, Heptinstall et al., 1970), biofilm formation (Gross et al., 2001, Holland et al., 2011), release of secreted proteins (Nouaille et al., 2004), adhesion (Wobser et al., 2014, Baur et al., 2014), pathogenicity (Fittipaldi et al., 2008, Morath et al., 2001), antibiotic resistance (Kovacs et al., 2006, Bertsche et al., 2013) and autolysin regulation (Biswas et al., 2012). In pathogens, the TAs, particularly LTA, have been demonstrated to be antigenic and are recognised by the innate immune system (Fedtke et al., 2004). In addition, the WTA and LTA have been shown to have important roles in the regulation of cell elongation and division (Schirner et al., 2009). These functions will be discussed at length later. As the structures of WTA and LTA are basically the same, it is thought the different roles are due to the spatial distribution of

these molecules, as opposed to any biochemical difference. It has been speculated that the charged nature of the TAs results in a microenvironment surrounding the cell that acts as periplasmic space similar to that seen in Gram negative organisms. It is thought that d-alanylation affects some of these functions, both positively and negatively, probably by altering the electromechanical properties of the cell envelope (Neuhaus and Baddiley, 2003). It has also been suggested that d-alanyl-LTA provides a source of free energy for chemical processes in the wall, though this hypothesis has not been proven (Neuhaus and Baddiley, 2003).

1.1.4.1 Wall teichoic acid

WTA is far better understood than the LTA, with most of the enzymes involved known; the synthesis of WTA has recently been comprehensively reviewed in (Brown et al., 2013). Unlike the synthesis of PG, WTA synthesis takes place within the cell cytoplasm, with the completed polymer exported across the membrane and then attached to the pre-existing wall (figure 1.4). WTA synthesis is carried out by enzymes encoded by the *tag* operon. The first gene in the pathway, *tagO*, encodes a protein that catalyses the attachment of GlcNAc to the undecaprenyl pyrophosphate (C_{55}-PP) carrier. TagA then attaches the linkage unit N-acetylmannosamine (ManNAc). ManNAc is created in an epimerisation reaction from GlcNAc by the enzyme MnaA. The building blocks of the WTA, CDP-GroP are synthesised by TagD, the first of these subunits are attached to the ManNAc residue by TagB. These initial steps are conserved in all the WTA synthetic pathways characterised thus far. However, the rest of the description will concern the synthetic pathway present in *B. subtilis*. Further extension of the WTA is catalysed by TagF, which links more of the CDP-GroP subunits until the chain is 45-60 residues in length. Glycosylation of the subunits is carried out by TagE. The extent of the glycosylation is dependent on the growth conditions. After the polymer is synthesised it is exported across the membrane to the exterior of the cell by the ABC transporter TagGH. Outside of the cell, the WTA is attached to PG in a process that was for some time poorly understood. It is now believed that members of the LytR–Cps2A–Psr (LCP) protein family encoded by *tagT*, *tagU* and *tagV* act as phosphotransferases to attach the polymer to the PG (Hubscher et al., 2008). Addition of d-alanyl esters is carried out by proteins encoded by the *dlt* operon. It is thought that the d-alanyl esters are added first to LTA, before they are transferred onto WTA (Neuhaus and Baddiley, 2003).

Deletion of any of these genes prevents the formation of WTA. Initially, it was believed that WTA was essential for cell survival (Bhavsar et al., 2001, Bhavsar et al., 2004). However, it was later demonstrated that deletions of the genes were viable, provided that the first gene in the pathway, *tagO*, was deleted (D'Elia et al., 2006a). Deletions of the later genes in the pathway in the absence of *ΔtagO* were non-viable, probably due to a build-up of a toxic intermediate or sequestration of an important metabolite (D'Elia et al., 2006b). Loss of WTA in *B. subtilis* results in cells that are affected in cell

elongation. The cells are able to divide, but are unable to maintain the normal rod shape. Localisation studies found that the synthetic enzymes localised to the sites of nascent PG synthesis along the lateral cell axis. This localisation was highly similar to that of the cytoskeleton proteins of the MreB family, which are believed to regulate PG synthesis and cell shape (Kawai et al., 2011, Formstone et al., 2008). This agrees with earlier work that demonstrated using radiolabelling that WTA was attached only to newly synthesised PG in *B. subtilis* (Mauck and Glaser, 1972). Work in *S. aureus* has shown further evidence for a functional interaction between the WTA and the PG synthesis machinery. Deletion of *S. aureus* WTA results in delocalisation of PBP4 and FmtA, and reduced PG crosslinking (Farha et al., 2013, Atilano et al., 2010).
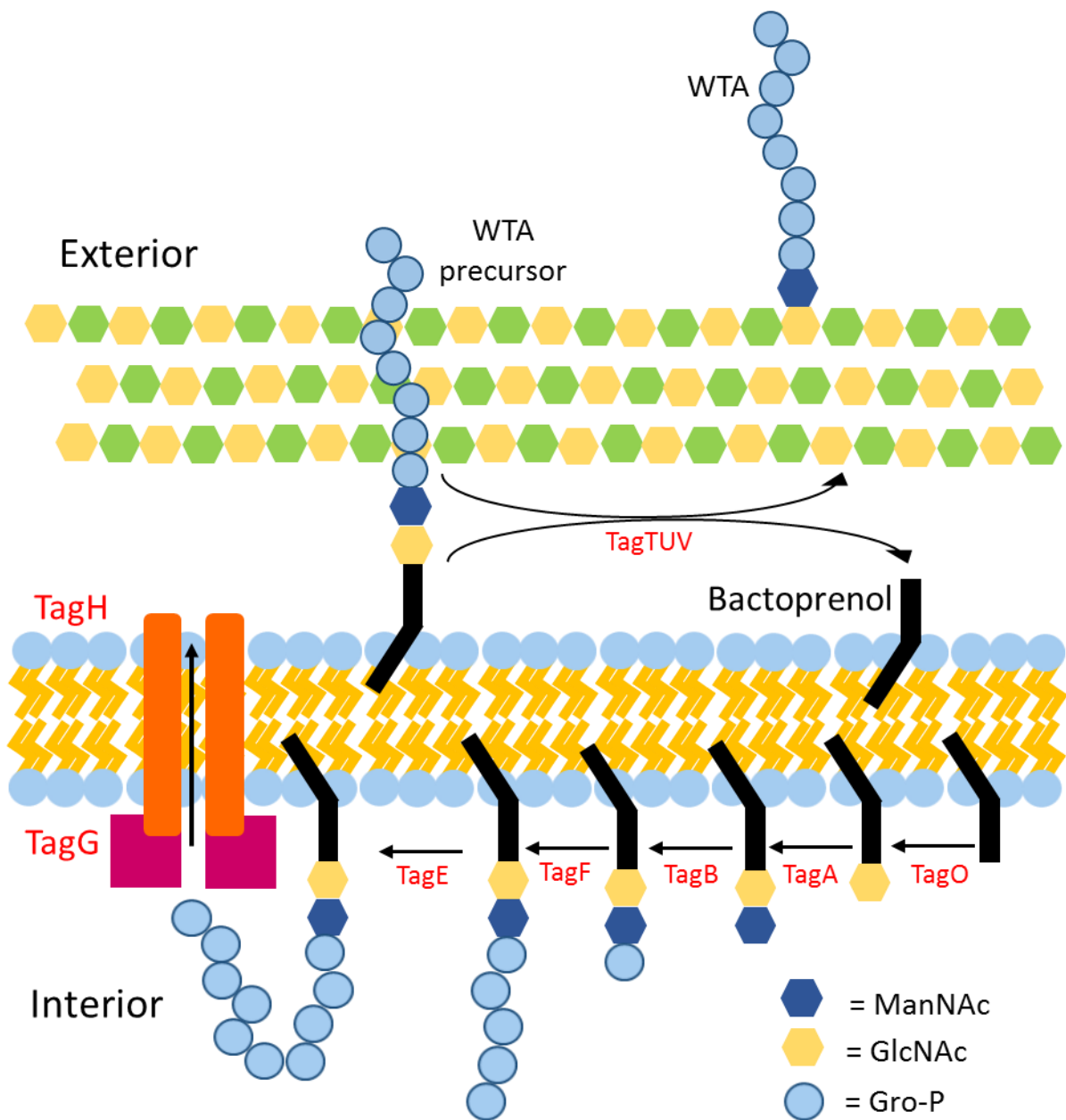
Figure 1.4. Pathway of wall teichoic acid synthesis in *B. subtilis*. Enzymes involved are indicated in red. WTA=wall teichoic acid; ManNAc=N-acetylmannosamine; GlcNAc=N-acetylglucosamine; Gro-P=glycerol phosphate.

1.1.4.2 Lipoteichoic acid

Unlike WTA, the synthetic pathway of LTA is poorly understood and characterised, with the genes involved only identified in the last 5 to 10 years. The majority of the research into LTA has been performed in a *S. aureus* background as it has been found to be important for the growth and pathogenicity of this organism. However, comparative work in *B. subtilis* has found the pathways between the two species to be largely similar.

As with WTA, the LTA in *B. subtilis* is composed of repeat units of Gro-P, although the Gro-P involved in LTA synthesis is derived from the head groups of the membrane lipid, phosphatidylglycerol. The Gro-P is anchored into the membrane by diglycosyldiacylglycerol (Glc$_2$-DAG). Glc$_2$-DAG is synthesised inside the cell by UgpP which catalyses the attachment of UDP-glucose to diacylglycerol (DAG). In *S. aureus*, the Glc$_2$-DAG anchor is thought to be flipped across the membrane by the transmembrane protein and putative flippase LtaA (Grundling and Schneewind, 2007a). No homologues of LtaA have been identified in *B. subtilis*, where the movement of the Glc$_2$-DAG across the membrane remains a mystery. The gene responsible for the attachment of Gro-P to the anchor, *ltaS*, was identified first in *S. aureus,* with a homologue identified by a BLAST search in *B. subtilis*. The BLAST search identified a further two homologues of *ltaS*: *yqgS* and *yfnI* (Grundling and Schneewind, 2007b). These are thought to play specialised roles in sporulation and stress, respectively. An additional homologue was also found, *yvgJ*, though this was later shown to be a primase rather than a synthase (Wormann et al., 2011). LtaS in both *S. aureus* and *B. subtilis* consists of five transmembrane domains with an extracellular catalytic C-terminal domain (Schirner et al., 2009). It is currently thought the attachment of subunits by the enzyme occurs at the distal end of the growing LTA molecule. As the subunits and the LtaS are both located in the membrane, it has been postulated that the terminal end of the LTA molecule remains close to the membrane. As with WTA, LTA can be d-alanylated. This is one of the few pathways shared between the two TAs, with the gene products of the *dlt* operon also responsible for d-alanylation of LTA.

Much like the differing synthetic pathways, it has been shown that LTA and WTA have different physiological roles. Loss of *ltaS* is lethal in *S. aureus*, with growth only possible at permissive temperatures or by development of suppressor mutants in osmotically

stabilising conditions. In *B. subtilis, ltaS* is dispensable, though a fitness cost is incurred. Further deletion of the homologues, *yqgS* and *yfnI,* renders the cell sicker, but is not lethal for *B. subtilis*. However, upon deletion of *ltaS* in *B. subtilis*, the cells develop a filamentous phenotype. In addition, it was shown that a double mutant of *ltaS* and the homologue *yqgS* blocks sporulation. In both vegetative and sporulating cells, LtaS and YqgS localise mainly to the sites of cell division. This supports the idea that LTA is involved in the regulation of division, whereas WTA is involved in elongation. Exactly how LtaS and LTA contribute to division is unclear. It is thought that LTA may increase the availability of magnesium to the division machinery. The role of LTA in cation homeostasis is supported by the observation that even very low concentrations of Mn^{2+} was extremely toxic to *B. subtilis* cells that were LtaS-null (Schirner et al., 2009). This suggests that LTA is able to bind the cations, preventing access to the cell.

In species such as *S. aureus,* the *ltaS* deletion mutants are viable when grown in high sucrose or salt media. They can also be rescued by increases in the cellular concentration of the signalling molecule cyclic-diadenosine-monophosphate (c-di-AMP). This molecule has been implicated in the regulation of the transport of potassium and other ions (Corrigan et al., 2011). It has therefore been postulated that LTA may play a role in the osmoprotection of the cell.
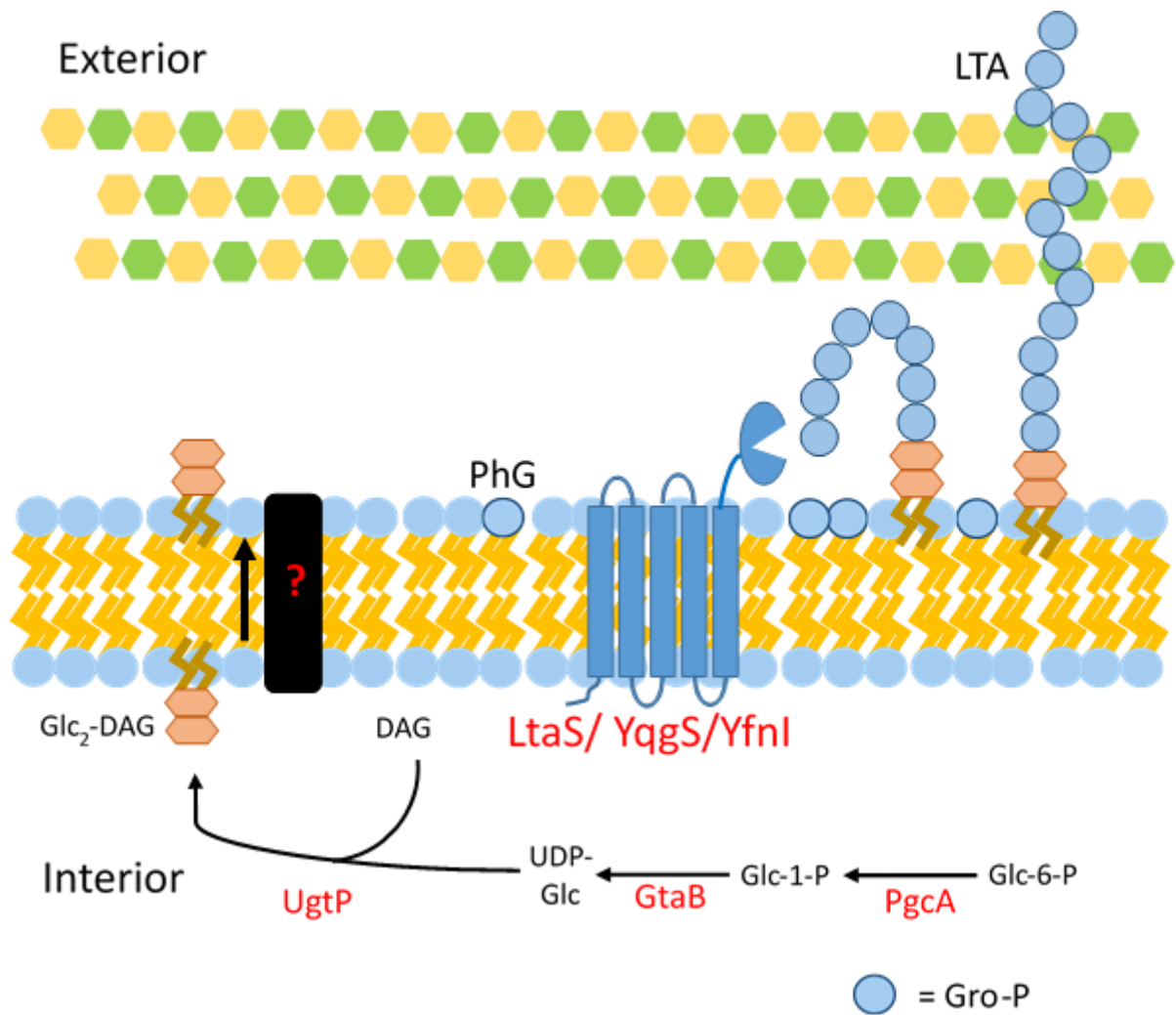
Figure 1.5. Pathway of LTA synthesis in *B. subtilis*. Enzymes involved are indicated in red. Unknown proteins are indicated with a question mark. LTA=lipoteichoic acid; Gro-P= glycerolphosphate; PhG=phosphatidylglycerol; Glc-6-P=Glucose-6-phosphate; Glc-1-P=Glucose-1-phosphate; UDP-Glc=UDP-Glucose; DAG=Diacylglycerol.

1.2 The bacterial cytoskeleton

For a significant period of time, the cytoskeleton was considered a uniquely eukaryotic characteristic. In the eukaryotes the cytoskeleton plays a role in cell shape determination, motility, chromosome segregation and the architecture of intracellular space. However, it has since emerged that bacteria possess a homologous system.

The first homologue identified in bacteria was FtsZ. FtsZ is a highly conserved tubulin-like protein that forms the Z-ring at the site of septum formation (Adams and Errington, 2009). This was followed by the discovery of another filamentous protein – MreB. Crystallisation of MreB showed a clear structural homology to the eukaryotic actin, even though there is very little homology at a nucleotide level or in the primary structure. MreB belongs to a super family of other actin-like proteins, which includes important proteins such as FtsA. However, for the purposes of this work only MreB and its homologues in *B. subtilis* will be discussed. More recently, a homologue to the intermediate filaments was identified in *Caulobacter crescentus.* Crescentin, as the homologue was called, was found to be a cell shape determinant in this species. It should be noted that the level of homology between crescentin and the intermediate filaments is very low; the only conserved characteristics are a nucleotide hydrolysing activity and some structural features (Ausmees et al., 2003).

1.2.1   MreB

The *mreB* genes were among the first to be associated with the regulation of cell shape in *E. coli* and *B. subtilis*. The *mreB* genes are highly conserved, but also widely distributed. They are found in most non-spherical bacteria, and are absent in almost all of the coccoidal bacteria. Those bacteria which lack a copy of MreB, but are still rod-shaped, tend to grow via more uncommon methods, such as through addition of new PG at the cell poles (Flardh, 2010). This contrasts with the conventional mode of elongation seen in *E. coli* and *B. subtilis* in which new material is added along the lateral cell axis. Deletion of *mreB* in rod-shaped bacteria results in the loss of this cell shape, with the bacteria instead adopting a spherical shape (Wachi et al., 1987). Taken together, this was a strong indication that MreB is involved in the addition of cell wall material along the lateral cell axis. MreB null mutants are very sick, though can be stabilised with the addition of high concentrations of magnesium(Formstone and Errington, 2005). This

suggests a possible role for the MreB in stabilising the membranes, though admittedly the actual role of the magnesium has yet to be elucidated. Original localisation studies indicated that MreB forms helical filaments along the lateral cell axis; the helical distribution of MreB matched that of nascent peptidoglycan synthesis (Daniel and Errington, 2003, Jones et al., 2001). At the same time, it was observed that many of the interaction partners as well as components of the elongation complex were similarly distributed, though it must be said that the localisation of some of these proteins was more tenuous than others. It is thought that through the interaction partners of MreB such as MurG, MraY, RodZ, MreC and MreD (Muchova et al., 2013, van den Ent et al., 2006, Defeu Soufo and Graumann, 2005), MreB is able to couple the cytoplasmic and extracellular cell wall synthesis steps. These proteins are also involved in cell shape determination. They are known to act as a bridge between MreB and other members of the elongation complex. Unfortunately, they are far less understood than MreB. From the results described it was therefore presumed that the MreB filaments were directly involved in the morphogenesis of rod shaped bacteria by coordinating the locations of peptidoglycan synthesis.

In 2011, this paradigm was contested by the release of a number of papers. These papers used more sophisticated microscopy techniques to re-examine the nature of the MreB assemblies in both *E. coli* and *B. subtilis*. The papers showed that instead of helical, stationary filaments, MreB instead form dynamic patches that move in a circumferential motion rather than in a helical movement. This movement appears driven not by actin-like dynamics, but rather by the action of the cell wall synthetic enzymes (Garner et al., 2011, Dominguez-Escobar et al., 2011, van Teeffelen et al., 2011). The conflicting observations were ascribed to various limitations regarding the techniques for the visualisation of MreB. The results raised many questions, namely, how do the short patches of MreB control the rod shaped morphology of the cells; it is difficult to imagine how the patches would be able to measure or coordinate the cell geometry, particularly as MreB has been demonstrated to be essential for the recovery of a rod shape in cells growing a cell wall *de novo* (Billings et al., 2014, Errington, 2015). More recently, both *in vitro* studies and high-resolution imaging techniques found that MreB could form extended filaments. It was demonstrated *in vitro* that MreB could form filaments that

could assemble into antiparallel proto-filaments (van den Ent et al., 2014). It was also shown that MreB can interact with the membrane via a membrane insertion loop or an N-terminal amphipathic helix (Salje et al., 2011); these interactions would be increased within a proto-filament. Alongside the biochemical work, use of new microscopy techniques such as structured illumination microscopy (SIM), stimulation emission depletion (STED) microscopy and total internal reflection fluorescence-SIM (TIRF-SIM) was able to shed new light on the nature of MreB within the cell (Olshausen et al., 2013, Reimold et al., 2013). The papers once again found that MreB forms extended filaments of variable length whose movement is based upon the activity of peptidoglycan synthesis. The extended filaments they observed using the various microscopy techniques moved in a circumferential motion, as reported in the work from 2011. However, some of these filaments were orientated in such a way as to appear helical using traditional fluorescent microscopy. The model they propose states that MreB does indeed form extended filaments, with these filaments connecting spatially separated complexes of PG synthesis machinery. The extended filaments are suggested to allow the protein to 'sense' information regarding the geometry of the cell (Olshausen et al., 2013). This model has been further enriched by recent work into the geometrical control of the cell shape by MreB. As mentioned earlier, MreB can directly interact with the membrane. In liposomes, this interaction is sufficient to impose curvature on the membrane (Salje et al., 2011). In the more recent work it was found that MreB preferentially localises to regions of negative curvature whilst depleting from areas of positive curvature. It was seen that this localisation was coupled with localised cell wall synthesis. Bursts of localised peptidoglycan synthesis result in the cell straightening, and the loss of negative curvature. *In silico* experiments agreed with the hypothesis that PG synthesis at negatively curved sites helps to straighten cells (Ursell et al., 2014).

The assembly of MreB into filaments appears to be further controlled by the availability of the PG precursor molecule lipid II. Depletion of lipid II either genetically or through use of antibiotics results in the disassociation of MreB from the membrane. The disassembly of the MreB filaments causes cell elongation to cease (Schirner et al., 2015). Whilst PG synthesis would presumably be halted due to the absence of a substrate, autolytic enzymes also make up the elongation complex organised by MreB, and would

continue degrading the PG at these sites. This mechanism therefore provides a nice system through which the activity of these enzymes could be regulated. Consistent with this study, recent work has indicated that MreB is linked to regions with increased membrane fluidity, as are the lipid II molecules (Strahl et al., 2014, Janas et al., 1994, Ganchev et al., 2006). These regions of increased fluidity are believed to be created by MreB, though is unclear how, as MreB in *B. subtilis* (in which this work was performed) lack the membrane interacting domains that have been shown to generate lipid domains (Garcia-Saez et al., 2007, Cornell and Taneva, 2006). It is hypothesised that the regions of increased membrane fluidity may facilitate catalytic activity or protein diffusion, though this is just speculation.

1.2.2 Mbl and MreBH

Gram negative bacteria tend only to have a single copy of *mreB* on their genome. *B. subtilis,* like many Gram positive organisms carries two homologues of *mreB*; *mbl* (**m**re**B**-**l**ike) and *mreBH* (**mreB** **h**omologue). MreB and Mbl have roughly equal abundance in the cell, whereas MreBH is significantly less abundant (Jones et al., 2001). The *mreB* gene is defined primarily by its genomic position in an operon alongside *mreC* and *mreD*. The other two homologues are organised into monocistronic units (Kobayashi et al., 2003). As with deletions of MreB, loss of any of the homologues is lethal. Like with MreB-null strains, growth can be restored through supplementation of the growth media with magnesium, though the magnesium dependence of MreBH is far more subtle, requiring Mg^{2+} concentrations less than 100 µM (Carballido-Lopez et al., 2006). Interestingly, MreBH is essential for growth in low magnesium conditions (Carballido-Lopez, 2006). In addition to the single deletions, the only viable double mutation has deletions of *mreBH* and *mbl* (Kawai et al., 2009, Defeu Soufo and Graumann, 2006). Deletions of *mbl* were found to be viable in the absence of magnesium at first (Abhayawardhane and Stewart, 1995, Jones et al., 2001), though it appears now that this instead provokes the development of suppressor mutations (Schirner and Errington, 2009, Schirner et al., 2009). It was discovered that the gene responsible for LTA synthesis, *ltaS*, is one of the genes identified to be lost in response to deletion of *mbl*. It remains unclear exactly how disruption of LTA enables Δ*mbl* cells to grow in the absence of Mg^{2+} supplementation; the strongest hypothesis is that the loss of LTA increases the

access of Mg^{2+} to the cell (Schirner et al., 2009). Another of genes whose mutation suppresses the magnesium dependence of Δ*mbl* was *rsgI*. *rsgI* encodes the anti-sigma factor of $σ^I$, a $σ^{70}$-type sigma factor that is involved in the response to external stress. As with the mutation in *ltaS* it remains unclear how derepression of $σ^I$ results in the suppression, though modifications to the cell wall are suspected. What is remarkable, however, is that Δ*rsgI* enables triple mutations comprising Δ*mreB*, Δ*mbl* and Δ*mreBH* to be constructed, something which is not possible in a wild type background (Schirner and Errington, 2009). The triple mutant was observed to adopt a spherical shape as was an increase in the membrane fluidity (Strahl et al., 2014).

All three of the MreB homologues are believed to interact with each other, but also to colocalise to the elongation complex discussed earlier (Carballido-Lopez, 2006, Defeu Soufo and Graumann, 2006, Challis, 2014, Formstone and Errington, 2005). The three homologues have overlapping functions, making it difficult to prise apart their individual functions. The different single mutations do not result in identical phenotypes, with the cells instead taking on different morphologies depending on which of the homologues was deleted. When MreB is lost cells become fatter, but remain straight; loss of Mbl results in fatter, twisted cells; loss of MreBH causes cells to become straight and thin.

It has also been demonstrated that the homologues have different roles in the regulation of the autolytic enzymes CwlO and LytE. As mentioned earlier, the cell wall is a highly dynamic structure that is constantly growing and remodelled. Where the PBPs attach new PG, the autolytic enzymes are able to remove the PG. As with PG synthesis machinery, the spatial and temporal activities of the autolytic enzymes must be tightly regulated. Loss of regulation would have disastrous results. In *B. subtilis* it has been demonstrated that CwlO and LytE play an essential role in the elongation of the cell (Bisicchia et al., 2007). Loss of both the enzymes results in cell death, likely as a result of an inability to elongate (Hashimoto et al., 2012). It was found that the two autolytic enzymes are differentially regulated by the MreB homologues, with MreB and MreBH controlling LytE activity, whereas Mbl controls the activity of CwlO (via the FtsEX complex) (Dominguez-Cuevas et al., 2013). In addition to the differential control, it was discovered in the same work that the autolytic enzymes have differing roles in the control of bacterial morphogenesis. Loss of LytE affects the control of the cell diameter,

whereas disruption of CwlO appears to affect the control of the longitudinal axis. Such phenotypes are broadly similar to the morphologies seen when MreBH and Mbl are deleted respectively. These results strongly indicate that the MreB and its homologues possess differentiated roles in the control of bacterial morphogenesis. It makes sense that the Gram positive bacteria have additional MreB homologues to allow them to more tightly coordinate the structure of the cell wall, particularly as they lack the ability to do so from an outer membrane like in Gram negative organisms.
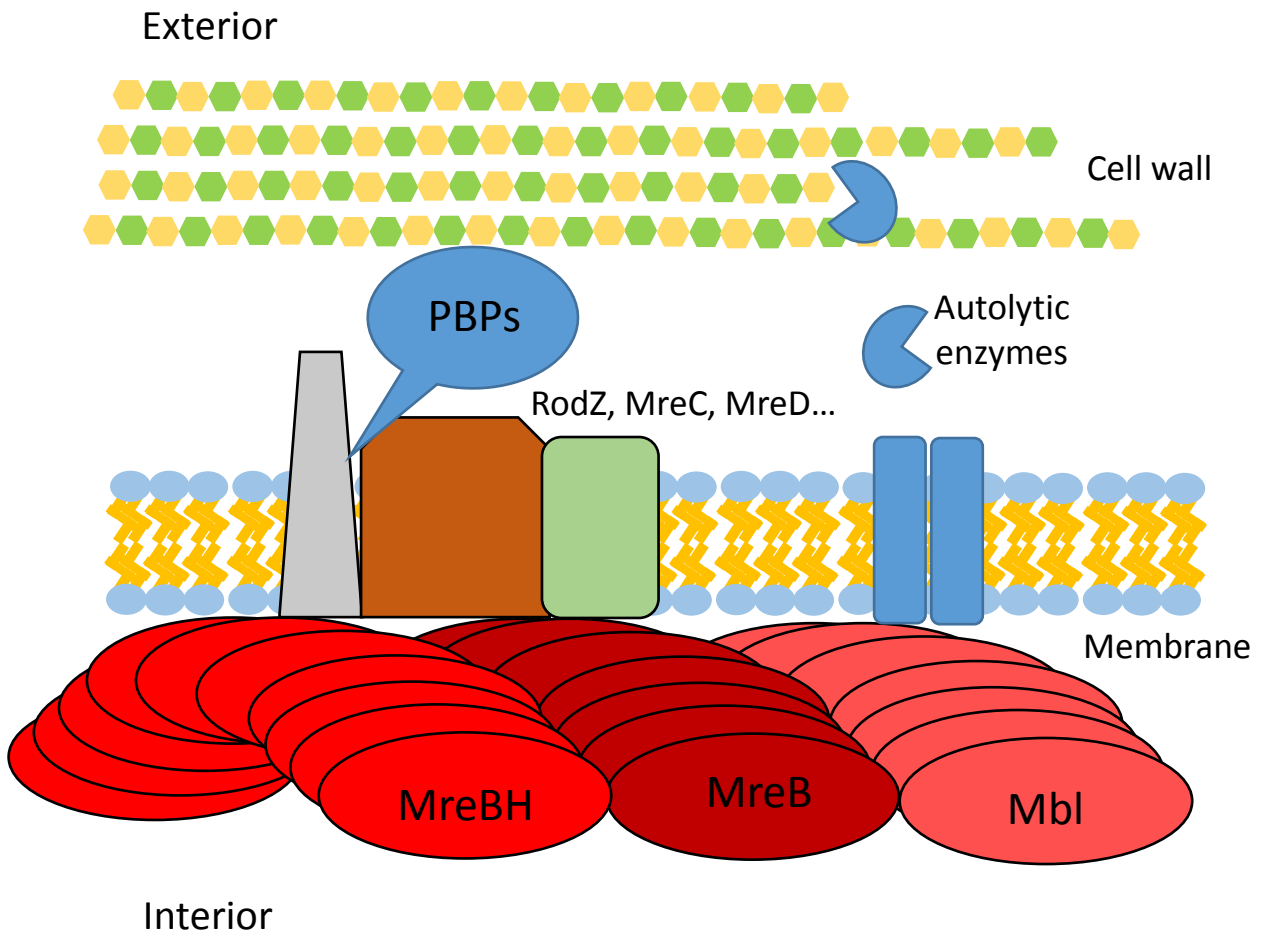
Figure 1.6. Model of the MreB homologues and their orchestration of the cell wall elongation machinery. MreB and its homologues form helical filaments that colocalise underneath the cell membrane. Here they interact with transmembrane proteins such as MreC and RodZ, which in turn coordinate the cell wall synthesis machinery (the PBPs). The MreB homologues also coordinate the activity of the autolysis enzymes.

1.3 Regulation of osmolarity in bacteria

Most bacteria will face changes in the osmolarity of its external environment. *B. subtilis* will face drastic changes of osmolarity in the soil due to the effects of precipitation and evaporation, whereas bacteria such as urinary pathogenic *E. coli* (UPEC) will experience changes as a result of the concentration or dilution of urine. As the external osmolarity rises or falls water will pass across the membrane to either concentrate or dilute the cytoplasm. Bacteria strive to maintain a constant cytoplasmic volume so as to enable optimum cell function and structure. Unlike eukaryotes, prokaryotes lack a means to actively transport water across their membranes. Instead, prokaryotes must instead modulate the levels of solutes within their cytoplasm. Broadly speaking the milieu of components within the cell cytoplasm can be divided into two camps. Firstly, there are the molecules that contribute that affect the osmolarity of the cell, but are involved in an essential cell process or are toxic to the cell. The second camp are known as the compatible solutes (Whatmore et al., 1990). These are soluble molecules and ions that can be accumulated to very high levels without affecting protein functions or cellular physiology (da Costa et al., 1998, Arakawa and Timasheff, 1985). As osmotic pressure is a physical function arising from the water activity, both affect the intracellular osmolarity. However, the cell is able to alter the levels of compatible solutes in response to changes in the external osmolarity, whereas the other solutes remain largely stable. The various routes by which the levels of compatible solutes can be controlled will be discussed below. Before that, the key role of the cell wall in withstanding the effects of changing osmolarities must be reiterated. As mentioned in 1.1.2.2.1 the cell wall provides the first line of defence in withstanding the effects of the influx of water. Without a cell wall large influxes of water will inflate the cell cytoplasm to the extent that the cell membrane loses its integrity, resulting in cell lysis.

Bacteria respond to osmotic changes through modulating the cytoplasmic concentrations of the compatible solutes. These compatible solutes come in several guises and include both organic and inorganic molecules. The inorganic molecules are generally limited to K^+ and Na^+ ions, whereas the list of organic molecules used as compatible solutes is far more extensive. Organic compatible solutes include molecules such as glycine betaine, proline and glutamate. The organic solutes used varies widely

from species to species (da Costa et al., 1998). K^+ is the most ubiquitous, being maintained in *B. subtilis* at basal levels of around 350 mM due to its involvement in many key functions. Upon osmotic upshock, the concentration of K^+ can increase as high as 650 mM as the bacterial cell utilises uptake systems to accumulate K^+ to counteract turgor. However, high concentrations of K^+ are difficult to sustain and are detrimental to the bacterial physiology. As such, following an initial osmotic upshock, bacteria will begin to accumulate the organic solutes, replacing the K^+ in combatting the turgor pressure (Whatmore et al., 1990).

Bacteria will respond to changes in osmolarity first on a protein based level, then as time progresses the cell will respond at a transcriptional level (Wood, 1999). The initial protein response largely concerns the osmosensing proteins distributed throughout the membrane. These proteins generally are dual-functional, with an additional role as a transporter. The dual function is necessary as changes in the hydration of the cell affects the functions of many proteins.

Upon an osmotic upshock the cell will start to dehydrate, resulting in cytoplasm shrinkage and even plasmolysis. Loss of cytoplasmic volume is known to inhibit many cellular functions. It was originally thought that the turgor was necessary for driving cell wall synthesis and cell expansion, though this no longer appears to hold true, as turgor is not significantly affected during osmotic upshocks (Rojas et al., 2014). It remains unclear how osmotic stress limits cell growth, though various deleterious effects on the molecule crowding in respiration, transcription, translation, precursor synthesis and replication have all been suggested (Wood, 1999, Wood, 2015).

Most of the membrane transporters become inactivated, except for the osmotransporters. The osmotransporters are bifunctional proteins in that they also possess an osmosensory function. The three models for understanding these osmoregulator proteins are ProP from *E. coli*, BetP from *Corynebacterium glutamicum* and OpuA from *B. subtilis* and *Lactobacillus lactis*. As the name suggests, ProP is involved in proline transport, though it has an equal affinity for glycine betaine. BetP and OpuA, on the other hand, transport glycine betaine exclusively. Despite being the best studied systems, both *in vivo* and *in vitro,* the exact mechanisms through which they are activated have not been elucidated. It is known that the C-terminal domain of all three

of these proteins, whilst not conserved, is a sensor for the direct or indirect changes as a result of changing osmolarities. There is a long list of potential stimuli which include the osmolarity gradient across the membrane, membrane thickness, bilayer curvature and the cytoplasmic osmolarity amongst others. Current work using proteoliposomes (liposomes prepared from protoplasts) suggest that the cytoplasmic osmolarity is the driving force in the activation of BetP and ProP (Rubenhagen et al., 2001). Unlike the other two model proteins, activation of OpuA is thought to be a result of changes in the ionic strength of the cytoplasm (Biemans-Oldehinkel et al., 2006). An alternative explanation for the results is that the activation of the transport functions is driven by the hydration of the proteins (Wood, 2011). Importantly, they do not appear to require the presence of additional protein; important as many proteins are inactivated by changes in osmolarity. As much of this work has been carried out in artificial systems it is probable that the regulation of the activation is far more complex. There is some evidence that the membrane plays an important role in the activation of these proteins, as the osmolarity required to activate the proteins in the proteoliposome systems varies depending on the quantity of anionic lipids in the liposome. In addition, both BetP and OpuA contain C-terminal domains that are thought to be able to interact with both the membrane and the rest of the protein, thereby acting as an osmoswitch. ProP on the other hand exhibits a preference for cardiolipin domains within the membrane; absence of CL causes attenuation of activation (Tsatskis et al., 2005).

Upon activation, the proteins transport the compatible solute of choice into the cell. Osmotransports are unique to any one protein family, with BetP belonging to the betaine-carnitine-choline transporter family, ProP belonging to the major transport facilitator superfamily (MFS) and OpuA being an ATP binding cassette (ABC) transporter. In the same vein, the bioenergetic mechanism by which the compatible solutes enter the cell is not specific either; BetP is a Na^+-compatible solute symporter; ProP is an H^+-compatible solute symporter; OpuA is an ABC transporter. Overall, the transporters are believed to adhere to the alternate access mechanism of transport. In this mechanism the compatible solutes binds to a cleft in an outward facing domain of the protein. Solute binding triggers a conformational change in which the protein will adopt an intermediate structure occluding the solute within the protein. The protein then

undergoes a second conformational change which results in the solute gaining access to the cell cytoplasm (Kaback et al., 2007).

In addition to accumulating glycine betaine from the environment, the cell can make its own (Boch et al., 1994). Glycine betaine is synthesised from either choline or glycine betaine aldehyde. These precursor molecules still have to be taken up from the external environment, usually via the same osmotransports described earlier, and as a result of the same stimuli. However, expression of the genes required for the conversion of the precursors into glycine betaine are only mildly upregulated in response to osmotic stress (Boch et al., 1994). The process of conversion has been best studied in *E.coli,* though the synthetic genes have been identified in *B. subtilis*. The synthesis from choline consists of a two-step oxidation step, featuring glycine betaine aldehyde as an intermediate step. The first step is catalysed by GbsB, a choline dehydrogenase, whereas the second step is catalysed by GbsA, a glycine betaine aldehyde dehydrogenase (Boch et al., 1996). A similar system for the generation of proline exists in *B. subtilis*. In addition to directly taking up proline from the environment, *B. subtilis* can instead take up oligopeptides via the App and Opp oligopeptide transporters. Uptake of proline-rich oligopeptides is followed by degradation by the amino-peptidases PapA and PapB into the amino acid subunits, thereby resulting in an increase in cellular proline (Zaprasis et al., 2013).

The bacterial response to osmotic downshocks is somewhat simpler, but less well understood. Upon entry into a hypotonic environment water will cross the membrane and cause the cell volume to increase. This increase in size is constrained by the cell wall which possesses some elasticity to deal with the increase in internal pressure. In *E. coli* it has been demonstrated that the cell wall is able to swell by up to 12% to accommodate the influx of water (Yao et al., 1999). However, to maintain the integrity of the cell envelope the cell must release excess solutes so as to minimise the influx of water. Bacteria are able to do so via mechanosensitive (MS) channels. These channels are ubiquitous across the prokaryotic kingdom and may be divided into two families; MscL and MscS. MscL proteins are highly conserved whereas the MscS proteins are far more varied, with the different forms only united by a conserved pore domain close to the C-terminus (Booth and Blount, 2012, Levina et al., 1999, Naismith and Booth, 2012). Often, a bacteria will only carry a single copy of MscL, but several different variants of

the MscS protein. These different copies are probably expressed in response to different stimuli (Booth and Blount, 2012). In *E. coli* it has been demonstrated that MscS and MscL are essential for survival in hypotonic conditions, whilst the MscS variants it carries merely affect the threshold of osmotic pressure that the cells can survive (Levina et al., 1999, Schumann et al., 2010). The cell death that arises from cells lacking the MS channels is a mix of cells that undergo catastrophic lysis and some that form lesions from which the essential macromolecules diffuse out (Reuter et al., 2014).

Returning back to the function of the MS channel proteins; it is thought that the MS channels open in response to lateral tension in the lipid bilayer that arises due to an increase in turgor pressure (Sukharev et al., 1999). It should be noted that exactly how the proteins sense the changes in membrane tension is still disputed. Typically, the MscS proteins form a pore of 12-16 Å in diameter (Sukharev, 2002, Wang et al., 2008). In contrast, the MscL proteins form a much larger pore, some 30 Å in diameter (Cruickshank et al., 1997). It is thought that the MscL channel is opened as a last line of defence (Berrier et al., 1996), an opinion that would be supported by the huge channel size, which could have deleterious effects on the cell; artificially opening the channel has catastrophic effects for a cell (Ou et al., 1998, Maurer and Dougherty, 2001, Batiza et al., 2002). The open channels allow for excess solutes to rapidly escape the cell by diffusion, thereby reducing the disruptive effects of extreme turgor pressure.
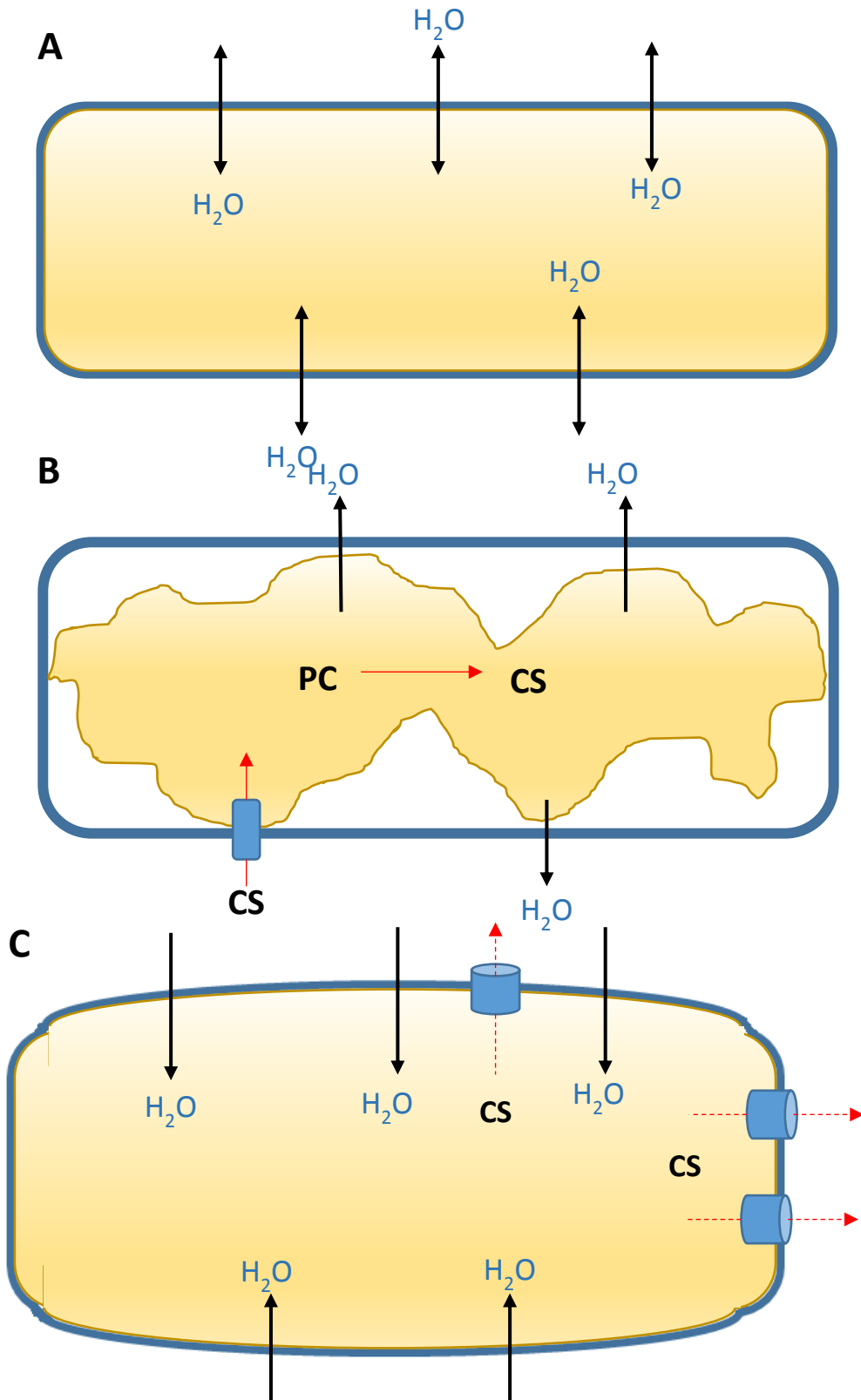
Figure 1.7. Cartoon depiction of the bacterial response to isotonic (A), hypertonic (B) and hypotonic (C) environments. Black arrows indicate the net movement of water. Red arrows indicate the movement of compatible solutes. CS=compatible solutes; PC=precursors.

1.4 L-form bacteria

1.4.1 L-form biology

It may come as some surprise that cell wall is dispensable under certain conditions. The bacteria that are able to grow and divide indefinitely in the absence of the cell wall are called 'L-forms' (Klieneberger, 1935), so named after the Lister Institute where they were originally discovered. Bacteria are able to survive without a cell wall as protoplasts, though they are unable to grow and divide indefinitely. The ability to grow in the L-form state does not appear to be limited to any one species, with many bacterial species displaying an ability to grow in this manner (Mercier et al., 2014, Gilpin et al., 1973, Williams, 1963). As L-forms lack a cell wall, they generally require high osmolarity media to ameliorate the effect of turgor on the cell (Onoda et al., 1987). In laboratory settings, L-forms can be generated via a number of different routes. Historically, the most common method to generate L-forms was to disrupt the cell wall synthesis with drugs such as the β-lactams. This method has largely fallen out of favour, with a genetic route the more common route for L-form development (Leaver et al., 2009). To induce an L-form state genetically it requires the overproduction of the cell membrane (Mercier et al., 2013). In *B. subtilis* this is achieved either through the depletion of MurE or the overexpression of *accDA*. The exact mechanism by which depletion of the PG synthesis protein MurE results in membrane overproduction remains unclear. The role of overexpression of *accDA* is far clearer, with the proteins directly involved in fatty acid synthesis (Mercier et al., 2013, Cronan and Waldrop, 2002). Alongside the primary mutation driving membrane overproduction a secondary mutation appears essential. In *B. subtilis* this mutation is often in the gene *ispA.* IspA catalyses the formation of farnesyl pyrophosphate in the isoprenoid synthetic pathway (Fujisaki et al., 1990). Farnesyl pyrophosphate is used as the substrate for synthesis of two lipid molecules: heptaprenyl diphosphate (HPP) and C_{55}-PP. HPP is in turn required for the synthesis of menaquinone, which is involved in the electron transport chain. C_{55}-PP is required for the synthesis of lipid II and WTA. It appears that the loss of *ispA* counteracts an increase in cellular levels of reactive oxygen species (ROS), which inhibit L-form growth. The requirement for the mutation can be bypassed by including ROS scavengers in the growth medium (Kawai et

al., 2015). The exact reason for an increase in ROS in L-forms is unclear, but the current hypothesis is that disruption of PG synthesis in L-forms results in fluxes in the TCA cycle.

Remarkably, most if not all of the traditional cell division machinery or cytoskeleton is redundant in the L-form state (Leaver et al., 2009, Mercier et al., 2012). Instead of dividing by binary fission, L-forms reproduce through the release of irregularly sized progeny through membrane blebbing or tubulation. Reproduction by the generation of intracellular vesicles has also been reported (Briers et al., 2012). It was initially thought that like binary fission, a protein or proteins must be directing and coordinating the reproduction of L-forms. Surprisingly, this turns out not to be the case. Instead it appears that L-forms are able to reproduce as a function of excess membrane production. It has been demonstrated both *in vivo* and *in vitro* that the production of excess membrane results in an increase in the surface area relative to the cytoplasmic volume. This imbalance results in increased tortional stress on the cell, which is resolved through the spontaneous release of membrane. Some of the released membrane will trap sufficient quantity of the cellular material to grow and reproduce itself (Mercier et al., 2014, Hanczyc et al., 2003). This agrees with bottom-up approaches in which similar reproductive events are observed when the additional fatty acids are added to simple vesicles (Zhu and Szostak, 2009) or when the internal volume is reduced by evaporation (Budin et al., 2012). This is perhaps not the case for the reproduction via vesicle formation mentioned previously, though it is likely some form of membrane dynamics is involved. As a result of such a simplistic mechanism of division, relying on the biophysical properties of the membrane, it has been suggested that L-forms could represent a form of division that existed prior to the evolution of the peptidoglycan cell wall (Svetina, 2009, Errington, 2013).

It has been demonstrated in both the recent genetic studies as well as in the historical research that L-forms are able to revert back to the walled state when the ability to produce PG is restored (Onoda et al., 1987, Leaver et al., 2009), though the frequency of L-forms reverting back to the walled state is low (Dominguez-Cuevas et al., 2012). It had been thought that morphogenesis in bacteria required a pre-existing peptidoglycan template (Holtje, 1998). Use of the L-form system has demonstrated that L-forms are able to recover their cell shape when peptidoglycan synthesis is allowed to recommence

(Dominguez-Cuevas et al., 2012). It has also been shown that upon transition into the walled state reacquisition of the cell shape is rapid, indicating that the cell shape is programmed into the peptidoglycan synthesis machinery. In the same work it was demonstrated that the cytoskeletal protein is essential for restoring the rod shape in *E. coli* (Billings et al., 2014).
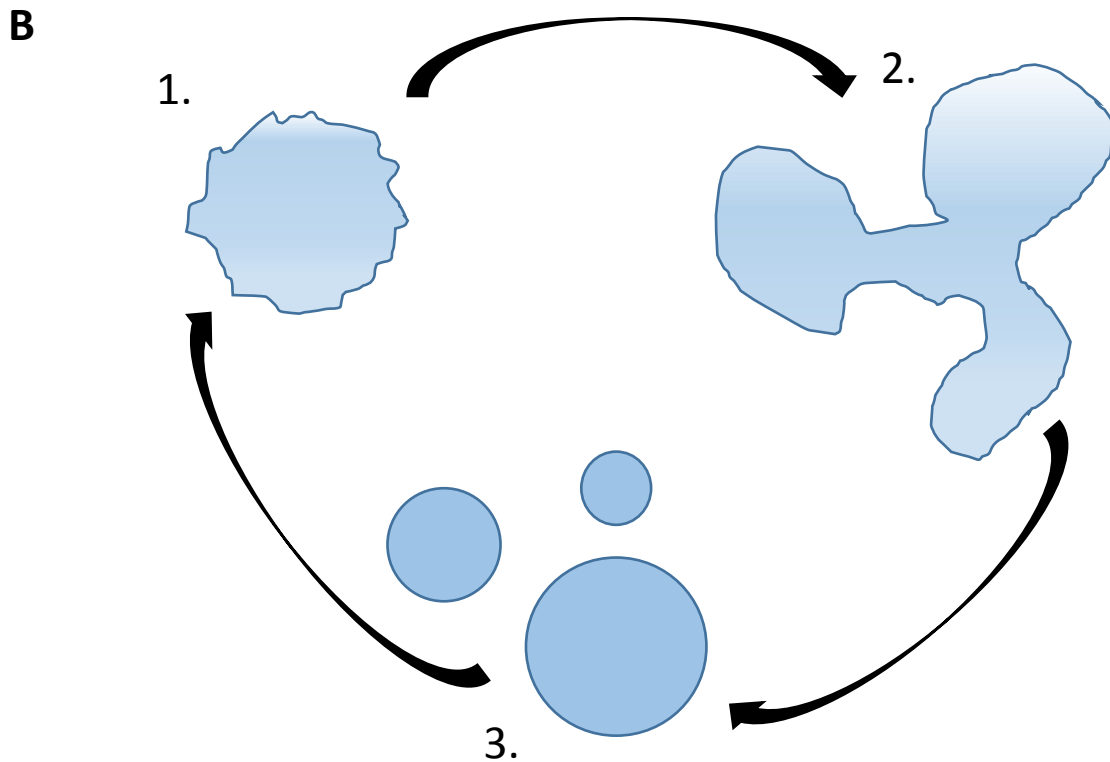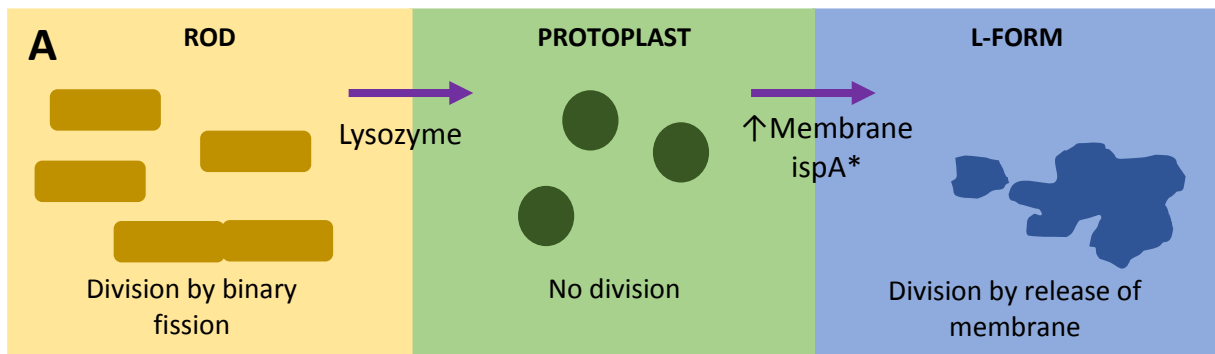
Figure 1.8. (A) Cartoon depicting the difference between bacterial growth as rods, protoplasts and L-forms. Purple arrows indicate the factors that permit the growth in each form. (B) Mechanism of L-form division as suggested by (Mercier et al., 2013). 1). L-form produces excess membrane leading to an imbalance in the surface area to membrane ratio. 2).The resulting torsional stress causes spontaneous shape deformations. 3). Deformities are resolved spontaneously by the release of excess membrane, resulting in the creation of daughter cells.

1.4.2   L-forms in disease

Despite the apparent fragility of L-form bacteria, they have been implicated in a host of various diseases. That L-forms could represent an infectious agent should not be that surprising. The cell envelope and in particular the cell wall represent the bulk of the pathogen-associated molecular patterns (PAMPs) recognised by the Toll-like receptors of the innate immune system (Murphy et al., 2008). Further, the peptidoglycan is the target for many of the most commonly used antibiotics and is a target for components of the host defences such as lysozyme. It can therefore be imagined that the L-form state represents a stress response to the adverse conditions encountered during infection. This is supported by the fact that L-form division is driven by the biophysical properties of the membrane as opposed to the division and cytoskeletal proteins that are apparently dispensable in this growth state. This renders the form of L-form division a highly redundant process.

Since their discovery in the 1930s, L-forms have been suspected in causing persistent bacterial infections and also as the aetiological agent in a number of chronic inflammatory diseases. However, the role of L-forms in disease is highly controversial. Much of the work is inconclusive at best, and highly dubious at worst. Much of the body of literature regarding L-form infections largely consists of case reports in which non-culturable, filterable bodies, presumed to be L-forms, were observed in various tissue biopsies or samples. These bodies are reported from a variety of body sites and a number of different diseases. These diseases range from common bacterial infections, through to multifactorial diseases such as multiple sclerosis and cancer (Domingue and Woody, 1997, Domingue, 2010). As stated previously, the work into L-form involvement in disease is generally circumstantial. It's debatable whether the bodies observed truly represent L-forms, and if they do, an actual involvement in the disease state is yet to be proven (Lantos et al., 2014).

1.4.3 L-form infection of plants

In addition to the speculation regarding L-forms with disease, L-forms have been found in association with plants. Unlike their relationship with mammals, it appears that the relationship between L-forms and plants is symbiotic in nature. *B. subtilis* has long been known to have a growth promoting effect on plants, with the inclusion of various strains in different commercially available biocontrol formulations (Nagorska et al., 2007, Lahlali et al., 2013). The primary appearance of *B. subtilis* in its relationship with plants is the formation of biofilms on the root system. It has been demonstrated that *B. subtilis* can be induced to grow in a biofilm by the release of L-malic acid and other exudates by plants (Chen et al., 2012). These biofilms are thought to be the main way *B. subtilis* is able to protect plants from pathogens (Morikawa, 2006), though the exact mechanism of protection is not known. The most likely explanation for protection is either by blocking the colonisation of the plant by the pathogen or by the release of antimicrobial compounds.

In addition to the formation of biofilms, *B. subtilis* as well as other species such as the plant pathogen *Pseudomonas syringae* have been shown to infect plants as L-forms. Such infection have been reported in strawberry plants (Ferguson et al., 2000), Chinese cabbage (Walker et al., 2002), radishes, soybeans (Aloysius and Paton, 1984) and French dwarf beans (Paton and Innes, 1991). The level of infection appears to remain minimal, with the growth of the plant remaining unaffected. L-form distribution throughout the plant is apparently not uniform, with the L-forms favouring cells that have few chloroplasts present. Within the plants, L-forms apparently remain biologically active, with bacterial products able to be detected in the plant (Ferguson et al., 2000, Aloysius and Paton, 1984). When treated with non-pathogenic bacteria such as *B. subtilis*, only the cells in the L-form state are able to successfully infect the plant. Treatment of the plants with either L-forms derived from plant pathogens or non-pathogenic organisms fail to elicit a hypersensitive reaction in the host plant. L-form infection appears to protect the plant from infection from both the walled version of the bacteria, but also from infection by other pathogens such as the fungal cause of grey mould; *Botrysis cinera* (Walker et al., 2002, Waterhouse et al., 1996). This phenomena remains

unexplained, with no clear mechanism through which the L-forms would be able to protect the plant.

How L-forms are able to penetrate the outer leaflet of plant cells remains entirely unknown. In addition, how L-forms arise in these plants naturally is unknown – what environmental triggers exist to stimulate L-form generation and how these L-forms survive long enough in the soil to be taken up by the plants. Interestingly, it has been reported previously in *E. coli* that many of the genes expressed in unstable L-forms are typical of genes expressed when grown as part of a biofilm (Glover et al., 2009). This perhaps indicates that L-forms could develop spontaneously as a function of the biofilm lifestyle, though this is mere speculation.

1.4.4   L-forms and osmolarity

Taken together, it suggests that L-forms may be more robust than what would be expected from the laboratory observations. The appearance of L-forms in a variety of natural conditions indicates that the L-forms are more tolerant to low osmolarities than one would expect. This is because the high levels of osmoprotectant used in the laboratory to maintain L-forms are generally unachievable in the environment. It would be expected in these conditions that the influx of water into the L-form cells would result in uncontrolled swelling and lysis as the L-form cell is unable to withstand turgor. Therefore, it can be assumed that L-forms will never be in 'hypotonic' or 'hypertonic' conditions, but will always be isotonic conditions due to this inability to withstand turgor. This raises issues regarding the regulation of the internal contents of the L-form cell, as discussed earlier all cells maintain a pool of K^+. The K^+ ions are involved in cellular processes, but also contribute to the cell turgor. When walled cells encounter hypotonic conditions they must release some of the internal osmolytes to withstand the effects of the water entering the cell. However, the cells must retain some of their osmolytes, K^+ included, for cellular functions to continue. The presence of the peptidoglycan helps the cells to maintain a degree of turgor under these conditions.

L-forms do not have this luxury, instead to survive in such conditions, presumably cells must either reduce their internal osmotic pressure, or the membrane integrity must be maintained, preventing the expected lysis. Remarkably, a number of papers have suggested that L-forms derived from a range of species can be adapted to grow in low osmolarities. It should be noted that the ability to survive and grow varied depending on the species and the osmoprotectant used. The definition of hypotonicity varied in the different reports as well (Dienes and Sharp, 1956). In the adapted L-forms changes in the ratio of saturated to unsaturated fatty acids in the membrane was observed, as was changes in the cytoplasmic ion content and the protein profiles of the strains (Leon and Panos, 1976, Montgomerie et al., 1972, Montgomerie et al., 1973).

Unfortunately, the work into the ability of L-forms to survive in low osmolarities were performed at a time where the suite of genetic tools we now enjoy were unavailable. In addition, the L-forms utilised in the work were not characterised to the same level as today; it is unclear whether the L-forms were 'true' L-forms or whether some residual

PG was present in the cells (Gilpin and Patterson, 1976). Regardless of these limitations, they demonstrate several interesting mechanisms through which L-forms of various species could adapt to survive and propagate in hypotonic conditions. It should be noted however that the changes reported in the L-forms could be either a cause or an effect of their growth in a medium with lower osmolarity. A role for the fluidity of the membrane is probably more as the cause of survival due to the observation that addition of the polyamine spermine enables protoplasts to withstand turgor (Harold, 1964, Mager, 1959). The authors assert this is a result of spermine binding to the lipid head groups of the cell membrane, as the spermine could be displaced, and osmotic fragility restored by addition of salts and cations. However, spermine possesses a number of alternative roles, including in transcription and stress responses (Yoshida et al., 2004, Rhee et al., 2007). It is possible that the changes in the cytoplasmic ion content (along with the protein profile) could represent the modulation of the levels of compatible solutes, though again this remains a speculation.

1.5 Exploitation of Actinobacteria for antibiotic discovery

1.5.1 Actinobacteria diversity

Actinobacteria are some of the most diverse and complex bacteria on the planet. They are Gram positive microorganisms that can be found in almost all marine and terrestrial environments, including from those that are uniquely hostile to life, such as the Atacama Desert in Chile (Okoro et al., 2009). As a result of habitation in these niches, the Actinobacteria encounter ever changing environments and nutrient scarcity. The first examples of Actinobacteria had a fungus-like growth, with branching filaments. It is to this morphology the genus owes its name. Despite this, the Actinobacteria are now known to encompass a broad range of different morphologies. At the simplest the phylum contains genera such as the *Corynebacterium* which exist as unicellular rods. Other genera like the *Mycobacterium* have greater complexity; growing as filamentous cells. Generally, the most complex of the Actinobacteria are the *Streptomyces.* These form mycelium composed of extensively branching, filamentous hyphae that reproduce through the production of aerial branches that develop into spores. Many of the species in the phylum are pathogenic, though for the majority of the members this is not the case; the *Streptomyces* are largely non-pathogenic, existing as decomposers in the soil or the water where they contribute to the 'earthy' smell of soil due to the production of metabolites called geosmins. The geosmins are one example of the complex secondary metabolism present in the Actinobacteria that results in a vast wealth of natural products (Madigan et al., 2009).

1.5.2 Secondary metabolism in Actinobacteria

One of the reasons that *Streptomyces* as well as other Actinobacteria are so widespread is as a result of their complex secondary metabolism. The exact role of many of the secondary metabolites is unclear. The function of some of the metabolites such as the pigments and geosmins remain a complete mystery (Davis and Chater, 1990, Gust et al., 2003), though an actual function is almost certain. Other metabolites are far clearer in their function. For example, siderophores are produced by many *Streptomyces* strains as a means to scavenge iron from their environment (Challis and Ravel, 2000, Neilands, 1995). In addition to these secondary metabolites Actinobacteria are a major source of naturally derived medicines, including antibiotics, antifungals, antiparasitics and

antineoplastic drugs. It is presumed that the production of these compounds enables the bacteria to outcompete its neighbours in the environmental niches they occupy (Laskaris et al., 2010). This is supported by the observation that expression of the gene involved in synthesis of these compounds is frequently linked to phosphate or glucose exhaustion. However, it has been argued that the natural compounds could have an alternative function such as a signalling molecule (Kitani et al., 2011).

The genes responsible for secondary metabolism are grouped in the genome into individual biosynthetic clusters. These clusters can be thought of as modular assemblies, with a simple building block type of relationship between the genes and the chemical structure of the secondary metabolite. The biosynthetic clusters can be split into three types of modules; those containing polyketide synthases (PKS); those containing non-ribosomal peptide synthases (NRPS); or those containing both PKS and NRPS (Cane et al., 1998). These modules are in turn split into domains based on activities. For instance, all PKS modules will include a keto synthase, an acyl-transferase and an acyl carrier protein, but can include a ketoreductase, a dehydratase and so on. The differences in the number of modules as well as their specificities enables the *Streptomyces* to produce a huge range of secondary metabolites (Diminic et al., 2014). There are currently two models for how the complexity of the PKS modules evolved (NRPS diversity has been less studied and therefore less well understood). The first proposed model is the amplification model, in which a module become amplified over time, with recombination events and random mutations leading to development of diversity (Jenke-Kodama et al., 2006). The other model is that diversity arises due to single crossover recombination events that results in the exchange of domains (Zucko et al., 2012). The ability to recombine between different modules and different biosynthetic clusters has facilitated the horizontal gene transfer of the most advantageous secondary metabolites. Hence why the same classes of antibiotics reappear again and again in different species of *Streptomyces*.

1.5.3 Antibiotic discovery

As touched upon, the secondary metabolism of Actinobacteria and in particular *Streptomyces* has proved to be an incredibly bountiful source for the discovery of a number of antibiotics. The history of antibiotic discovery from Actinobacteria began in 1943 with the isolation of Streptomycin from *Streptomyces griseus* by Waksman and Schatz (Waksman and Schatz, 1943). Following this landmark work, many of the most familiar antibiotics in the therapeutic arsenal were isolated from the Actinobacteria. This list of antibiotics includes but is not limited to vancomycin, tetracycline, chloramphenicol and daptomycin. The discovery of these important antibiotics occurred between the 1950s and the 1980s. During the 1990s the search for natural products dried up. The decline in research occurred for a number of reasons. Firstly, there was a problem with rediscovery of already known compounds; those antibiotics that were readily discovered in the past now proved to be hindrances, acting now as background noise. Secondly, discovery of new antibiotics became less and less lucrative; natural product screening is very costly as thousands of strains need to be grown and screened to elicit a single novel compound (Baltz, 2008). In addition, bacterial infections became a disease of the developing world, resulting in a minimal return on the money invested in research and development. Finally, there was a shift in focus towards more modern drug discovery methods such as *in silico* screening and the use of combinatorial chemistry. Unfortunately, these modern techniques have largely failed to generate new antibiotics. One of the best described abortive efforts to use the combinatorial chemistry approach was that carried out by GlaxoSmithKline (Payne et al., 2007). There are several reasons for the failure; the chemical libraries lack the complexity seen from natural products; most of the targets that are essential for bacterial survival are not easily druggable; the best antibiotic targets such as the growing peptidoglycan or the ribosomes are difficult to screen against *in vitro*.

The lack of new antibiotics has been coupled with an explosion in the cases of antibiotic resistance. We now face growing resistance from both Gram positive and Gram negative pathogens in both community and hospital based infections. Of particular concern are the 'ESKAPE' pathogens: *Enterococcus faecium, Staphylococcus aureus, Klebsiella pneumoniae, Acinetobacter baumanii* and *Pseudomonas aeruginosa*. These species

cause the bulk of infections in the USA, but frequently possess resistance to the frontline drugs, and are thus able to 'escape' the effect of the antibiotics. Many of these species are becoming pan-resistant either through the adoption of multiple drug resistant cassettes (as is the case with MRSA) or through intrinsic resistance resulting from the modulation of the envelope permeability (as is the case with *Acinetobacter baumanii*) (Boucher et al., 2009). Increasing levels of resistance result in therapeutic failures, with rises in mortality and morbidity. To tackle this issue we urgently require new antibiotic therapies against these microorganisms.

However, several advances have started somewhat of a gold rush for natural product discovery. The greatest impact has been in the spread of high-throughput sequencing. This sequencing was originally used to screen pathogens for potential drug targets; sequencing can instead be used to discover novel biosynthetic clusters in Actinobacteria. *Streptomyces coelicolor* was the first antibiotic-producing *actinomycetes* species sequenced (Saitou and Nei, 1987). Within the genome of *S. coelicolor* a significant number of biosynthetic clusters identified. Similarly, sequencing of *Steptomyces avermitilis* revealed the presence of 25 putative biosynthetic clusters composed of over 300 genes. In total, it appeared 6.6% of the genome of *S. avermitilis* was involved in the synthesis of secondary metabolites (Ikeda et al., 2003). The number of biosynthetic clusters in these two species is not unique, with many *Streptomyces* species carrying multiple clusters (Gomez-Escribano et al., 2015, Iftime et al., 2015, Komaki et al., 2015). The problem is that very few of the predicted secondary metabolites are observed when the strains are grown in the standard media. It is therefore of great interest to be able to identify and characterise the unknown compounds. There are three main routes by which novel compounds may be investigated. The first approach is the simplest – growing the strains on alternative media as a means to express the secondary metabolites in the original species. The second approach is to clone the biosynthetic gene clusters into cosmid or bacterial artificial chromosome vectors before transformation into alternative host strains. These strains are typically those that are well characterised, are fast growing, genetically tractable or are able to produce a particular class of secondary metabolite readily. An additional benefit of this route is that the compound of interest can be more readily identified when it is being produced

against a background of known compounds (Penn et al., 2006). An example of this method is the cloning of a 53kb biosynthetic cluster from a marine *Micromonospora* strain into *Streptomyces albus* and *Streptomyces lividans*. Expression of the cluster in these hosts resulted in the production of a compound with anti-tumour properties (Lombo et al., 2006). Thirdly, identification of the biosynthetic clusters enables the ability to make structural predictions of the secondary metabolite. Such a method accelerates chemical dereplication and improves the identification of the compound in the milieu of secondary metabolites. This approach was validated in 2000, when the structure of the siderophore coelichelin was predicted in the *S. coelicolor* genome and subsequently identified *in vitro* (Challis and Ravel, 2000).

In addition to using novel techniques to search known strains for new antibiotics, it is possible to search for new strains of actinobacteria. The pharmaceutical industry has screened soil samples for 50 years, but this represents only a small fraction of the diversity of the actinobacteria. Ongoing work is exploring the levels of actinobacteria diversity around the globe; from regions as high as the Tibetan plateau to as deep as the Mariana trench (Zhang et al., 2010, Pathom-Aree et al., 2006). Exploration of novel environments such as the marine sediments has already paid off; the antibiotic abyssomicin was isolated from a novel species of *Verrucosispora* that originated from the Sea of Japan (Bister et al., 2004).

1.5.4 Lipoteichoic acid synthase as an antibiotic target

With ever increasing levels of resistance there is a pressing need for new antibiotics with activities against novel targets. Most of the pre-existing antibiotic targets concern aspects of the peptidoglycan cell wall. This is largely because the cell wall fulfils all the criteria that make an optimal antibiotic target (Projan and Shlaes, 2004). Firstly, under most conditions the cell wall is essential for the growth and survival of the bacterial cell. In addition, this essentiality means that many of synthetic enzymes required for synthesis are conserved across the prokaryotic kingdom, resulting in broad spectrum activity to antibiotics. Secondly, the cell wall is unique to bacteria – homologues are not present in humans. This reduces the level of toxicity and side effects of the antibiotics. Finally, the cell wall is easily accessible, lying on the exterior of the cell. This contrasts with alternative antibiotic targets such as transcription and translation lie within the cell.

Cells can alter the envelope permeability, or increase expression of exporters, resulting in non-specific resistance to some of these compounds.

Lipoteichoic synthase fulfils many, though not all of the criteria listed. As discussed earlier, LTA is essential for the growth of many important Gram positive pathogens, including *S. aureus*. However, it is not present in Gram negative organisms and is non-essential in other Gram positive species. In species or conditions where LTA is dispensable, antibiotics targeting the synthesis may be useful anti-virulence agents (Weidenmaier et al., 2004, Collins et al., 2002). Further, disruption of LTA and the related WTA has been demonstrated to affect the efficacy of other antibiotics, probably through the change in the electrochemistry of the cell envelope. Similarly, disruption of WTA in MRSA has been shown to sensitise the bacteria to β-lactams (Farha et al., 2013). The resistance in MRSA is conferred by acquisition of a gene coding for a resistant copy of the PG transpeptidase PBP2A. The function of this protein depends on the numerous factors including WTA. It is thought that loss of WTA disrupts the cooperative effects of the numerous factors, which include additional PBPs (Sewell and Brown, 2014). Taken together; a compound targeting LtaS may also be useful in a combination treatment with conventional antibiotics in treating many Gram positive infections. Whilst not present in all bacteria, LTA is unique to bacteria. This addresses the problem of potential antibiotic toxicity in the eukaryotic hosts.

In regards to the final criteria – the target accessibility – the LTA is positioned in the cell envelope, tethered to the lipid head groups of the cell membrane. Importantly, the synthase is embedded within the membrane, with an extracellular catalytic group. This renders the catalytic group highly accessible to any potential compounds.

Despite the potential for antibiotic development, the majority of discovered compounds that act against teichoic acid synthesis target components of the WTA pathway (Swoboda et al., 2009, Lee et al., 2010, Hancock et al., 1976, Farha et al., 2014). Only a single compound, a small molecule called 1771, is believed to possess an inhibitory effect against LtaS in *S. aureus*. No spontaneous mutations were identified in the work and were therefore unable to definitively confirm a mechanism of action. However, production of LTA was reduced in a heterologous expression system when treated with the compound (Richter et al., 2013).

Aims

Previous work has demonstrated that L-forms are able to persist and grow in conditions that would be expected to be lethal for the cells (Domingue and Woody, 1997, Amijee et al., 1992, Gilpin and Patterson, 1976). The principal aims for this part of the project are two-fold. First, to develop a reproducible method for the adaptation of L-forms to low osmolarities. Second, to identify and characterise any mutations that enable L-forms to survive in these challenging situations. This work hopes to address some fundamental questions regarding the molecular biology of L-forms, as well as the maintenance and regulation of the cell membrane and cytoplasm. It is hoped that this work will inform our understanding of osmotic regulation and support the development of models to explore the role of L-forms in the natural environment.

The second part of this work will utilise a novel screening method (Errington J, 2009) to identify inhibitors of the attractive antibiotic target, LtaS, from a unique collection of actinomycetes. The primary aim of this project is to identify and characterise a potential inhibitor using the screening method and to demonstrate its effect on LtaS in *B. subtilis* and *S. aureus*.

2. Materials and methods

2.1 Solutions and media

Tables of solutions and media are given in appendices 1 and 2.

2.2 Strains and plasmids

Strains and plasmids used in this work are given in tables 2.1 and 2.2 respectively.

Table 2.1.

Name	Genotype	Source
Bacillus subtilis		
168CA	*trpC2*	(Kunst et al., 1997)
Marburg NCIB 3610		Laboratory strain
JB57	*trpC2 ltaS::spc*	(Schirner et al., 2009) into 168CA
JB24	*trpC2 yfnI::cat*	(Schirner et al., 2009) into 168CA
JB25	*trpC2 yqgS::spc*	(Schirner et al., 2009) into 168CA
JB26	*trpC2 yvgJ::erm*	(Schirner et al., 2009) into 168CA
JB84	*trpC2 mbl::cat*	(Schirner et al., 2009)
LR2	*ispA* ΩspoVD::cat* P_{xyl}-*murE*	(Leaver et al., 2009)
LR2-M	*Tn ispA Pspac-hepT ΩspoVD::cat* P_{xyl}-*murE*	(Leaver et al., 2009) into Marburg background
YK1694	*ispA* amyE::*P_{xyl}-*accDA*	(Mercier et al., 2013)
JB104	*ispA* ΩspoVD::cat* P_{xyl}-*murE amyE::PrpsD-gfp spc*	(Syvertsson, unpublished) into LR2
JB105	*ispA* ΩspoVD::cat* P_{xyl}-*murE amyE::PrpsD-mCherry spc*	(Syvertsson, unpublished) into LR2
M1	*ispA* ΩspoVD::cat* P_{xyl}-*murE amyE::PrpsD-mCherry spc* *yhaG⁻ yhaH⁻ scoC⁻ yhaI⁻ yhaJ⁻*	This work

JB112	ispA* ΩspoVD::cat P_{xyl}-murE yhaG::erm	NBRP (NIG,Japan): B. subtilis into LR2
JB113	ispA* ΩspoVD::cat P_{xyl}-murE yhaI::erm	NBRP (NIG,Japan): B. subtilis into LR2
JB132	ispA* ΩspoVD::cat P_{xyl}-murE scoC::zeo	This work
JB155	ispA* ΩspoVD::cat P_{xyl}-murE aprE::scoC spc	This work
JB156	ispA* ΩspoVD::cat P_{xyl}-murE amyE::PrpsD-mCherry spc yhaG$^-$ yhaH$^-$ scoC$^-$ yhaI$^-$ yhaJ$^-$aprE::scoC spc	This work
JB114	ispA* ΩspoVD::cat P_{xyl}-murE mreB$^-$pit$^-$ftsE$^-$	This work
JB115	ispA* ΩspoVD::cat P_{xyl}-murE mreB$^-$rpoB$^-$	This work
JB116	ispA* ΩspoVD::cat P_{xyl}-murE ydbL$^-$	This work
JB117	ispA* ΩspoVD::cat P_{xyl}-murE hom$^-$SPβ^-	This work
JB118	ispA* ΩspoVD::cat P_{xyl}-murE	This work
JB119	ispA* ΩspoVD::cat P_{xyl}-murE gbsB$^-$	This work
JB120	ispA* ΩspoVD::cat P_{xyl}-murE	This work
JB121	ispA* ΩspoVD::cat P_{xyl}-murE nusG$^-$ppsB$^-$	This work
JB122	ispA* ΩspoVD::cat P_{xyl}-murE ypzK$^-$	This work
JB125	ispA* ΩspoVD::cat P_{xyl}-murE	This work
JB126	ispA* ΩspoVD::cat P_{xyl}-murE	This work
3725	Ωneo3427 ΔmreB	(Formstone and Errington, 2005)
JB133	ispA* ΩspoVD::cat P_{xyl}-murE Ωneo3427 ΔmreB	3725 into LR2
JB134	JB114 ispA* ΩspoVD::cat P_{xyl}-murE Ωneo3427 ΔmreB	3725 into JB114
JB135	JB115 ispA* ΩspoVD::cat P_{xyl}-murE Ωneo3427 ΔmreB	3725 into JB115
JB139	168CA gbsB::erm	This work
JB140	LR2 gbsB::erm	This work

JB155	*ispA* ΩspoVD::cat* P$_{xyl}$-*murE aprE::scoC spc*	This work, pJB2 transformed into LR2
JB156	M1 *aprE::scoC spc*	This work, pJB2 transformed into M1
JB158	*ispA* ΩspoVD::cat* P$_{xyl}$-*murE Ωneo3427 mreB^{Δ20}*	This work
PG67	*aprE::P$_{spac}$-yfp-zapA-spc*	(Richter et al., 2013)
JB162	*ispA* ΩspoVD::cat* P$_{xyl}$-*murE aprE::P$_{spac}$-yfp-zapA-spc*	PG67 into LR2
JB163	JB114 *aprE::pspac-yfp-zapA-spc*	PG67 into JB114
JB164	JB115 *aprE::pspac-yfp-zapA-spc*	PG67 into JB115
JB175	*ispA* p$_{xyl}$-murE-spc Ωneo3427 ΔmreB aprE::p$_{spac}$-gfp-mreB-cat*	(Weigel et al., 2003); pAPMreB1 into LR2
JB176	*ispA* p$_{xyl}$-murE-spc Ωneo3427 ΔmreB aprE::p$_{spac}$-gfp-mreB^{Δ20}-cat*	This work
RM119	168CA *ΔmurC::spc pLOSS-P$_{spac}$-murC erm*	(Mercier et al., 2013)
JB180	*ispA* ΩspoVD::cat* P$_{xyl}$-*murE murC::spc pLOSS murC-erm*	RM119 into LR2
JB181	*ispA* ΩspoVD::cat* P$_{xyl}$-*murE murC::spc pLOSS murC-erm Ωneo3427 ΔmreB*	RM119 into JB133
JB182	JB115 *ispA* ΩspoVD::cat* P$_{xyl}$-*murE murC::spc pLOSS murC-erm*	RM119 into JB115
JB189	JB114 *ispA* ΩspoVD::cat* P$_{xyl}$-*murE murC::spc pLOSS murC-erm*	RM119 into JB114
PDC594	168CA *ftsE::neo*	(Dominguez-Cuevas et al., 2013)
JB-PDC594	168CA *ftsE::(neo::spc)*	PDC594 transformed with pKV71
JB183	*ispA* ΩspoVD::cat* P$_{xyl}$-*murE ftsE::(neo::spc)*	LR2 transformed with JB-PDC594

JB184	*ispA* ΩspoVD::cat* P_{xyl}-*murE Ωneo3427 ΔmreB ftsE::(neo::spc)*	JB133 transformed with JB-PDC594
2566	168ED *amyE::P_{xyl}-gfp-mreB-spc*	(Challis, 2014)
JB185	*trpC2 amyE::P_{xyl}-gfp-mreB-spc*	2566 into 168CA
JB186	*trpC2 amyE::P_{xyl}-gfp-mreB^{Δ20}-spc*	This work
JB187	*trpC2 Ωneo3427 ΔmreB amyE::P_{xyl}-gfp-mreB-spc*	2566 into 3725
JB188	*trpC2 Ωneo3427 ΔmreB amyE::P_{xyl}-gfp-mreB^{Δ20}-spc*	JB186 into 3725
Escherichia coli		
DH5α	F⁻ψ80*lacZ*ΔM15 Δ(*lacZYA-argF*) U169 *recA1 endA1 hsdR17* (r_k-,m_k+) *gal⁻ phoA supE44* λ⁻ thi⁻1 *gyrA96 relA1*	Invitrogen
Staphylococcus aureus		
RN4220	Δ*rbsU* Δ*tcaR* Δφ11 Δφ12 Δφ13 r⁻m⁻	(de Azavedo et al., 1985)
Actinomycetes spp.		
DEM30616		This work
DEM30345		This work
DEM20435		This work
DEM30618		This work
DEM20657		This work

Table 2.2

Name	Genotype	Construction	Reference
pAPMreB1	P_{spac}-mgfp-mreB cat bla		(Jahn et al., 2015)
pAPNC213	spc bla		(Morimoto et al., 2002)
pBEST501	bla neo		(Itaya et al., 1989)
pHM457	bla cat zeo		(Lautru et al., 2005)
pJB1	scoC::zeo	(oJB33/oJB34) and (oJB35/oJB36) ligated into pHM457	This work
pJB2	aprE::scoC spc	(oJB77/oJB78) ligated into pAPNC213	This work
pJB3	aprE::p_{spac}-gfp-mreB$^{\Delta20}$ cat	(oJB84/oJB85) amplification of pAPMreB1	This work
pJB4	P_{xyl}-gfp-mreB$^{\Delta20}$ bla spc	(oJB84/oJB85) amplification of pSG1729	This work
pMUTIN4	erm		(Vagner et al., 1998)
pSG5451	P_{xyl}-gfp-mreB bla spc		(Formstone and Errington, 2005)
pVK71	neo::spc replacement		(Arbeit et al., 2004)

2.3 Oligonucleotides

The oligonucleotides used in this work are given in appendix 3.

2.4 Media supplements

The media supplements and their respective concentrations are given in table 2.3

Antibiotics	Stock solution	Final concentration
Ampicillin	50 mg/ml	100 µg/ml
Chloramphenicol	10 mg/ml	5 µg/ml
Erythromycin	20 mg/ml	0.5 µg/ml
Kanamycin	25 mg/ml	2 µg/ml
Phleomycin	2 mg/ml	1 µg/ml
Spectinomycin	100 mg/ml	50 µg/ml
Tetracycline	10 mg/ml	10 µg/ml
Zeomycin	100 mg/ml	10 µg/ml
Inducers		
IPTG	1 M	up to 3 mM
Xylose	25%	up to 0.1%

2.5 Experimental methods

2.5.1 DNA methods

2.5.1.1 Oligonucleotides

Oligonucleotides were purchased from Eurogentec. Aliquots were stored at -20°C at a concentration of 10 µM.

2.5.1.2 Polymerase chain reaction (PCR)

PCR reactions were carried out according to the manufacturers' recommendations. GoTaq polymerase (Promega) was used to confirm insertions or deletions. Q5 (NEB) polymerase was used for creating genetic constructs.

2.5.1.3 Purification of PCR products

PCR products were purified using QIAquick PCR purification kit (Qiagen) according to the manufacturer's recommendations

2.5.1.4 Purification of plasmids

Plasmids were purified using QIA miniprep kit (Qiagen) according to the manufacturer's recommendation.

2.5.1.5 Agarose gel electrophoresis of DNA fragments

Agarose gel electrophoresis of DNA fragments was performed on 0.8-1.2% agarose gels containing 0.1 mg/ml ethidium bromide in 1x TAE buffer. Prior to loading samples were mixed with loading dye. The voltage used for electrophoresis was 90-120 V. Bands were visualised using a G-box transilluminator (Syngene) with built in camera.

2.5.1.6 Restriction endonuclease digests

Digests were carried out following the manufacturers' recommendations. Digests were carried out for 1-3 hrs in the appropriate buffer and temperature. The restriction enzymes were removed using a QIAquick PCR purification kit (Qiagen).

2.5.1.7 Ligation of DNA fragments

Ligation of DNA fragments was catalysed by T4 ligase (Roche) in the supplied buffer. The reaction volume was typically 10-20 µl and was incubated for 1-2 hr at room temperature.

2.5.1.8 In-Fusion cloning

Construction of some plasmids was facilitated by In-Fusion cloning. DNA fragments were fused using In-Fusion HD cloning kit (Clontech), according to the manufacturer's recommendations.

2.5.1.9 DNA sequencing

PCR products or plasmids were sent to the sequencing service of Dundee University for sequencing.

2.5.1.10   Full genome sequencing

Bacterial genomes for full genome sequencing were sent to GATC Biotech ltd or given to the Wipat research group for sequencing on their MiSeq platform.

2.5.1.11   Analysis of full genome sequencing

Genome sequencing data was analysed using the commercial software CLC genomics workbench (Qiagen). The sequence data was imported and mapped to the appropriate reference genome.

2.5.2 Protein methods

2.5.2.1 Preparation of protein samples

Cultures were grown in 5 ml PAB or LB media. Protein overexpression was induced using 1 mM IPTG or 0.5% xylose where appropriate. Cells were grown to an OD_{600}=0.6 at 37°C before harvesting by centrifugation. Cells were resuspended in 200 µl 50 mM Tris HCl pH 7.3 containing protease inhibitor (Roche). The samples were either held on ice and the cells broken by sonication (30 seconds, amplitude 40) or lysed using 10 µl 10 mg/ml lysozyme and 5 µl DNase. The soluble fraction was separated from the insoluble fraction by centrifugation at 13,000 rpm for 15 minutes.

2.5.2.2 SDS-polyacrylamide gel electrophoresis

 Samples were prepared by mixing with NuPAGE LDS sample buffer (Invitrogen) and NuPAGE reducing agent (Invitrogen). Samples were heated at 85°C for 10 minutes then loaded on Novex midi gels 4-12% Bis-Tris (Invitrogen). The electrophoresis was performed in 1x MOPS buffer (Invitrogen) at 200V.

2.5.2.3 Coomassie Staining

For Coomassie staining, gels were washed briefly with dH_2O and then stained by the addition of 10 ml Coomassie stain. Gels were incubated with the stain overnight. Destain of the background was achieved by incubating the gel at room temperature in destain solution (10% methanol, 10% propan-2-ol, 10% acetic acid, 5% glycerol).

2.5.2.4 Western Blotting

Following electrophoresis, the gel was soaked in transfer buffer. The transfer onto nitrocellulose membrane (GE Healthcare) was performed using a Hoeffer Scientific semi-dry transfer cassette according to the manufacturer's instruction at 0.8 mA/cm² for 1 hr. Following the transfer the nitrocellulose membrane was incubated with shaking in blocking solution (PBS + 0.1 Tween20 + 5% milk powder) overnight at room temperature. The next day the membrane was washed briefly in PBS + 0.1% Tween20 (PBST) then incubated for 1 hr with shaking in blocking solution containing the primary antibody diluted to an appropriate concentration. After incubation the membrane was washed 3 times for 10 min in PBST then incubated for 1 hr in blocking solution containing the secondary antibody diluted to an appropriate concentration. The

membrane was then washed 3 times for 10 min in PBST. The ECL+ kit (GE Healthcare) was used, following the manufacturer's recommendations to visualise the protein bands of interest.

2.5.3   Manipulations in *Escherichia coli*

2.5.3.1 Preparation of competent cells

E.coli DH5α competent cells were prepared using the RbCl method. Here, cells were grown to an OD_{600} of 0.3-0.4 in 2TY medium, then chilled on ice for 10 minutes. After chilling, cells were pelleted and then resuspended in 0.3 (v/v) RF1. The mixture was incubated on ice for 15 minutes, then pelleted and resuspended in 0.1 (v/v) RF2. Aliquots of the competent cells were frozen rapidly in liquid nitrogen and stored at -80°C for future use.

2.5.3.2 Transformation of competent *E.coli* cells

Aliquots of competent cells were removed from -80°C and thawed on ice. After thawing, 100 µl of competent cells were added to plasmid or ligation reaction mixture. The cells were incubation on ice for 30 minutes and then heat shocked at 42°C for 90 seconds after which the cells were returned to ice for 1 minute. 200 µl of LB medium was added, and the cells were incubated at 37°C for 1 hour. After incubation the cells were plated on agar containing the appropriate antibiotics.

2.5.3.3 *E.coli* colony PCR

To screen *E.coli* transformations for correct clones, colonies were picked and resuspended in 50 µl dH_2O and incubated at 100°C for 10 minutes. After cooling to room temperature, 10 µl of the cell suspension was used in a standard PCR reaction employing the GoTaq polymerase.

2.5.4   *Bacillus subtilis* methods

2.5.4.1 Preparation of competent *B. subtilis* cells

To make *B. subtilis* competent for transformation, a 5ml culture was grown in minimal media overnight. The next day 300 µl of the culture was used to inoculate 5 ml fresh minimal media and was incubated with shaking at 37°C for 3 hours. At this point, 5 ml starvation medium was added and the culture incubated for a further 2 hours at 37°C. 400 µl of the now competent cells were used immediately for transformation.

2.5.4.2 Transformation of competent *B. subtilis*

400 µl of competent cells were mixed with 5 µl plasmid/ligation product or 10 µl genomic DNA. The mixtures were incubated at 37°C for 1 hour before plating agar containing the appropriate antibiotics.

2.5.4.3 Preparation of genomic DNA for transformation

Genomic DNA for transformation was prepared as described by (Ward and Zahler, 1973). In brief, the strain of interest was streaked onto a nutrient agar plate and grown at 37°C overnight. The next day, a small scoop from the plate was suspended in 4 ml PAB and incubated with shaking at 37°C for 4 hours. The culture was then pelleted, resuspended in 1 ml SSC. 10 µl lysozyme solution (10 mg/ml) was added and the solution incubated at 37°C for 20 minutes. 1 ml 4 M NaCl was then added and the mixture filtered (0.45 µm pore size).

2.5.4.4 Preparation of genomic DNA for PCR

To prepare genomic DNA for use in PCR, cells were grown overnight at 37°C in LB. The next day 2 ml of overnight culture was pelleted and resuspended in 100 µl 50 mM EDTA solution containing 10 µl lysozyme solution (10 mg/ml) and 5 µl RNase (10 mg/ml). The suspension was incubated at 37°C for 1 hour then 500µl nuclei lysis solution (Promega) was added and the mixture incubated for 5 minutes at 80°C. The mixture was allowed to cool down to room temperature, then 200 µl protein precipitation solution (Promega) was added and the mixture vortexed vigorously for 20 seconds. They were incubated on ice for 10 mins before centrifugation at 13,000 rpm for 10 mins. The resulting supernatant was carefully decanted into a fresh Eppendorf tube containing 600 µl isopropanol. The tube was gently inverted until the DNA formed a visible precipitate. The DNA was pelleted by centrifugation at 13,000 rpm for 10 minutes and the supernatant removed. The pelleted was washed with 600 µl 70% ethanol before being centrifuged for a further 5 mins at 13,000 rpm. The DNA was air dried, then resuspended in 100 µl H_2O and incubated at 65°C for 15 minutes or at 4°C overnight. Typically, for PCR 2-5 µl of template was used.

2.5.4.5 Preparation of genomic DNA for whole genome sequencing

To prepare DNA for whole genome sequencing, cells were grown in 10 ml PAB until OD_{600}=3.0 at which point the cells were harvested and washed with 10 ml TES. The cell

pellet was resuspended in 0.5 ml TES before being stored overnight at -20°C. The next day the cells were removed from the freezer and placed at room temperature. Once defrosted 25 µl lysozyme (10 mg/ml) and 5 µl RNase (10 mg/ml) were added and the mixture at 37°C for 30 mins. At this point 50 µl pronase and 30 µl sarkosyl was added, with the mixture incubated for a further 30 mins at 37°C. Following this treatment 600 µl phenol-chloroform was added and the components mixed by shaking. The tubes were then centrifuged at 10,000 rpm for 10 minutes to separate the phases. The upper aqueous phase was aspirated off into a clean Eppendorf tube. The process of adding phenol-chloroform was repeating 3 times. In the final repetition, the phenol-chloroform is replaced with just chloroform. After the final cleaning step 3 volumes of 100% ethanol was added to 1 volume of the aqueous phase and mixed by gentle inversion. The DNA was picked up by moving a heat-sealed sterile Pasteur pipette in a clockwise motion around the Eppendorf. After collection the DNA was washed by dipping the pipette into 70% ethanol, the ethanol was evaporated off the by placing the pipette near a Bunsen flame. The DNA was resuspended by moving the pipette in an anticlockwise motion in an Eppendorf containing a volume of H_2O appropriate for the quantity of DNA. The concentration and purity of the DNA was measured using a Nanodrop spectrophotometer (Thermoscientific). For whole genome sequencing 30µl of DNA and concentration of 200 ng/µl with for purity an $OD_{260/280}$ ratio 1.8-2.0 and an $OD_{260/230}$ ratio 2.0-2.2 were required.

2.5.4.6 Construction of deletion strains

Genes were deleted through replacement of the gene with an antibiotic resistance marker. Integration of the antibiotic resistance marker was achieved either through transformation with a plasmid system or a ligation product. For both of these methods approximately 2500bp up- and downstream of the target gene was amplified using the appropriate primer pair. For transformations with plasmids the upstream and downstream regions were sequentially cloned either side of the antibiotic resistance cassette. Following each step the plasmid was transformed into competent *E.coli* DH5α. Transformants were selected using ampicillin. Insertion of the flanking regions was verified using PCR. Following plasmid construction the deletion plasmid was transformed into competent *B. subtilis* cells. Transformants were plated on the

appropriate antibiotic and the deletion verified by PCR. Plasmids used for deletion were pBEST501 (Itaya et al., 1989) and pHM457 (Murray et al., 2006). For transformations with ligation products, the PCR products were digested with the appropriate restriction endonuclease and ligated to the appropriate antibiotic resistance cassette. Competent *B. subtilis* cells were transformed with the ligation product. Transformants were selected using the appropriate antibiotic and the deletion verified by PCR. The antibiotic resistance cassettes were derived by PCR amplification from plasmids [*cat* from pAPNC213cat (Morimoto et al., 2002); *erm* from pMUTIN4 (Vagner et al., 1998); *neo* from pBEST501 (Itaya et al., 1989); *spc* from pAPNC213 (Morimoto et al., 2002)].

2.5.4.7 Construction of *mreB*$^{\Delta 20}$

Construction of the partial 60bp deletion of *mreB* was based off a pre-existing *ΔmreB* strain that featured an upstream *neo* cassette (Challis, 2014, Webb et al., 2009, Formstone and Errington, 2005). Using the primers featured in this work (LENm1-m4) the partial deletion was amplified from JB114/115 and ligated to *neo* cassette digested from the pBEST501 plasmid.

2.5.4.8 Construction of fusion protein GFP-MreB$^{\Delta 20}$

Construction of the fusion protein was based off a pre-existing plasmid carrying a functional *gfp-mreB* [pSG1729 (Strahl et al., 2014)]. The partial deletion in *mreB* was introduced using an In-Fusion cloning kit (Clontech), according to the manufacturer's instructions. In brief, the plasmid was amplified using primers JB84 and JB85. The binding site of these oligonucleotides lay either side of the deletion region, as a result fusion of the PCR product resulted in the loss of the region. The fused plasmid was transformed into competent *E.coli* DH5α cells and the sequence of the plasmid confirmed by PCR and sequencing. Transformation of competent *B. subtilis* cells with the plasmid resulted in strain JB166, which carried *gfp-mreB*$^{\Delta 20}$ under a xylose-inducible promoter at the *aprE* locus.

2.5.4.9 Preparation of *B. subtilis* L-forms

L-forms were generated via an intermediate protoplast preparation step as described in (Wu and Errington, 1998). Briefly, *B. subtilis* cells were grown in 4 ml LB at 37°C until an OD$_{600}$ between 0.3 and 0.5 was reached. The cells were harvested by centrifugation and resuspended in 2 ml NB/MSM containing 2 mg/ml lysozyme. The suspension was then

incubated at 37°C with gentle shaking for 45 min-1 hr until >99% of cells were protoplasts (as estimated using light microscopy). 10 µl of the protoplast culture was used to inoculate 10 ml fresh MSM/NB containing 200 µg/ml PenG (Sigma). Protoplasts were allowed to develop as L-forms through stationary incubation at 30°C for 24-72 hrs.

2.5.4.10   Growth of *B. subtilis* L-forms on solid and liquid media

For growth in liquid media L-forms were inoculated 1/1000 into 10 ml of either MSM/NB or MNM/NB containing 200 µg/ml PenG (Sigma) and incubated at 30°C. For growth on solid media, L-forms were streaked on MSM/NA containing 200 µg/ml PenG (Sigma) and incubated at 30°C.

2.5.4.11   Growth of L-forms in low osmolarities

L-forms were prepared and then grown in 0.5 M MSM/NB or 0.5 M MNM/NB until they reached mid-late exponential phase (OD_{600}=0.5-1.0). L-forms were inoculated into 10 ml media containing low osmoprotectant concentrations of interest in a 1/1000 dilution ratio. Cultures were grown for up to 30 days at 30°C with no shaking. Growth was primarily monitored by eye, with the OD_{600} measured on average every 5 days. Presence of L-forms was confirmed using light microscopy. Alternatively, the walled cells were streaked on 0.5 M MSM/NA or 0.5 M MNM/NA plates and grown until colonies appeared. A loop of cells was streaked onto nutrient agar containing a reduced concentration of sucrose or NaCl. The plates were sealed within a plastic bag and incubated at 30°C for up to 30 days.

2.5.4.12   Regeneration of L-forms to the walled state

100 µl L-forms were used to inoculate the defined protoplast recovery medium DM3 (Chang and Cohen, 1979) that was supplemented with 0.5% xylose. Plates were incubated at 30°C for up to 14 days or until colonies appeared. Colonies were restreaked on nutrient agar containing 0.5% xylose and the appropriate antibiotic markers.

2.5.4.13   Fatty acid analysis

Fatty acid composition of *B. subtilis* L-forms was determined from cells grown at 30°C in MSM/NB. Cells were harvested when cultures reached an OD_{600}≈0.5. Cells were washed three times in 0.4 M NaCl followed by lyophilisation. Fatty acids were analysed as fatty

acid methyl ester using gas chromatography. All analyses were carried out in duplicate by the Identification Service of DSMZ, Braunschweig, Germany.

2.5.4.14   Analysis of membrane fluidity

For measurement of membrane fluidity, *B.subtilis* cells were grown as walled cells in LB supplemented with 0.5% xylose and 0.1% glucose at 37°C. *B. subtilis* L-forms were grown in MSM/NB at 30°C. When OD_{600}=0.3 was reached, 10 µM Laurdan dye (6-dodecanoyl-2-dimethylaminoaphthalene) was added. The walled cells were incubated for 10 minutes at 37°C, the L-forms were incubated at 30°C. After incubation cells were washed three times at 37°C or 30°C with phosphate buffered saline (pH 7) containing either 0.1% glucose (walled cells) or mixed in a 1:1 ratio with MSM (L-forms). The fluorescence was measured using a BMG optima plate reader, warmed to 37°C or 30°C, with a 350 nm excitation wavelength and emission wavelengths of 435 and 490 nm. Background fluorescence was measured using buffer supernatant removed after removal of cells by centrifugation. Following background subtraction, the Laurdan GP value was measured using the formula GP = $(I_{435nm}-I_{490nm})/(I_{435nm}+I_{490nm})$ (Parasassi et al., 1990).

2.5.4.15   Δ*mbl* recovery screen

Strain JB84 was grown overnight at 37°C in nutrient broth supplemented with 20 mM $MgCl_2$. 5 µl of Δ*mbl* diluted 10^{-4} was used to inoculate 185 µl nutrient broth in each well of a 96 well plate as necessary. Unless specified otherwise, 10 µl of material derived from the Actinobacteria to be tested was added to each well. Addition of 20 mM $MgCl_2$ was used as a positive control for growth and the addition of no $MgCl_2$ was used as a negative control. Cells were grown for 16 hrs at 37°C in a BMG plate reader with the OD_{600} measured every 60 seconds. Unless specified otherwise all experiments had at least two technical repeats and two biological repeats.

2.5.5   Experiments using *Actinomycetes*

2.5.5.1 Growth of *Actinomycetes* on solid media

From freezer stocks *actinomycetes* strains were streaked onto oatmeal agar and grown at 30°C. Once growth was established, strains were restreaked onto GYM agar and grown at 30°C.

2.5.5.2 Growth of *Actinomycetes* in liquid media

Actinomycetes grown on solid media were used to inoculate 10 ml GYM medium. Cultures were grown at 30°C with orbital shaking for about 7 days. Once dense 10 ml cultures were used to inoculate 50 ml GYM medium.

2.5.5.3 Growth of *Actinomycetes* large scale cultures

For scaling up compound purification *Actinomycetes* strains of interest were grown in 20 L bioreactors. *Actinomycetes* were grown in feeding flasks containing 500 ml GYM media for 4 days at 30°C with orbital shaking.

2.5.6   Compound purification

2.5.6.1 Compound collection

Secondary metabolites of the *Actinomycetes* strains were harvested from either solid or liquid media. For harvesting from solid media, agar plates were passed through a 50 ml syringe and frozen at -20°C. Crushed agar was defrosted and centrifuged at 9000 rpm for 30 mins, then the released liquid was passed through low-binding 0.45 µm filters. The resulting extract was stored at -20°C until needed. For collection from liquid media, cultures were centrifuged at 9000 rpm for 10 mins. The supernatant was passed through low-binding 0.45 µm filters and stored at -20°C until needed.

2.5.6.2 Ethyl acetate extraction

An aliquot of culture supernatant (~30 ml) obtained from a 500 ml fermentation of DEM30616 was mixed with an equal volume of ethyl acetate in a rotary flask. The aqueous phase was then removed into a separate rotary flask. From both phases the ethyl acetate was removed in a rotary evaporator heated to 37°C. Prior to the complete evaporation of ethyl acetate in the solvent phase dH_2O was added to keep compounds present in solution.

2.5.6.3 Reverse phase chromatography

Reverse phase chromatograpy was performed on an Isolera Prime flash purification system (Biotage). 50ml crude extract was loaded onto a C18 30 g silica SNAP Biotage cartridge and eluted with methanol+0.1% formic acid (325 ml; 13 CV) at a flowrate of 25 ml/min and a fraction size of 10 ml. Methanol was removed from the 96 well plate in

a centrifugal evaporator run at 27°C 1725 rpm and 40 mBar pressure for 45 minutes prior to testing of the compounds.

2.5.6.4 Preparative and analytical HPLC

Both types of HPLC were performed on an Agilent 1260 Infinity system. For preparative HPLC, 900 μl was injected whilst for analytical HPLC 5 μl was run. Both volumes were run on a Phenomenex 150x4.50 mm column with an attached precolumn. The column was eluted with acetonitrile+0.1% formic acid at a flow rate of 1 ml/min over 48 minutes. UV absorption was measured using a diode array detector (DAD) at 254, 210, 350, 230, 400, 273, 300 and 250 nm. During preparative HPLC compounds were eluted into 96 well plates based on fixed time intervals. Acetonitrile was removed from the 96 well plate in a centrifugal evaporator run at 27°C 1725 rpm and 40 mBar pressure for 45 minutes prior to testing of the compounds.

2.5.6.5 Mass spectroscopy

Purified compounds were analysed by mass spectroscopy using a Voyager DE-STR instrument (Applied Biosystems). Compounds were identified using searches of the Dictionary of Natural Products.

2.5.7   Microscopy

2.5.7.1 Phase contrast and Fluorescence microscopy

Both walled cells and L-forms were visualised at various points in their growth. For L-forms, 2 μl of culture was mounted directly onto a microscope slide. Walled cells were mounted on microscope slides covered with a thin film of 1.2% agarose in SMM (Glaser et al., 1997). Membranes were stained by addition of 0.4 $\mu g.ml^{-1}$ FM5-95 dye (Invitrogen), nucleoids were stained by addition of 1 μl DAPI (Sigma) solution (1 mg/ml) to 10 μl of the culture prior to mounting. Images were acquired using either a Sony CoolSnap HQ2 cooled CCD camera (Roper scientific) attached to a Zeiss Axiovert M200 microscope or Qimaging Rolera em-c^2 cooled CCD camera attached to a Nikon Eclipse T_i microscope. Metamorph (MolecularDevices) was used to manipulate the images, which was limited to cropping the images and altering the brightness and contrast. Photoshop (Adobe) was used to apply scale bars to the images. The ImageJ (Schneider et al., 2012)

plugin, ObjectJ, was used to analyse the microscope images. This included cell counting and measurement of cell size.

3. Osmoresistant L-form generation and characterisation

3.1 Introduction
3.1.1   L-forms

In the majority of bacterial species the cell membrane is constrained by a cell wall composed of peptidoglycan. This complex mesh of interlocked glycan strands acts to protect the bacterium from external assault, to restrain the cell membrane against the effects of turgor and to provide shape to the cell. Despite the key roles the cell wall plays, remarkably it is dispensable under certain conditions. Many bacteria of a variety of species can grow and propagate in the absence of the cell wall as 'L-forms' (Klieneberger, 1935, Mercier et al., 2014). In laboratory settings, L-forms can be generated through disruption of the cell wall by antibiotics such as the β-lactams or fosfomycin (Mercier et al., 2014) or by blocking peptidoglycan synthesis genetically (Leaver et al., 2009). Without the cell wall to resist turgor pressure L-form growth requires the presence of high osmolarity media (typically in the form of sucrose or NaCl) to reduce the turgor pressure and prevent massive lysis. In the absence of the peptidoglycan, the cell shape is no longer maintained with the L-forms typically adopting an enlarged, amorphous and roughly spherical shape. This morphology is similar to that observed in protoplasts as a result of inflation by turgor pressure.

Despite the requirement for high concentrations of osmoprotectant, L-forms are not a laboratory artefact, as the dramatic phenotypic shift to the L-form state may be a natural response to compounds that affect wall integrity or to escape phage or immune system predation.   L-forms have been found in plant material (Waterhouse et al., 1996, Ferguson et al., 2000) and also from clinical isolates, particularly from patients with persistent or recurrent bacterial infections (Domingue and Woody, 1997).

A paradox begins to emerge - L-forms are exquisitely sensitive to changes in osmolarity, yet can be isolated from environments in which the high concentrations of osmoprotectant cannot be found. Several, mostly older, studies describe L-forms that have been adapted to minimal levels of osmoprotection. The adapted L-forms were characterised biochemically and shown to have lower concentrations of internal Na^+ and K^+ (Montgomerie et al., 1972), changes in their fatty acid profile (Montgomerie et al., 1973, Leon and Panos, 1976) and a higher protein content (Leon and Panos, 1976).

However, little is known about the molecular genetics that allow L-forms to grow and propagate under these adverse conditions.

In this work we reinvestigate the remarkable ability of L-forms to grow with minimal osmoprotection. Here we adapt the well-defined L-forms derived from the Gram positive model organism *B. subtilis* to a range of low sucrose or salt environments and use modern genome sequencing methods as well as more traditional techniques to identify and characterise a number of mutations that enable L-forms to grow in these hostile conditions.

3.2 Results

3.2.1 Growing L-forms in decreasing concentrations of osmoprotectant is not an effective method for osmoadaptation

As shown, L-forms have been a well-studied phenomena. However, much of this research took place during the pre-genomic era where many of the tools required for in-depth investigation did not yet exist. Following the landmark paper in 2009 (Leaver et al., 2009) in which the genetic changes required for L-form development in *B. subtilis* were elucidated it has become possible to generate and investigate L-forms in a highly reproducible and robust fashion.

L-forms derived from the Gram-positive model organism *B. subtilis* are typically grown in nutrient broth enriched with MSM (20 mM magnesium chloride, 0.5 M sucrose and 20 mM maleic acid). This growth medium is well defined, having been used in both L-form and protoplast studies for many years.

The osmolarity of nutrient broth and nutrient agar is currently unknown. However, work relating to osmotic regulation indicates that these media is of low osmolarity and is therefore unlikely to contribute significantly to the overall osmolarity of the media (Schirner et al., 2015). In turn, the 20 mM concentrations of $MgCl_2$ and maleic acid are unlikely to have significant bearing on the overall osmolarity of the media. As such, it can be considered that the primary source of osmotic stabilisation in L-form cultures is from sucrose. Throughout the experiments the concentrations of $MgCl_2$, maleic acid and nutrient broth were maintained as a means to control for only the contributions of the sucrose within the media.

This initial investigation utilised the strains JB104 and JB105. These two strains are derived from the well characterised LR2 strain (Leaver et al., 2009) which carries *murE* under a P_{xyl} promoter alongside a point mutation in *ispA* in the 168CA laboratory strain background. JB104 and JB105 carry GFP and mCherry respectively under a constitutive P_{rpsD} promoter (Grundy and Henkin, 1992). The presence of the fluorescent markers allowed for rapid and robust verification that the 'output' bacteria were the same as the 'input' bacteria.

As discussed in the introduction, we hoped to establish whether L-forms could grow in more biologically relevant conditions than those normally used in the laboratory. Whilst there is evidence that *B. subtilis* can grow as an L-form in nature, the LR2 strain is in the 168CA background, a laboratory adapted strain. To examine if the strain background affects the ability to grow in low osmolarities the mutations in LR2 were recreated in the *B. subtilis* Marburg strain (LR2-M). The Marburg strain lacks many of the mutations that arose in the domestication of 168CA laboratory strain and retains the ability to produce biofilms (Zeigler et al., 2008). These differences notwithstanding the two strains from the different backgrounds behaved similarly and were treated the same both when grown as walled cells and L-forms in the normal conditions.

The first approach of the L-form adaptation experiment was to dilute L-forms, step-wise, into a medium with a lower concentration of sucrose. The experiment started with a parent L-form culture derived from the walled cells as described in 2.4.5.8 and grown until dense in 0.5 M MSM/NB. The parent culture was then used to make 1/1000 inoculations into test tubes containing 5 ml 0.4 M MSM/NB. These were grown for roughly 10 days at 30°C. The adaptation experiments were set up with replicates of 10. To control for any factors affecting L-form growth that were not related to the osmotic conditions, L-forms from the parent culture were also used to inoculate 3 tubes of 5 ml fresh 0.5 M MSM/NB cultures. To minimise the risk of contamination the growth rate was only tracked in three of the 10 tubes during each adaptation experiment. As shown in figure 3.1A L-form growth in 0.4 M MSM/NB was robust, though at a lower rate than growth in 0.5 M MSM/NB. The presence of L-forms within all the cultures was verified using light microscopy. To further verify the L-forms, fluorescence microscopy was used to detect the presence of the constitutively expressed GFP or mCherry. Excluding occasions of contamination with walled bacteria (typically cocci, though instances of rods and yeast were observed) L-forms were observed in 100% of all 0.4 M MSM/NB cultures.

For easy storage and characterisation of the adapted L-forms, L-forms grown in 0.4 M MSM/NB were plated on DM3 protoplast recovery media (Chang and Cohen, 1979) supplemented with xylose. This medium supports the L-forms and alongside the xylose facilitates regeneration of cell wall and therefore reversion of the bacteria back to the

walled state. Correct isolation was verified using the constitutively expressed GFP and mCherry markers. Stocks of the adapted L-forms were stored at -80°C only after they have been reverted back to the walled state.

Following growth in 0.4 M MSM/NB L-forms were used to inoculate medium containing 0.3 M MSM/NB. In addition, the L-forms were also used to inoculate fresh 0.5 M and 0.4 M MSM/NB for use as controls. Where contamination arose fresh L-forms were prepared from the freezer stocks of the walled strains regenerated from L-forms adapted to 0.4M sucrose and were used to reinoculate fresh media.

Again growth in the '0.3 M sucrose' medium was observed in 100% of cultures (barring occurrences of contamination). As before, the presence of L-forms was verified using light and fluorescence microscopy, and a portion of the adapted cells were reverted back to the walled state via streaking on DM3 plates containing xylose for storage.

The step from 0.3 M to 0.2 M sucrose was repeated additional times, with occurrences of growth averaging at 5% (range=0-20%) in the separate cultures. None of the L-forms seen in the step down to 0.2 M sucrose achieved high optical densities, and neither could they be propagated further on DM3 media or in fresh L-form media.

This work suggested that the limit to which L-forms could readily grow in reduced levels of sucrose ranged between 0.3 M and 0.2 M sucrose. To confirm this and to resolve the boundary with greater resolution L-forms derived from LR2 were used to inoculate a range of sucrose concentrations between 0.3 M and 0.2 M. As can be seen in figure 3.1D growth becomes progressively less robust until it is effectively abolished at a concentration between 0.2125 M and 0.2 M sucrose.
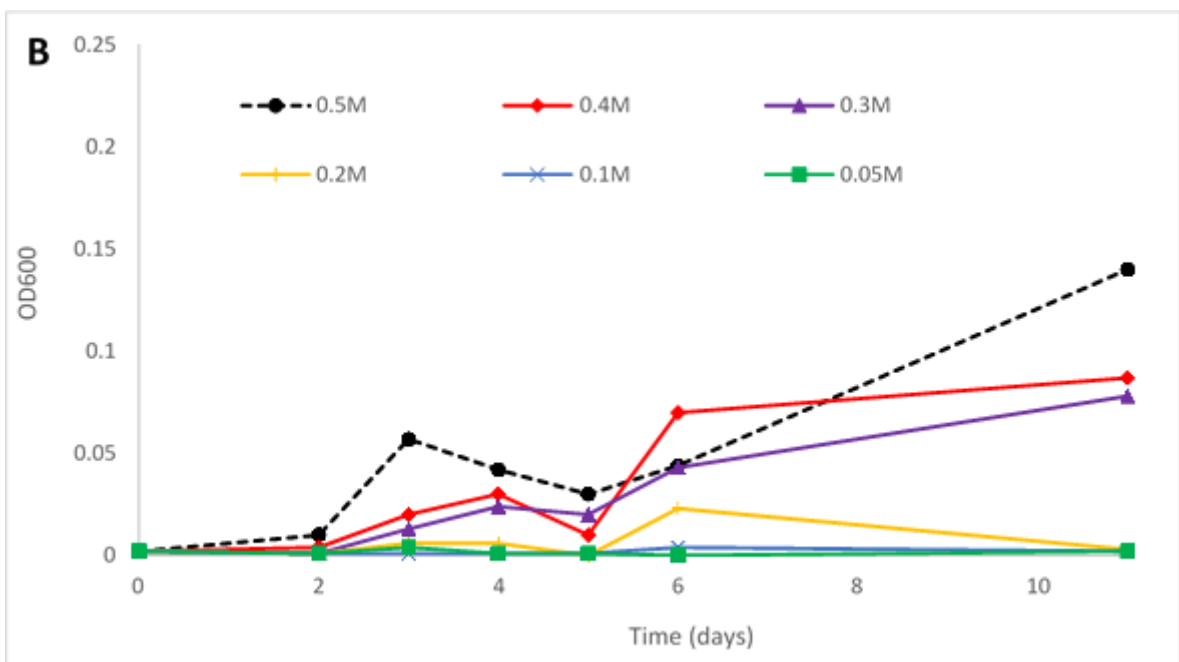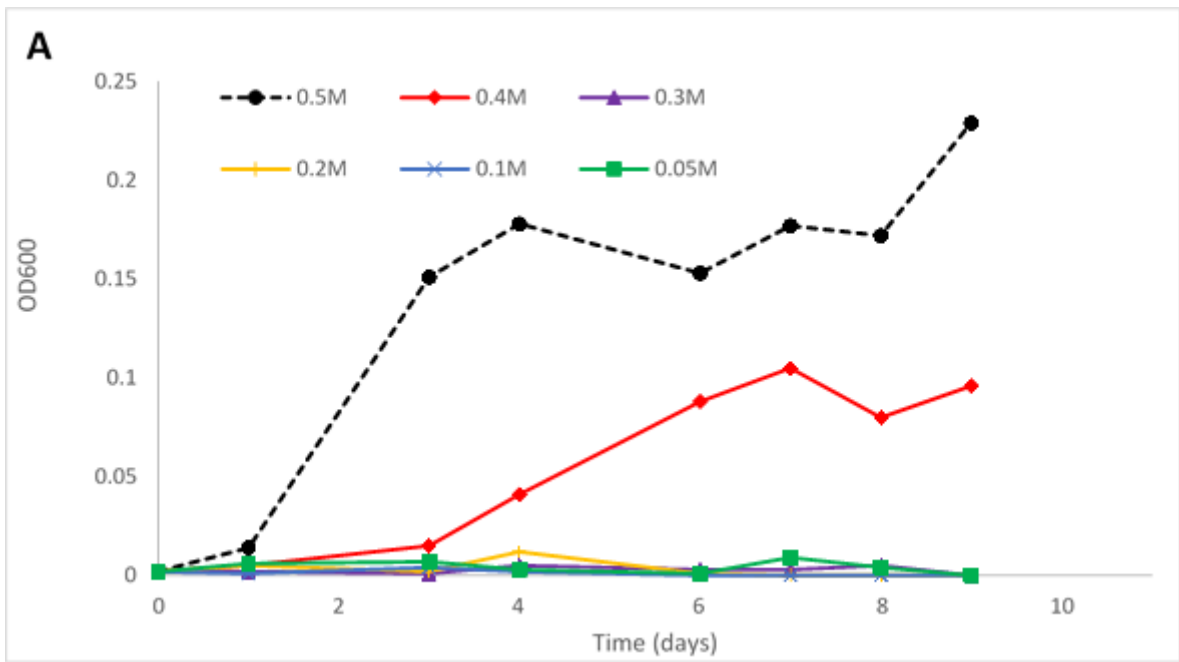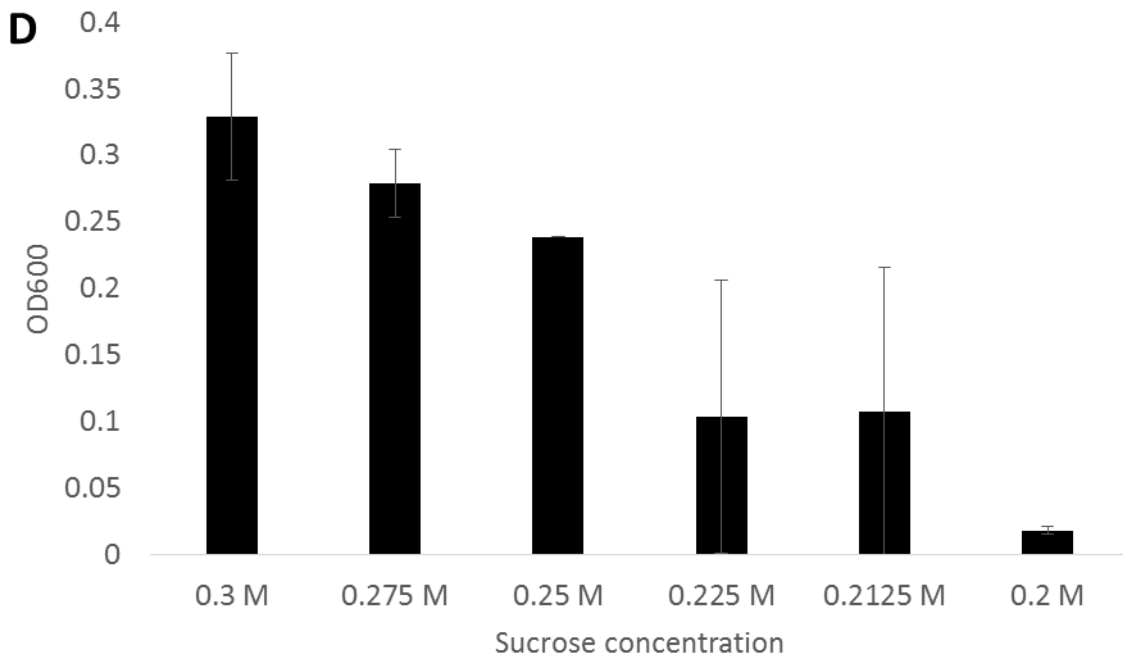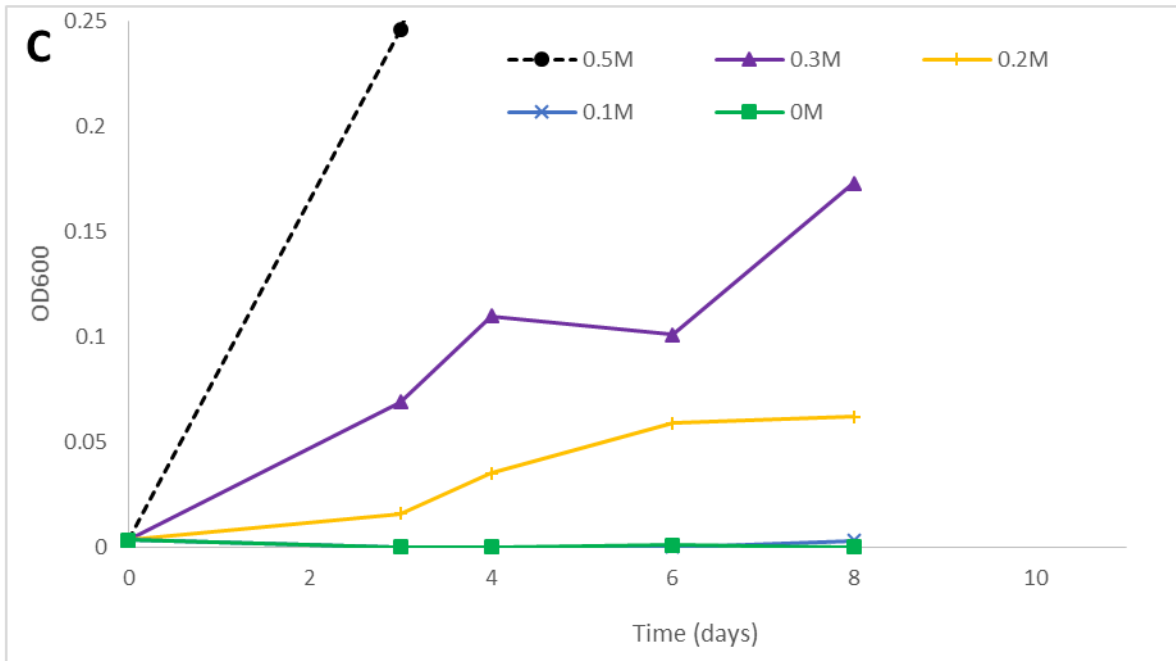
Figure 3.1. Growth of LR2 L-forms in varying concentrations of MSM/NB. L-forms derived from LR2 were grown in 0.5 M MSM/NB until dense. L-forms from this culture were used to inoculate a range of concentrations from 0.5 M to 0.05 M (A). After incubation, growth was only observed in cultures containing 0.5 M MSM or 0.4 M MSM. The same experiment was repeated using the L-forms grown in 0.4 M MSM/NB (B). After

11 days, L-forms were observed in media containing sucrose concentrations as low as 0.3 M. L-forms grown in 0.3 M MSM/NB were used to a fresh range of sucrose concentrations (C). L-forms were able to grow in sucrose concentrations of 0.2M, though these L-forms were not able to be propagated further. Graphs are illustrative of the growth of 12 biological replicates, each with 12 technical replicates. D). L-form growth in a range of sucrose concentrations after 10 days incubation.

To characterise the L-forms that have adapted to grow at sucrose concentrations below 0.3 M, the strains, stored at -80°C as walled cells, were grown on nutrient agar plates supplemented with 0.5% xylose. On plates no differences between the adapted strains in colony morphology was observed (Figure 3.2), examination of the strains by light microscopy also revealed no clear differences. Finally, there were no significant differences in the growth rates between the various adapted strains and the parent strain. Taken together, this indicated strongly, but not absolutely, that the L-forms had not acquired adaptive mutations and instead any changes were likely to have been transient.

This method of adaptation was ultimately abandoned. The primary reason was the inability to grow and recover L-forms at sucrose concentrations below 0.3 M. Secondly, the extended periods of growth and repeated inoculations rendered the risk for contamination high. Finally, the prolonged periods of growth would likely result in the accumulation of multiple mutations within the *Bacillus* genome. Such a build-up of mutations has the potential to confound attempts to analyse any whole genome sequencing performed.
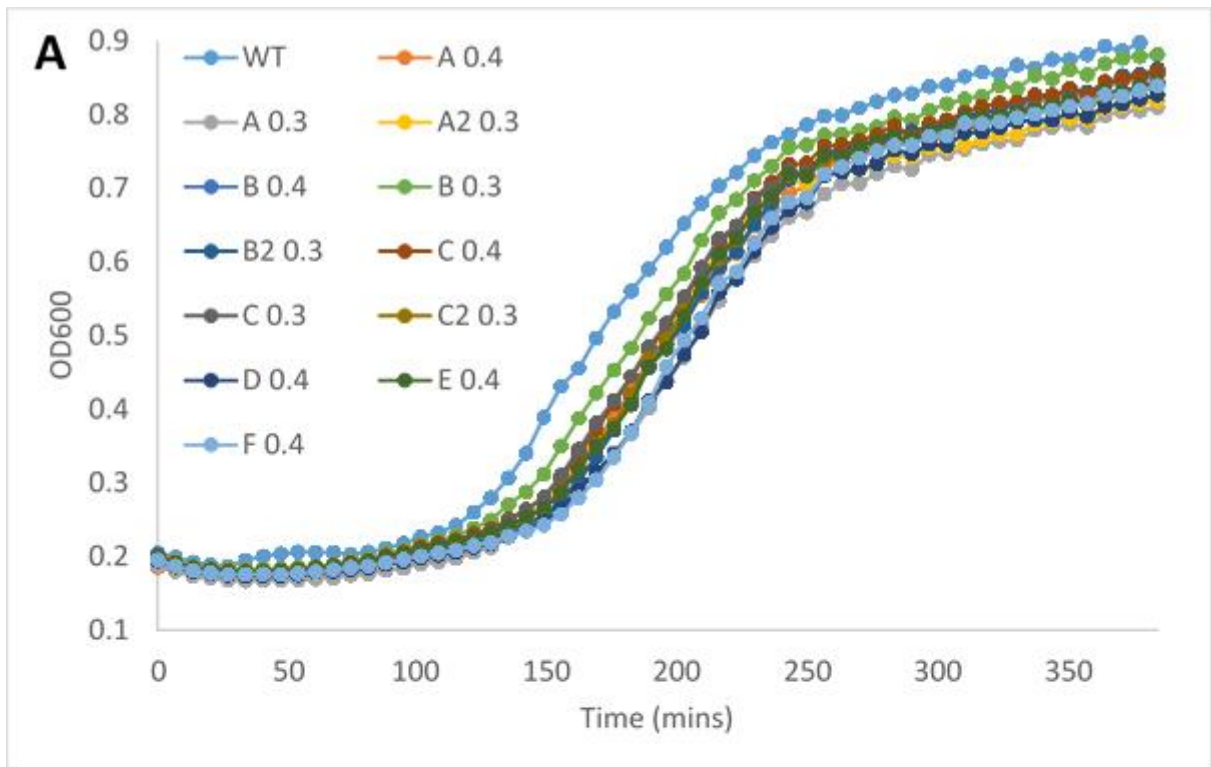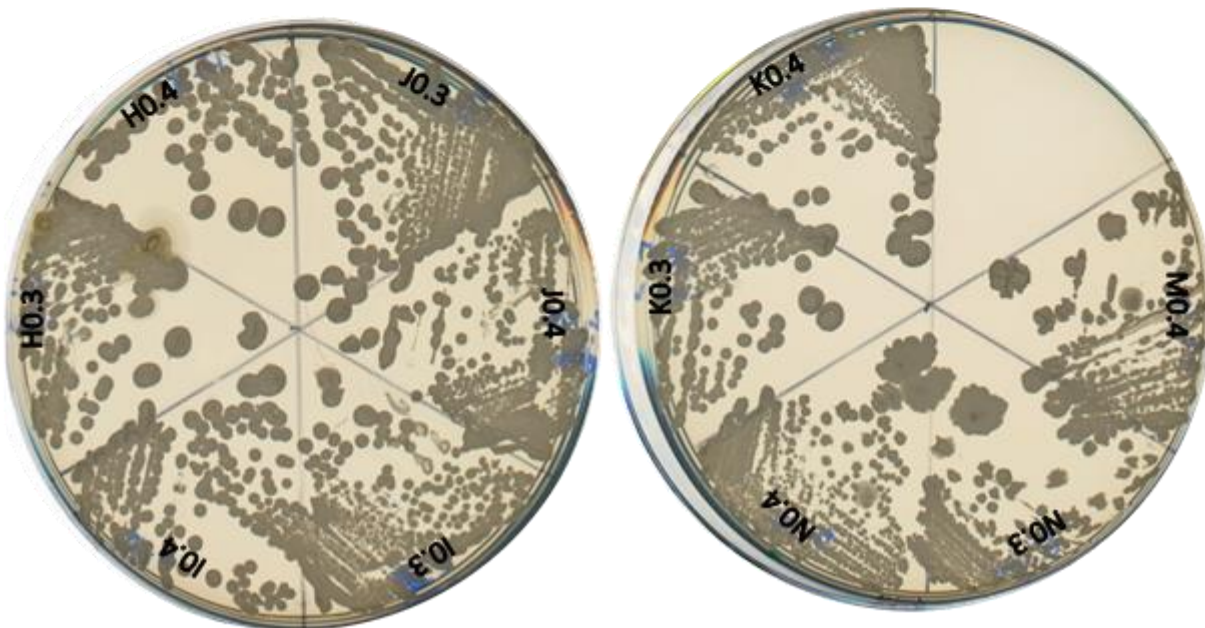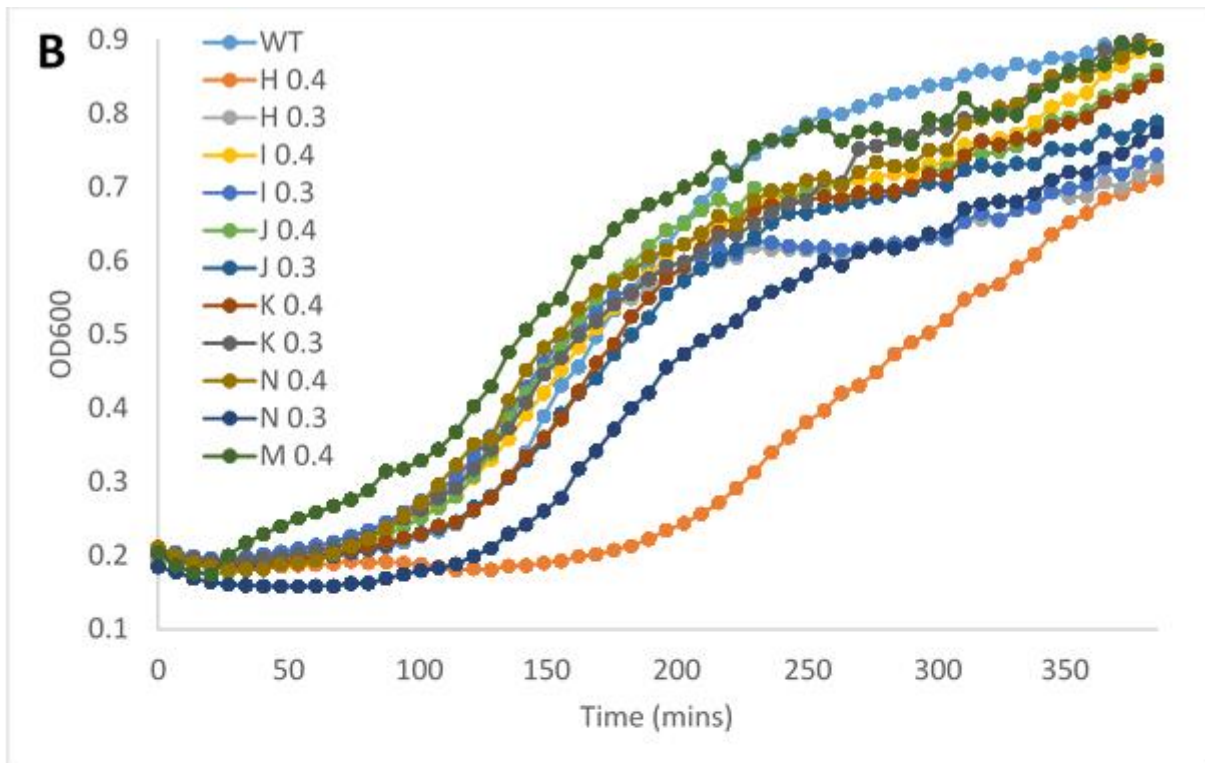
Figure 3.2. Regenerated L-forms derived from LR2 (A) and LR2-M (B) isolated from the adaptation experiments are phenotypically identical in both liquid and solid media. L-forms from the adaptation experiment were regenerated on DM3 protoplast recovery media and restreaked on nutrient agar containing the appropriate selection marker(s), frozen in liquid nitrogen and stored at -80°C. For measurement of the growth rates, bacteria were diluted from overnight cultures into fresh LB media on a 96 well plate. Bacteria were grown for 6 hours and the OD_{600} measured in a plate reader heated to 37°C. For growth on solid media the strains were streaked on nutrient agar

supplemented with 0.5% xylose. Each letter in the strain name refers to each biological replicate in the adaptation experiment, whilst the number refers to the sucrose concentration the strain was isolated from.

3.2.2 Direct inoculation of low sucrose media can be used to generate osmoadapted L-forms

As an alternative route for generation of osmoresistant L-forms, it was considered whether L-forms could be directly inoculated into media containing low levels of sucrose. Such a method was preferable to that described in the previous section as it would reduce the long growth times during each stage of adaptation. It would also reduce the level of manipulation required, thereby limiting the opportunities for contamination to be introduced.

This method was attempted with both the LR2 derivatives mentioned previously and an *accDA* overproduction strain (though the majority of the experiments utilised the LR2-based strains). *accDA* encodes an acetyl-CoA carboxylase, an enzyme involved in the FAS II pathway. Overexpression of *accDA* results in membrane overproduction, which can enable growth in the L-form state. In normal growth conditions these strains proliferate as L-forms in an identical fashion (Mercier et al., 2013). However, it was not known whether their behaviour in low osmolarities would be identical to each other. Apart from the requirement for xylose for growth as an L-form the *accDA* overexpression strain was handled exactly the same as the L-forms derived from the LR2 strains.

L-forms were grown in 0.5 M MSM/NB until they reached either mid-exponential or stationary phase and were then diluted 1/10 into MSM/NB containing either 0.1 M, 0.05M or no sucrose. As a result of these dilutions there were significant alterations to the final sucrose concentration in the media. These final concentrations are listed in table 3.1. For the sake of clarity the original sucrose concentrations will be used when describing the experiment.

Start sucrose concentration	Final sucrose concentration
0.1 M	0.136 M
0.05 M	0.091 M
No sucrose	0.045 M

Table 3.1. Sucrose concentration pre- and post- direct 10^{-1} inoculation from L-forms grown in 0.5M MSM/NB. Final sucrose concentration assumes minimal technical error in pipetting.

As with the previous adaptation experiment, the optical density was only tracked in a single culture and only in those exhibiting sign of growth (where media was observed to become turbid). As hoped, with the reduction in handling with the current method a reduction in the level of contamination was observed.

Crucially, growth was observed in a number of the flasks, across a number of the sucrose concentrations. An interesting phenomenon was observed in a small minority of the media containing no sucrose. In these cultures turbidity was observed 2-3 days post inoculation, and examination by light microscopy confirmed the presence of L-forms. However, the majority of these L-forms appeared phase negative, suggesting that they were more likely empty vesicles. This view was confirmed by the collapse in optical density over the 48 hours after examination. Subsequent examination by microscopy failed to detect any intact or viable L-forms within the culture. This observation suggests that proliferating L-forms were releasing empty vesicles as opposed to viable progeny.

In two cases *accDA* L-forms derived from strain JB150 (P_{xyl}-*accDA*) were able to grow in 0.1 M sucrose (Figure 3.3), though these L-forms were not able to be regenerated to grow in walled state nor propagated when re-diluted into the same (0.1 M sucrose) medium. However, what made these bacteria unique was that under the microscope these L-forms appeared to be clumping into dense clusters. Initially, this behaviour was thought to be unique to the *accDA* strain, though later work with osmoadapted L-forms derived from LR2 also exhibited this behaviour at a low frequency. The reason and significance of forming dense clumps was not known and not investigated further, though it is possible that many cells lysed and released a large amount of DNA, trapping some cells and perhaps even protecting them from lysis.
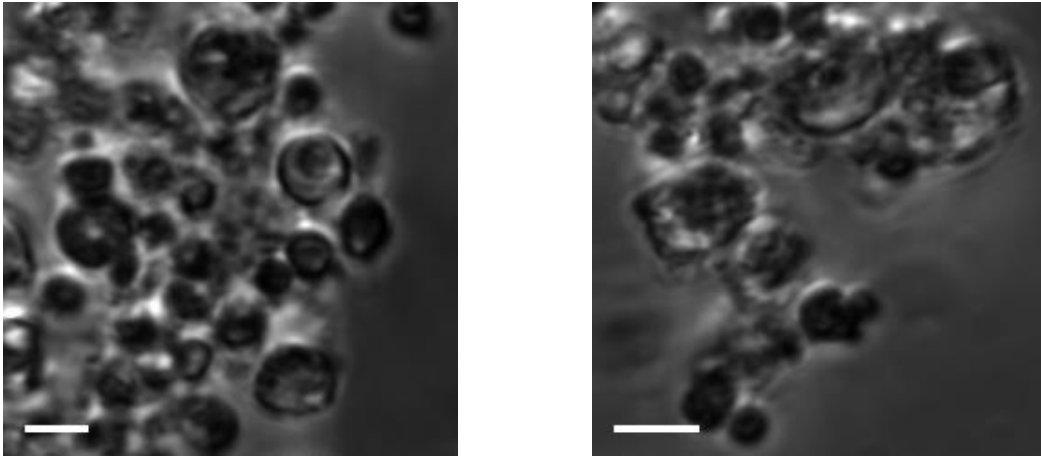
Figure 3.3. Despite observations of some growth, Growth in 0.1 M MSM/NB was observed following direct inoculation with L-forms derived from the *accDA* strain (JB150). Under the microscope L-forms appeared clustered together, along with a large number of dead L-forms. L-forms are assumed to be alive when phase bright and when recognisable as L-forms. Optical density was measured after 7 days. Scale bar=3 µm

In contrast to the *accDA* L-forms, one of the cultures derived from LR2 showed sustained growth in 0.1 M MSM/NB (figure 3.4), and could be propagated when diluted in fresh 0.5 M MSM/NB. Furthermore, after plating on DM3 (+xyl) protoplast recovery medium the walled cells could be isolated. Again presence of the fluorescent marker (in this case mCherry) and the selection marker was checked, which confirmed that the walled cells from the 'recovery' plates were regenerated L-forms. From the recovery plate four colonies were isolated and stored at -80°C. The four strains isolated from the colonies were called M1, M2, M3 and M4.
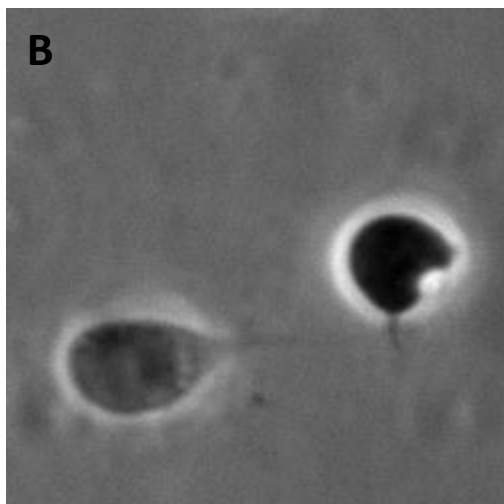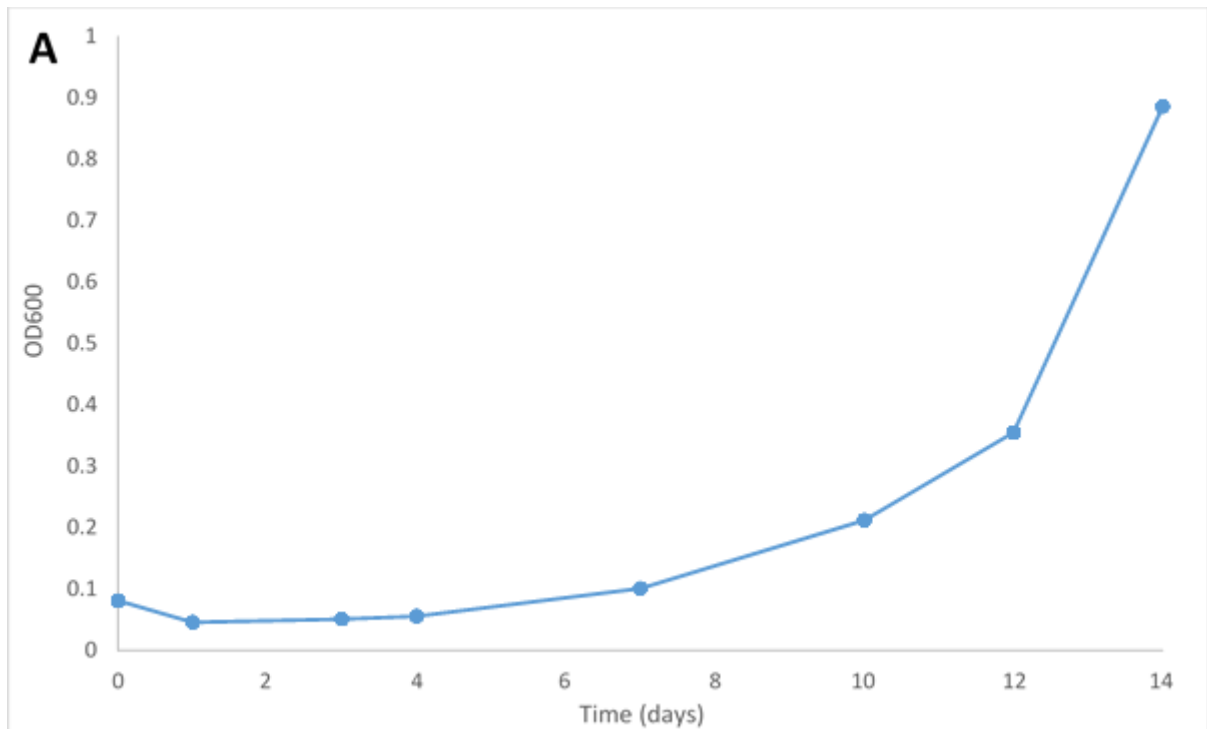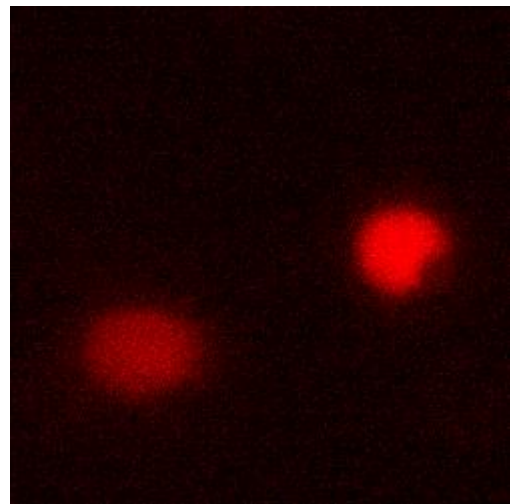
Figure 3.4. A). Growth of the isolated M1 strain in 0.1 M MSM/NB at 30°C over two weeks. **B).** L-form validation was achieved by the continued presence of a constitutively expressed copy of the fluorescent marker mCherry.

3.2.3 The ability of L-forms to survive resuspension in hypotonic conditions does not appear to be growth phase dependent

In the direct inoculation experiment described earlier it was considered whether the ability of L-forms to survive in the low osmolarity medium used was growth phase dependent; whether the ability to grow was dependent on early exponential growth for instance. To investigate this, the ability of L-forms derived from LR2 grown in 0.5 M MSM/NB to survive following suspension in either 0.1 M MSM/NB or H_2O was examined. L-form cultures were grown in triplicate for 3, 5, 7 and 9 days in 10 ml 0.5 M MSM/NB. The L-forms from each culture were centrifuged, and the resulting pellet was resuspended in either 0.3 M MSM/NB or in just water.

As can be seen in figure 3.5 the age of a culture has no bearing on the ability of the L-forms to survive the initial hypotonic shock. The caveat of the experiment is that it did not track whether the L-forms were able to grow following resuspension. Therefore, it remains possible that the age of an L-form culture could affect the ability to grow, just not survive.
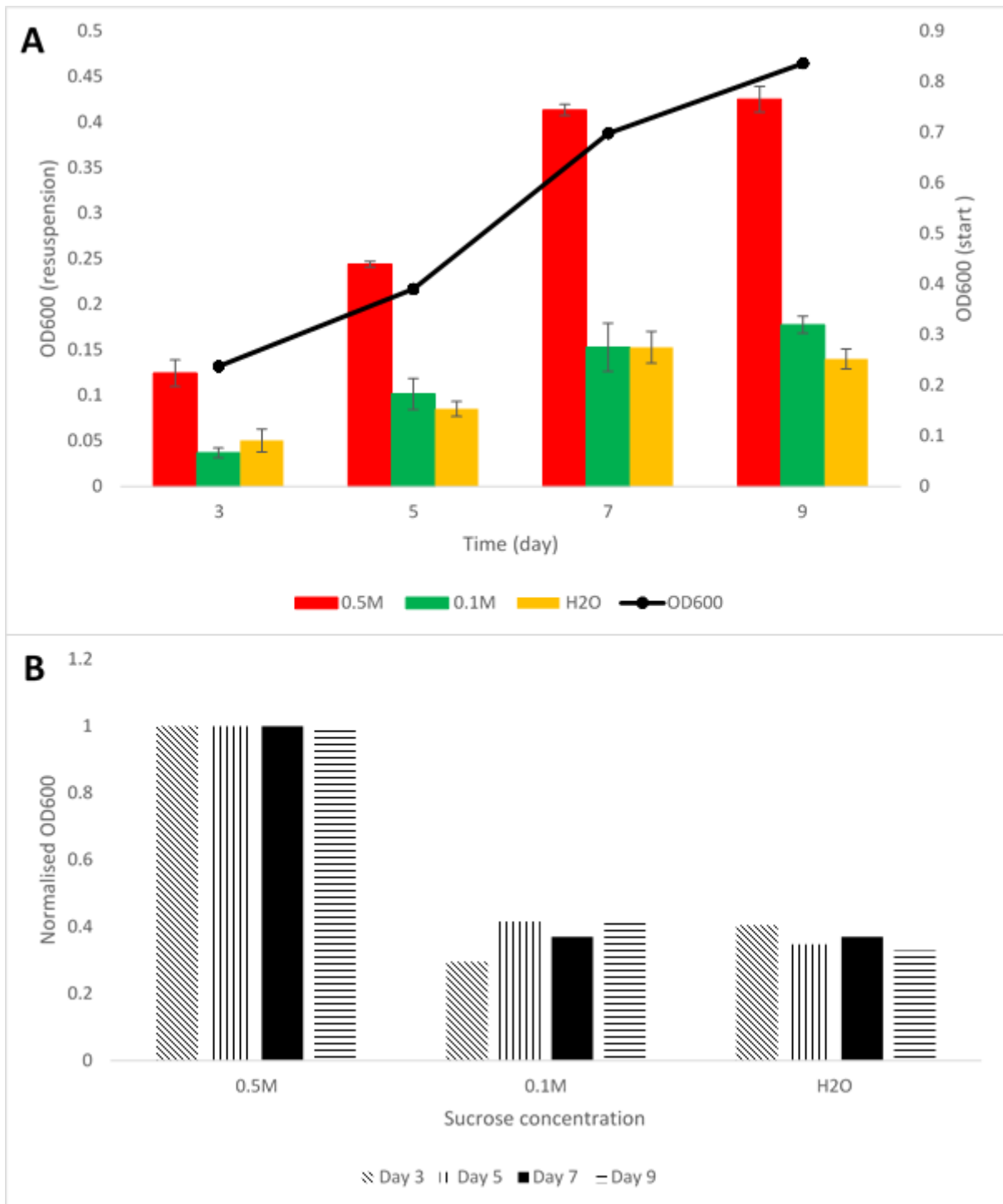
Figure 3.5. The age of an L-form culture has no effect on the levels of lysis following resuspension in low osmolarites. L-forms were diluted 10^{-3} into 10 ml 0.5 M MSM/NB and grown at 30°C. Every two days the OD_{600} was measured and 2 ml of the L-form culture pelleted. The pellet was resuspended in 2 ml of either 0.5 M MSM/NB, 0.1 M MSM/NB or H_2O and incubated at 30°C for 10 minutes. After 10 minutes the OD_{600} was measured. Little to no lysis is observed following resuspension in 0.5 M MSM/NB, whilst identical levels of lysis are observed between the two low osmolarities. The data were

normalised against an OD$_{600}$=1 at 0.5 M MSM/NB (B). Error bars are representative of the standard deviations of three replicates.

3.2.4 The adapted L-form strain retains the ability to grow in low osmotic conditions after regrowth as walled cells and in high sucrose

It was of interest to examine whether the L-forms that have adapted to grow with 0.1 M sucrose retained the ability to grow in low sucrose indicative of a mutation(s), or if what was observed was instead a transient adaptation. To test this, L-form cells in the 0.1 M sucrose culture (henceforth called M1) was firstly used to inoculate fresh 0.5 M MSM/NB and grown until dense, then diluted by either 1/10, 1/100 or 1/1000 back into 0.1 M MSM/NB. As a control the parental strain, JB105 was diluted by the same factors into 0.1 M MSM/NB. Even at dilutions of 1/1000 the L-form M1 strain was able to regrow in the low osmolarities, whereas the parental strain was unable to do so (figure 3.6). This provided the first evidence that the M1 strain had indeed picked up a mutation or mutations enabling it to grow in low sucrose environments.

The second piece of evidence was provided by the walled cells that were regenerated from L-forms adapted to grow in 0.1 M MSM/NB. The four colonies that had been isolated from the regeneration (M1, M2, M3 and M4) were investigated in case the adapted L-form culture was a mixed population. From these four strains L-forms were prepared as described in 2.4.5.8 and grown in 0.5 M MSM/NB until dense. The L-forms of these strains were then used to inoculate 0.1 M MSM/NB alongside the parental JB105 strain. All four of the strains were able to grow in the low sucrose media whereas the parental strain was not (figure 3.7A). This was further evidence that the isolated L-forms had indeed picked up a mutation or mutations that enabled growth in low sucrose environments.

Additionally, the ability of the adapted L-forms to grow in sucrose concentrations of 0.05 M was tested; no growth was observed, therefore the lowest concentration that L-forms could adapt to was 0.1 M sucrose (data not shown).
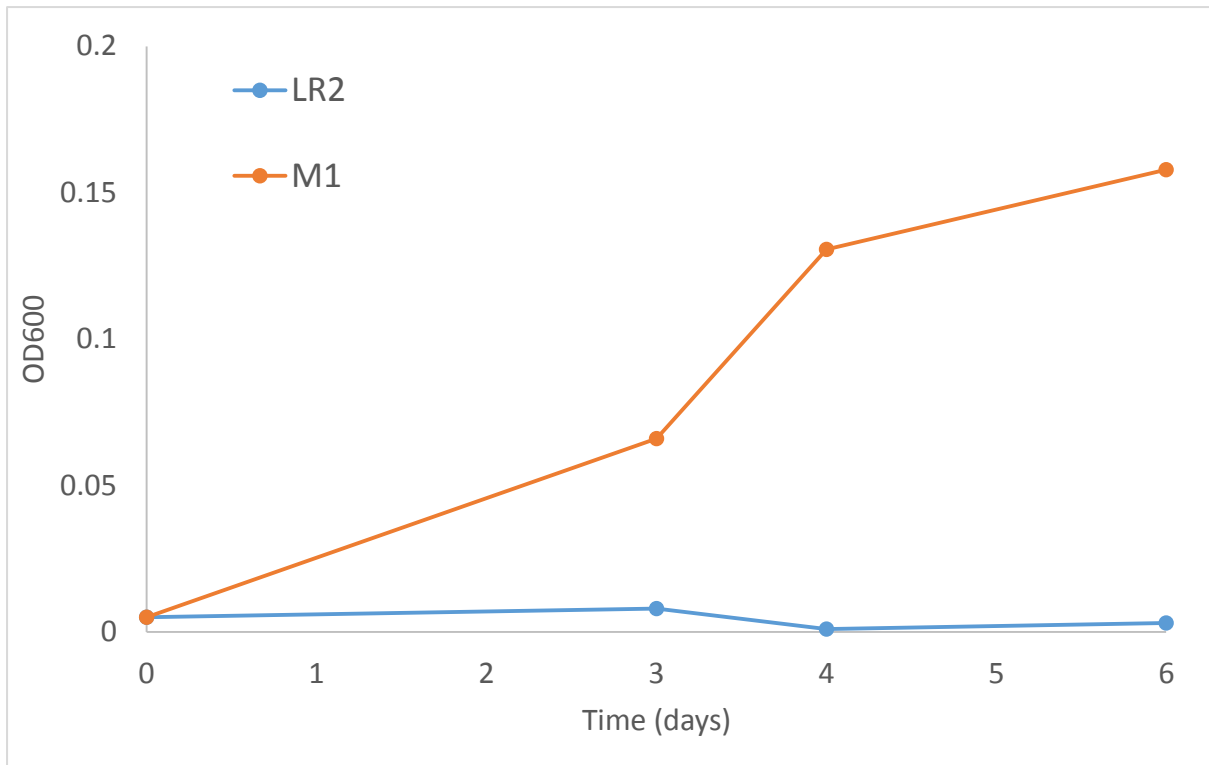
Figure 3.6. L-forms isolated from a 0.1 M MSM/NB culture can regrow in low osmolarities environments following growth in 0.5 M MSM/NB. The M1 strain isolated in the previous experiment was grown in 0.5 M MSM/NB for three days at 30°C. Cells were diluted into the low sucrose media by a factor of 10^{-2}. L-form growth was tracked via measurement of the OD_{600}.

3.2.5 The isolated osmoadapted L-forms M1-M4 have similar growth rates and similar cell morphologies indicating that the parent L-form culture did not represent a mixed population

It was possible that the osmoadapted L-form culture contained a mixed population of mutants. To probe this issue the four colonies obtained from regenerated L-forms in 0.1 M MSM/NB (M1-M4), which all retained the ability to grow in low sucrose conditions, were characterised by comparing their growth rates and cell morphology.

All four of the strains had the same slower growth rate than the parental strain, with growth improved but not restored by the addition of 20 mM $MgCl_2$ (figure 3.7). Microscopic analysis showed that all four of the strains exhibited the same striking morphological aberrations, in particular the strains appear to produce minicells as well as perturbations in the ability to maintain a uniform peptidoglycan wall.

Taken together, it seems likely that the four strains are identical and that they do appear to possess at least one mutation, which also hinders their growth and development in the walled state.

Early exponential phase   Late exponential phase

Phase contrast   Membrane   Phase contrast   Membrane
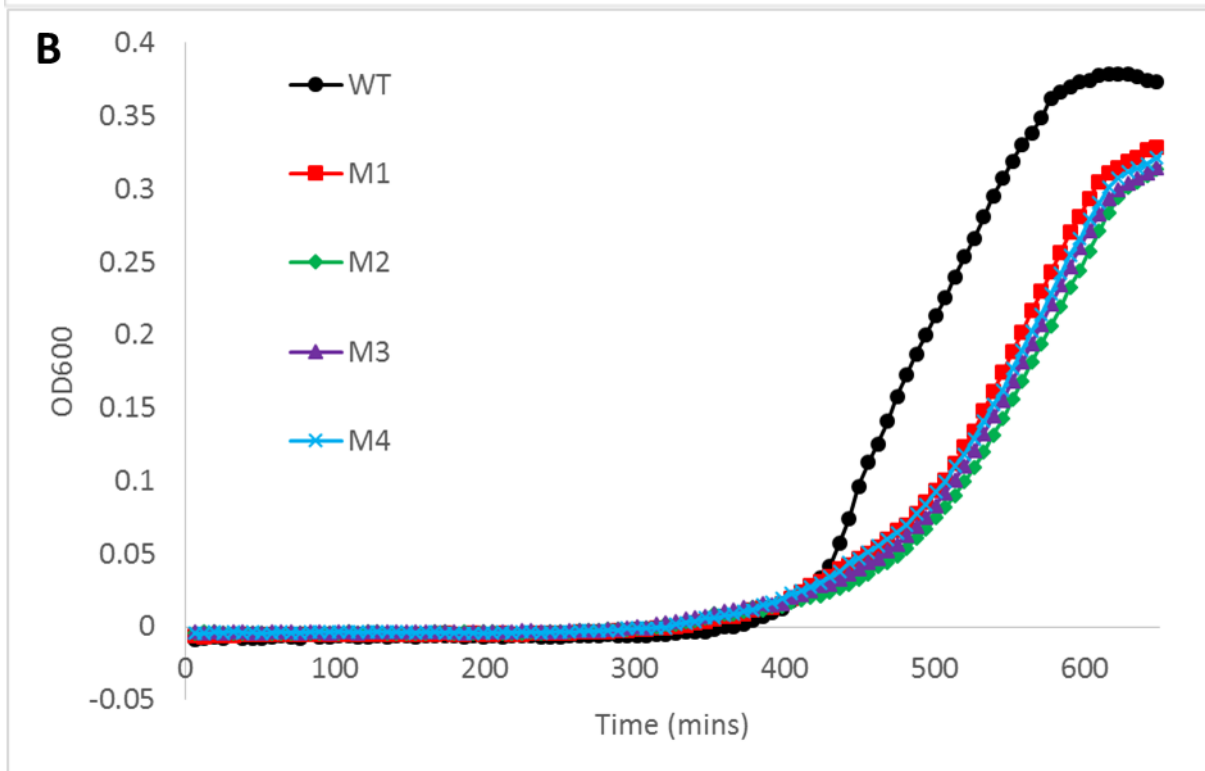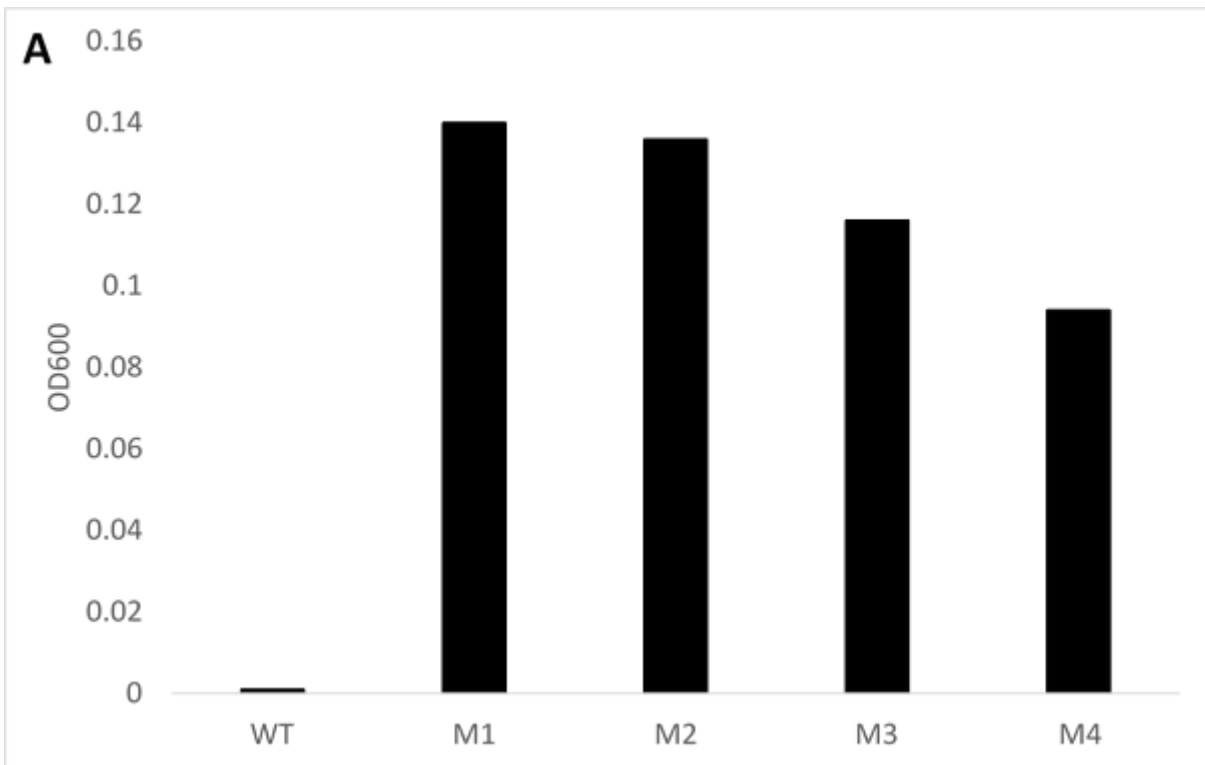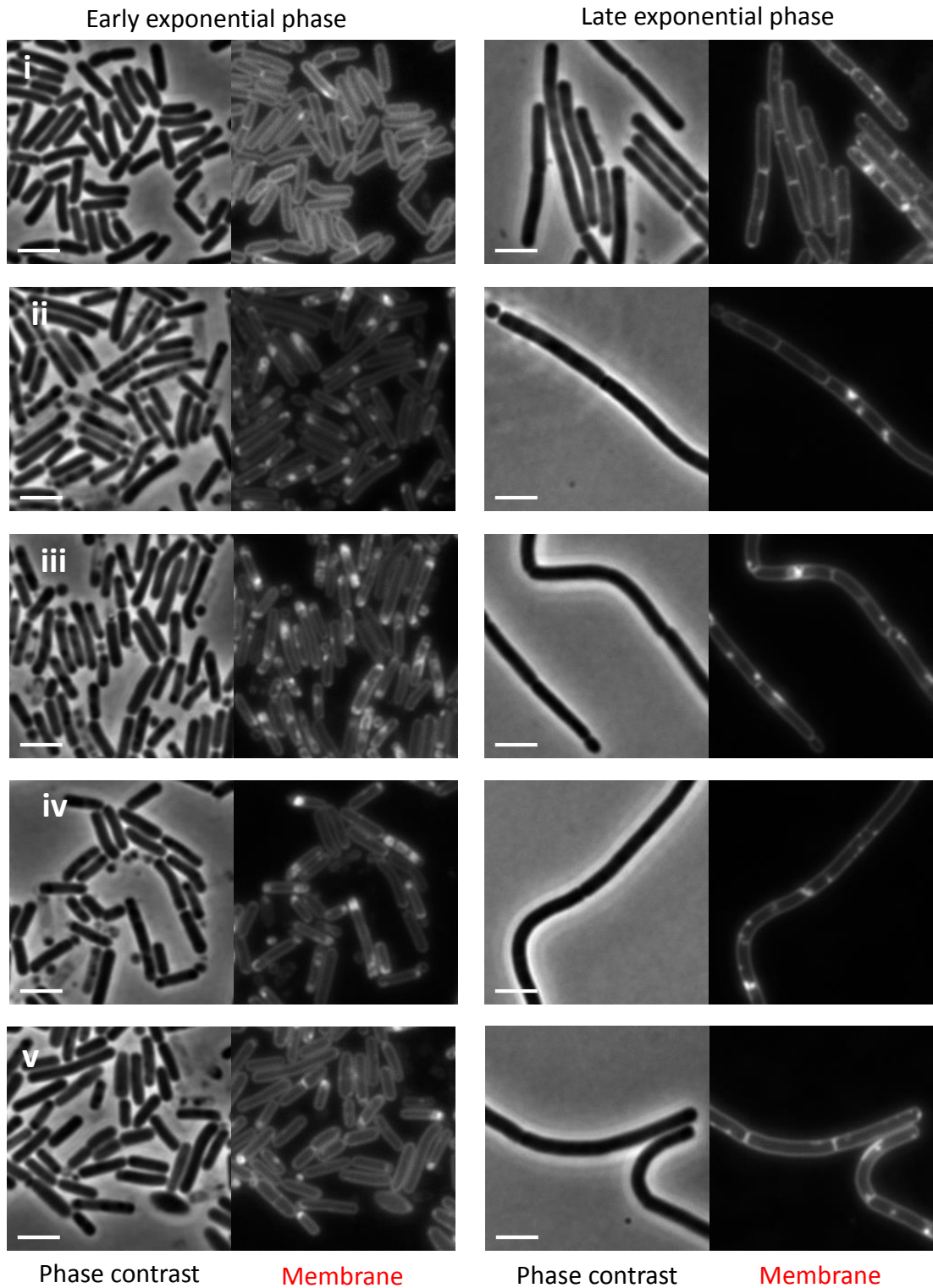
Figure 3.7. The four strains isolated from the DM3 recovery plate are phenotypically similar, but distinct from the parent strain. Following growth in low osmotic conditions L-forms were recovered on DM3 plates and the cell wall regenerated. Four colonies were stored to assess if the original culture was contained a mixed population. All four of the strains were able to regrow in low sucrose **(A)** and all four had a similar growth

rate when grown in LB as walled cells, though this growth rate was lower than the parental JB105 strain (B). **C).** Microscopy of the four strains during early and mid-exponential phase. The strains isolated from the osmoadaptation experiment M1 (ii), M2 (iii), M3 (iv) and M4 (v) all had similar morphologies to each other. These differed from the morphology of the wild type strain (JB105; i). Scale bar = 3μm.

3.2.6 Development of an adaptation method for the generation of osmoadapted L-forms proves successful

The above described adaptation method did prove successful, allowing for isolation of 4 mutants (probably clonal). To improve the efficiency of the 'adaptation' experiments, it was considered whether the method described in 3.2.1 could be adjusted so that instead of growing L-forms at each lower concentrations of sucrose for a prolonged period of time, the L-forms were instead adapted to progressively lower concentrations of sucrose for only 1-2 hours at each intermediate concentration. For this method a 50 ml L-form culture of the strain LR2 was grown until dense. Cells were harvested by centrifugation for 10 minutes at 3000 rpm. The supernatant was then discarded and the cell pellet was resuspended in 20 ml 0.4 M MSM/NB. The culture was incubated at 30°C for 1.5 hrs and 100 µl was removed to inoculate 10ml fresh 0.4 M MSM/NB; this was then grown at 30°. The main culture was centrifuged again at 3000 rpm for 10 mins, with the pellet resuspended in 20 ml 0.3 M MSM/NB and then incubated at 30°C once again for 1.5 hrs. This whole process was repeated at the sucrose concentrations listed in table 3.2 until the L-form pellets were resuspended in media containing no sucrose.

[Sucrose] or [NaCl]
0.5 M
0.4 M
0.3 M
0.2 M
0.1 M
0.075 M
0.05 M
No addition

Table 3.2. The concentration of osmoprotectant at each stage in the adaptation experiment. The concentrations listed do not reflect the effect the addition of residual osmoprotectant from a previous step on the overall molarity.

All the cultures were grown at 30°C for up to a month to see if growth develops. Unsurprisingly, the L-forms at the 0.4 M and 0.3 M sucrose concentrations grew rapidly and robustly. In the majority of cases no growth was observed in any of the flasks containing sucrose concentrations below 0.3 M. However in three independent experiments L-form growth was observed in flasks containing minimal sucrose, in two of these experiments L-forms were observed growing in several of the different concentrations, some containing as little as 0.05 M sucrose. The concentrations that the 5 isolated L-form strains were able to grow in following adaptation is listed in table 3.3.

Strain name	Osmoprotectant	Concentration (M)	Lineage
JB114	Sucrose	0.075	A
JB115	Sucrose	0.05	A
JB116	Sucrose	0.1	B
JB117	Sucrose	0.1	-
JB118	Sucrose	0.05	B
JB119	NaCl	0.1	C
JB120	NaCl	0.1	D
JB121	NaCl	0.05	C
JB122	NaCl	0.05	D
JB123	NaCl	0.1	-
JB124	NaCl	0.1	-
JB125	NaCl	0.1	-
JB126	NaCl	0.1	-

Table 3.3. Strains isolated from the adaptation experiment. Strains are listed with the osmoprotectant used and the concentration of osmoprotectant from which they were isolated. The lineage refers to the starting culture the L-forms were derived from.

As stated earlier, in the literature L-forms have been successfully grown with a variety of different osmoprotectants, amongst these osmoprotectants NaCl has been one of the most commonly used. It was speculated whether changing the osmoprotectant used from sucrose to NaCl would facilitate adaptation to low osmolarities more readily. To this end, L-forms derived from the LR2 strain were prepared as described, but the sucrose was replaced with 0.5 M NaCl thereby making MNM/NB. L-form growth in this media was slower than in sucrose, but still comparable; under the microscope cells grown with either osmoprotectant were indistinguishable (figure 3.8). The adaptation protocol established earlier was repeated with the sucrose concentrations substituted with equal concentrations of salt. The type of osmoprotectant used does not seem to have a significant effect on the ability of L-forms to adapt to low osmolarities – L-forms were able to adapt to minimal salt concentrations at a rate comparable to those adapted to low sucrose concentrations. In total eleven adapted L-form strains were isolated from six independent adaptation experiments. The salt concentrations that these strains are adapted to is listed in table 3.3**.**
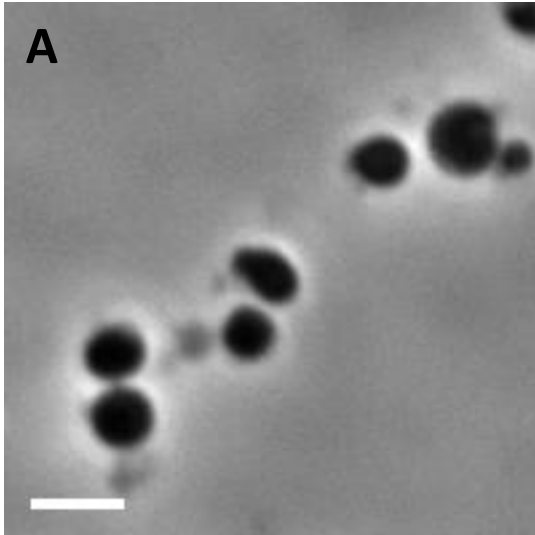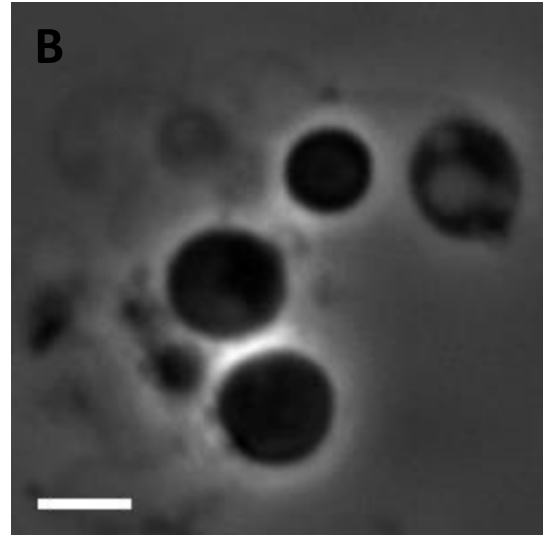
Phase contrast   Phase contrast

Figure 3.8. L-forms grown in MSM/NB (A) and in MNM/NB (B) are indistinguishable.

L-forms were grown from protoplasts in MSM/NB before inoculation of the two media.

L-forms were grown for 72hrs at 30°C then examined by light microscopy. Scale bar =

3 μm.

3.2.7 Adapted L-forms can be successfully regenerated into the walled rod form

Unlike the experiments described in 3.2.2 the osmo-resistant L-form mutants obtained in 3.2.6 were not introduced back in either 0.5 MSM/NB or MNM/NB. This was not intentional, but instead an unfortunate oversight. Instead, all the adapted cultures were directly plated onto the DM3 regeneration media to allow reversion to the walled state and remarkably, all the adapted strains were able to regenerate cell wall and grow as rods. The parent strain used for these experiments was LR2, without the GFP or mCherry tags used in the previous experiments. As such the identity of the regenerated strains was confirmed just by seeing if the bacteria retained their resistance to chloramphenicol, a marker linked to the p_{xyl}-$murE$ construct. All the strains were able to grow on nutrient agar containing the appropriate concentrations of xylose and chloramphenicol. Following this confirmation all the strains were given a name (table 3.3) and stored at -80°C for further analysis.

3.2.8 Most of the adapted L-forms retain the ability to grow in low osmotic conditions after regrowth as walled cells and in high sucrose or salt

To see whether the new osmo-resistant mutants retained their resistance after being reverted back into the walled state, the regenerated osmo-resistant mutants, now in walled form, alongside the parental strain LR2, were prepared as L-forms and grown in 0.5 M MSM/NB or MNM/NB where appropriate. Once the L-form cultures became dense they were diluted 1/100 into media containing either 0.1 M sucrose or 0.1 M NaCl as required and grown at 30°C for up to a month. Two of the L-form strains were unable to regrow in 0.1M salt despite repeated attempts; therefore for these two strains it must be assumed that they experienced a transient adaptation that allowed them to grow in low osmolarities. The remaining adapted L-form strains were able to grow with minimal osmoprotection (Figure 3.9), whereas the parent (LR2) could not, suggesting that these strains had picked up a mutation or mutations that enabled them to grow in these conditions. How reliably and robustly L-forms could grow in low osmolarities varied from strain to strain. The strains JB114, JB115 and JB118 were able to grow following inoculation into low osmotic media in ˜95-99% of the cases, for the other strains the ability to grow, was limited to roughly 50% of all inoculations.
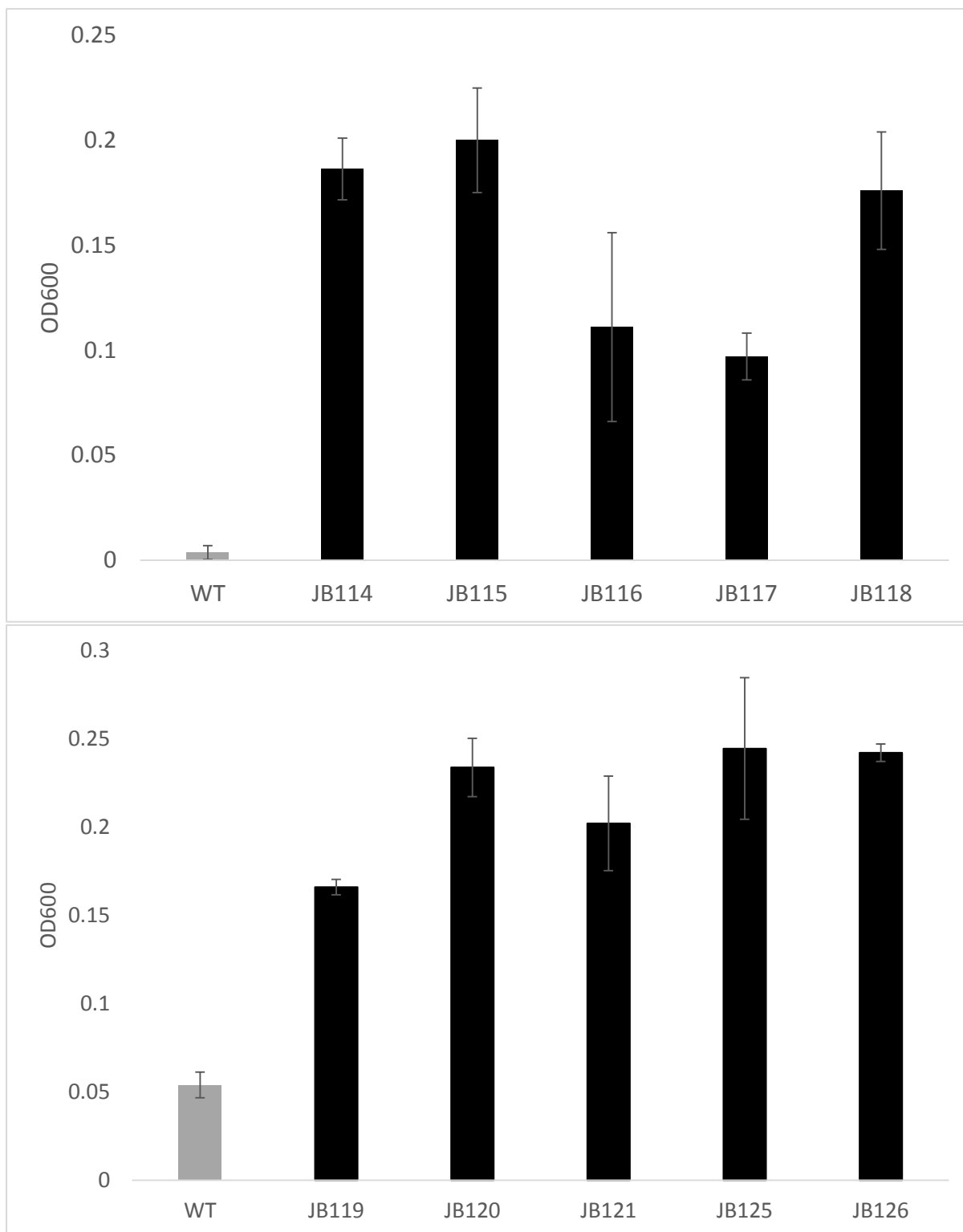
Figure 3.9. The L-form strains isolated from the adaptation experiment are able to regrow in low sucrose (A) or salt (B) concentrations. All the strains were grown in either 0.5 M MSM/NB or MNM/NB where appropriate before 10^{-3} dilutions into either 0.1 M MSM/NB (A) or 0.1M MSM/NB (B). OD_{600} was measured after 7 days incubation at 30°C. Errors bars represent the standard deviation of three replicates.

3.2.9 Growth of the adapted strains is identical to the parent strain under normal L-form growth conditions

As the adapted strains were able to grow in low osmotic media it was wondered whether the adaptations in these strains affected their ability to grow under normal growth conditions. To this end, L-forms were diluted to an $OD_{600}=0.05$ in either MSM/NB or MNM/NB and grown for 3 days at 30°C. All the strains had a growth rate roughly comparable to the parental LR2 strain (data not shown). It's possible that subtle differences do exist between the strains, though as a result of the heterogeneity of L-form division any differences have to be significant to be observed.

3.2.10 Mutants grown in the walled state exhibit a diverse array of growth rates

After the initial characterisation of the adapted strains in the L-form state the behaviour of the strains in the walled state was probed. On nutrient agar plates containing xylose the strains exhibited a multiplicity of colony morphologies (figure 3.10), this was unlike the M1 strain which appeared visually similar to the parental JB105 strain. Particularly striking were strains JB114, JB115 and JB118 which struggled to grow, forming small colonies. In addition, strain JB121 grew well initially but then underwent rapid lysis on the plate. JB125 growth was unremarkable, but appeared to develop suppressor mutants rapidly, that seem to improve the growth of the strain. Supplementation of media with magnesium chloride has long proved to be an effective remedy at restoring the growth of bacteria carrying mutations affecting the cell envelope. Addition of 20 mM $MgCl_2$ to the nutrient agar did indeed improve the growth of several of the strains, particularly those with the poorest growth.
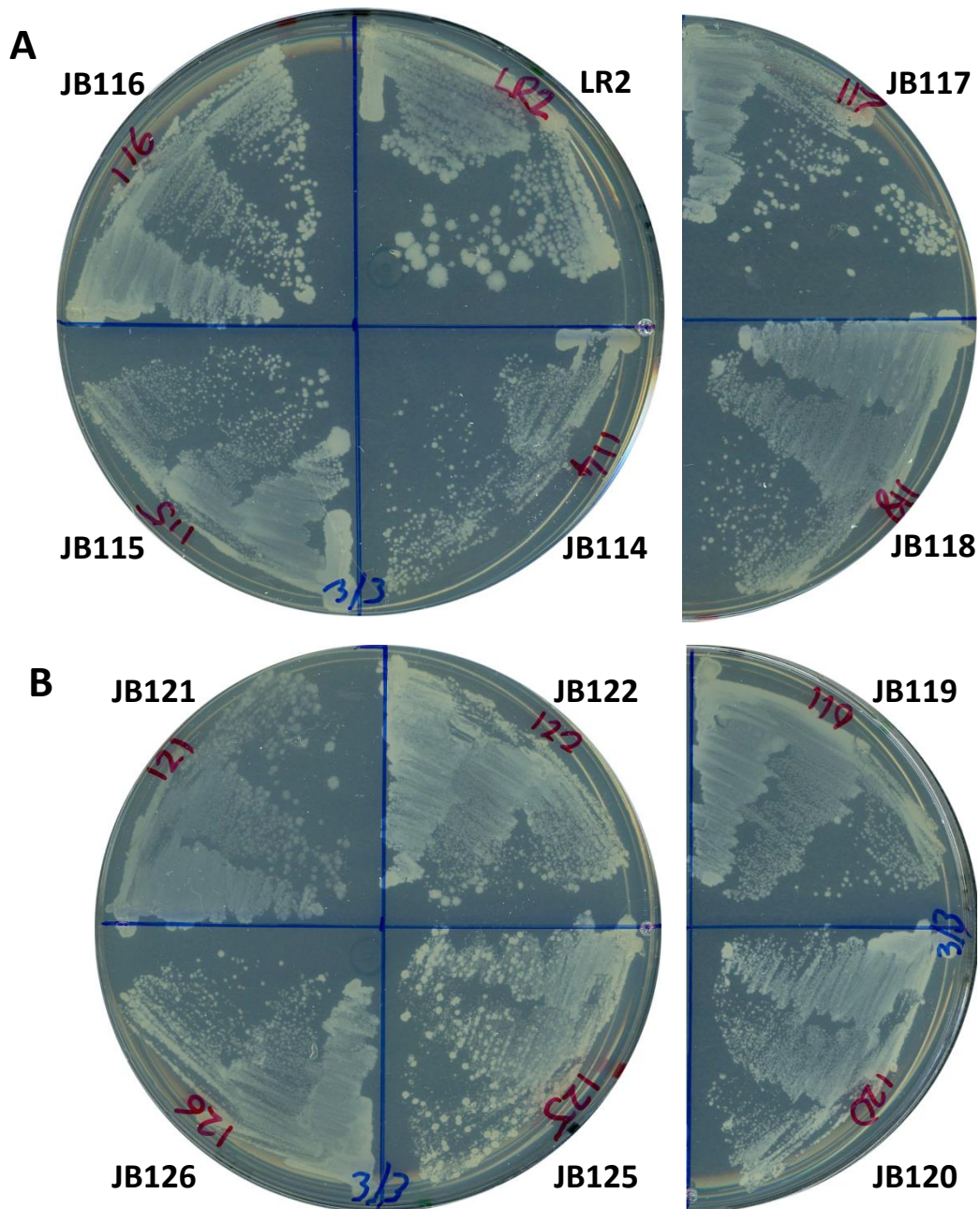
Figure 3.10. Colony morphologies of the osmoadapted strains on nutrient agar. The regenerated strains were streaked on nutrient agar containing 0.5% xylose and incubated overnight at 37°C. The strains adapted to sucrose are shown in (A), the salt adapted strains shown in (B).

To further characterise the mutants, the growth rate in PAB medium supplemented with xylose was measured in the presence or absence of 20 mM Mg^{2+}. As can be seen in figure 3.11 there was a great level of variation in the growth rate of the different strains regardless of whether 20 mM Mg^{2+} Is present. In particular, the growth of several of the salt-adapted strains, such as JB120, JB122 and JB125 was severely attenuated, with only minimal recovery following the addition of 20 mM $MgCl_2$. Growth of JB119, on the other hand, improved significantly with the addition of magnesium. Among the sucrose-adapted strains, JB114 had the poorest growth rate, though this was still superior to the rates seen with JB120, JB122 and JB125. JB115 appeared to have growth rate that ranked between that seen with JB114 and the parental LR2 strain.

Such a variety of growth rates and colony morphologies was very promising as it indicates that the strains have picked up a variety of different mutations. In addition the sensitivity to Mg^{2+} suggests some of these mutations involve the cell envelope – magnesium has been found to enable the recovery of a wide variety of mutations involving the wall such as *mbl* (Schirner and Errington, 2009), *ponA* (Murray et al., 1998) and *tagO* (D'Elia et al., 2006a).
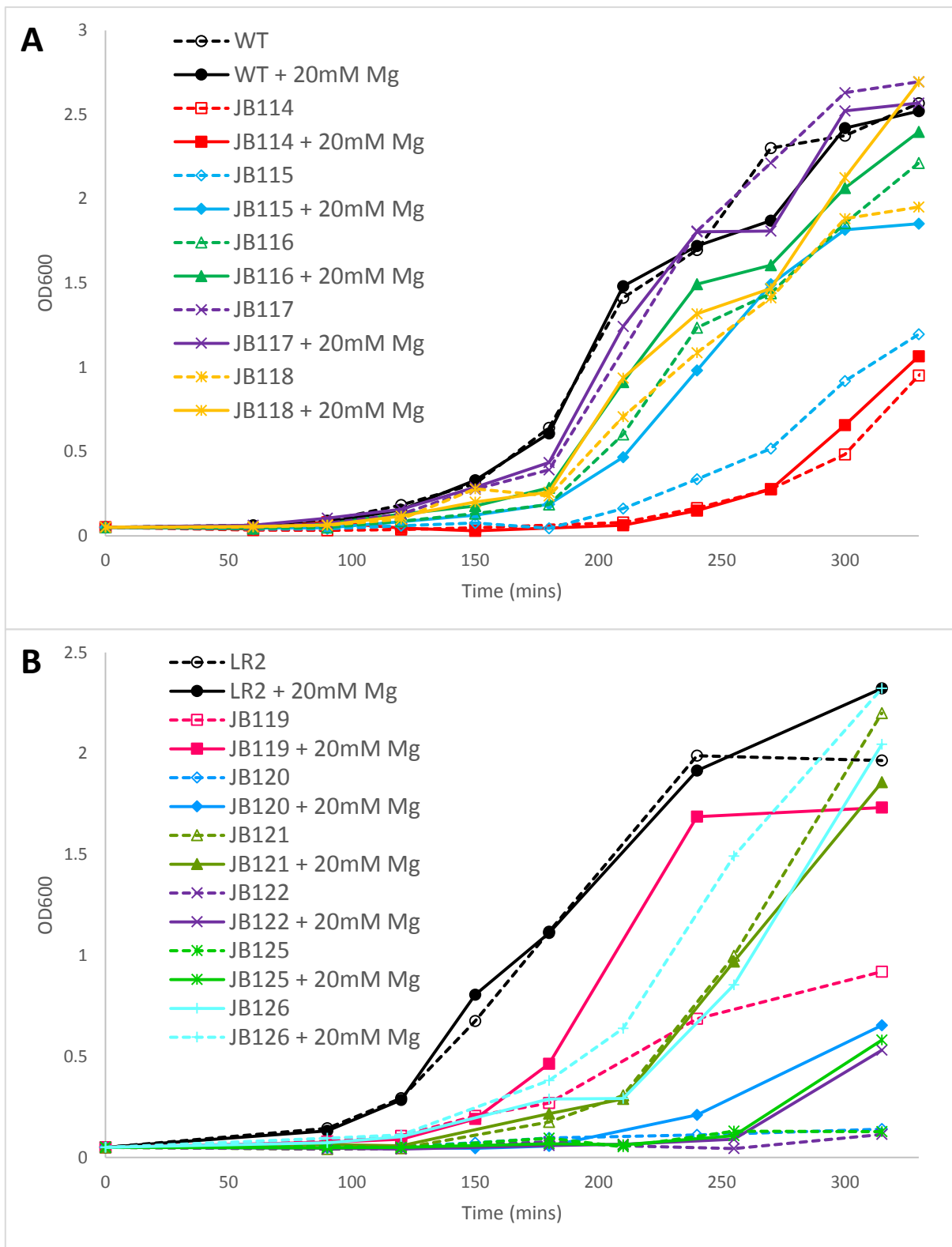
Figure 3.11. Growth rate of the strains adapted in sucrose (A) and salt (B) in the walled state. Strains were diluted to OD_{600}=0.01 in PAB+0.5 % xylose +/- 20 mM $MgCl_2$. Cultures were grown with shaking at 37°C with OD_{600} measured every 30 minutes.

3.2.11 Microscopy of the mutant strains display a multitude of phenotypes

To further characterise the strains the cells were examined using fluorescence microscopy during early exponential, mid exponential and stationary phases. A multitude of different phenotypes was observed for the various strains. The phenotype of the strains JB114 and JB115 was particularly arresting. As can be seen in figure 3.12, JB114 cells are very sick in the absence of Mg^{2+}, with pronounced dysregulation in the cell shape. Magnesium dependency was also observed with JB115, which displayed a similar morphology to JB114 during early exponential phase. However, unlike JB114 the morphology of JB115 generally recovered as the cells moved through exponential phase into stationary phase. Whilst the overall morphology did improve, the cells began to develop a curious budding/branching phenotype more reminiscent of *Streptomyces* rather than *Bacillus*. During stationary phase, where the branching phenotype is most pronounced, 12% of cells exhibited some degree of the branching or budding phenotypes. For comparison, in the parental strain 0% of cells demonstrated this phenotype. Some level of branching/budding was also seen in JB115 supplemented with 20mM $MgCl_2$ but at much reduced levels. To see how much cell division was affected in these mutants, a *zapA-gfp* construct was introduced into the strains. ZapA is a cell division protein that is recruited to the Z-ring and therefore a GFP-tagged copy allows for visualisation of the Z-ring positioning. As can be seen in figure 3.13 both strains displayed aberrant positioning of the Z-ring, though in JB114 this was far more pronounced. Unsurprisingly, the positioning of the Z-ring in JB115 improved during growth as the morphology improved as described earlier. These results show that the Z-ring does remain intact in growth, implying that the mutation is not directly involved in Z-ring formation. However, any substantial conclusion is not possible as the Z-ring mislocalisation phenotype could be arising as a result of a mutation in a protein directly involved in localisation of the Z-ring or as a result of a more general change affecting the cell shape (which would in turn affect the positioning).
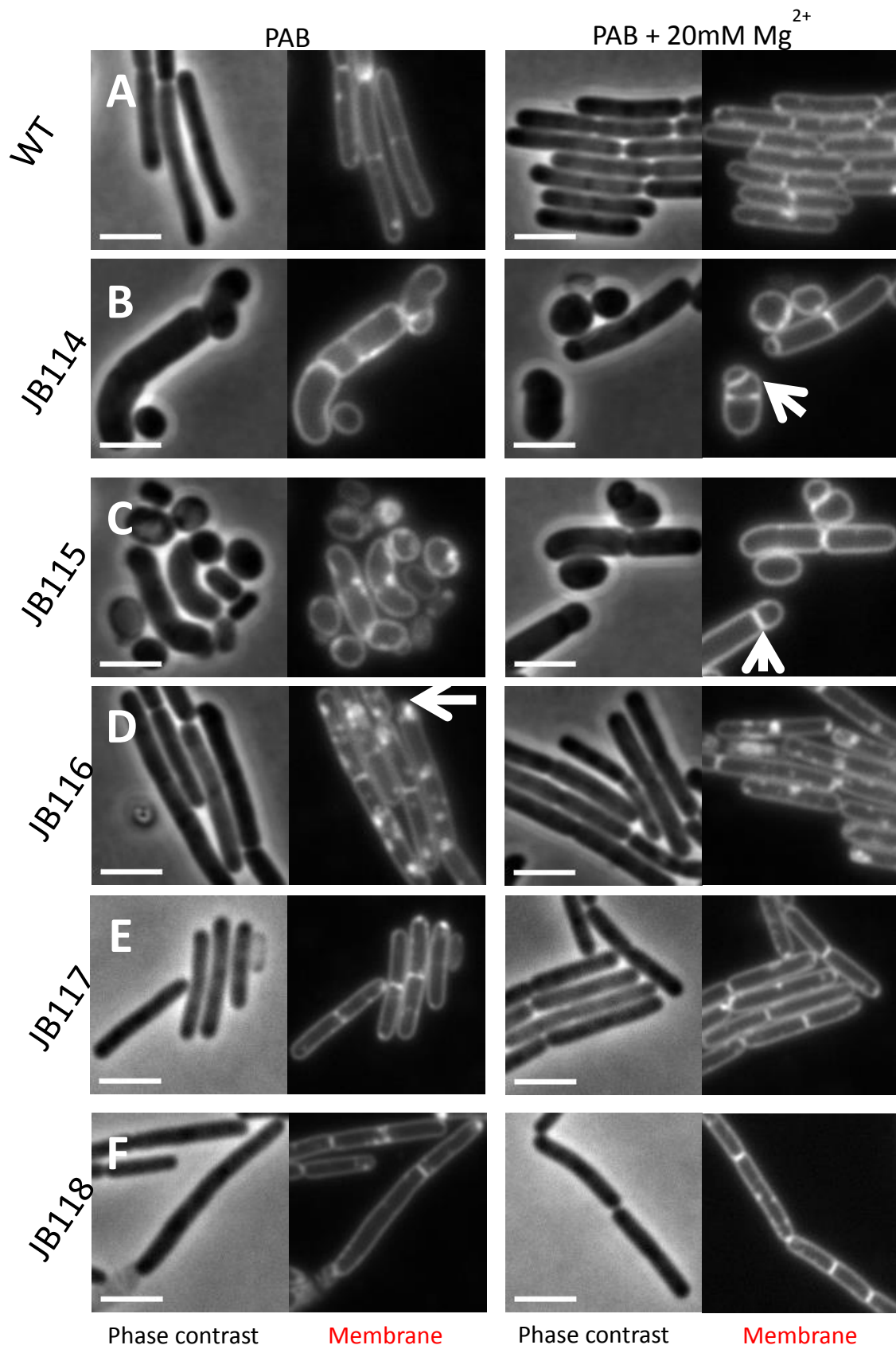
Figure 3.12.A. Cell morphology of the wild type (LR2;A), JB114 (B), JB115 (C), JB116 (D), JB117 (E) and JB118 (F) during early exponential phase (OD_{600}=0.3). Arrows in panel B

and C indicate misplaced septum. The arrow in panel E indicates membrane over production.
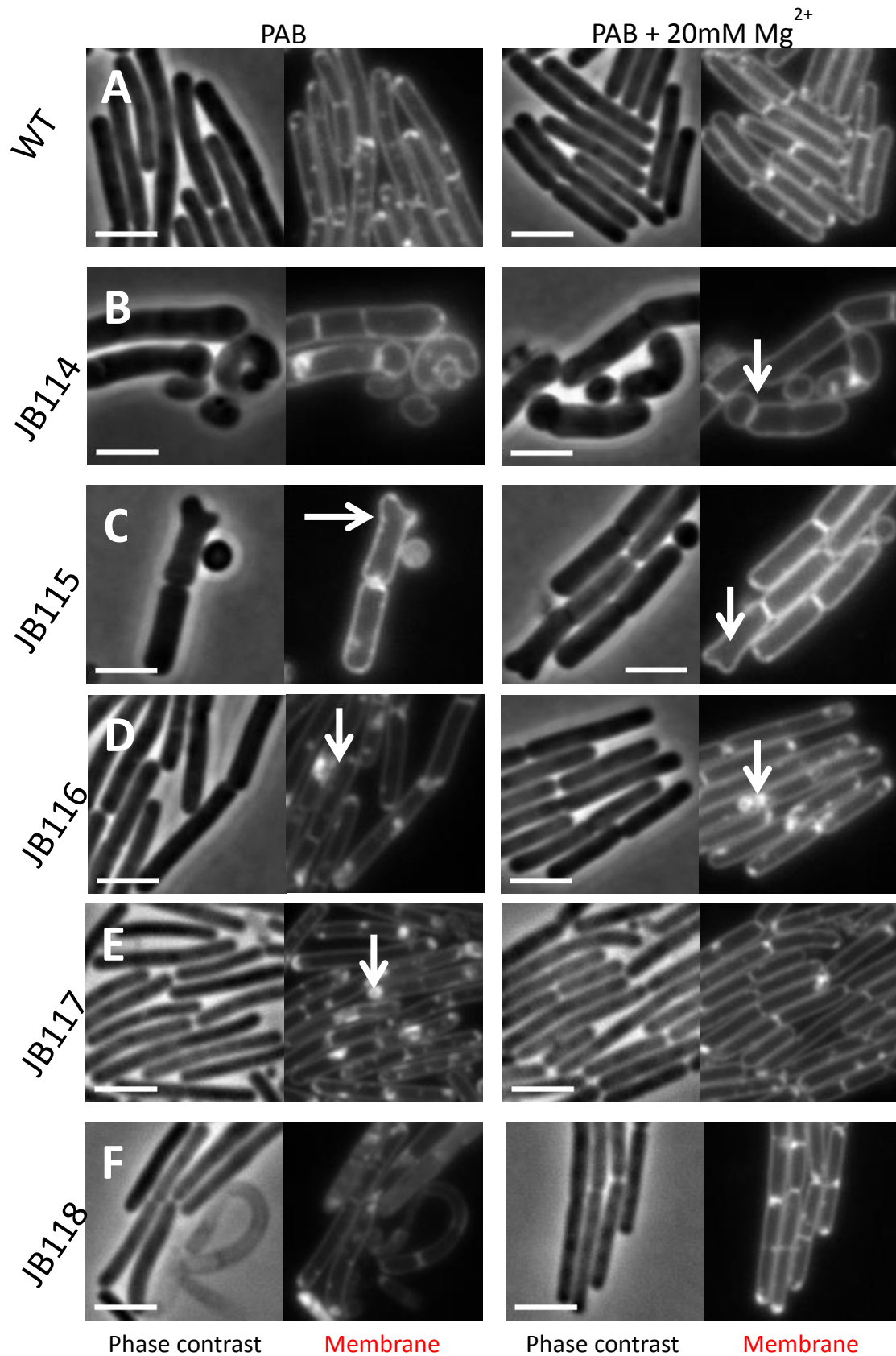
Figure 3.12.B Cell morphology of the wild type (LR2; A), JB114 (B), JB115 (C), JB116 (D), JB117 (E) and JB118 (F) during mid-exponential phase (OD$_{600}$=1.0). Arrow in panel B points to a misplaced septum. The arrows in panel C indicate the clubbing/early

branching described in the text. The arrows in panels D and E indicate the membrane overproduction.
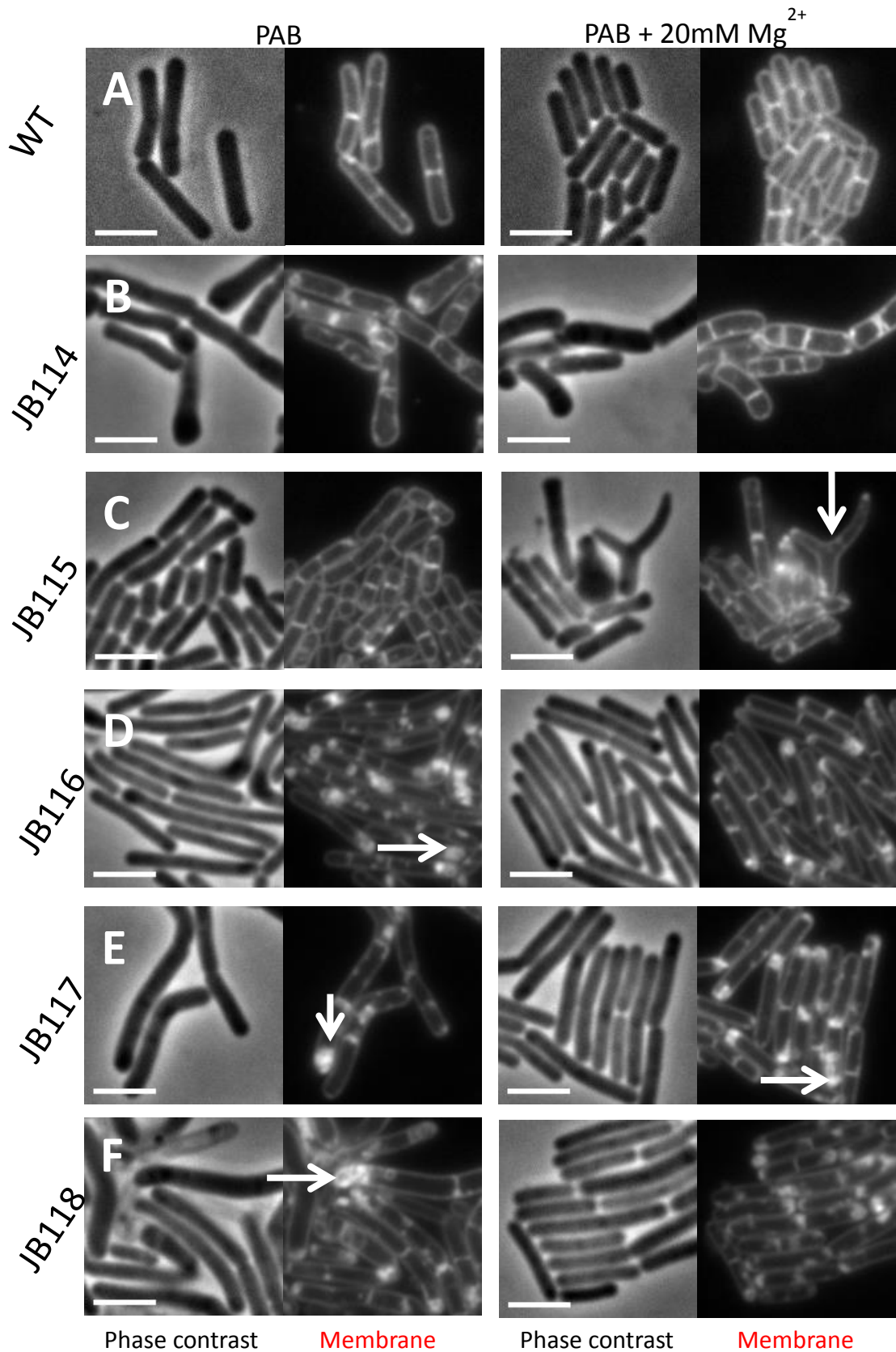
Figure 3.12.C Cell morphology of the wild type (LR2; A), JB114 (B), JB115 (C), JB116 (D), JB117 (E) and JB118 (F) during stationary phase. Arrow in panel C points to the budding in 10% of JB115 cells. Arrows in panels D, E and F point to membrane overexpression.

Phase contrast   GFP   Overlay

Phase contrast   GFP   Overlay
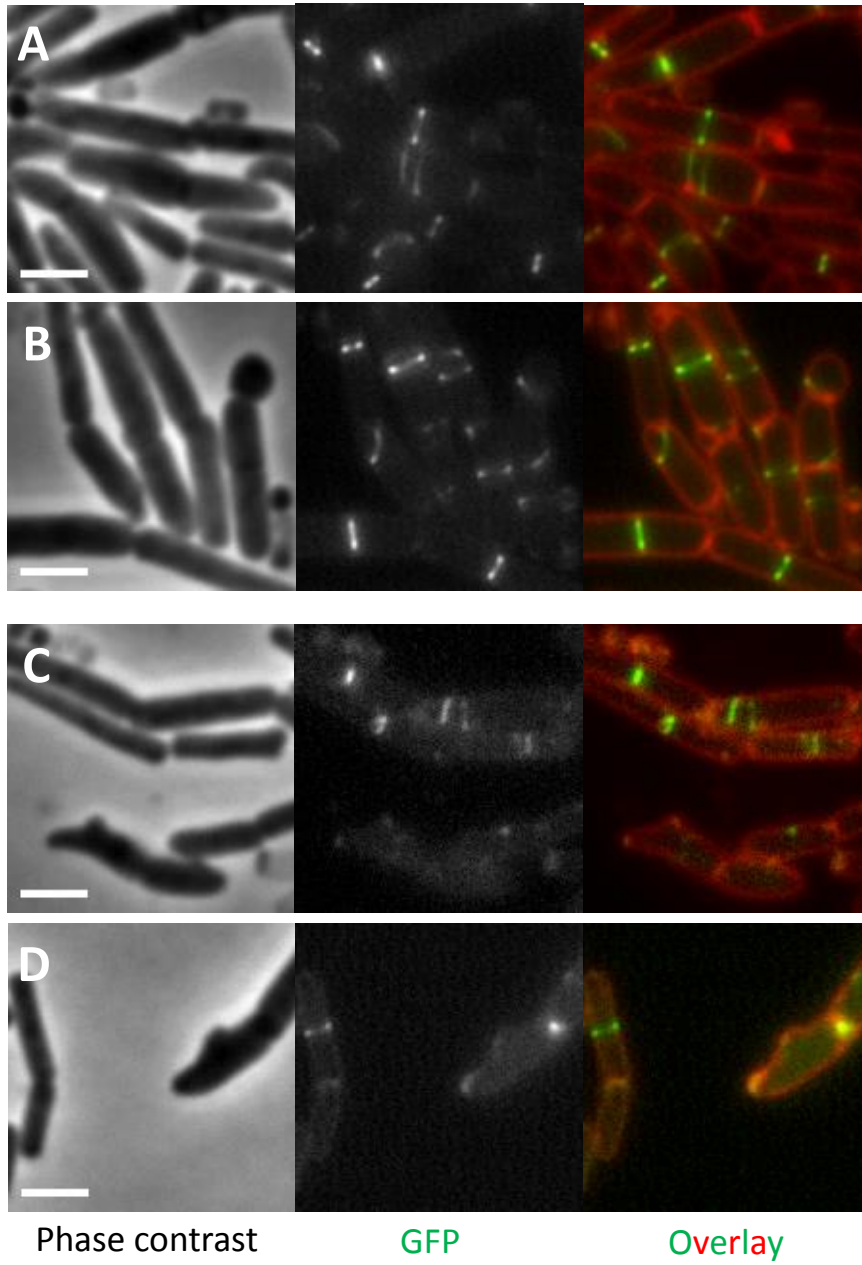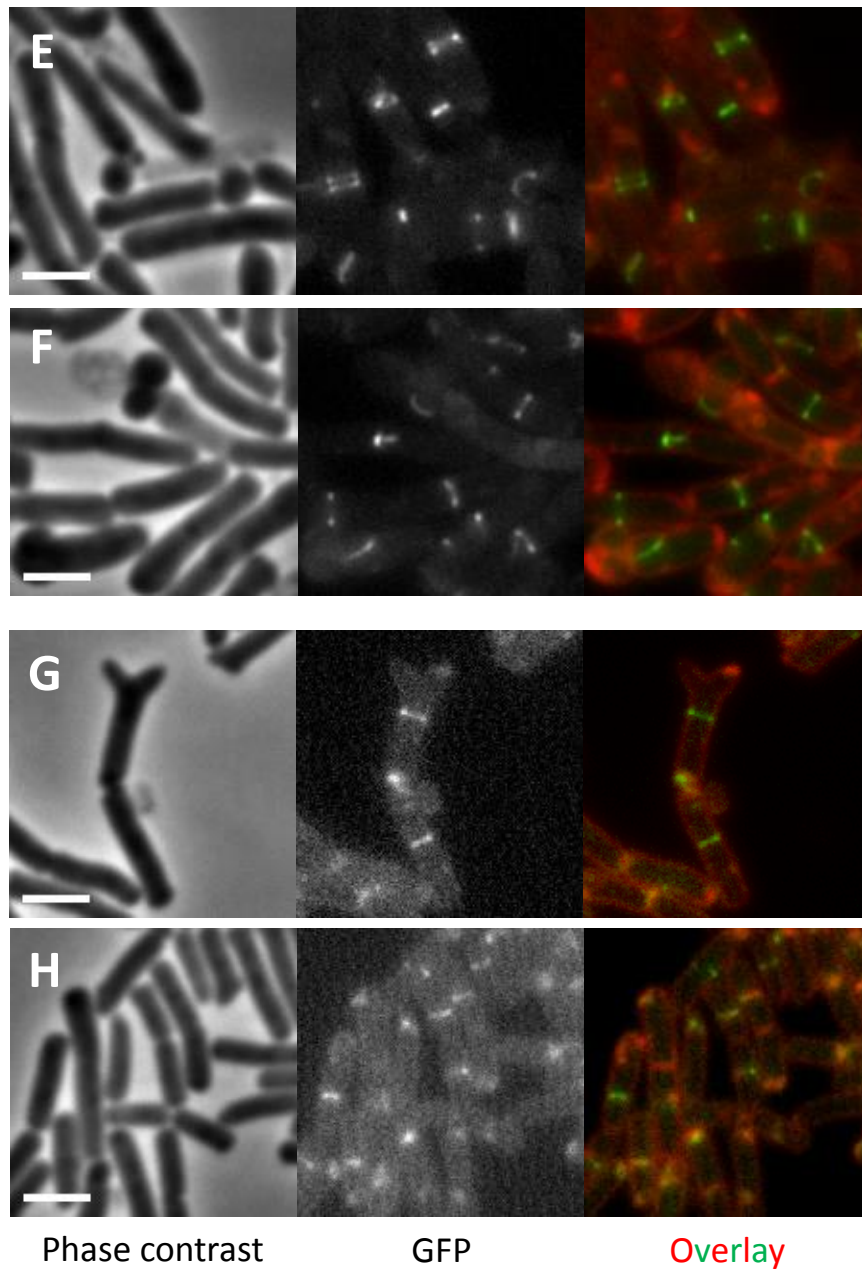
Figure 3.13. ZapA-gfp localisation in JB114 grown with (A) and without (B) 20mM Mg^{2+} and in JB115 grown with (C) and without (D) 20mM Mg^{2+} during mid-exponential phase and the localisation during stationary phase with the respective strains and conditions (E-H).

In contrast to JB114 and JB115, JB116 and JB117 have morphologies far more similar to the parental strain. Whilst their cell width and length is identical to LR2 (figure 3.12), they appeared to produce bundles of excess membrane, particularly towards the cell poles. The final sucrose adapted strain, JB118, was largely healthy, though appeared to suffer from lysis when grown in the absence of 20 mM magnesium. Interestingly, this lytic behaviour did not seem to affect the growth rate of the strain.

The first of the salt adapted strains, JB119 is perhaps one of the healthiest of the strains. Some cell shape perturbations were observed, but generally the cells were highly similar to the parent, with identical cell length and width to LR2. Strains JB120 - JB125 were remarkably sick with substantial changes to the cell morphology (figure 3.14), with significant levels of shape perturbations and high degrees of lysis. Taken with the growth rate results, these results were not that surprising, except in the case of JB121. This strain initially grows well on nutrient agar, but then undergoes rapid lysis. In addition, under the microscope the cells are morphologically aberrant. Remarkably, despite these observations, JB121 possesses a growth rate comparable to the parent strain. JB126 appeared as one of the healthier strains, without any significant growth defects. However, quantification of the cell length revealed a significant increase in both the cell length and width in comparison with the parent strain (figure 3.15). Cell length/width measurements were also made for a number of the other strains though the clear appearance of distinct phenotypes largely rendered these measurements unnecessary.
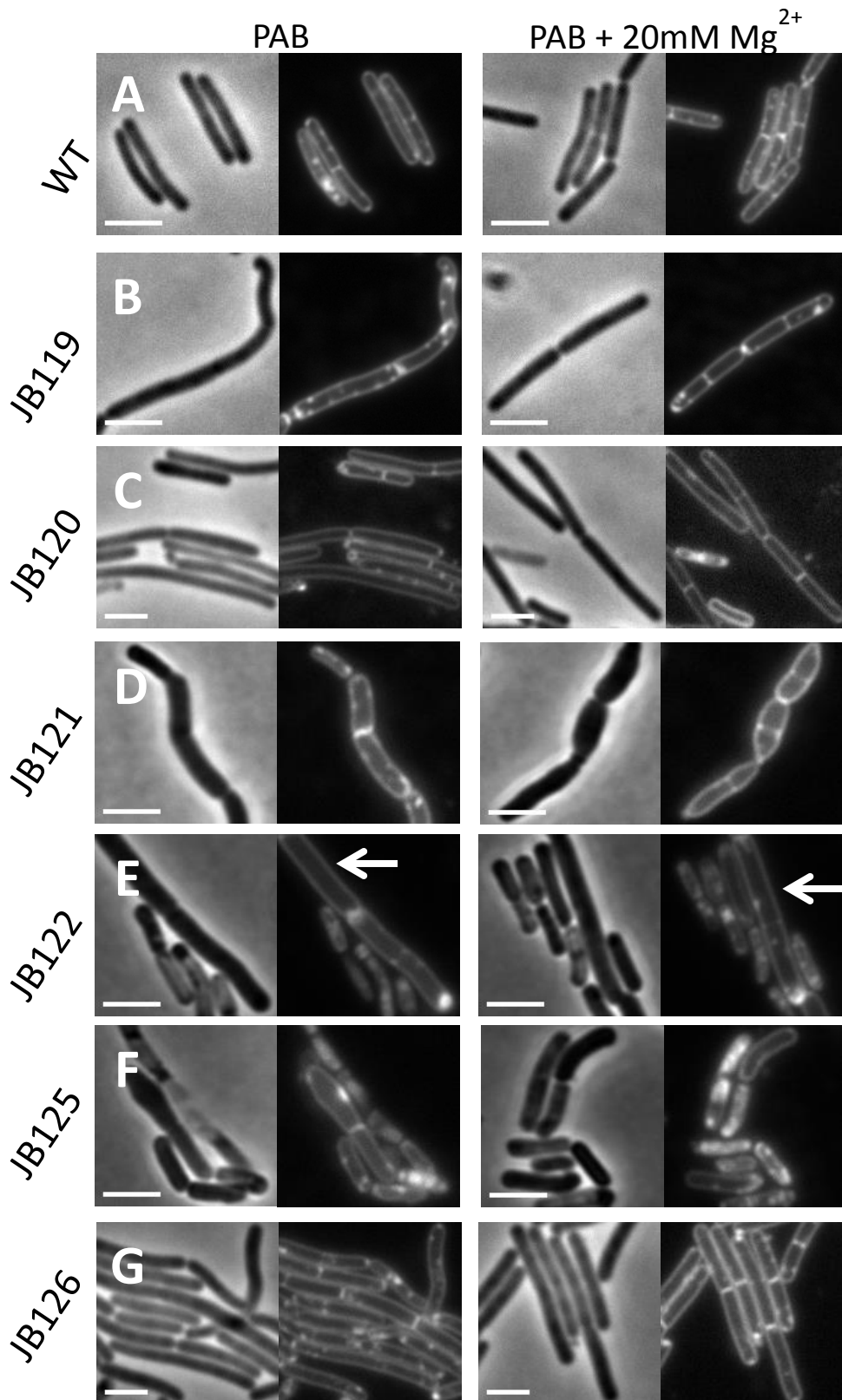
Figure 3.14.A. Cell morphology of the parent strain LR2 (A), JB119 (B), JB120 (C), JB121 (D), JB122 (E), JB125 (F) and JB126 (G) during early exponential phase (OD_{600}=0.3).The arrows in panels E highlight the long cells present in JB122. Scale bar = 3μm.
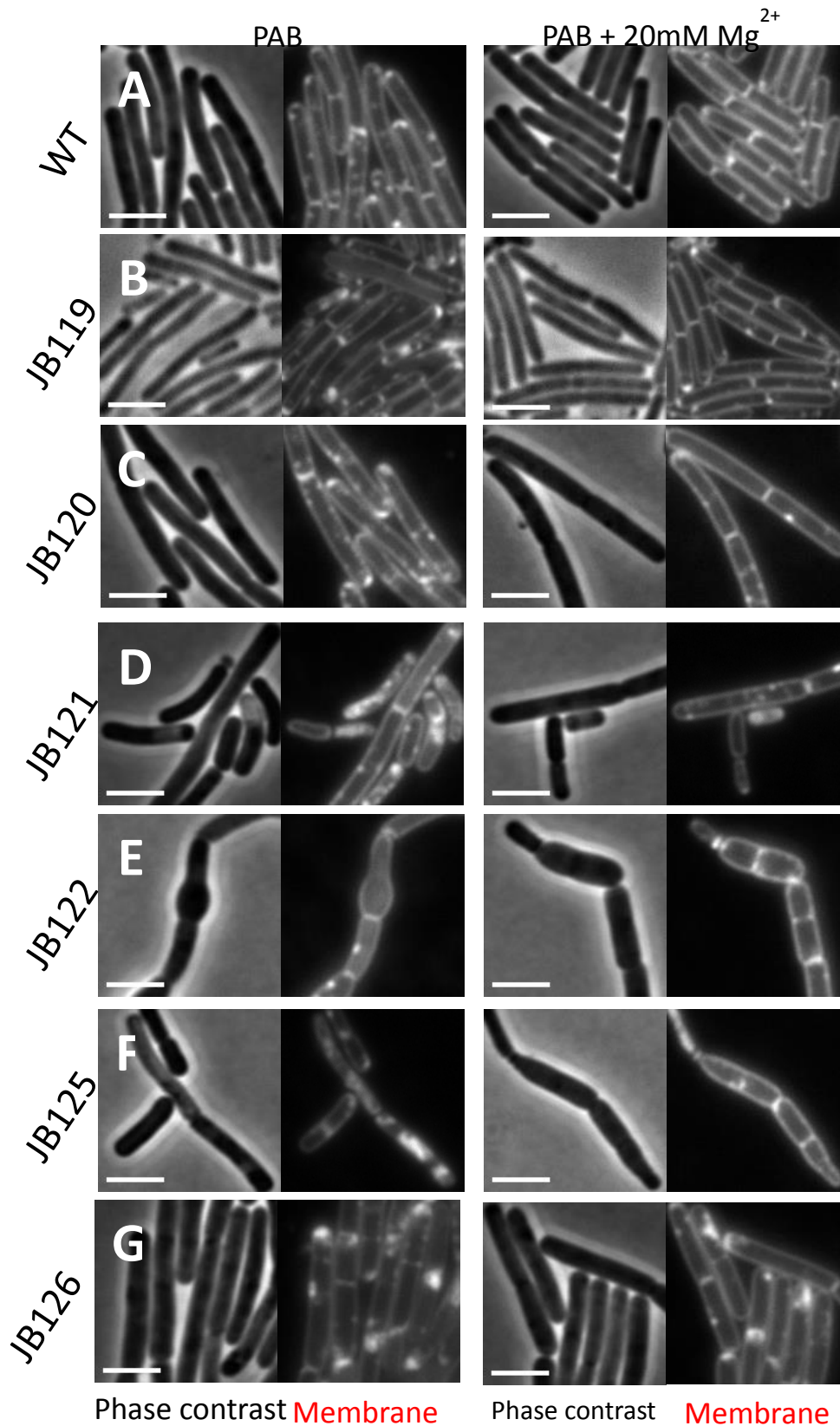
Figure 3.14.B Cell morphology of the parent strain LR2 (A), JB119 (B), JB120 (C), JB121 (D), JB122 (E), JB125 (F) and JB126 (G) during exponential phase (OD$_{600}$=1.0. Scale bar=3μm
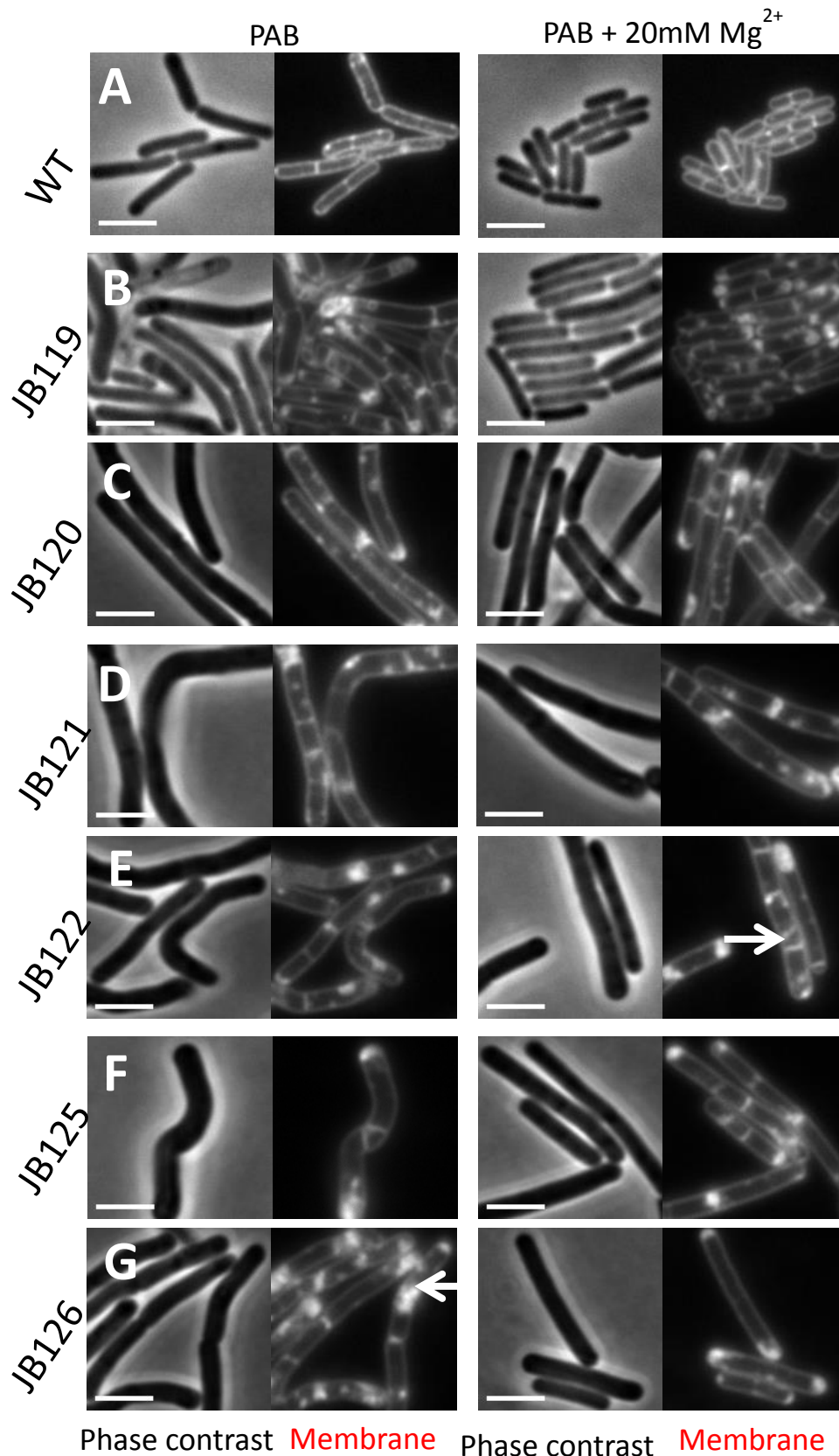
Figure 3.14.C Cell morphology of the parent strain LR2 (A), JB119 (B), JB120 (C), JB121 (D), JB122 (E), JB125 (F) and JB126 (G) during stationary phase. Arrow in panel E

highlights aberrant septa, whilst the arrow in panel G indicates membrane

overexpression.
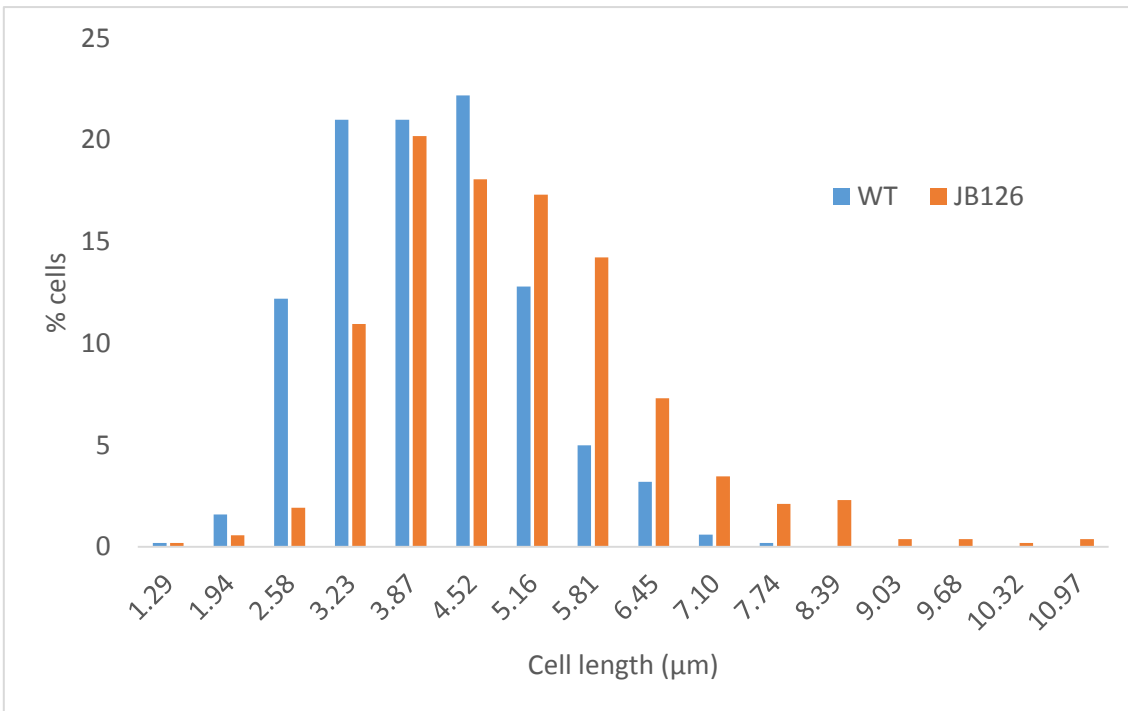
Figure 3.15. Cell length of strain JB126 in comparison to the wild type strain (LR2) when grown in PAB supplemented with 20 mM $MgCl_2$. Cell length was measured during mid-exponential phase (OD_{600}=1.0); at least 500 cells were measured for each strain.

It was feared that one or more of the phenotypes might have arisen due to mutations in the P$_{xyl}$ promoter, which controlled the expression of the *murE* gene essential for the growth of the walled cells, resulting in a depletion of MurE. To test for this possibility xylose was titrated away from LR2. As expected, a reduction in xylose levels did result in morphological aberrations in strain LR2 (figure 3.16). However, the aberrations observed in the mutant strains appeared quite distinct from those seen for LR2 in the absence of xylose. Therefore it seemed likely that xylose or the absence of xylose was not responsible for the phenotypes presented above.

Early exponential **Late exponential**

Phase contrast Membrane Phase contrast Membrane
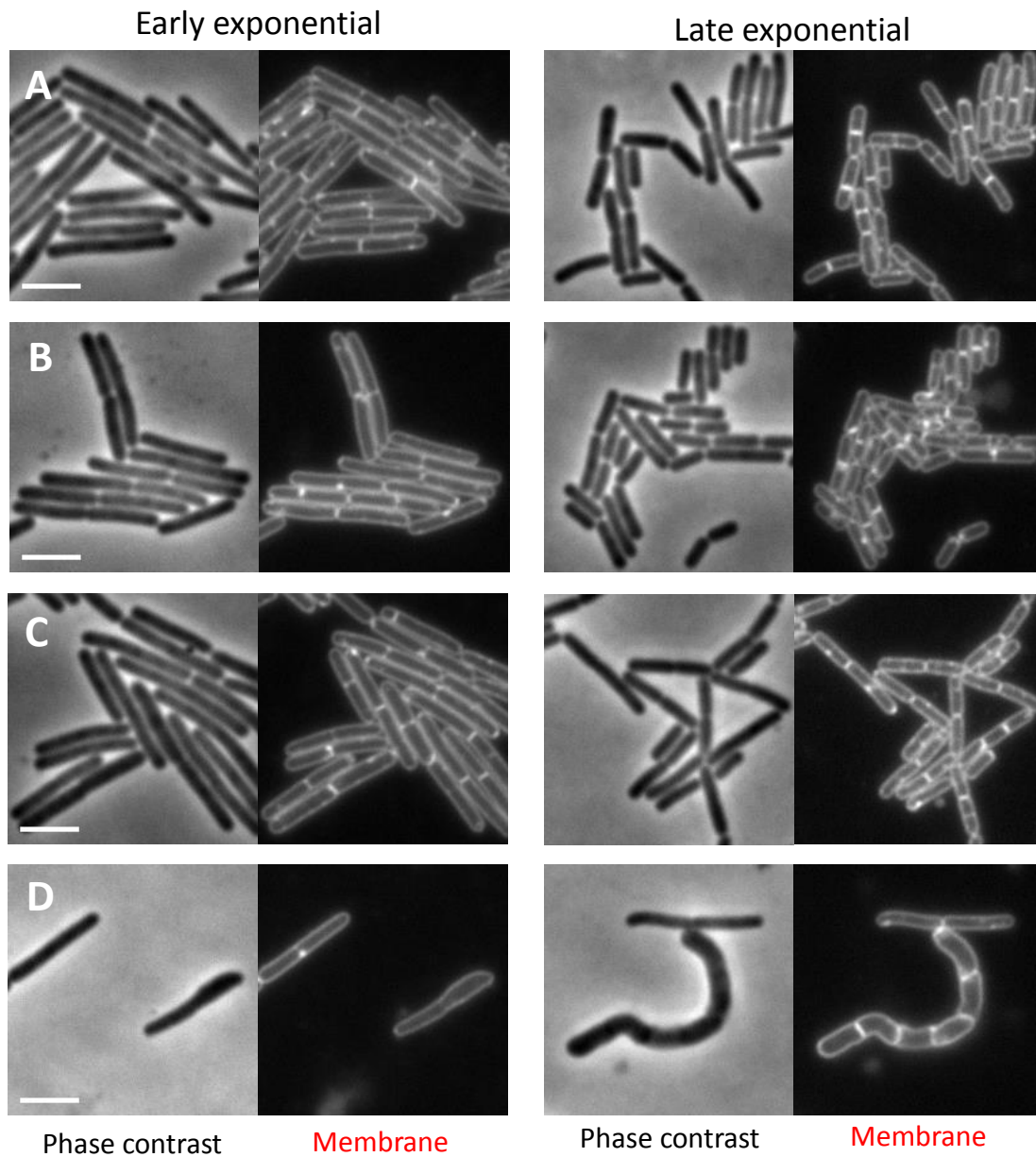
Figure 3.16. The effect of decreasing concentrations of xylose on the cell morphology of the wild type strain (LR2). Cells were grown in PAB supplemented with 20mM $MgCl_2$ and 0.5% (A), 0.25% (B), 0.125% (C) or no (D) xylose.

3.2.12 Genome sequencing of the adapted strains revealed a range of mutations

After the initial characterisation of the adapted strains it was clear that a number of mutations were present. To identify the mutation(s) responsible for the ability to grow in low osmotic media, the genomes of all the strains isolated as well as the wild type strain were determined by sequencing using an Illumina MiSeq system. The mutations detected are listed in table 3.4. Mutations of interest were validated by PCR then sequencing the relevant regions using Sanger sequencing. The full list of mutations, including those present in the parent strain are given in appendix 4.

Gene	Description	Coding region change	Amino acid change
		M1	
yhaG/trpP	Tryptophan uptake		81% deletion
yhaH	Unknown		Complete deletion
scoC	Transcriptional repressor	3541bp deletion	Complete deletion
yhaI	Unknown		Complete deletion
yhaJ	Putative bacteriocin		Complete deletion
		JB114	
mreB	Cytoskeleton	568/60bp del	I192>I211del
ftsE	ABC transporter/autolysis	523/G>T	E175*
pit	Phosphate transporter/proton symporter	932/ins TG	W331*
nucA	Membrane associated nuclease	163/delA/insCG	T55R
adeC	Adenine deaminase	1654/delT	L552*
accD	Acetyl-CoA carboxylase	789/T>C	N/A
yvgJ	Lipoteichoic acid synthesis primase	194/AC>GG	N65R
		JB115	
mreB	Cytoskeleton	568/60bp del	I192>I211del
rpoB	RNA polymerase	3181/C>A	Q1061K
nucA	Membrane associated nuclease	163/delA/insCG	T55R
adeC	Adenine deaminase	1654/delT	L552*
accD	Acetyl-CoA carboxylase	789/T>C	N/A
yvgJ	Lipoteichoic acid synthesis primase	194/AC>GG	N65R

JB116

Gene	Function	Mutation	Effect
ydbL	Unknown	874/G>C	A292P
hom	Homoserine dehydrogenase	568<>711/inversion	48aa inversion
yqhY	Unknown	38/delA	D13*

JB117

Gene	Function	Mutation	Effect
	Intergenic	1731572 delA	
hom	Homoserine dehydrogenase	641/90bp deletion	F214>G243 del
yqpP-yodU	SPβ prophage	134.4kb deletion	N/A
nucA	Membrane associated nuclease	163/delA/insCG	T55R
adeC	Adenine deaminase	1654/delT	L552*
yrdQ	Transcriptional regulator	865/T>G	STOP289E
accD	Acetyl-CoA carboxylase	789/T>C	N/A
yvgJ	Lipoteichoic acid synthesis primase	194/AC>GG	N65R

JB118

Gene	Function	Mutation	Effect
nucA	Membrane associated nuclease	163/delA/insCG	T55R
adeC	Adenine deaminase	1654/delT	L552*
yrdQ	Transcriptional regulator	865/T>G	STOP289E
accD	Acetyl-CoA carboxylase	789/T>C	N/A
yvgJ	Lipoteichoic acid synthesis primase	194/AC>GG	N65R

JB119

Gene	Function	Mutation	Effect
acdA	acyl-CoA dehydrogenase	709/ 126bp deletion	K237>Q279 del
gbsB	Glycine betaine synthesis	965<>1097/ inversion	44aa inversion
ytzB	Unknown	89/insT	S31*

yqhY	Unknown	38/delA	D13*

JB120

nucA	Membrane associated nuclease	163/delA/insCG	T55R
adeC	Adenine deaminase	1654/delT	L552*
yrdQ	Transcriptional regulator	865/T>G	STOP289E
accD	Acetyl-CoA carboxylase	789/T>C	N/A
ytzB	Unknown	89/insT	S31*
yvgJ	Lipoteichoic acid synthesis primase	194/AC>GG	N65R
yqhY	Unknown	38/delA	D13*

JB121

nusG	Antitermination factor	227/G>A	W76STOP
ppsB	Plipastatin synthetase	3218/C>G	A1043G
nucA	Membrane associated nuclease	163/delA/insCG	T55R
adeC	Adenine deaminase	1654/delT	L552*
yrdQ	Transcriptional regulator	865/T>G	STOP289E
accD	Acetyl-CoA carboxylase	789/T>C	N/A
ytzB	Unknown	89/insT	S31*
yvgJ	Lipoteichoic acid synthesis primase	194/AC>GG	N65R
yqhY	Unknown	38/delA	D13*

JB122

ribT	Unknown	242G>C	G81A
adeC	Adenine deaminase	1654/delT	L552*
yrdQ	Transcriptional regulator	865/T>G	STOP289E

accD	Acetyl-CoA carboxylase	789/T>C	N/A
ytzB	Unknown	89/insT	S31*
yvgJ	Lipoteichoic acid synthesis primase	194/AC>GG	N65R
yqhY	Unknown	38/delA	D13*
JB125			
blt	Spermidine efflux	28/ 159bp deletion	T10>P63 del
yhfC	Unknown	526/ 153bp deletion	L176>I229 del
ytzB	Unknown	89/insT	S31*
yqhY	Unknown	38/delA	D13*
JB126			
rrnG-23S	rRNA	T>C	N/A
yvrJ	Unknown	452bp	Loss of gene
ytzB	Unknown	89/insT	S31*
yqhY	Unknown	38/delA	D13*
	Intergenic	176143 delT	N/A
	Intergenic	176185^6 insC	N/A

* denotes frame shift mutation

Table 3.4. Strains isolated from the adaptation experiment and the mutations they carry. Table lists the unique SNPs and structural variations identified in each strain and the effect these have on the translated protein. Mutations found in the wild type strain (LR2) are not listed.

The sequencing revealed a series of common SNPs that are present in most of the osmomutants but are absent in the parent strain. As several of the strains isolated do not apparently carry unique mutations, it seems likely that the diverse phenotypes observed in these strains resulted from the mutations identified. Where these mutations arose is not clear.

Perhaps the most interesting mutation is that seen in the strains JB114 and JB115. Both of these strains carried an identical 60bp in-frame deletion in *mreB*. That they carried the same mutation is not wholly remarkable, being that they were both derived from the same starting culture in the adaptation experiment. What is surprising is the mutation itself. MreB has long been associated primarily with directing and coordinating the various components of the cellular machinery involved in peptidoglycan synthesis during cell elongation (Errington, 2015). Further, it is very curious that the two strains have such differing phenotypes, despite the identical mutation in *mreB*. It is therefore likely that one or all of the mutations presumed to be 'secondary' have an effect on the health of the strain(s) and perhaps a role in the ability to grow in low osmotic conditions. JB114 and JB115 and the mutations they carry will be explored in greater detail in the next chapter.

Several of the genes identified in the sequencing, such as *gbsB* have a known role in osmoprotection (Boch et al., 1996), or like *acdA* and *blt*, affect membrane fluidity (Fujita et al., 2007, Woolridge et al., 1997), a property that has been associated with L-form growth in hypotonic conditions previously (Harold, 1964). Several of these mutations were recreated in the wild type background (LR2). However, preliminary testing did not indicate a clear osmoprotective role for these mutants and were therefore not pursued further (data not shown).

Many of the additional mutations such as the complete loss of the prophage SPβ from the genome have no clear involvement in the regulation of osmosis, and a further number of mutations are in genes of unknown function. These mutations have not been investigated further in this work.

3.2.13 Deletion of *scoC* enables growth in low sucrose environments

As befits the first mutant to be isolated, M1 was also the first to be sequenced. As shown in table 3.4 this strain lost a 3.8kb region resulting in the complete loss of five genes (*scoC, yhaG, yhaH, yhaJ* and *yhaI*). Amongst these genes was *scoC* (also referred to as *hpr* or *catA* in the literature), a transcriptional repressor of the App and Opp peptide transporters (though App exists as a pseudogene in the 168CA background) (Koide et al., 1999). It had been shown that these transporters are involved in the uptake of proline rich peptides, with the subsequent degradation resulting in an increase in the compatible solutes within the cell (Zaprasis et al., 2013). Therefore out of the five genes deleted, it seemed likely that *scoC* was the most important, though the other genes were later deleted. A *scoC* deletion strain was therefore constructed and the L-forms derived from this strain were able to survive and grow in 0.1 M MSM/NB. The other mutations (*yhaG, yhaH, yhaJ* and *yhaI*) had no effect on the ability of LR2 L-forms to grow in low sucrose conditions. Oddly, complementation of *scoC* in the M1 with *scoC* expressed under its native promoter at the *amyE* locus did not abolish the ability to grow in 0.1 M MSM/NB, though L-form viability in these conditions was reduced (figure 3.17).
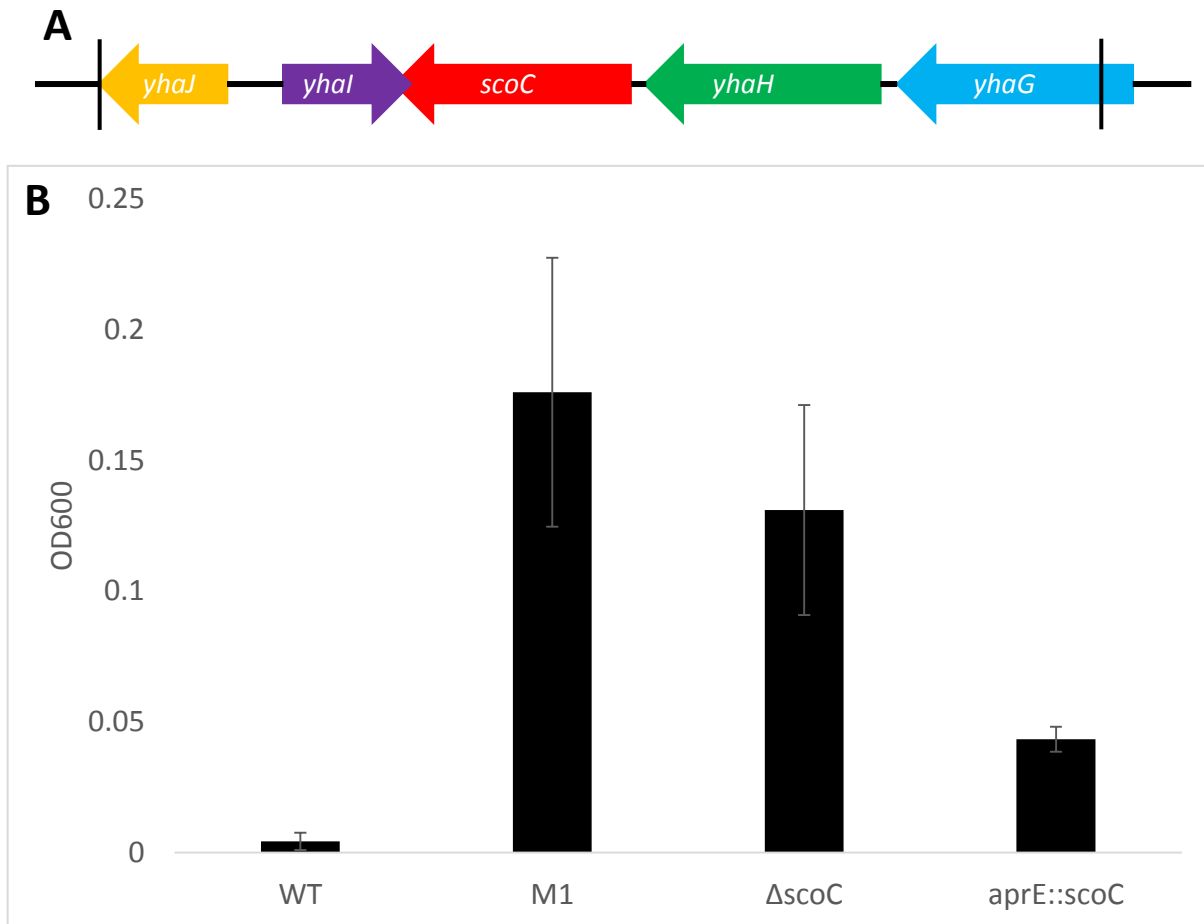
Figure 3.17. The effect of Δ*scoC* on L-form growth in low osmotic media. **A.** Schematic diagram of the 3.8kb deletion in M1. Vertical bars represent the limits of the deletion. Confluent arrows between *yhaI* and *scoC* indicate overlapping exons. **B.** Growth of the wild type (LR2), M1, Δ*scoC* (JB132) and LR2 *aprE::scoC* (JB156) in 0.1 M MSM/NB after 9 days at 30°C.

3.3 Discussion

In the past L-forms have been demonstrated to be able to grow in media with minimal levels of osmoprotection. However, as explained in the introduction, these studies were carried out in an age when L-form biology was poorly characterised, with low levels of reproducibility and challenges in ensuring 'true' L-forms were being used. Therefore it can be considered that this work provides the first evidence in a reproducible, well defined system that L-forms can indeed survive and grow in low osmolarities. The presence of a broad range of phenotypes suggests that the method allows for the acquisition of multiple different mutations. That many of these mutations appear to affect the cell envelope is of some interest. It is possible that the techniques utilised in this work allowed for the accumulation of mutations that might not otherwise have arisen in the conventional walled state, as it allowed for the development of mutants that were involved in stress responses, but were otherwise selected against in the walled state due to fitness costs. It is possible that the requirement for growth in the walled state by the adapted L-forms selected against strains that had developed mutations that allowed them to grow in low osmolarities, but not in the walled state. It may be of interest to repeat the established adaptation experiment in the future, but to sequence the genomes of the L-forms immediately after growth in low sucrose or salt environments. It is possible that such a protocol would enable a greater number of interesting mutations to be found.

By far the most significant mutation is the 60bp in-frame deletion observed in the strains JB114 and JB115. This was surprising as MreB is primarily involved in peptidoglycan synthesis along the lateral cell wall, by directing and coordinating the elongation machinery (Errington, 2015). Further, it has been shown that MreB filaments dissociate from the cell membrane in the absence of cellular lipid II (Schirner et al., 2015), a molecule that is not present in L-forms derived from LR2. Alongside this work, it had previously been shown that *mreB* is redundant when cells are in the L-form state (Mercier et al., 2012). It therefore seemed likely that *mreB* would have no role in the cell wall-less L-forms. This no longer appears to be the case. As this is such an important and fascinating mutation and so will be focussed on for the remainder of the investigations into L-form growth in low osmotic conditions.

Whilst such mutations as the one seen in *mreB* is exciting, it is reassuring that the adaptation of L-forms to low osmolarities also identified several genes which have a known role in response of walled *B. subtilis* to changes in its osmotic environment. These genes, such as *gbsB* and *scoC,* act by mediating the levels of compatible solutes within the cell. Disruption of these genes would be expected to affect the ability of the bacterium to maintain the pools of compatible solutes. In the case of *scoC*, it would be expected that the loss of this gene would result in an increase in the level of proline within the cell as a result of the de-repression of the Opp transporter. How an increase in the levels of compatible solutes would protect the L-forms from low osmolarities is unclear, as generally it would be imagined that this would increase the osmotic gradient across the membrane. As this is mostly speculation, further investigation would require examining the role of the Opp system – for example, to see whether disruption or overexpression would result in increased or decreased resistance to low osmotic environments. Assuming that proline import allows for L-form to survive and grow in low osmotic conditions, use of radioactive proline may be helpful in following what is going on inside the cell.

Due to time constraints many of the mutations identified in this work were not pursued further. It would be an interesting avenue of future research to explore these mutations in greater depth. Not only do many of the genes affected not have a clear role in response to osmotic response, their role in the generation of the broad range of morphologies is also unclear. Further research into these genes and their mutations may prove useful in uncovering the response of L-forms to low osmolarities, but also in understanding the control of cell morphogenesis in the normal walled state.

This work had established reproducible methods that allow for the adaptation of L-forms to low osmolarities. Whilst this work only utilised L-forms derived from the Gram-positive model organism *Bacillus subtilis* there is no theoretical reason why the methods generated could not be extended to L-forms derived from other bacterial species. This includes pathogenic bacteria that have been implicated in L-form mediated chronic or recurrent bacterial infections. Current work on this issue is limited by the difficulty and complexity of establishing L-forms in relevant disease models. Development of osmotically stable versions of these strains may allow for greater ease

at investigation of possible roles L-forms may play in disease. It would be interesting to examine what mutations enable different species to grow in low osmolarities and whether the mutations generated would reflect the physiology of the host species. Similarly, such an approach may allow for fresh investigations into the relationship that *B. subtilis* plays with plants. Unlike their association with mammalian tissues, the relationship between L-forms and plants is thought to be symbiotic (Walker et al., 2002, Ferguson et al., 2000). As with the infection models, robust investigation into this subject has been limited, partly due to the difficulty in establishing L-form growth in these systems.

As such this work provides some support towards somewhat controversial theories that consider L-forms an aetiological agent for a number of chronic or recurrent bacterial infections (Leon and Panos, 1976). One of the major criticisms of this hypothesis regards the fragility of the L-form cells; the results of this work would disagree with such a statement.

Finally, the simple fact that wall-less cells could propagate in low osmo-protectant environments is somewhat surprising. The prevailing wisdom is that under normal conditions the peptidoglycan cell wall is essential; it is necessary to resist the effects of turgor pressure acting against the cell. As such, this work validates the older work demonstrating that L-forms could survive in low osmolarities. In addition, it suggests that regulation of the membrane and the internal composition of the bacterial cell may be far more important in relation to the cell wall in resisting the effects of turgor.

4. The role of MreB in osmoresistance in L-forms

4.1 Introduction

4.1.1   MreB and the bacterial cytoskeleton

The MreB proteins are homologues of the eukaryotic actin and are highly conserved and widespread amongst both Gram-positive and Gram-negative bacteria that have adopted a complex, non-spherical cell shape (Errington, 2015). Unlike Gram-negative organisms that often only encode a single MreB homologue, Gram-positive organisms tend to carry two or three homologues. The Gram-positive model organism, *Bacillus subtilis* is no exception, carrying three paralogues of MreB – Mbl (**M**re**B**-**l**ike) and MreBH (**MreB h**omologue) in addition to MreB.

Traditionally, these proteins have been proposed to be involved in the positioning and regulation of the cell division machinery, thereby controlling cell shape (Daniel and Errington, 2003, Challis, 2014). More recently, it has been shown that MreB in *B. subtilis* is involved in the organisation of the cell membrane (Strahl et al., 2014), though it has been proposed that this organisation of the membrane is to facilitate colocalisation between MreB and the peptidoglycan precursor molecule lipid II (Schirner et al., 2015). The same work shows that this colocalisation is important, as lipid II stimulates the polymerisation of MreB into filaments. The nature of these filaments has proved to be somewhat controversial, with a conflict between the theory that MreB forms filaments along the longitudinal axis of the cell (Jones et al., 2001) and the alternative view that MreB instead forms discrete, dynamic processive patches that traverse the cell (Dominguez-Escobar et al., 2011, Garner et al., 2011). As stated earlier, *B. subtilis* possesses three MreB homologues. It has been demonstrated that all three colocalise and interact with each other and with other interaction partners. The three homologues have differentiated, but overlapping functions (Defeu Soufo and Graumann, 2004, Kawai et al., 2009).

All the functions that have been ascribed to MreB are in relation to the maintenance and regulation of the peptidoglycan cell wall – a structure that is absent in L-form bacteria. Despite this, a mutation in *mreB* was identified in the genome of two related strains that possessed the ability to grow in low osmolarities as L-forms. Here I show *in vitro* and *in vivo* that the small deletion in *mreB* present in the osmo-resistant strains JB114 and JB115 has the same phenotypic effect as a null mutation. I show that this loss of function

is sufficient to enable L-forms to grow in osmolarities, including conditions in which supplemented osmoprotection is entirely lacking. The ability to grow under these conditions is unusual, as the peptidoglycan is normally essential in resisting the turgor pressure resulting from osmotic downshock. As discussed in the previous chapter, L-forms have been adapted to low osmolarities in the past. Unfortunately, due to the technical limitations of the time, these adaptations were not explored to the same depth that is possible in the current day.

It has been shown that deletion of all three of the MreB homologues in *B. subtilis* (rendered viable by a Δ*rsgI* mutation) results in cells with increased membrane fluidity. In the historic L-form literature there have been accounts of L-forms from a variety of species adapted to low osmolarities (Harold, 1964, Montgomerie et al., 1973). Taken together, it suggested a possible membrane-associated role for MreB in permitting L-forms to grow in low osmolarities.

 In this work I demonstrate that membrane fluidity was unchanged between cells in the L-form state and the walled state. Further, I show that loss of a single copy of MreB did not affect the fluidity of *B. subtilis* cells. However, whilst membrane fluidity was not affected, L-forms of both the osmo-resistant mutant strain JB114 and the Δ*mreB* strain had an increase in the fatty acids of the membrane. A causal relationship between the thickness of the cytoplasmic membrane and the ability to survive in low osmolarities has not been previously established.

4.2 Results

4.2.1 The 20 amino acid deletion does not appear to affect a known interaction site

The structure of MreB was first resolved in 2001 (van den Ent et al., 2001). The knowledge of the structure has allowed for the identification of the membrane interacting domains and the nucleotide binding cleft, as well as the binding sites of some of its interaction partners and other MreB molecules (van den Ent et al., 2010, van den Ent et al., 2014).

The structure was resolved from an MreB molecule belonging to the Gram positive organism *Thermotoga maritima.* Whilst there are differences, the sequence of *B. subtilis* MreB is similar enough to that of *T. maritima* that it is possible to map the sequence of MreB$_{BS}$ onto that of MreB$_{TM}$. Using the structure of MreB it was possible to locate the deleted region found in the mutant strains JB114 and JB115. As can be seen in figure 4.1, the 20 amino acid deletion region is found in domain II of the protein and comprises part of two α-helices as well as the linker region connecting them. This domain is cytoplasmic facing, and has not been previously shown to be a binding or a polymerisation surface. This led us to hope that the mutant in the two strains could represent a loss or gain of function, possibly involved in the interaction with an unknown partner. Of course, with such a deletion it could not be discounted that the mutation may affect another part of the protein structure or could result in a non-functional protein.

A

```
551  gtgatgagat ggatgacgcg atta tcaact acatcagaaa aacgtacaat ctgatgatcg gtgaccgtac ggctgaagcg atta aaatgg aaatcggatc tgcagaagct
                                                              Deletion
     >................................................................mreB.............................................................>
       g  d  e  m  d  d  a  i  i  n  y  i  r  k  t  y  n  l  m  i  g  d  r  t  a  e  a  i  k  m  e  i  g  s  a  e  a
```

B
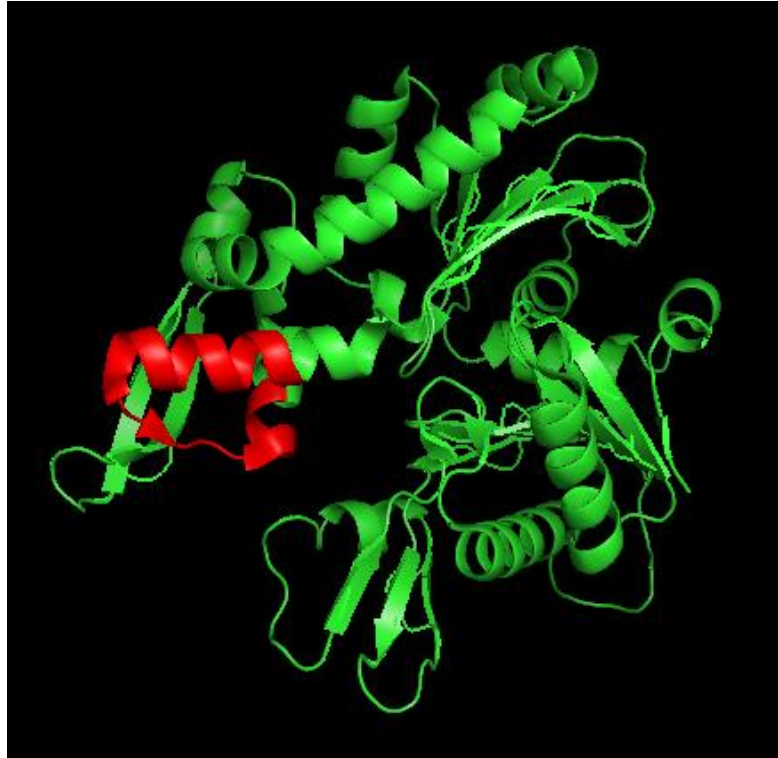
Figure 4.1. A). The 60bp deletion at position 575 in *mreB* is flanked by two direct repeats. The deletion is highlighted in red, whilst the direct repeats are in the two boxes. **B).** The 20 amino acid deletion is highlighted in red. The deletion is located in domain IIB. This region is cytoplasmic facing and has not been previously identified as an interaction surface. Model of *B. subtilis* MreB created by H. Strahl using Phyre service.

4.2.2 JB114 and JB115 can grow in both low sucrose and low salt and can even grow in the complete absence of osmoprotection

To try to understand the mechanism(s) of osmoprotection/osmo-resistance, we wanted to see whether the two mutant L-form strains isolated from the low sucrose growth media were able to grow when the osmoprotectant was changed from sucrose. As expected, both strains grew at a rate similar to the wild type in concentrations of 0.5 M MNM/NB. When the concentration of NaCl in the MNM/NB was reduced to 0.05 M, L-forms of the JB114 and JB115 strains were still able to grow, whereas the parental strain, LR2 was not (figure 4.2). It therefore appears that the mutations present in these two strains are not specific for growth in sucrose.
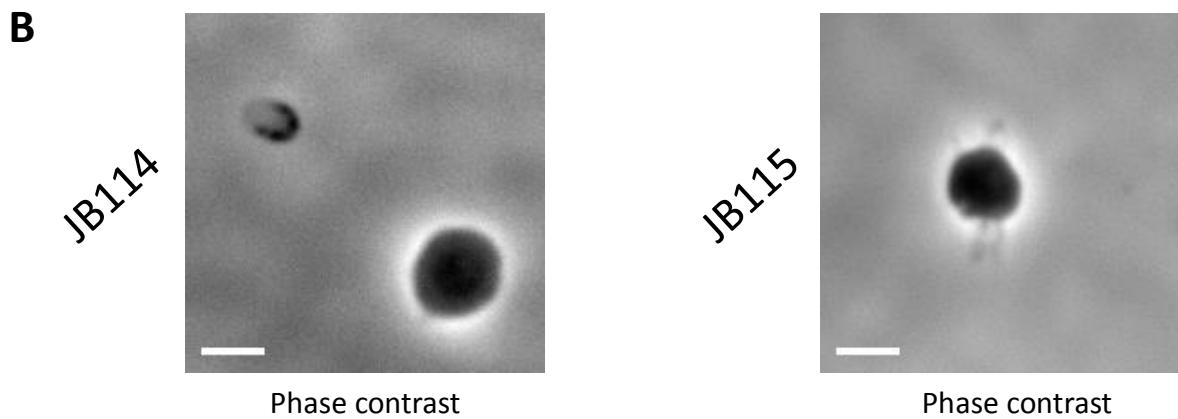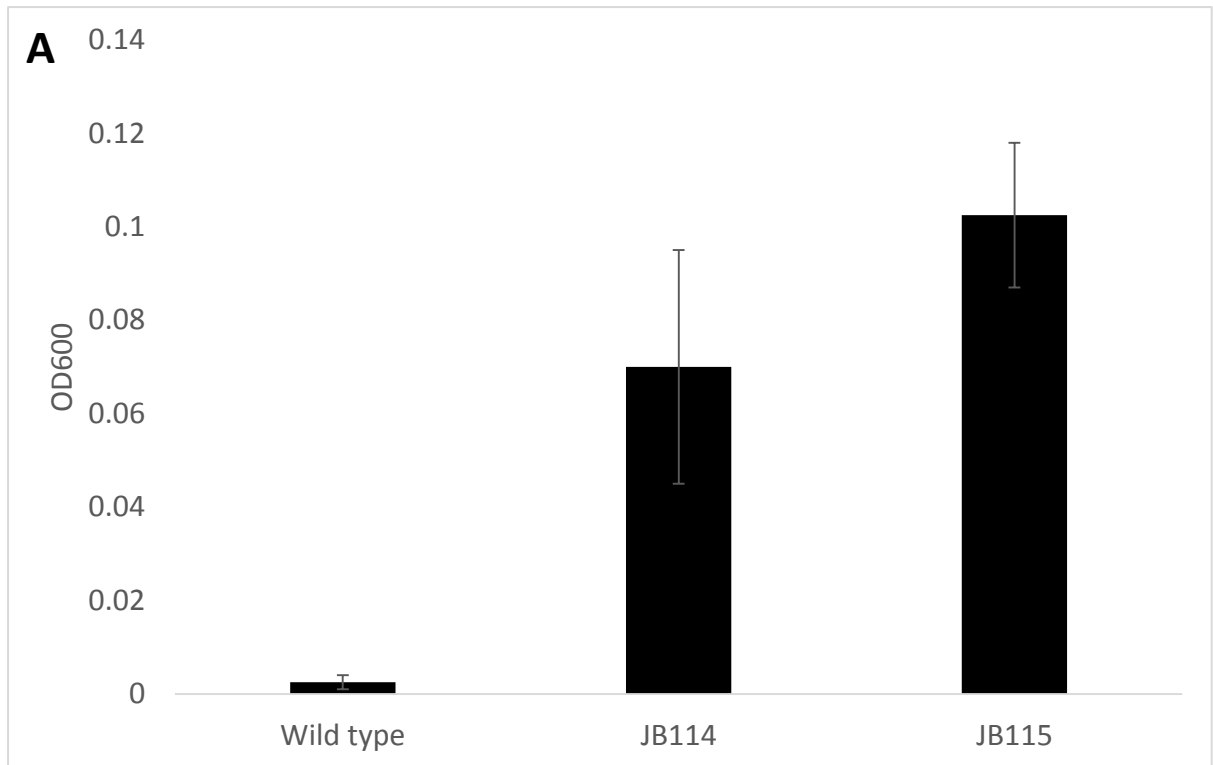
Figure 4.2. A). Osmo-resistant L-forms originally adapted in low concentrations of sucrose can grow in low concentrations of salt. L-forms derived from the wild type (LR2) and the mutant strains JB114 and JB115 were grown until dense in 0.5 M MNM/NB. L-forms were diluted 10^{-3} in 0.05 M MNM/NB and incubated at 30°C for seven days. OD_{600} was measured on the seventh day. **B).** Presence of L-forms in the low salt medium was confirmed by light microscopy. Scale bar = 3µm

However, the growth rates of the two mutants in 0.05 M MSM/NB were considerably lower than when grown in 0.5 M MSM/NB. It was possible that the mutation in *mreB* was merely allowing the cells to survive the initial osmotic shock, and that the strains had picked up additional mutations enabling their growth. This seemed somewhat unlikely due to the fairly minimal number of mutations present in the original isolates. Nevertheless, we tested this possibility by sequencing the genomes of JB114 and JB115 L-form cells grown in 0.05 M MSM/NB. Sequencing revealed a limited number of mutations in non-coding regions in the genomes of these cells. It can therefore be concluded that the mutations already present in the JB114 and JB115 strains are sufficient for growth in the challenging conditions.

JB114 and JB115 had been isolated from cultures containing the sucrose concentrations of 0.075 M and 0.05 M, respectively. However, much of the osmo-resistance testing of the two mutant strains was carried out at 0.05 M, indicating that the mutations may allow for the strains to grow in lower concentrations than originally adapted to. To see whether the mutants could grow at even lower concentrations of sucrose, the strains JB114 and JB115 were diluted from a 0.5 M MSM/NB culture by 10^{-4} into media with a range of different osmolarities. Remarkably, both strains could grow in sucrose concentrations as low as 0.01 M (unsurprisingly, the wild type strain (LR2) could not grow in any of the concentrations tested) (figure 4.3), though the ability to grow appeared to diminish as the concentrations decreased. Following a 10^{-4} dilution from 0.5 M MSM/NB, L-forms of both osmo-resistant strains were unable to grow in the medium without sucrose. As the strains were able to grow in very low sucrose concentrations, it was considered whether it was the initial osmotic down-shock that was preventing the L-forms to grow, probably causing majority of the cells to lyse. Therefore, instead of inoculating the sucrose-free medium with L-forms from the high sucrose culture, L-forms grown in 0.05 M MSM/NB was used instead. A second benefit is that this route removes much of the sucrose carried over from the original culture that would be introduced from the inoculation from 0.5 M MSM/NB. Amazingly, the L-forms derived from the two adapted strains were able to grow in the near complete absence of supplemented osmoprotectant (roughly 0.05 mM is present), though the growth was slow and the final optical density was low (figure 4.3).

A

B

Phase contrast
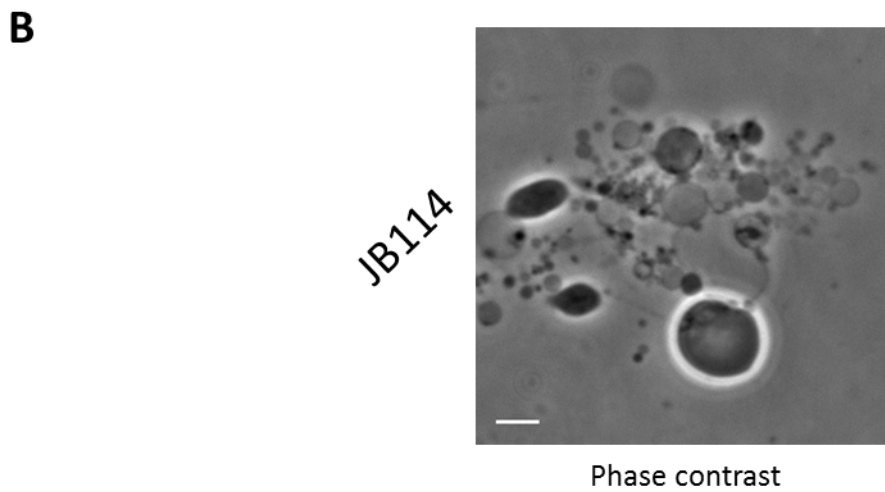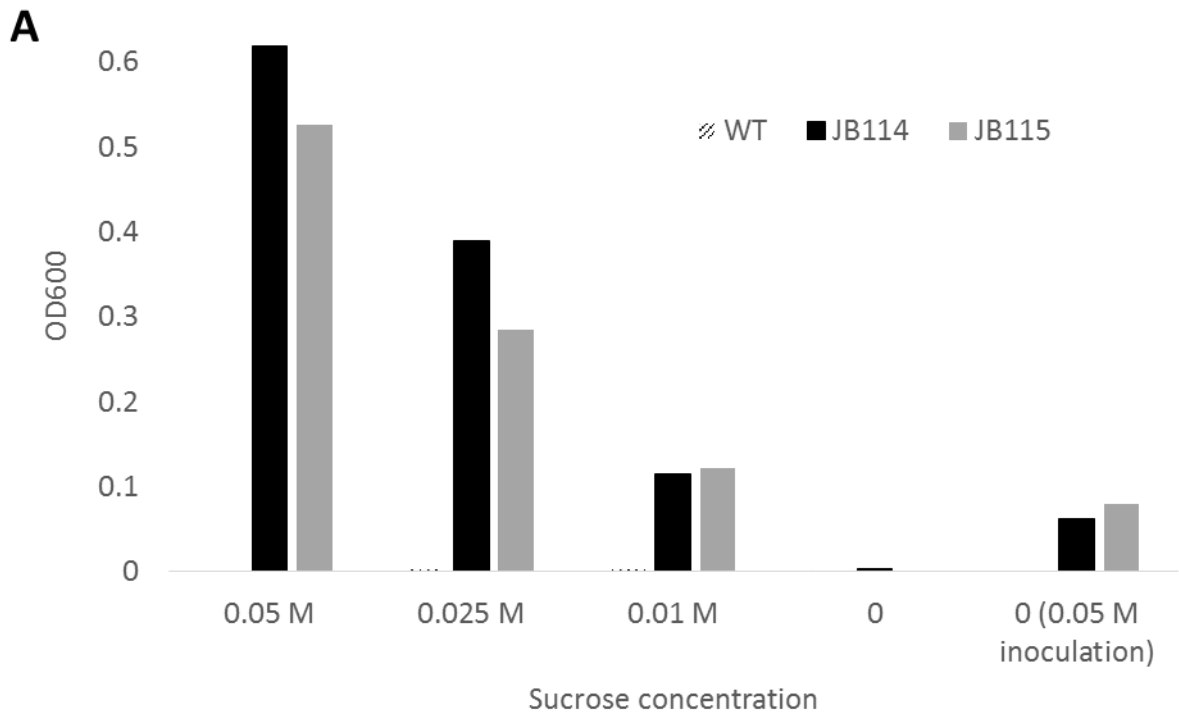
Figure 4.3. The mutant strains, JB114 and JB115, are able to grow as L-forms in sucrose concentrations as low as 0.01 M. L-forms derived from JB114 and JB115 are able to grow in the complete absence of osmoprotection following a 2×10^{-3} dilution from L-forms grown in 0.05 M MSM/NB. L-forms derived from the wild type (LR2), JB114 and JB115 were grown in 0.5 M MSM/NB until dense. The cells were diluted 10^{-3} into MSM/NB with a range of sucrose concentrations, including the complete absence of sucrose. L-forms were grown at 30°C for up to 24 days. OD_{600} was measured in the flasks with growth after 15 days. The wild type strain was unable to grow in any of the conditions tested,

the two mutant strains were unable to grow in the complete absence of sucrose.

L-forms from the 0.05 M MSM/NB cultures were used to inoculate NB with no sucrose.

These cultures were grown at 30°C, with the OD_{600} measured after 24 days growth.

B). The presence of L-forms was verified using light microscopy in the NB containing no osmoprotectant. Scale bar = 3µm.

4.2.3 The L-forms can still grow in low osmolarities even with a *murC* deletion

Most of the L-forms used in this research were generated by depleting MurE from strain LR2, in which *murE* was under the control of a xylose-inducible P_{xyl} promoter. However, it has been shown previously that these cells still contain low levels of peptidoglycan due to the leaky nature of the P_{xyl} promoter (Gartner et al., 1988). Whilst unlikely, it was a concern that the L-forms were able to grow in the adverse conditions as a result of residual amounts of peptidoglycan. To ensure this was not the case, a second gene in the lipid II pathway, *murC,* was deleted. To allow for this deletion, an additional copy of *murC*, carried on a pLOSS plasmid and under the control of a P_{spac} promoter was introduced into the LR2 background, before the native copy of *murC* was deleted (JB180). To maintain the plasmid when the cells were in the walled state, cells were grown with the appropriate concentrations of IPTG and the antibiotic, in this case, erythromycin. Removal of the IPTG and the antibiotic results in the loss of the plasmid and renders the walled cells carrying the Δ*murC* mutation non-viable. However, in the L-form state where the lipid II pathway is dispensable deletion of *murC* should be viable. As expected, in the L-form state there is no discernible difference between the WT and the Δ*murC* strains. Loss of the plasmid was verified using PCR. Δ*murC* L-form strains were generated from strains JB189 and JB182, the Δ*murC* derivative of JB114 and JB115, respectively, and an *mreB*-null strain (JB181) were able to grow in 0.05 M MSM/NB, whereas the Δ*murC* LR2 strain was unable to grow in these conditions (figure 4.4).
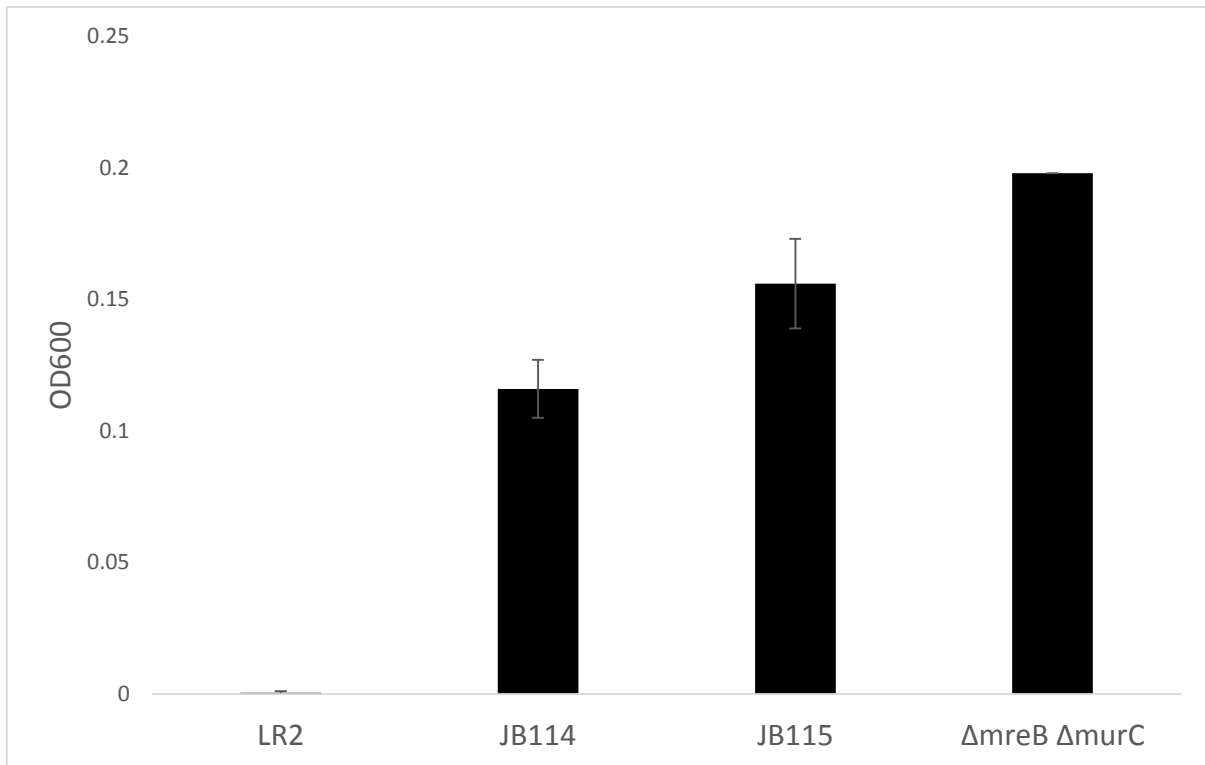
Figure 4.4. L-forms can still grow with minimal osmoprotection when the lipid II synthesis pathway is completely disrupted. L-forms derived from a LR2 strain carrying a *ΔmurC* and a functional copy on a pLOSS plasmid were grown in 0.5 M MSM/NB until dense. Loss of the pLOSS plasmid was verified by PCR. L-forms were diluted 10^{-3} into 0.05 M MSM/NB and grown for 14 days at 30°C. No significant difference was observed between the original mutant strains and the strains in which *murC* is deleted.

4.2.4 Deletion of *mreB* has some effect on the growth and cell morphology of JB114 and JB115

The nature of the *mreB* deletion present in JB114 and JB115 – a 60bp in-frame deletion – suggested a possible loss or gain of function as opposed to a null mutant. To examine this possibility, *mreB* was deleted from the two mutant strains, as well as the LR2 parent. Deletion of *mreB* was achieved using the established construct of Formstone and Errington, 2005 in which the expression of the downstream *mreC* and *mreD* genes is preserved (Formstone and Errington, 2005). In the walled state the JB133 mutant carrying the *mreB* deletion was largely similar to the growth rate and morphology of the JB115 mutant strain (figure 4.5). Whilst the growth of JB114 cells was sicker than that of Δ*mreB* in the LR2 background (JB133), deletion of *mreB* in the JB114 background did not significantly affect the growth and morphology of the strain. Taken together, this strongly suggested that the 60bp deletion was resulting in a non-functional protein. Interestingly, whilst the growth rate of JB114 did not change significantly with complete deletion of *mreB*, the *mreB* deletion in the JB115 background had significantly perturbed growth rates (figure 4.6). This observation instead suggested that the mutant copy of *mreB* may retain some functionality.

Complete deletion of *mreB* had no effect on the growth of the strains as L-forms in MSM/NB as was expected (data not shown).

PAB

PAB + 20mM Mg^{2+}

Wild type
A

ΔmreB
B

JB114
C

JB114 ΔmreB
D

JB115
E

JB115 ΔmreB
F

Phase contrast   Membrane   Phase contrast   Membrane
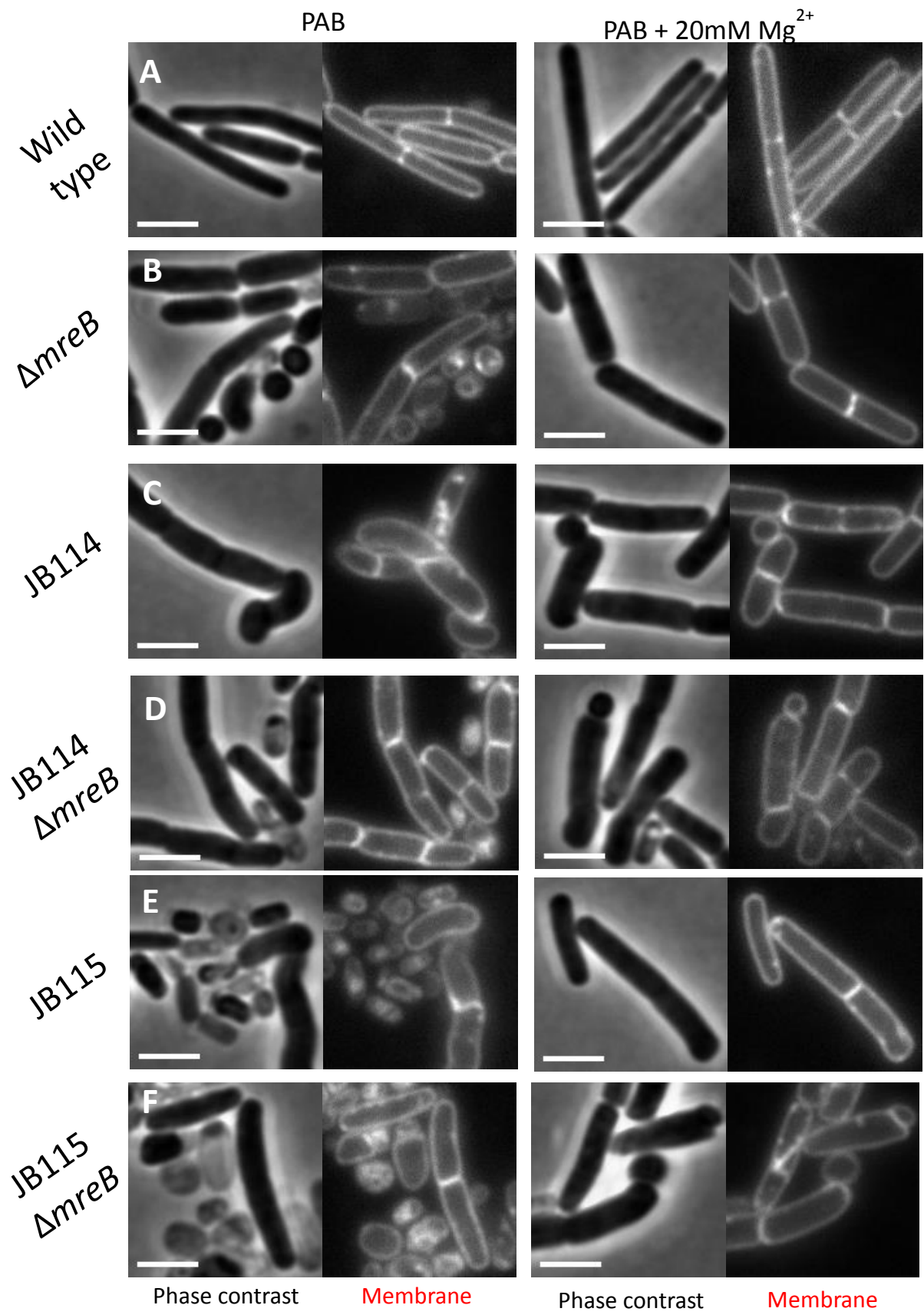
Figure 4.5.A. Cell morphology of the wild type (LR2; A), Δ*mreB* (JB133; [B]), JB114 (C), JB114 Δ*mreB* (JB134; [D]), JB115 (E) and JB115 Δ*mreB* (JB135; [F]) during early exponential phase (OD$_{600}$=0.3). Cells were grown at 37°C in PAB supplemented with 0.5% xylose and +/- 20mM MgCl$_2$. Membranes were visualised with FM5-95 dye. Scale bar=3μm

PAB   PAB + 20mM Mg^{2+}

Wild type

ΔmreB

JB114

JB114 ΔmreB
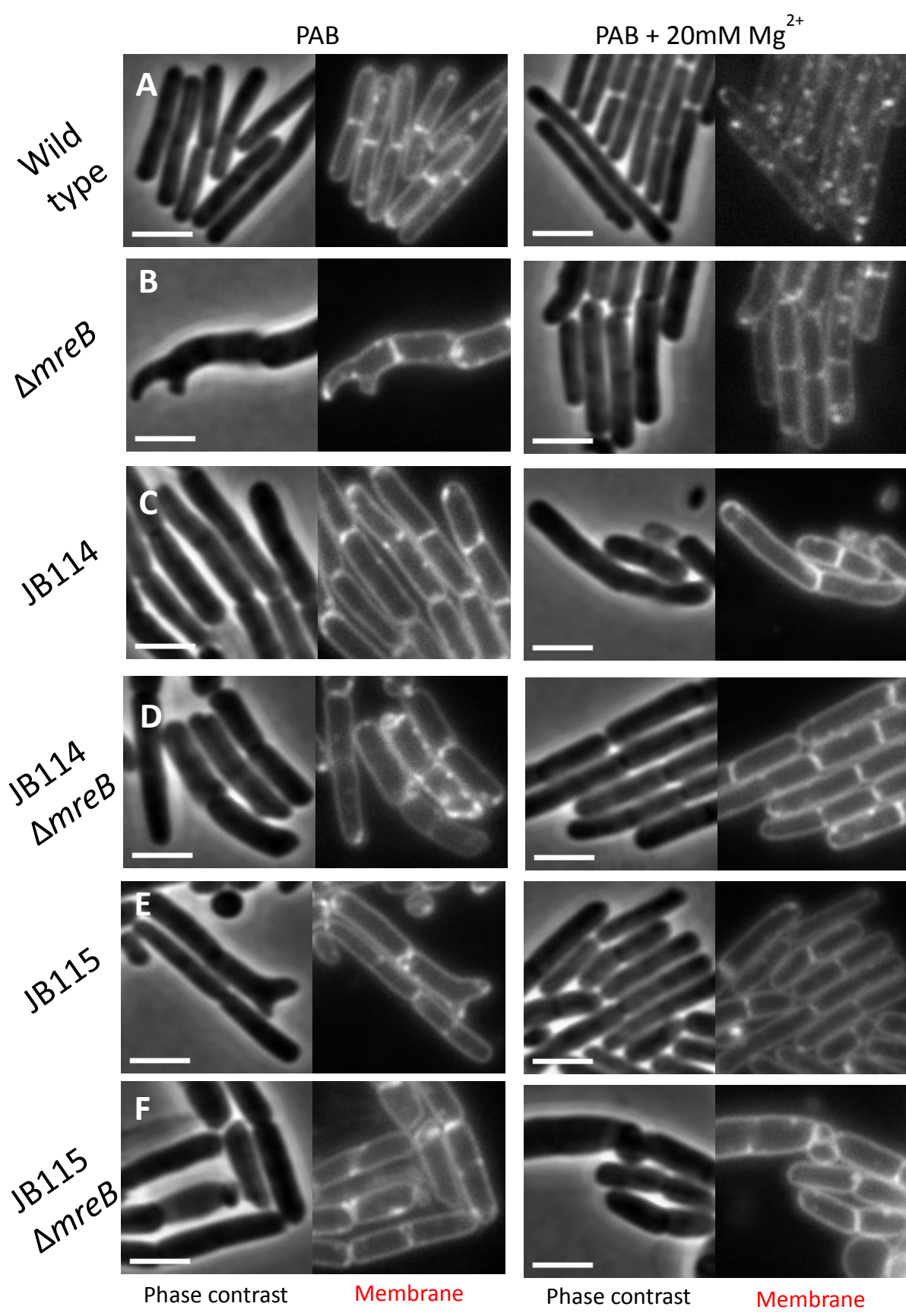
JB115

JB115 ΔmreB

Phase contrast   Membrane   Phase contrast   Membrane

Figure 4.5.B. Cell morphology of the wild type (LR2; [A]), Δ*mreB* (JB133; [B]), JB114 (C), JB114 Δ*mreB* (JB134; [D]), JB115 (E) and JB115 Δ*mreB* (JB135; [F]) during mid-exponential phase (OD_{600}=1.0). Cells were grown at 37°C in PAB supplemented with 0.5% xylose and +/- 20mM $MgCl_2$. Membranes were visualised with FM5-95 dye. Scale bar=3µm

PAB

PAB + 20mM Mg^{2+}

Wild type
A

ΔmreB
B

JB114
C

JB114 ΔmreB
D

JB115
E

JB115 ΔmreB
F

Phase contrast   Membrane   Phase contrast   Membrane
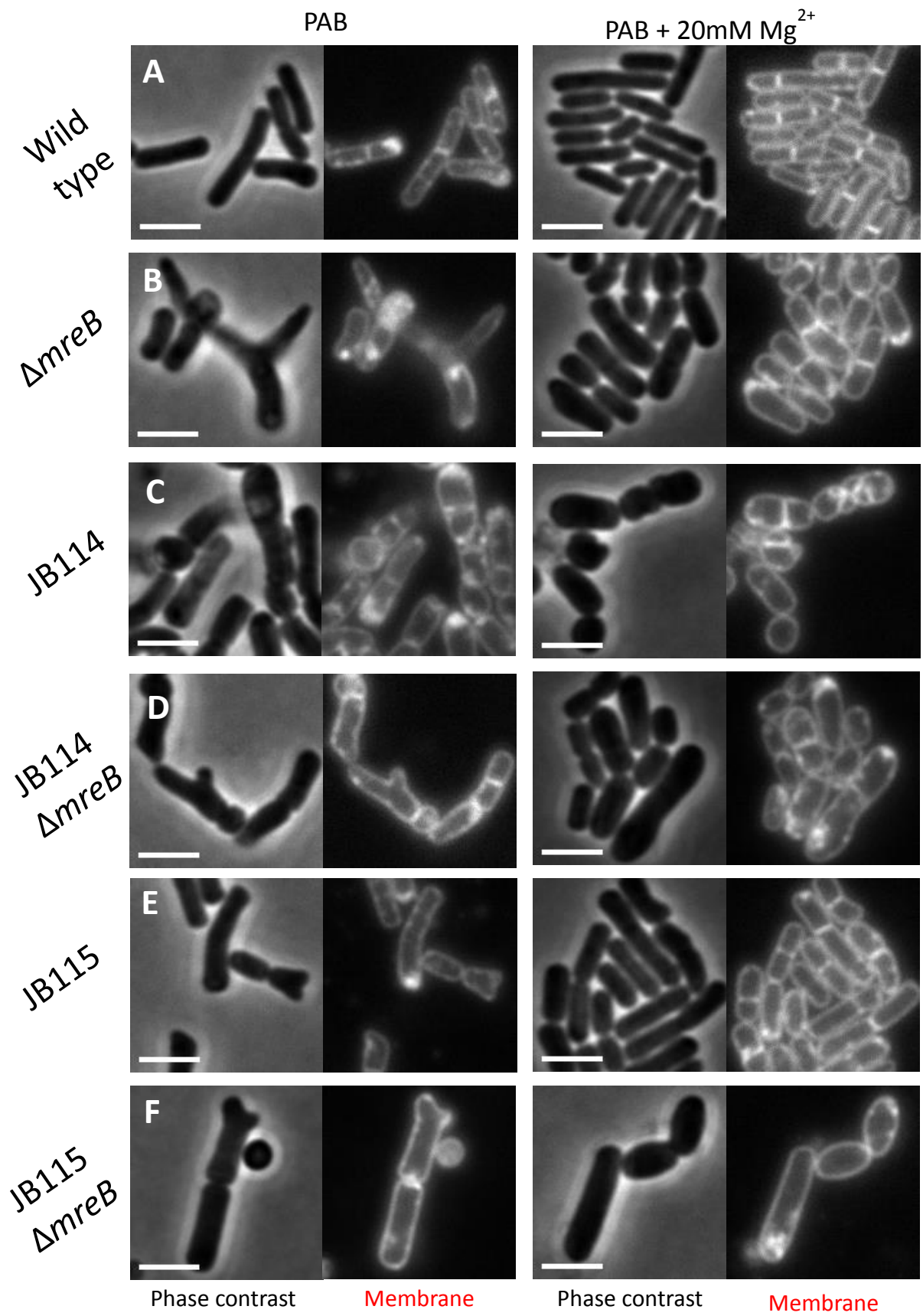
Figure 4.5.C. Cell morphology of the wild type (LR2; [A]), Δ*mreB* (JB133; [B]), JB114 (C), JB114 Δ*mreB* (JB134; [D]), JB115 (E) and JB115 Δ*mreB* (JB135; [F]) during stationary phase. Cells were grown at 37°C in PAB supplemented with 0.5% xylose and +/- 20mM MgCl$_2$. Membranes were visualised with FM5-95 dye. Scale bar=3μm
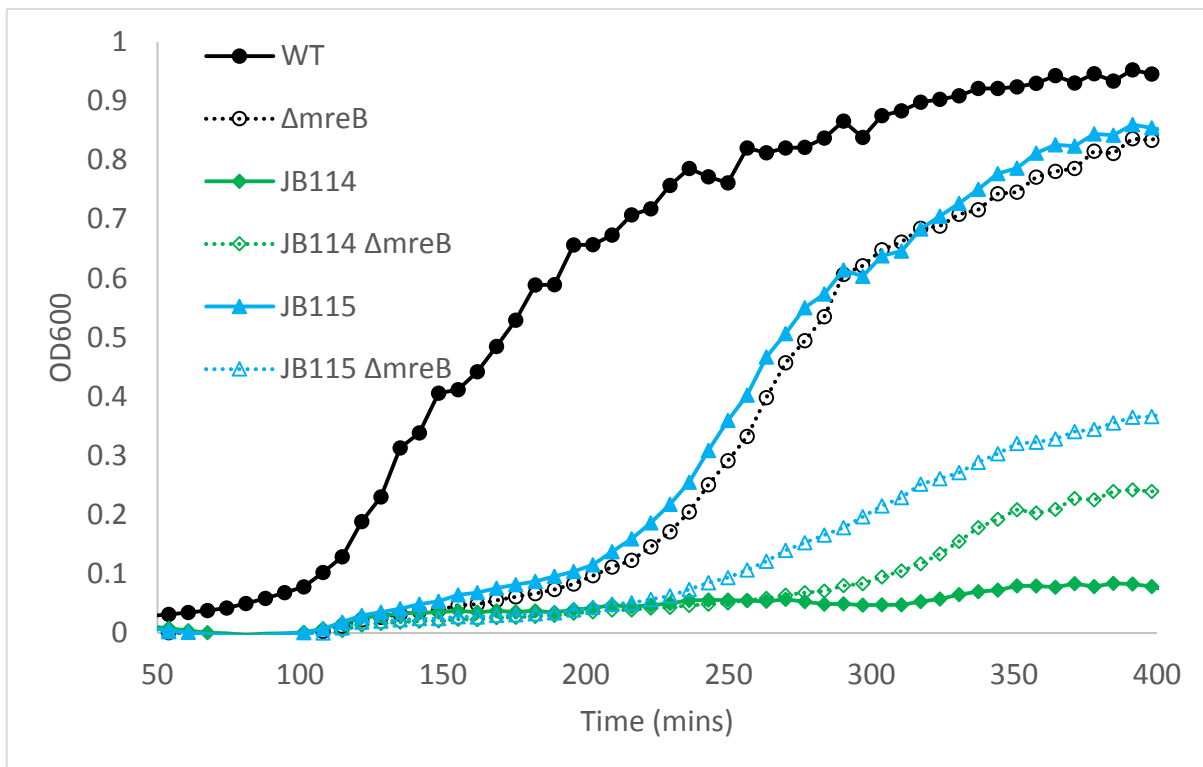
Figure 4.6. Growth rate of the *mreB*-null strains in PAB supplemented with 0.5% xylose and 20mM Mg^{2+}.

4.2.5 The 60bp deletion can be reconstructed in the LR2 strain

To further examine the effect of the mutation on *B. subtilis*, the 60bp deletion was recreated in a clean LR2 background. The strain was created via a three-piece ligation method as reported in Formstone and Errington, 2005, using an upstream insertion of the *neo* cassette to provide transcription for the essential downstream genes (figure 4.7). As expected from the previous results in 4.2.4 there was no difference in the growth rate or cell morphology between the *mreB*$^{\Delta 20}$ strain and the Δ*mreB* strain, providing further evidence that the in-frame deletion was effectively a null mutation.
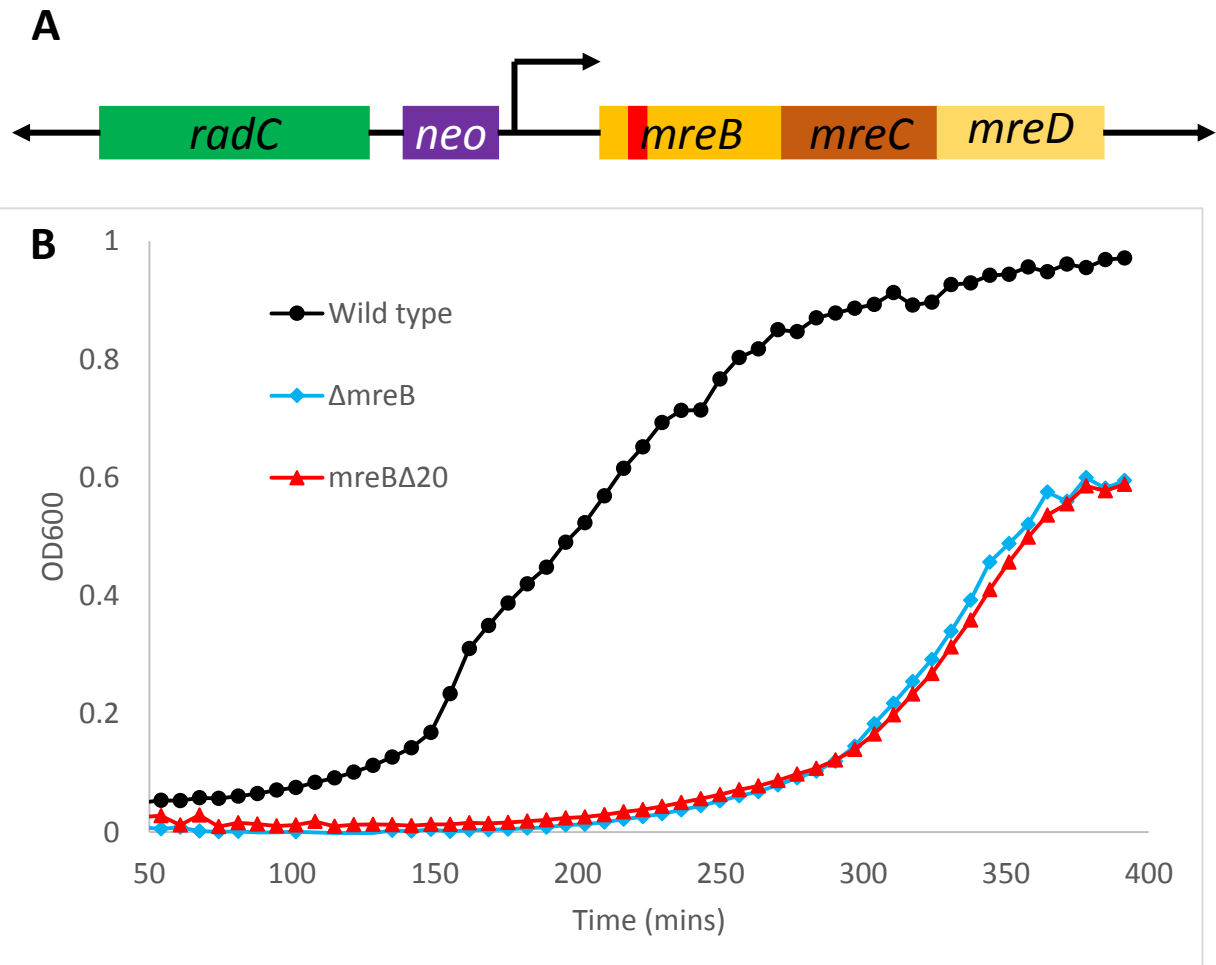
Figure 4.7. Reconstruction of the 60bp inframe deletion present in JB114 and JB115.

A). Schematic cartoon of the 60bp deletion in the LR2 background. The *neo* cassette was positioned after the terminator of *radC* and before the promoter region of the *mreBCD* operon. The 60bp deletion is indicated by the red vertical bar. **B).**The growth of the reconstructed mutant was lower than the wild type (LR2), and identical to the null mutant (JB133) when grown at 37°C in PAB.

4.2.6 Complementation of JB114, JB115 and *mreB*$^{\Delta 20}$ with *gfp-mreB* restores the growth of the strains

To examine whether the *mreB*$^{\Delta 20}$ mutation carried by JB114 and JB115 was in any way dominant in the walled state, a functional copy of MreB tagged with GFP was introduced into the strains. The GFP-MreB construct was under a xylose inducible P_{xyl} promoter, though as a result of the requirement for xylose by the LR2 strain to grow in walled state, the construct was always expressed. An alternative IPTG-inducible strain was trialled, but expression of the construct was minimal. Expression of the GFP-MreB construct was sufficient to fully restore the phenotype of the two mutant strains to that of the wild type (figure 4.8). The discrepancy between the growth reported in figure 4.6 is likely to have occurred as a result of the development of suppressor mutations.

A

	Wild type *gfp-mreB*	JB114 *gfp-mreB*	JB115 *gfp-mreB*
Phase contrast	A	B	C
Membrane			
gfp			
Overlay			
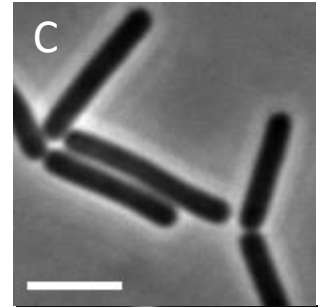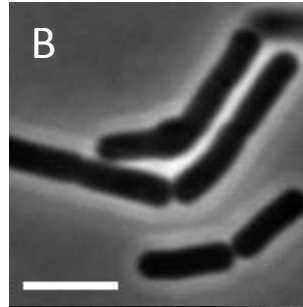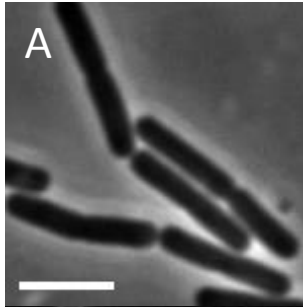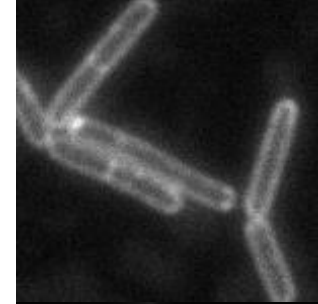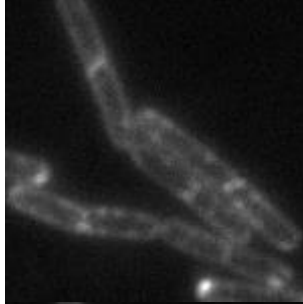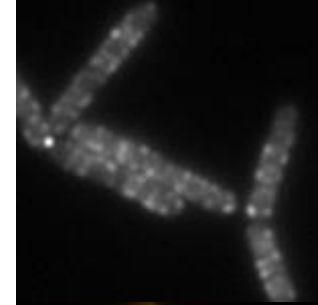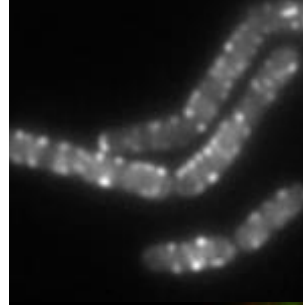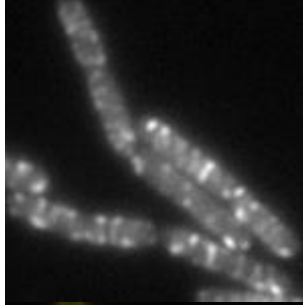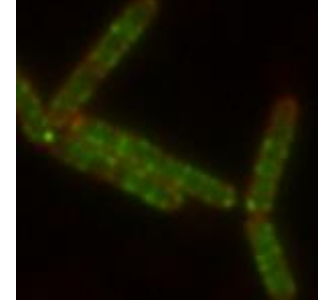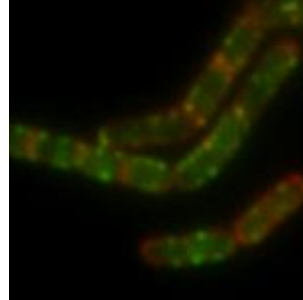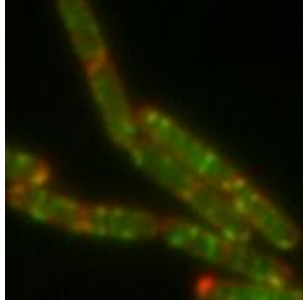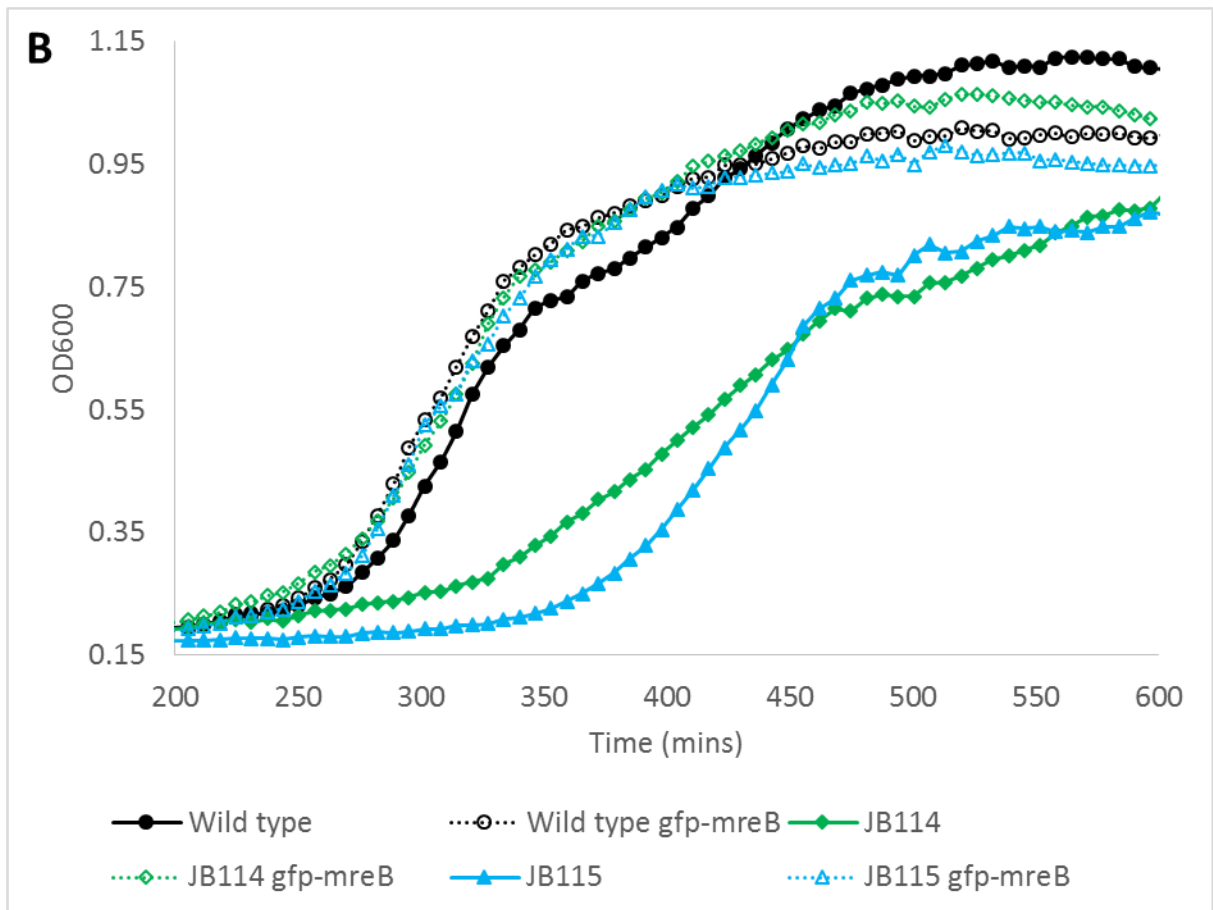
Figure 4.8. Morphology (**A**) and growth rate (**B**) of JB114 and JB115 can be restored by complementation with a functional GFP-MreB construct. **A).** Morphology of cells JB114 (JB137; [B]) and JB115 (JB138; [C]) is restored to that of the wild type (LR2; JB136; [A]) by expression of *gfp-mreB.* Cells were grown in PAB supplemented with 0.5% xylose at 30°C. Scale bar=3μm **B).** Growth rate of JB114 and JB115 is restored to that of the wild type (LR2) when complemented with a functional copy of *gfp-mreB* (JB137 and JB138 respectively). Cells were grown at 37°C in PAB supplemented with 20mM $MgCl_2$ and 0.5% xylose.

4.2.7 MreB cannot be detected by Western blotting in JB114, JB115 and $mreB^{\Delta20}$, though can be detected at low levels in an overexpression strain

Immunoblot analysis of MreB expression in JB114 and JB115 revealed that the mutated copy of *mreB* was either not being expressed or was unstable as MreB could not be detected in the cell lysates of these two strains, nor in the lysate of an $mreB^{\Delta20}$ strain in the 168CA background. As an alternative method to detect the MreB$^{\Delta20}$ protein, a P_{xyl}-*gfp-mreB$^{\Delta20}$* was constructed to overexpress the GFP-linker mutant copy of MreB in a 168CA wild type background. Upon expression a low level of GFP-MreB with the partial deletion could be observed in the relevant strains (figure 4.9). This indicates that the partial deletion maybe resulting in an unstable protein that is prone to degradation.
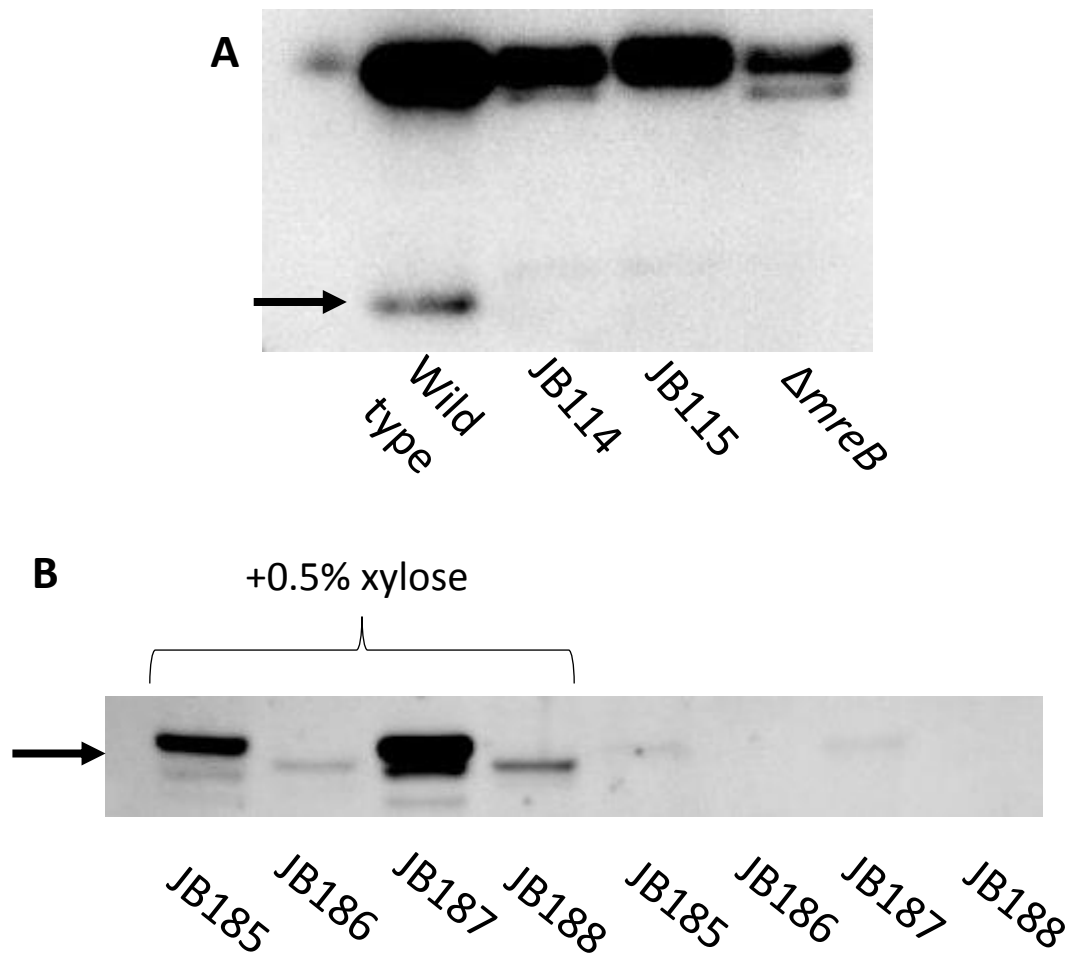
Figure 4.9. Western blotting against MreB in the mutant strains (**A**) and the overexpression strains (**B**). Arrows indicate the expected position of MreB and GFP-MreB where appropriate. **A).** MreB could only be detected in the wild type strain (LR2) and not in JB114, JB115 or an MreB-null strain (JB133). Cell lysate prepared from cells grown in PAB supplemented with 20mM $MgCl_2$ and 0.5% xylose reached an $OD_{600}=0.3$ **B).** Western blot against GFP-MreB held under an inducible P_{xyl} promoter. Strains JB185 (168CA *gfp-mreB*), JB186 (168CA *gfp-mreB$^{\Delta 20}$*), JB187 (Δ*mreB gfp-mreB*) and JB188 (Δ*mreB gfp-mreB$^{\Delta 20}$*) were grown in LB +/- 0.5% xylose.

4.2.8   Localisation of MreB$^{\Delta 20}$ in walled cells and in L-forms

To further investigate any potential role MreB$^{\Delta 20}$ may be playing the localisation of the protein was examined *in vitro*. In both a 168CA wild type background and in an *mreB*-null background, the MreB$^{\Delta 20}$ construct did not form filaments, but instead remained diffuse in the cytoplasm during exponential growth. As the cells progress into late exponential/stationary phase the protein began to aggregate to form foci throughout the cell (figure 4.10). These foci appear to be distributed randomly, and do not localise to important landmarks such as the cell poles, division septa and so on. Taken with the earlier work, it can be concluded that the 60bp deletion in *mreB* is resulting in a non-functional protein that is effectively equivalent to a complete knock out of the protein. As these results were performed in the walled state, it is a reasonable assumption that the null-phenotype observed for MreB$^{\Delta 20}$ would carry over to the L-form state.

A

P_{xyl} *gfp-mreB*

+0.5% xylose

P_{xyl} *gfp-mreB*^{Δ20}

+0.5% xylose

Phase contrast

Membrane

GFP

Overlay

B

P_{xyl} *gfp-mreB*
+0.5% xylose

P_{xyl} *gfp-mreB$^{\Delta 20}$*
+0.5% xylose

Phase contrast

Membrane

GFP

Overlay
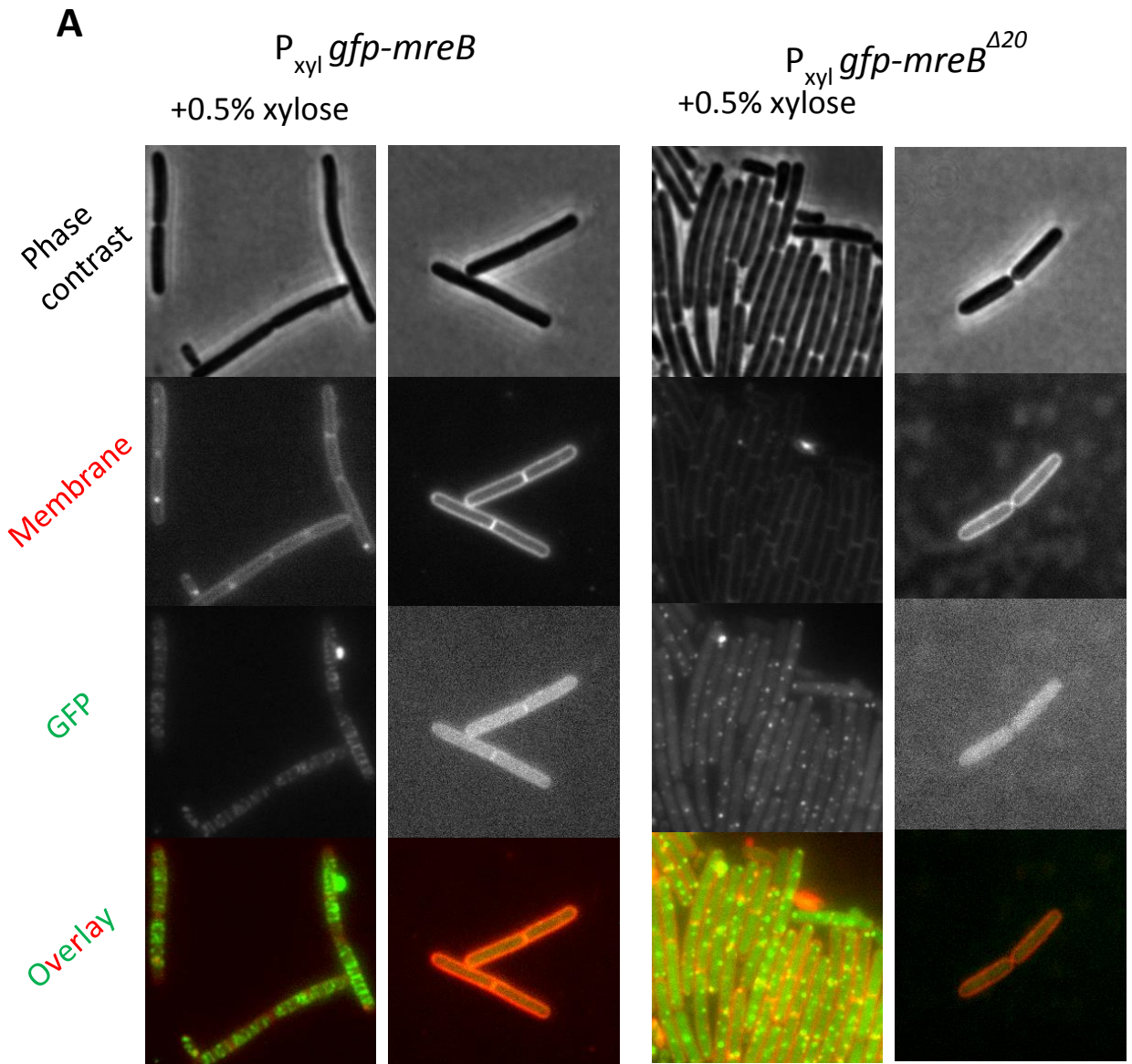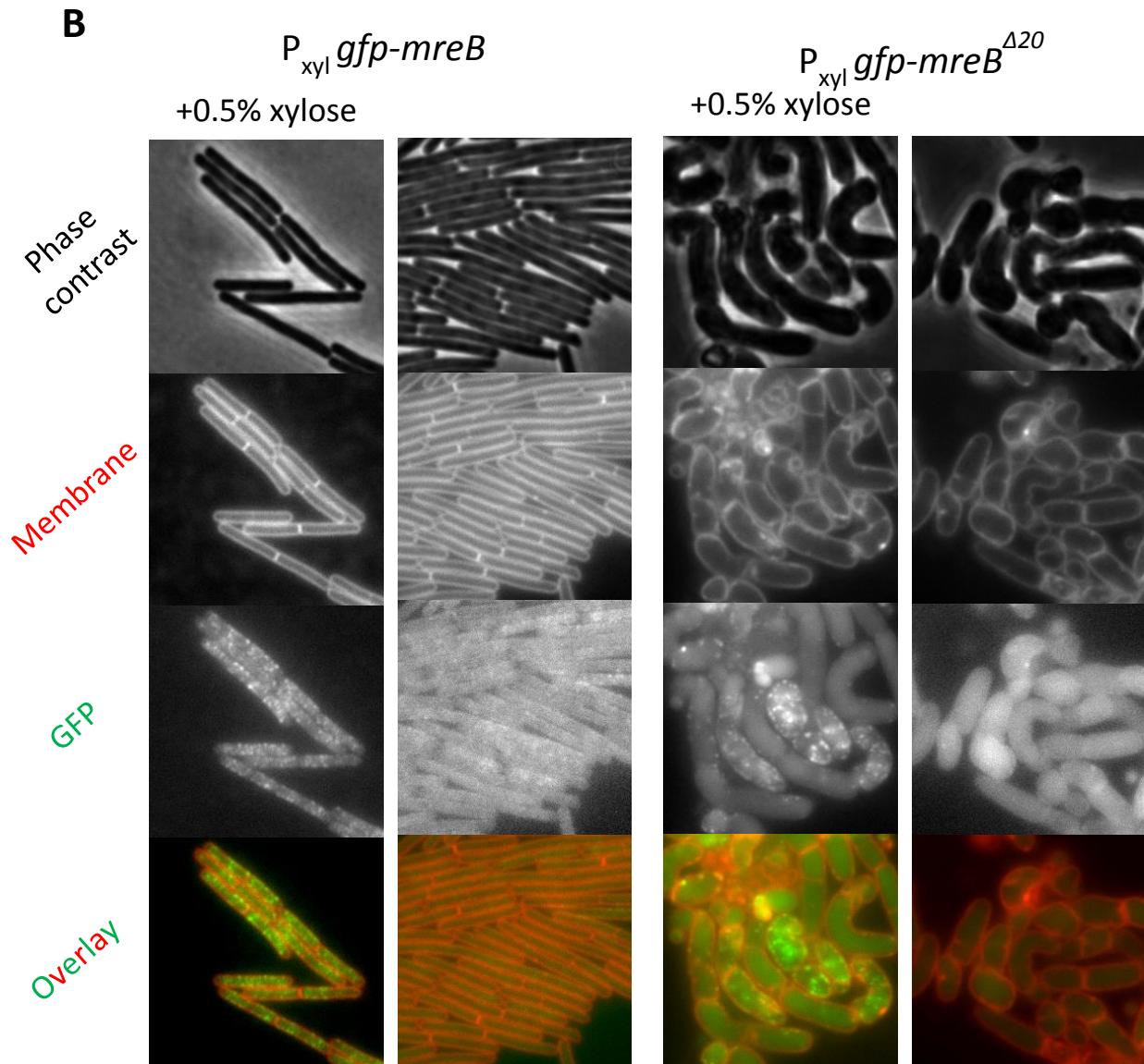
Figure 4.10. Localisation of GFP-MreB and GFP-MreB$^{\Delta 20}$ in a wild type (168CA [A]) and *mreB*-null background (B). The wild type copy of GFP-MreB forms the characteristic helical filaments in both the wild type (JB185) and *mreB*-null (JB187) strains when expression is induced with 0.5% xylose. The GFP-MreB$^{\Delta 20}$ copy remains cytoplasmic with a tendency to aggregate into foci in both the wild type (JB186) and *mreB*-null (JB188) strains when expression is induced with 0.5% xylose. Scale bar=3μm

4.2.9 Both $mreB^{\Delta20}$ and $\Delta mreB$ can grow in low sucrose environments, though at a lower efficiency than the original mutant strains

The effect of $\Delta mreB$ on the ability of L-forms to grow with minimal osmoprotection was carried out early on in the investigation when the $mreB^{\Delta20}$ mutation was first identified in JB114 and JB115. However, L-forms of the $\Delta mreB$ derivative of LR2 (JB133) was not able to grow in 0.05 M MSM/NB. It was therefore suspected that the partial deletion possessed either a gain or loss of function that enabled it to grow under these conditions. However, upon reconstruction and testing of the $mreB^{\Delta20}$ mutation it was realised that both the $\Delta mreB$ and $mreB^{\Delta20}$ constructs were able to grow in low sucrose, but far less reliably than either JB114 or JB115 (figure 4.11). Both JB114 and JB115 could grow in 0.05 M MSM/NB in roughly 95% of inoculations, whereas the $\Delta mreB$ and $mreB^{\Delta20}$ derivatives could only grow following about 50% of inoculations. This suggested a possible role for the secondary mutations that JB114 and JB115 carried. This possibility was confirmed by the observation that the null mutant in the JB114 and JB115 background was able to grow in 0.05 M MSM/NB in a similar manner to the original mutant strains (figure 4.12). It was considered that L-forms of the $\Delta mreB$ (JB133) strain might be able to grow in the presence of low sucrose only when they had acquired the necessary mutations. To examine this possibility, the L-forms of JB133 generated from these experiments were sequenced to identify any secondary mutations. Thus far, no mutations of interest have been discovered, indicating that the secondary mutations may facilitate, but are not essential for growth with minimal osmoprotection.
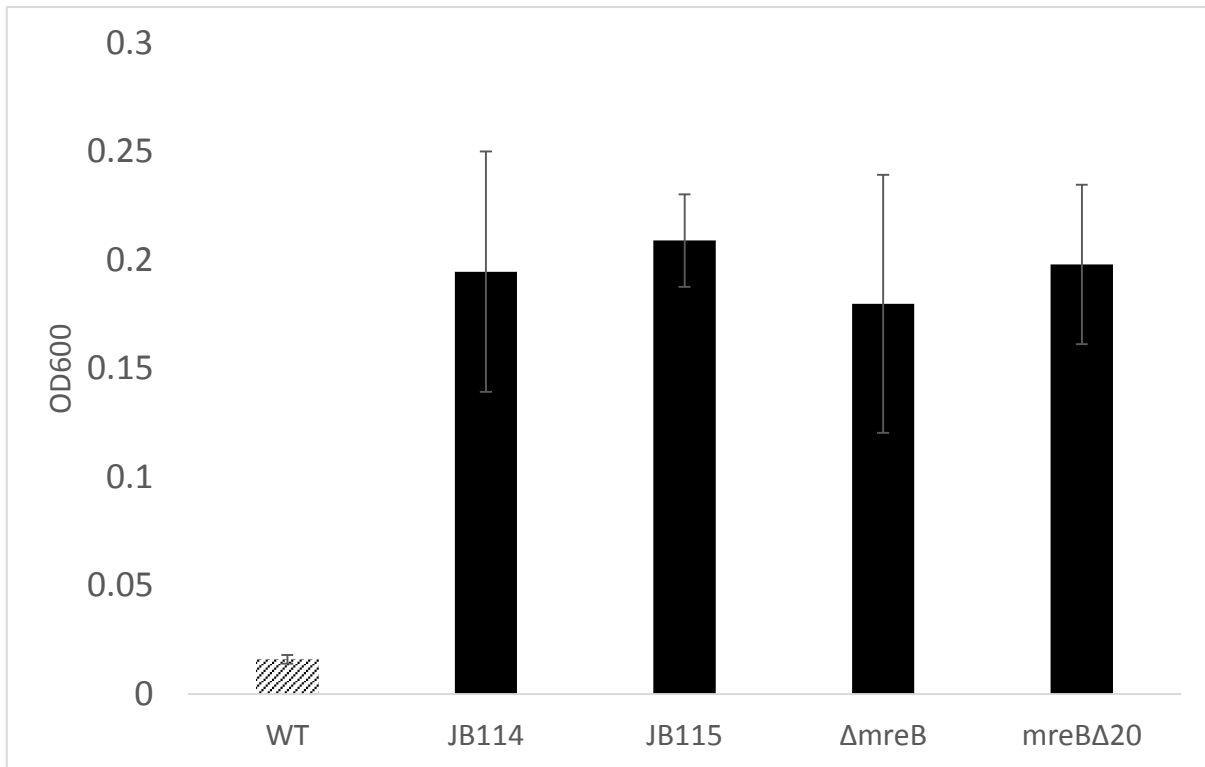
Figure 4.11. L-forms derived from an *mreB*-null strain (JB133) and a *mreB^{Δ10}* strain (JB150) are able to grow to a similar OD_{600} as L-forms derived from the osmomutant strains JB114 and JB115 in 0.05 M MSM/NB. L-forms were diluted 10^{-3} into 0.05 M MSM/NB from cultures grown in 0.5 M MSM/NB. Cultures were incubated at 30°C and the OD_{600} measured after 10 days.
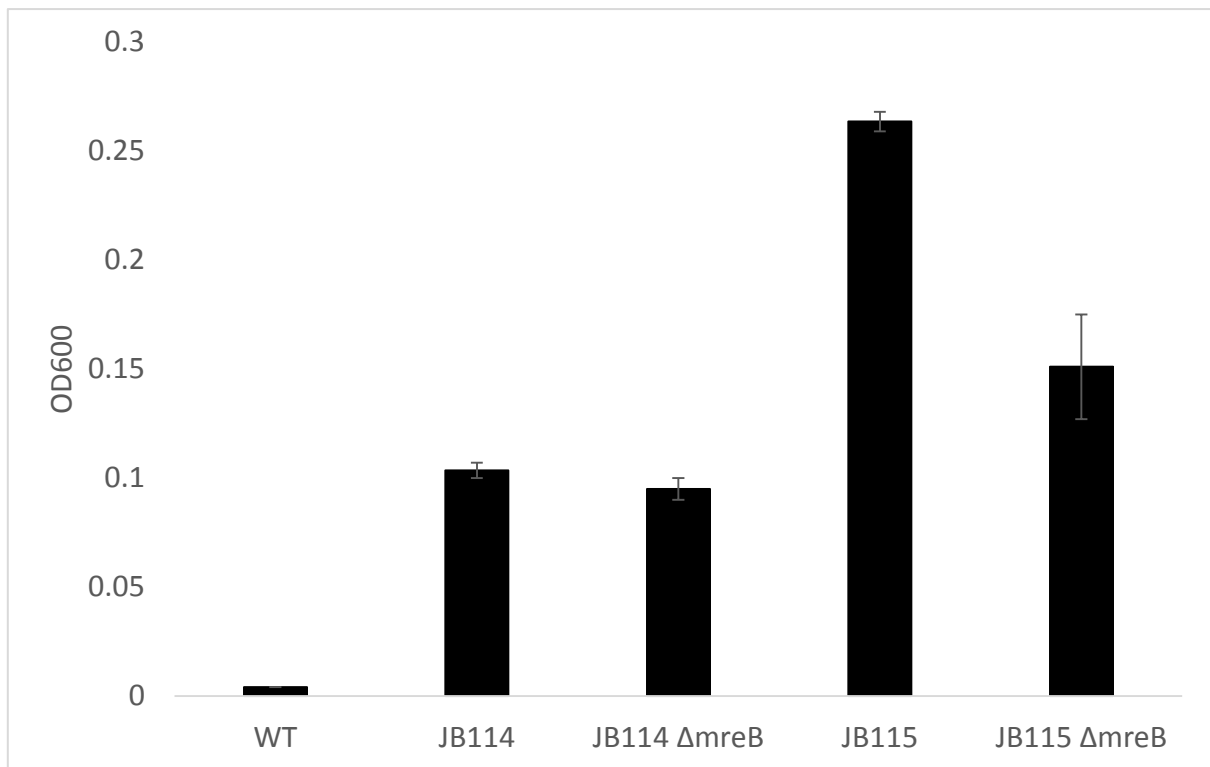
Figure 4.12. The osmomutant strains JB114 and JB115 can still grow in 0.05 M MSM/NB when *mreB* is completely deleted (JB134 and JB135 respectively). L-forms were grown until dense in 0.5 M MSM/NB and then diluted 10^{-3} into 0.05 M MSM/NB. Cultures were incubated at 30°C for 10 days at which point the OD_{600} was measured.

4.2.10 L-forms of the Δ*mreB* mutants can grow in the complete absence of osmoprotection

As discussed earlier, L-forms of both JB114 and JB115 can grow in the complete absence of supplemented osmoprotection (MgCl$_2$, maleic acid and the osmolytes in NB notwithstanding) following an intermediate step of growth in 0.05 M MSM/NB. The ability of JB133 (Δ*mreB* in the LR2 background) to grow at the intermediate step remained as reliable as reported in the previous section. Furthermore, once grown in 0.05 M the null mutant, JB133, was able to achieve a low level of growth (figure 4.13), in a similar fashion to the two original mutant strains (figure 4.3). This provided further evidence that Δ*mreB* was sufficient for growth in these conditions.
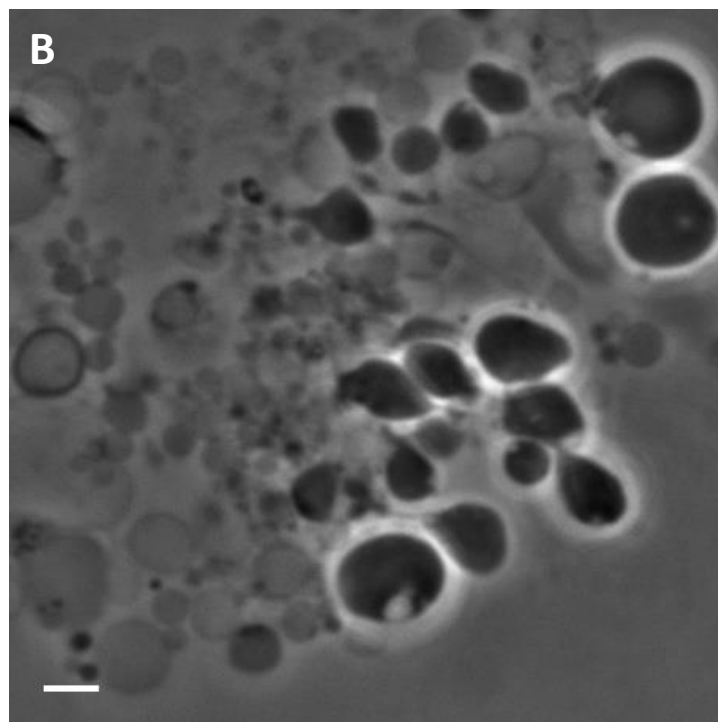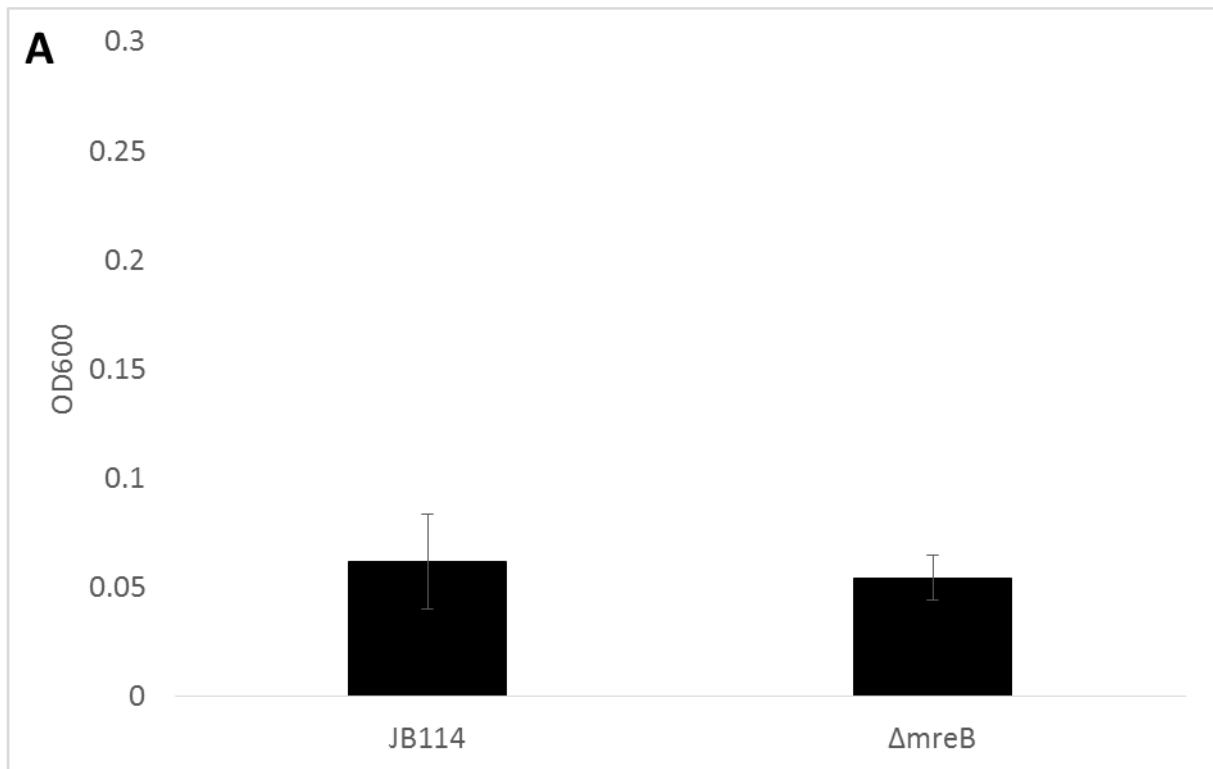
Figure 4.13. m*reB-null* L-forms can grow in the complete absence of osmoprotection in a similar fashion to the original mutant strains JB114 and JB115. **A).** L-forms were diluted 2×10^{-3} from a culture grown in 0.05M MSM/NB and incubated at 30°C. OD_{600} was measured after 15 days. **B).** The presence of L-forms in the Δ*mreB* culture was verified using light microscopy. Scale bar=3µm.

4.2.11 Deletion of *ftsE* does not improve the efficiency of the low osmotic growth of Δ*mreB*

The matter of the secondary mutations and the ease by which JB114 and JB115 grew in 0.05M MSM/NB in comparison to the Δ*mreB* strain was of some interest. Among the secondary mutations present was a mutation in *ftsE*. FtsE is an important protein; it is an ABC transporter that is involved in the autolysin activity, regulation of cell wall turnover and has been associated with the actin cytoskeleton (Dominguez-Cuevas et al., 2013). Any potential role in L-forms was therefore of some curiosity. After the strain carrying an *ftsE* deletion was constructed in a Δ*mreB* background (JB184) its ability to grow as an L-form in low sucrose concentrations was tested. Whilst able to grow in these conditions, its ability to grow was much like the Δ*mreB* single mutant. Testing of the Δ*ftsE* single mutant (JB183) revealed it was unable to grow at low osmolarities, thus supporting the idea that MreB (or its absence) was the main driving force of the phenotype (figure 4.14).

When the Δ*ftsE* Δ*mreB* double mutant was examined in its walled state, it was clear that the mutant did not possess the same growth inhibition that separated the JB114 strain from JB115 and Δ*mreB* (figure 4.15.B). Further, microscopy revealed a disturbed cell morphology, but a cell morphology that was identical to that of Δ*mreB* as opposed to JB114 (figure 4.15.A). From this work it was concluded that FtsE did not play any role in the observed phenotypes of JB114 either in the walled form or in the L-form.
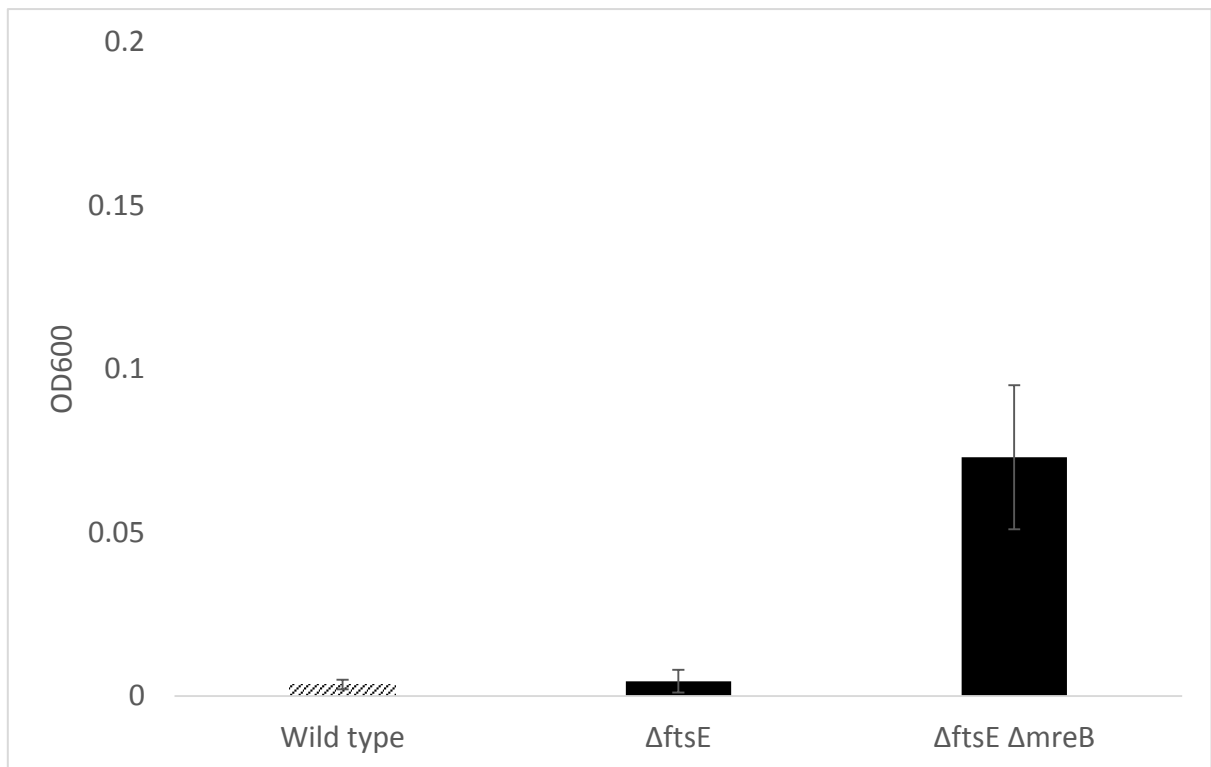
Figure 4.14. L-forms derived from Δ*ftsE* single mutants (JB83) are unable to grow in 0.05M MSM/NB. L-forms derived from the LR2 Δ*mreB* Δ*ftsE* double mutants (JB184) are able to grow in low sucrose in a manner identical to Δ*mreB* single mutants (JB133).

A

Early exponential

Mid-exponential

i Wild type

ii JB114

iii ΔmreB

iv ΔftsE

v ΔftsE ΔmreB
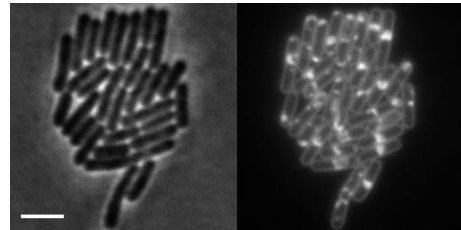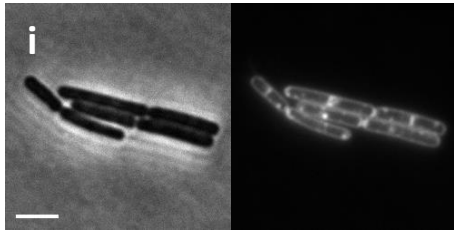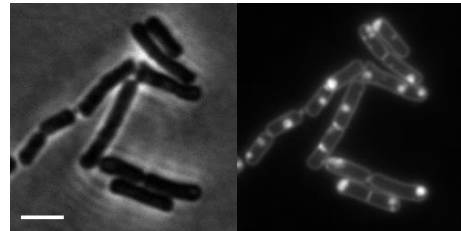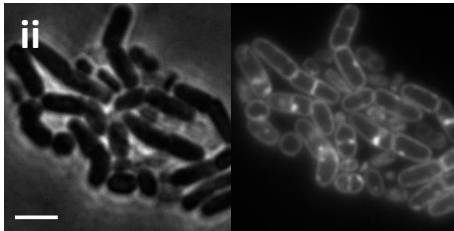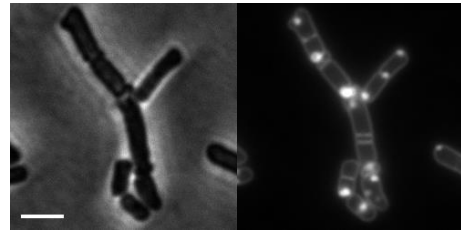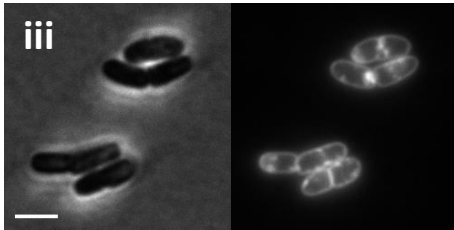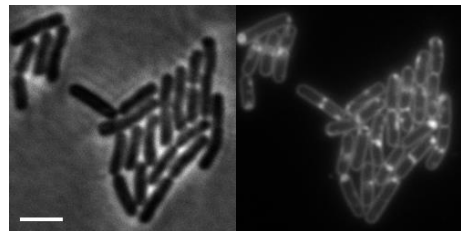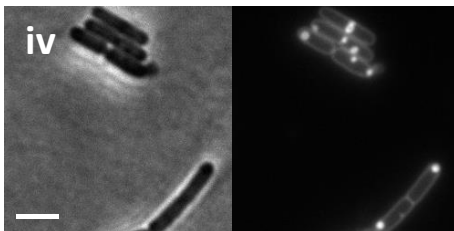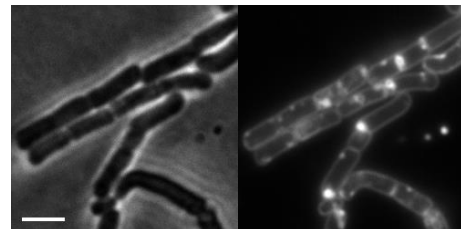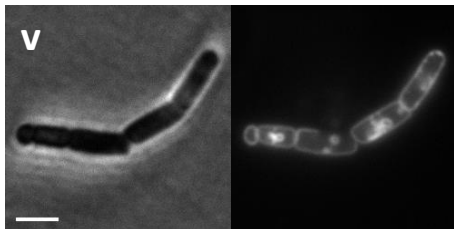
Phase contrast   Membrane   Phase contrast   Membrane
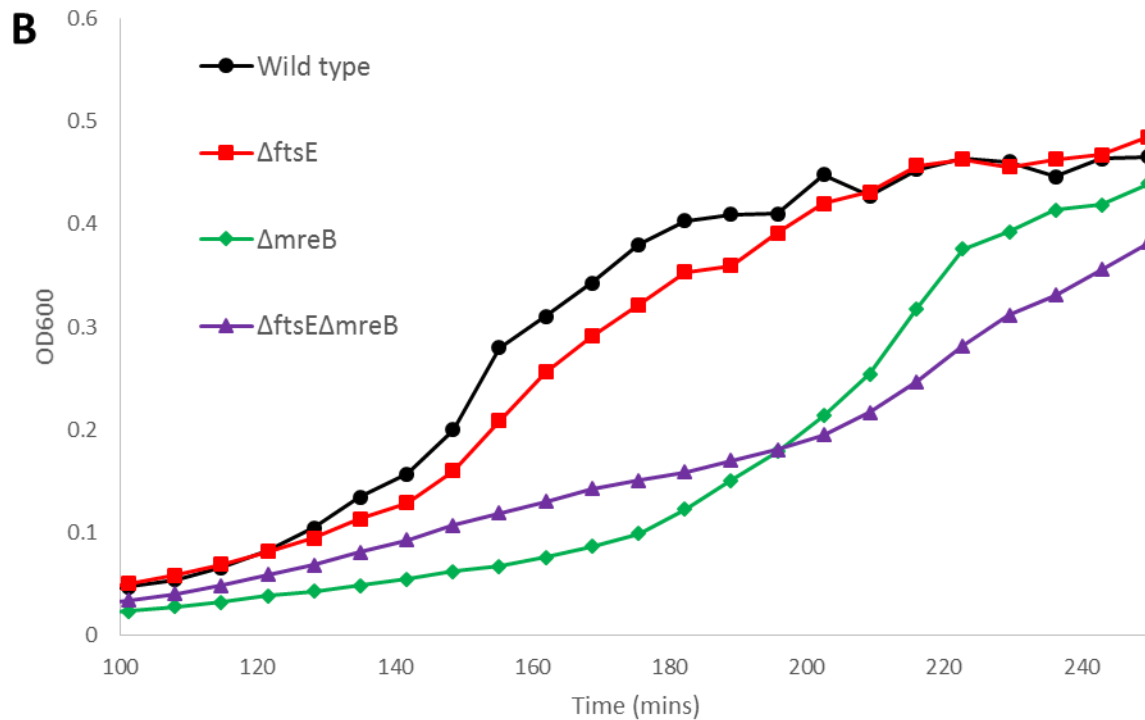
Figure 4.15. Effect of the deletion of Δ*ftsE* on the morphology (**A**) and growth rate (**B**).

A). Cell morphology of the wild type (LR2; [i]), JB114 (ii), Δ*mreB* (JB133; [iii]), Δ*ftsE* (JB183; [iv]) and Δ*ftsE* Δ*mreB* (JB184; [v]) during early exponential and mid-exponential phases. Cells were grown at 37°C in PAB supplemented with 0.5% xylose and 20mM MgCl$_2$. Membranes were visualised with FM5-95 dye. Scale bar=3μm. **B).** Growth rate of the wild type (LR2), Δ*ftsE* (JB183), Δ*mreB* (JB133) and Δ*ftsE* Δ*mreB* (JB184) at 37°C in PAB supplemented with 0.5% xylose and 20mM MgCl$_2$.

4.2.12 Absence of MreB changes membrane properties

It has previously been demonstrated that MreB creates islands with increased fluidity and that a triple deletion of all the three MreB homologues significantly elevates the overall membrane fluidity (Strahl et al., 2014). Taken alongside the historic L-form literature in which changes to the membrane were observed (Montgomerie et al., 1973), and the recent discovery that L-form proliferation requires increased membrane fluidity (Mercier et al., 2012), the hypothesis was that loss of *mreB* results in a change in membrane fluidity that enable the L-forms to grow with minimal osmoprotection.

When overall membrane fluidity was measured using Laurdan generalised polarisation (GP), it turned out that none of the osmo-resistant mutant strains tested either in the walled-form or L-form exhibited any significant change in membrane fluidity in comparison to the wild type (LR2) (figure 4.16). The Laurdan GP experiments showed that there was no overall change in the membrane fluidity. However, it was possible that loss of MreB influenced the membrane composition. To investigate this, the fatty acid compositions of the strains in the L-form state were analysed using gas chromatography (table 4.1). Surprisingly, JB114, Δ*mreB* and *mreB*$^{\Delta 20}$ all showed increased fatty acid length (more C_{17} species and fewer C_{15} species) relative to the parent strain, a result that would typically lower the membrane fluidity (figure 4.17.B). Intriguingly, JB115 has a similar fatty acid composition to the parent strain. However, the theoretical decrease in membrane fluidity in the three strains is offset by an increase in the percentage of *anteiso* fatty acids as compared to *iso* fatty acids (figure 4.17.A). The *anteiso* species carry a methyl group on their third-to-last carbon molecule, compared to the *iso* species in which the methyl group is carried on the penultimate carbon molecule. Placement of the carbon on the third to last position results in a significantly more fluid molecule than that of the *iso* species. Again, this change in the fatty acid composition is not seen in the JB115 strain. Taken together, it appears that loss of *mreB* does affect the membrane composition, with the deletion resulting in an increase in the fatty acid chain length. It is not obvious whether this phenotype allows L-forms to grow with minimal osmoprotection or whether it is a side effect of the loss of an important membrane protein. That JB115 possesses a membrane that is almost identical to the parental strain suggests that the latter guess is probably correct.
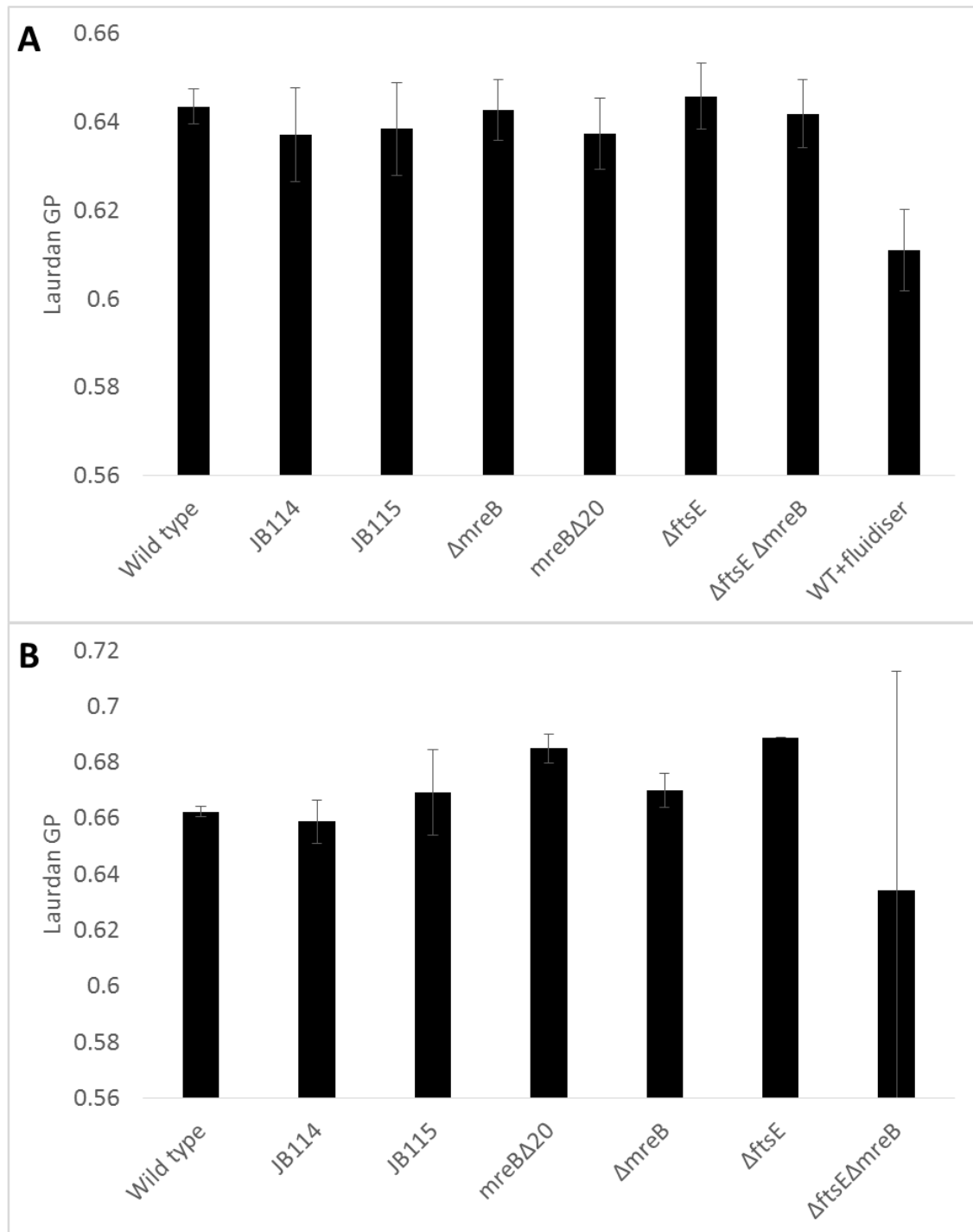
Figure 4.16. Overall membrane fluidity as measured by Laurdan GP of the wild type (LR2), JB114, JB115, *mreB*$^{\Delta 20}$ (JB150), Δ*mreB* (JB133), Δ*ftsE* (JB183) and Δ*ftsE Δmreb* (JB184) when grown as rods (A) and as L-forms (B). Decrease in the Laurdan GP value represents an increase in membrane fluidity. Treatment with membrane fluidiser (30 mM benzyl alcohol) was used as a positive control for increased membrane fluidity. The graphs depict the average values and standard deviations from three independent measurements.

Fatty Acid	Wild type	JB114	JB115	ΔmreB	mreB$^{\Delta20}$
C$_{14:0}$ iso	3.2±0.13	1.08±0.02	4.61±0.12	1.48±0.20	1.28±0.18
C$_{15:0}$ iso	15.2±0.26	11.3±0.65	15.0±0.71	10.0±1.20	10.0±1.50
C$_{15:0}$ anteiso	35.0±1.80	35.8±0.52	36.0±0.49	37.7±1.00	37.6±0.46
C$_{16:0}$	4.9±0.50	5.4±0.12	6.2±0.48	3.3±0.45	4.0±0.98
C$_{16:0}$ iso	9.5±0.14	5.2±0.03	12.3±0.03	7.53±0.96	6.36±0.79
C$_{17:0}$ iso	12.7±0.22	13.7±0.14	11.1±0.07	12.9±0.72	13.2±0.82
C$_{17:0}$ anteiso	13.0±0.08	20.1±0.86	11.3±0.70	21.7±2.15	23.0±2.205
C$_{18:0}$ iso	1±0.11	<1	<1	<1	<1
C$_{18:0}$	1.91±0.105	2.84±0.12	1.98±0.35	1.49±0.13	2.44±0.57
>C$_{18}$	<1	1.98±0.57	<1	1.34±0.33	1.69±1.19
sum	96.4%	97.5%	98.4%	98.5%	100%
C17/C15	0.51±0.02	0.72±0.02	0.44±0.02	0.73±0.03	0.76±0.05
<16/≥16	1.26±0.08	0.98±0.01	1.30±0.01	1.00±0.01	0.95±0.05
iso/anteiso	0.86±0.04	0.55±0.03	0.91±0.04	0.55±0.08	0.52±0.07
Laurdan GP	0.66±0.00	0.66±0.01	0.67±0.02	0.67±0.01	0.69±0.01

Table 4.1. The fraction of fatty acids which contribute to more than 1% of the overall fatty acid content are presented as mean and standard deviation of duplicate measurements. The corresponding *in vivo* Laurdan GP values are presented as mean and standard deviation of three independent measurements. Strains used: *Bacillus subtilis* LR2 (L-form wildtype), JB114 (osmomutant), JB115 (osmomutant), JB133 (Δ*mreB*) and JB150 (*mreB$^{\Delta20}$*).
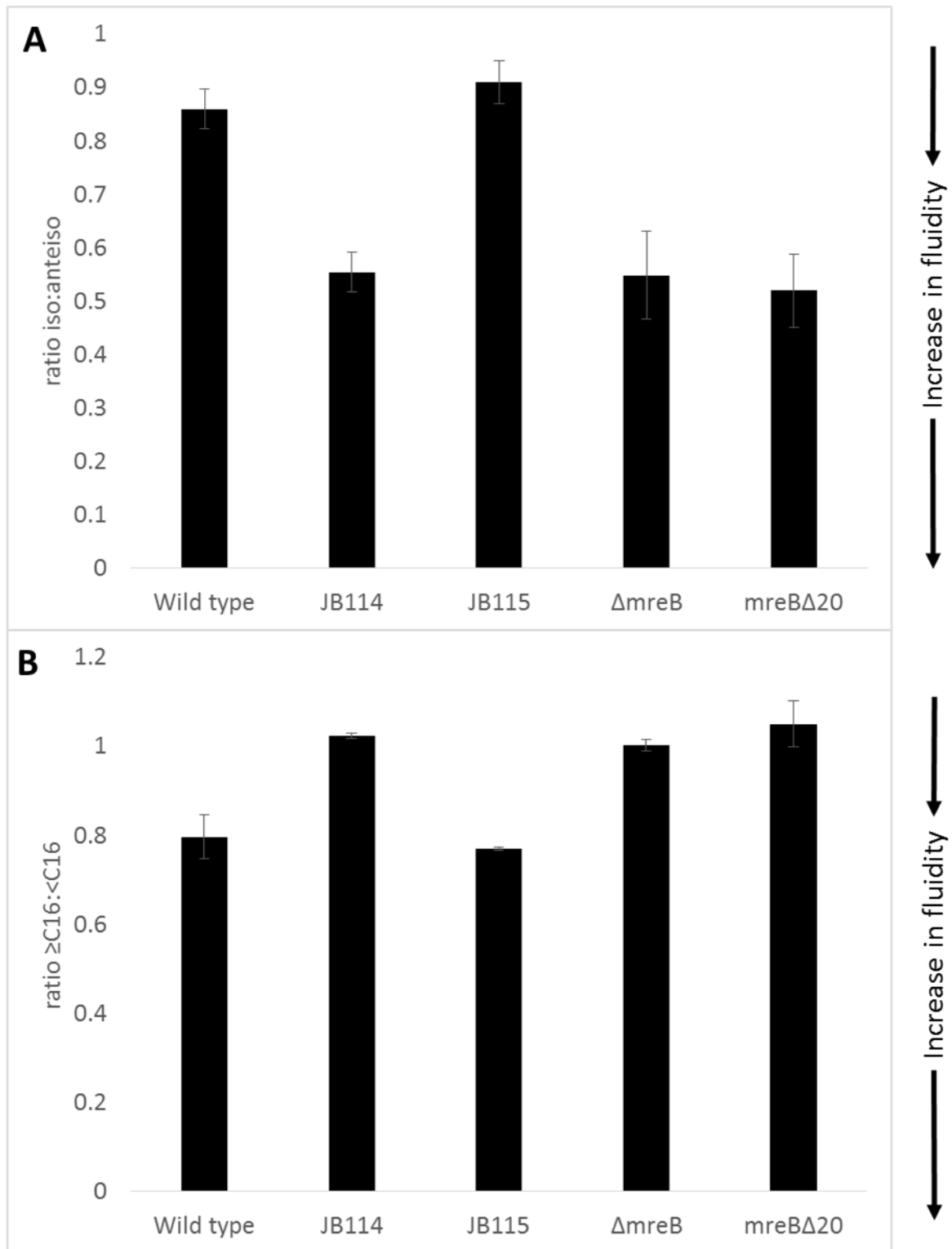
Figure 4.17. Graphical representation of data of the presented in table 4.1. **A).** the ratios between the *iso* and *anteiso* forms of the fatty acids of the different strains and **B).** the ratios between the chain lengths of the fatty acids as presented in the table. High *iso/anteiso* or high long chain/short chain ratios indicate reduced fluidity.

4.3 Discussion

In many regards, the work into the role that MreB plays on cells that lack a cell wall and how its absence enables L-forms to grow in the complete absence of osmoprotection has raised as many questions as it has answered. Upon identification of the in-frame deletion of MreB in the mutant strains it was hoped that this mutation might represent either a specific gain or loss of function. It now appears that the mutation is functionally identical to a null-mutation, with the in-frame deletion preventing disruption of the essential downstream genes; *mreC* and *mreD*. Despite this conclusion, this work has demonstrated that deletion of *mreB* is sufficient for L-forms to grow in low osmolarities; conditions that include the complete absence of osmoprotection. Such results fly in the face of what we should expect for L-forms, as it would be expected that turgor would result in cell death. To render this even more exciting, it suggests a novel role for MreB that is independent of the cell wall synthesis it has traditionally been involved in.

Recent work by (Schirner et al., 2015) has shown that lipid II is required for the formation of the MreB filaments on the cell membrane. The strain used in this work, LR2, grows as an L-form as a result of a depletion of MurE. As described earlier, MurE is involved in Lipid II synthesis. Therefore, depletion of MurE should be resulting in the disassociation of the MreB filaments. Dissociated from the filaments, MreB is no longer localising and positioning the biosynthetic complexes it interacts with. It is therefore not a stretch to presume that outside its normal filaments in the wall-less L-forms, MreB is inactive. However, by demonstrating that deletion of MreB plays a role in cells lacking a peptidoglycan cell wall it implies an additional role for MreB that is independent of the cell wall. What this precise role is remains unclear, but recent discoveries, as well as work presented here suggest a role in the regulation of the cell membrane.

It has recently been shown that MreB, along with its homologues help to organise the cell membrane (Strahl et al., 2014, Strahl and Hamoen, 2010). When MreB assembles into filaments it results in the formation of regions of increased fluidity, whilst loss of all the MreB homologues results in an overall increase in membrane fluidity. How MreB affects the cell membrane is unclear. Peripheral proteins have been shown to possess the ability to induce lipid domains (Garcia-Saez et al., 2007, Cornell and Taneva, 2006), though this requires binding of the lipid bilayer by intercalating amphipathic helices.

Such features are absent in the MreB homologues present in Gram-positive organisms (Salje et al., 2011). Despite this, it's within reason that one of the many interacting partners of MreB could be responsible. Alternatively, it's possible that MreB helps to organise the membrane by directly interacting with the lipid head groups and disrupting the electrostatic interactions between the different lipid head groups (Mbamala et al., 2005). Changes in the makeup of the membrane naturally affect its properties. For instance, increased viscosity will limit protein diffusion (Lee, 2004).

At this point in time it was not possible to establish whether the increase in fatty acid length as well as the change in the branching of the fatty acids were allowing the L-forms to grow in the low osmolarities or were merely the result of the loss of an important membrane-associated protein. Further, with the complexity of the complexes formed by MreB, it's entirely possible that either a known or unknown interaction partner is responsible for the ability of L-forms to survive in low osmolarities.

The fatty acid profile of JB115 renders making of any hypotheses related to the changes in membrane troublesome due to the surprising difference to the other mutant strains and the similarity to the parent strain.

In general, there are three probable explanations for the ability of the L-forms to grow in low osmolarities when *mreB* is deleted. Firstly, the loss of *mreB* enables the L-forms to retain some degree of turgor. As detailed earlier, it is assumed that L-forms are effectively isotonic with their environment due to their inability to maintain turgor. Therefore, when L-forms enter the low osmolarity medium they are unable to constrain their cellular machinery, resulting in cell death. It is possible that without MreB, the membrane is altered to an extent by which the L-form cells are able to maintain some degree of turgor, allowing them to maintain a functioning cellular machinery.

The second possibility is that the loss of MreB affects the uptake of K^+, with a lower cytoplasmic K^+ concentration reducing the amount of turgor generated by the cell, enabling the L-forms to survive in low osmolarities. It was demonstrated in the work of Strahl et al. 2015, that many different proteins are localised by the presence of the RIFs organised by the presence of MreB. It is conceivable that the loss of these RIFs could result in disruption of the K^+ uptake systems.

The other alternative is that the deletion of MreB enables the L-forms to survive when the cellular cytoplasm is isotonic with the low osmolarity medium, thereby removing the need for the cells to maintain turgor for survival. However, there is no clear mechanism through which loss of MreB could enable this process.

It may be beneficial not to look towards *in vivo* studies of MreB and the bacterial membrane, but instead turn towards some of the work in the field of synthetic biology. One of the myriad aims of synthetic biology is to create the simplest form of life. To explore the problem, giant vesicles are often used (Walde et al., 2010). These are simple lipid structures that separate an aqueous solute core from the surrounding aqueous environment. Such systems have been used to investigate and explore how primordial cells may have survived before the evolution of the bacterial cell wall. Like living cells, when these vesicles are placed in hypotonic conditions, water can readily cross the lipid membrane (Fettiplace and Haydon, 1980) whereas the passive movement of the solutes across the membrane is far slower (Deamer and Bramhall, 1986). As with living cells, this creates an osmotic gradient across the membrane resulting in an influx of water into and swelling of the vesicle. The membranes can only tolerate a certain degree of expansion (Needham and Nunn, 1990), at which point pores begin to form in the membrane (Ertel et al., 1993). Instead of lysis, a biophysical process has been observed wherein the transient pores allow for the release of solutes (Sandre et al., 1999). The release relaxes the membrane tension, enabling the pores to be resolved and preventing catastrophic lysis. The ability to resolve the pores depends on the osmotic pressure and the properties of the membrane (Ertel et al., 1993). Further, it has been shown that the swelling and release of solutes promotes changes in the membrane (Oglecka et al., 2014). It's possible that the absence of the membrane ordering effect by MreB in the osmoresistant L-forms enables the cells to survive and grow using such a biophysical process reported by the synthetic biologists. Again, such hypotheses are merely speculation.

5 A novel screen for inhibitors of LtaS

5.1 Introduction

5.1.1 Lipoteichoic acid

The Gram positive cell envelope consists of a classical cytoplasmic membrane surrounded by a thick peptidoglycan cell wall. The wall serves to protect the bacterium from external assault, to restrain the cell membrane against the effects of turgor and to provide shape to the cell. Peptidoglycan is a complex mesh of crosslinked glycan strands (Vollmer and Bertsche, 2008). The cell envelope is further enriched in Gram-positive bacteria with teichoic acids (TA). These are similar in overall mass to the peptidoglycan, but far less well understood. The teichoic acids are anionic polymers that can either be attached to the wall (WTAs) or to the lipid head groups in the membrane (LTAs) (Neuhaus and Baddiley, 2003). There have been several proposed roles for the TAs, including: cation homeostasis (Heptinstall et al., 1970, Schirner, 2009), placement of cellular machinery such as the division apparatus (Schirner, 2009, Formstone et al., 2008), efficient protein secretion (Nouaille et al., 2004), pathogenicity (Morath et al., 2001, Fittipaldi et al., 2008), biofilm formation (Gross et al., 2001) and antibiotic resistance (Kristian et al., 2003, Kovacs et al., 2006).

In many bacteria the WTAs and LTAs contain the same repeat units, though they have distinct genetic and biochemical synthetic pathways (Fischer, 1988). The two subject species in this work, *Bacillus subtilis* 168CA and *Staphylococcus aureus* RN4220 both have LTAs composed of repeat units of glycerol-phosphate (Gro-P), though in RN4220 the repeat unit of the WTA is ribitol-phosphate. These TAs can be further modified by D-alanylation (Neuhaus and Baddiley, 2003). In both species the WTA synthetic pathway is encoded by the *tagA-F* operon, with identified proteins for each catalytic step. The synthetic pathway of LTA is less well understood, though our understanding has significantly increased in recent years. The main synthase, LtaS, was discovered initially in *S. aureus*, with a homologue identified in *B. subtilis* (Grundling and Schneewind, 2007b). The synthase catalyses the formation of poly (Gro-P) as well as the attachment to the lipid head group.

Protein localisation studies have revealed that the WTA synthetic enzymes appear to colocalise with the MreB cytoskeleton in *B. subtilis* (Formstone et al., 2008), whereas LtaS localises at the site of division and sporulation (Schirner, 2009). Taken together, it

provides a strong indication that WTA is involved in elongation, whilst LTA is involved in division.

Interestingly, while the WTA synthetic pathway is largely dispensable in both *S. aureus* and *B. subtilis* (though mutants deficient in WTA exhibit reduced pathogenicity and viability), LTA is essential for growth at temperatures over 30°C in *S. aureus* but not in *B. subtilis*. It should be noted that in *B. subtilis* cells, whilst each system is dispensable, jointly they are essential (Schirner et al., 2009).

5.1.2   Redundancy of LTA synthases in *Bacillus subtilis*

S. aureus carries only a single copy of *ltaS*, whereas *B. subtilis* has three additional paralogues – *yqgS, yvgJ* and *yfnI*. Unlike *S. aureus*, in *B. subtilis ltaS* can be deleted, with only limited effects on the growth of the cell. Combinations of double or triple deletions of the paralogues have a moderate effect on the health of the cells, but otherwise they remain viable. Interestingly, double mutants of *ltaS* and *yqgS* are completely blocked in sporulation (Schirner, 2009), indicating a sporulation specific role for *yqgS*. *yfnI* appears to be involved in LTA production during a σ^M-mediated stress response (Kingston et al., 2013).

5.1.3   The MreB homologue Mbl

In rod-shaped bacteria such as *B. subtilis* the cell wall is modelled and sculptured through a series of interactions by the actin homologue MreB. This protein forms helical filaments along the cell periphery, where it interacts with and directs the elongation machinery. In a similar fashion to the LTA synthases, *B. subtilis* possesses two additional homologues, Mbl (**M**re**B**-**l**ike) and MreBH (**MreB h**omologue). All three appear to have overlapping, partially redundant functions, though some specialised roles have been ascribed to them (Kawai et al., 2009, Dominguez-Cuevas et al., 2013). Cells that have lost MreB or one of its homologues exhibit a progressive increase in cell diameter, ultimately leading to lysis. However, cell viability can be restored by the addition of high concentrations of Mg^{2+}, though the role of the magnesium is currently unclear (Challis, 2014). In the absence of magnesium, *mbl*-null mutants can acquire suppressor mutations that enable the growth of the strains in a magnesium-independent fashion. Using transposon mutagenesis (Schirner, 2009, Schirner and Errington, 2009) were able to identify several of these suppressor mutations. One of these mutations was the loss of *ltaS*.

It is not clear how $\Delta ltaS$ suppresses the magnesium dependency of Δmbl. One plausible explanation is that loss of anionic LTA increases the availability of magnesium in the cell, as less is sequestered by LTA at the cell surface. This hypothesis is supported by results that show $\Delta ltaS$ cells are highly sensitive to even low concentrations of the toxic cation Mn^{2+}.

5.1.4 Drug discovery

Antibiotic resistance of *Staphylococcus aureus* is an ever increasing problem, with resistance to β-lactams wide spread (MRSA), and emerging resistance to glycopeptides (VISA) (Menichetti, 2005). The increase in resistance results in a greater number of therapeutic failures leading to a rise in the morbidity and mortality associated with such infections. Novel antibiotics are required to combat the increasing burden of antibiotic-resistant infections.

For the development of novel antibiotics, a suitable drug target is required. The optimal targets should: (i) only be present in bacteria, not in eukaryotes; (ii) be easily accessible to the antibiotic and remain unaffected by the reach of multidrug efflux pumps. To this extent β-lactams and glycopeptides fulfilled all these criteria as their targets in the peptidoglycan synthesis machinery are extracellular and unique to bacteria. Attempts to find other such extracellular, essential targets have been problematic.

The lipoteichoic acid synthase in *S. aureus* is an attractive potential target for antibiotic development. Firstly, the synthase is essential for the growth of the bacterium under physiological conditions. Secondly, the catalytic head group of the synthase lies outside the cell (Schirner et al., 2009, Grundling and Schneewind, 2007b), rendering it accessible to antibiotics. In addition, $LtaS_{Sa}$ as an antibiotic target has previously been validated from a small molecule inhibitor screen (Richter et al., 2013). In the same work, they were unable to isolate any mutants resistant to their inhibitor, further increasing the attractiveness of LtaS as a target.

Almost two-thirds of antibiotics currently in use were originally isolated from bacteria belonging to the phylum Actinobacteria (Berdy, 2012). The actinomycetes are a rich source of antibiotics as well as antifungals, antiparasitics and anticancer agents, due to a highly complex secondary metabolism. Actinomycetes can be isolated from almost all

terrestrial and marine environments; it is thought that the production of secondary metabolites gives a competitive advantage against other bacteria in these niches. The work presented here was carried out in collaboration with Demuris limited, an antibiotic discovery company with a diverse, dereplicated collection of over 10,000 *actinomycete* strains. The observation that loss of LtaS in *B. subtilis* enables magnesium-independent growth of a Mbl null strain was developed into an assay to screen for potential inhibitors of LtaS and was subsequently patented (Errington J, 2009). Through use of this method and the Demuris collection we show that potential inhibitors of LtaS can be isolated.

5.2 Results

5.2.1 Validation of the LtaS inhibition assay

As discussed in the Introduction, loss of *ltaS* is sufficient to enable the growth of a Δ*mbl*
strain in the absence of high levels of magnesium. An assay was previously set up in the
lab to screen extracts derived from the Demuris actinomycetes collection for activity
against LtaS (Errington J, 2009). The hypothesis was that an inhibitory compound should
allow a Δ*mbl* strain to grow in the absence of magnesium. The assay developed is
described in section 2.5.4.14; however, in brief: in a 96 well plate 10 µl actinomycetes
extract was added to 190 µl of nutrient broth containing a 10^{-4} dilution of a stationary
phase Δ*mbl* strain (OD_{600} approx 7.0-9.0) and grown with shaking at 37°C for 16 h in a
plate reader, with the OD_{600} measured every 6 min. The previous work with this assay
was based on use of a Δ*mbl* mutation in the *B. subtilis* 168ED background, which was
recently discovered to carry multiple unexpected mutations (Dominguez-Cuevas et al.,
2012). Thus, the deletion of *mbl* was recreated in a 168CA background and tested in the
established assay with a variety of different magnesium concentrations. The strain
(JB84) responded to the varying concentrations of magnesium in the same manner as
reported for the deletion in the 168ED background (figure 5.1). For the purposes of this
work the highest concentration of $MgCl_2$ used, 20 mM, was used as a positive control,
and 0 mM $MgCl_2$ (i.e. no addition) as a negative control. In many of the tests growth was
observed in the negative control wells at later time points, probably representing the
emergence of mutants with suppressor mutations. On occasions in which the negative
control showed unusually rapid growth the experiment was terminated. Space
permitting, a blank was also included; if not, results were blanked against the negative
control.
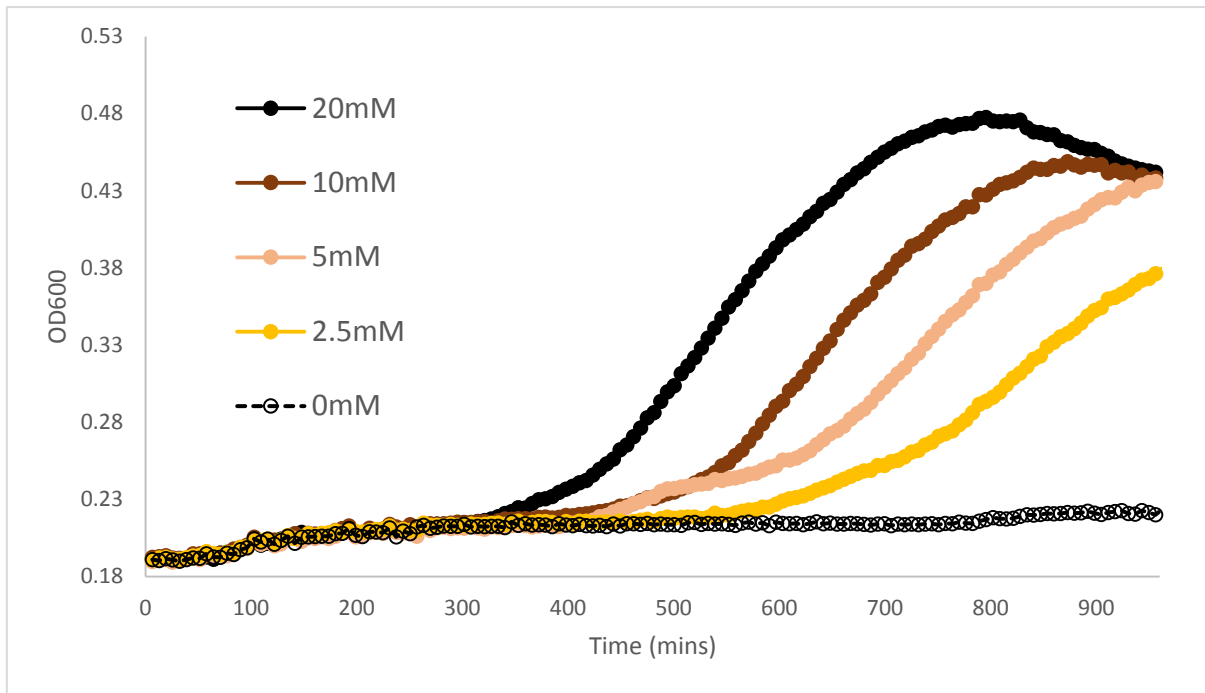
Figure 5.1. Growth rate of the *Δmbl* strain JB84 in the presence of varying concentrations of $MgCl_2$. Cells were diluted 10^{-4}-fold in nutrient broth and grown for 16 h in a plate reader at 37°C.

5.2.2 Identification of activity in the crude extracts from actinomycetes strains DEM30616, DEM29435 and DEM30549

The previous screen (Kim & Errington, unpublished) had highlighted 5 strains with possible activity against LtaS (figure 5.2), each with a distinct appearance. To confirm the production of possible LtaS inhibitors each strain was grown on GYM plates at 30°C. Once robust growth was achieved the plates were crushed, frozen and centrifuged. The supernatants were tested in the established assay. Activity was observed for three of the strains: DEM30616, DEM30549 and DEM20435 (figure 5.3). Despite several repeats, activity was not observed for the other two strains. Absence of growth in wells treated with the supernatant from the other strains indicate that growth restoration is not a result of the carry-over of magnesium from the growth medium. As growth of the strains on solid medium intrinsically limits the scalability in the production of an active compound, the three remaining strains were tested for production of the active compound in liquid medium. Unfortunately, regardless of when the medium was harvested and despite multiple repeats, activity was never detected for DEM29435. Of the remaining strains DEM30549 was relatively difficult to grow, whereas DEM30616 grew in planktonic culture rapidly and robustly. As such DEM30616 was taken forward for purification of an active compound. Addition of culture supernatant from DEM30616 filtered through a 0.45 µm low-binding filter was sufficient to restore the growth of the Δ*mbl* strain in the established assay (figure 5.4).
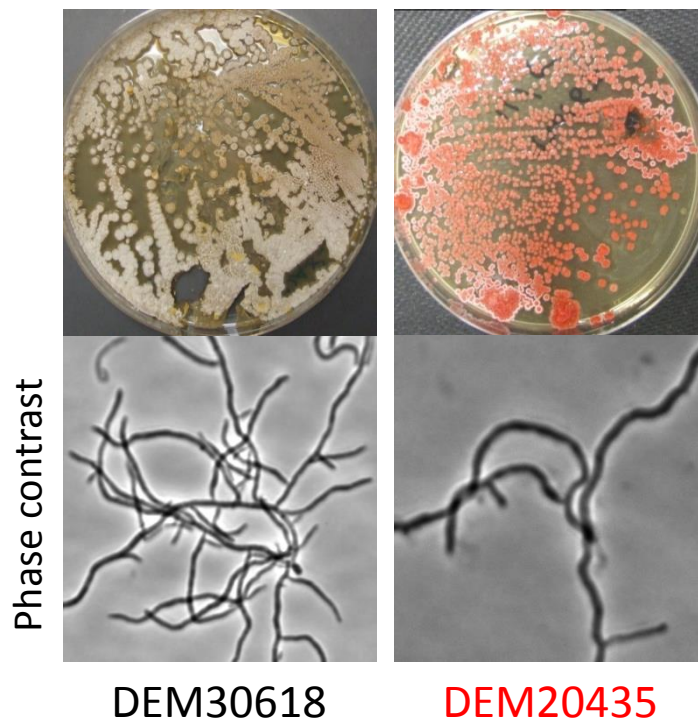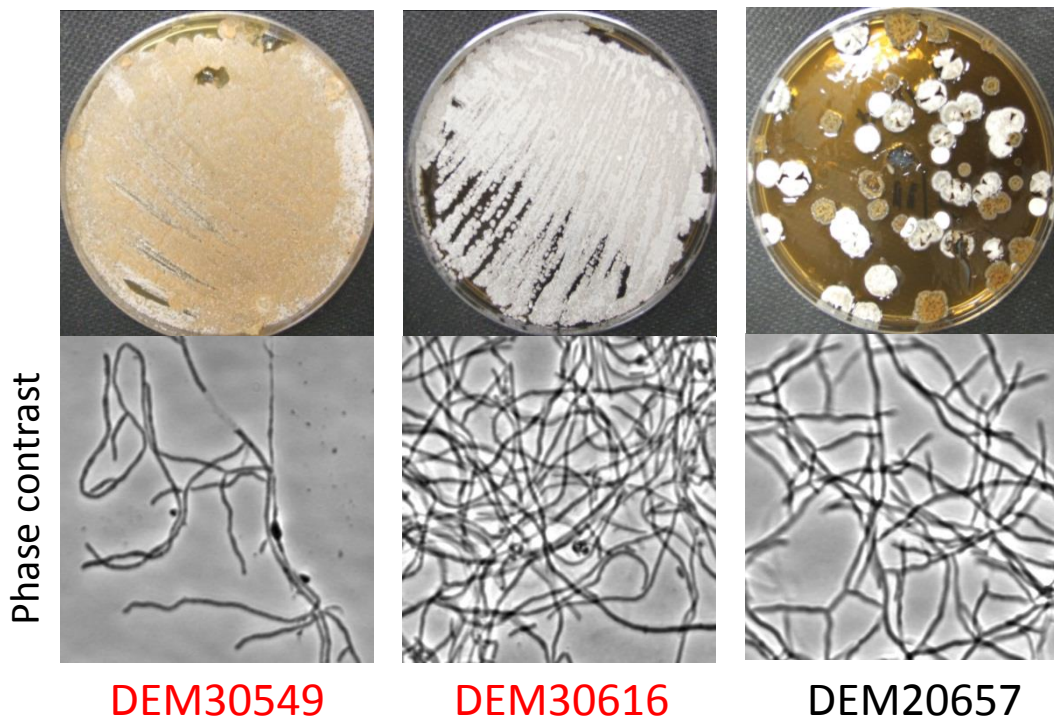
Figure 5.2. Colony and cell morphology of the five strains grown on GYM media at 30°C that were isolated in the screen by Byung-Yong Kim. The strains highlighted in red had the activity against LtaS verified in the established *Δmbl* growth assay.
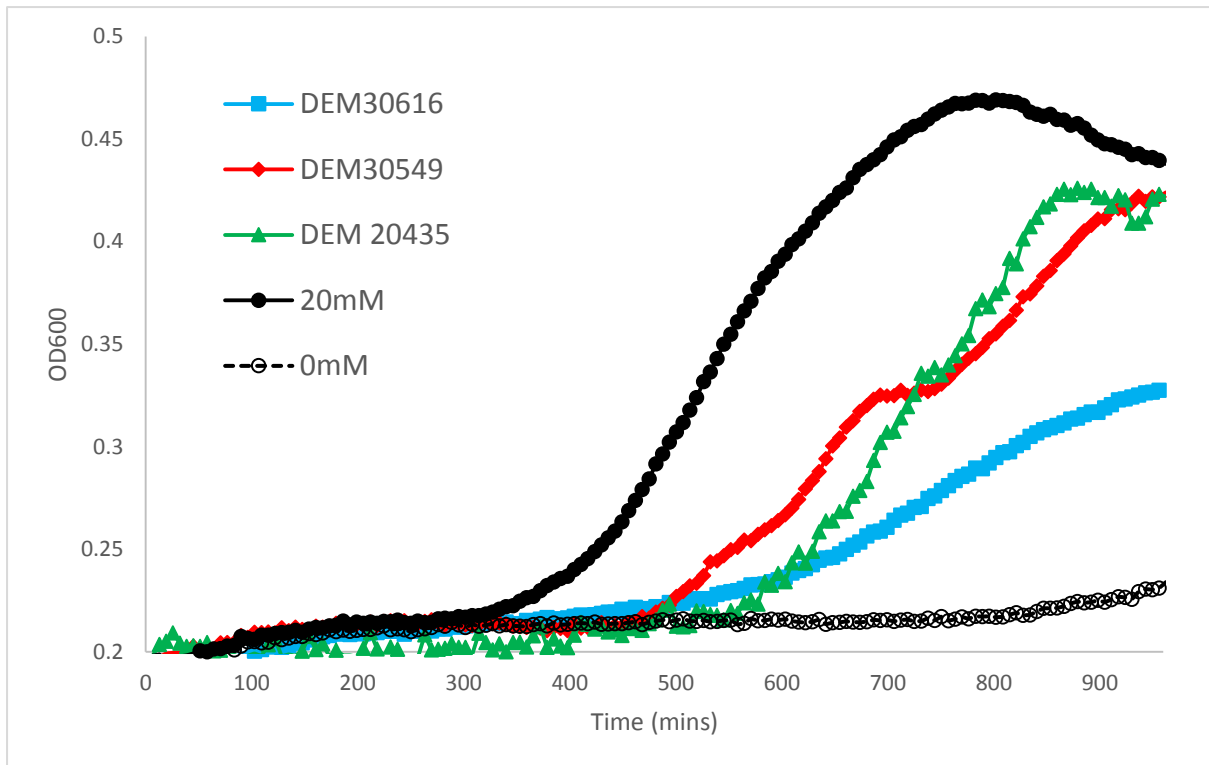
Figure 5.3. Growth of *Δmbl* (JB84) after treatment with extract from crushed GYM plates of DEM30616, DEM30549 and DEM20435. Results are illustrative of two biological replicates, each with eight technical replicates. Graph is composed of data from different, but comparable experiments.
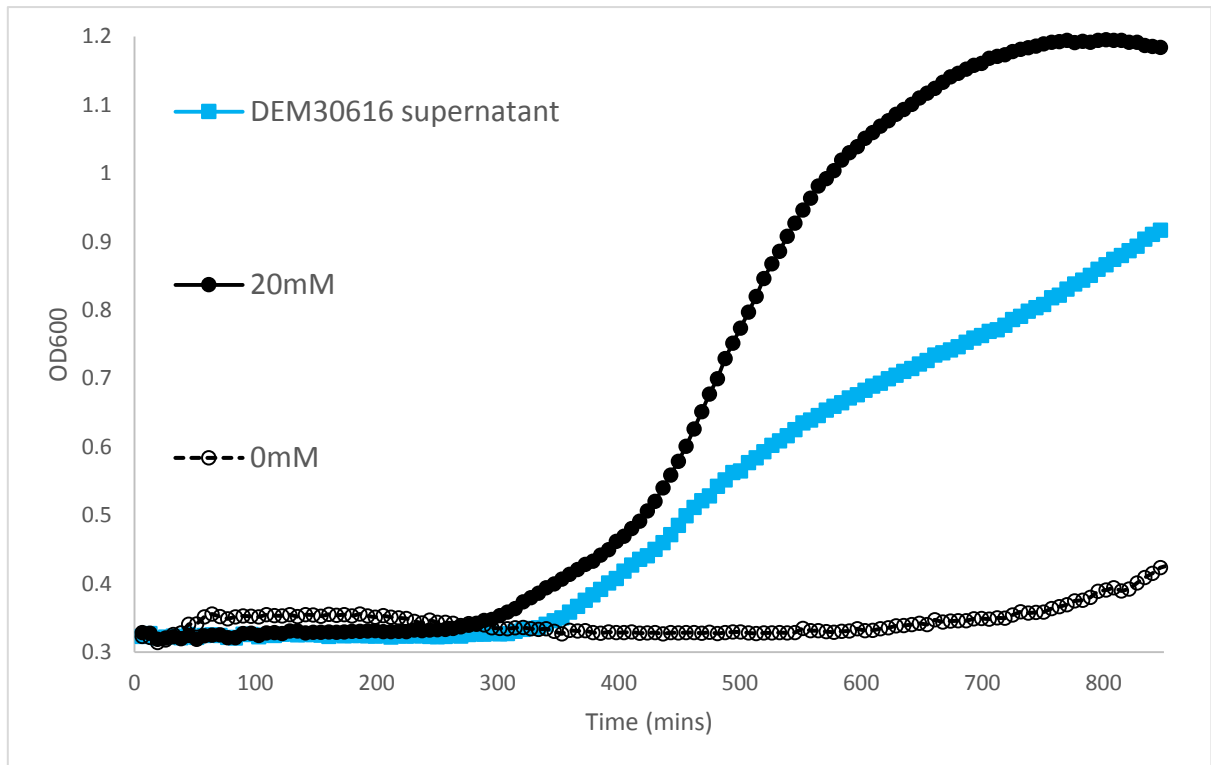
Figure 5.4. *Δmbl* (JB84) can grow in the absence of magnesium when treated with the culture supernatant from DEM30616 grown in GYM media at 30°C. *Δmbl* (JB84) cells were diluted 10^{-4} in nutrient broth and grown in a plate reader at 37°C.

5.2.3 Production of the active compound peaks at day 6 of growth of DEM30616

To characterise the time course for production of the active compound DEM30616 was first grown in 50 ml GYM for 7 days at 30°C, then diluted 10^{-1} into 500 ml GYM. This culture was then grown for 11 days at 30°C, with 10 ml aliquots of culture removed every day after the third day. The aliquots were filter sterilised, stored at -20°C until all samples had been collected, and then tested in the established assay. Figure 5.5 shows that activity peaked after six days, then fell to background by the 10th day. The early peak in activity seen at day 3 could be a result of the dilution at the start of the experiment.
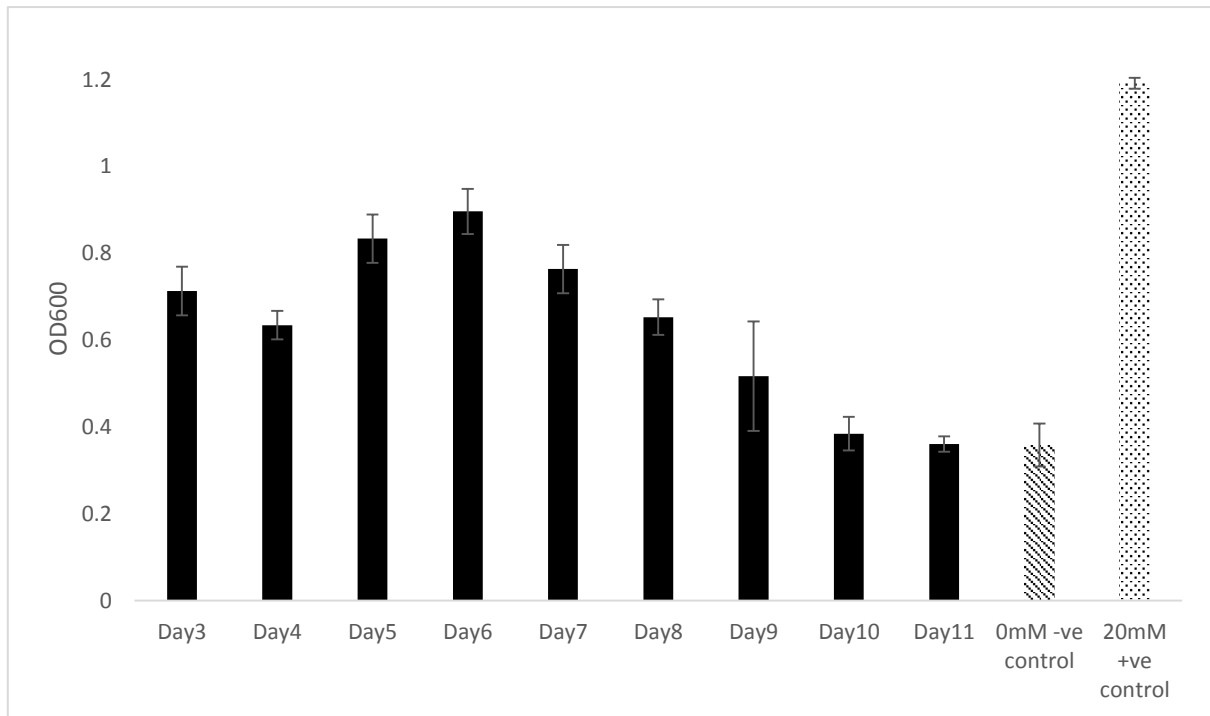
Figure 5.5. Growth of Δ*mbl* (JB84) after treatment with the filtered extract from DEM30616 grown in GYM. Negative control represents growth of JB84 in the absence of supplemented Mg^{2+}; positive control represents growth of JB84 when treated with 20 mM Mg^{2+}. OD_{600} shown is at t_{834}. Standard deviation of eight technical replicates.

5.2.4   16S sequencing identifies DEM30616 as a novel species

To further characterise strain DEM30616, the 16S rRNA gene was sequenced. Genomic DNA was isolated from DEM30616 growing in GYM media using a DNeasy kit (Qiagen). The DNA was amplified and Sanger sequenced. The identification of phylogenetic neighbours was carried out by BLASTN searches against the EzTaxon 16S database. The sequences obtained were exported for use in Mega (v.6.06) and the sequences aligned using ClusterW. The phylogenetic tree was constructed using the neighbour-joining method of (Saitou and Nei, 1987).

The closest taxon to DEM30616 in the EzTaxon similarity search was found to be *Streptomyces drozdowiczii* (GenBank accession no. AB249957), whose sequence was 99.79% identical, differing in 3 nucleotides. The relationship between DEM30616 and *Streptomyces drozdowiczii*, and to the phylogenetically nearest taxa can be seen in figure 5.6. None of the taxa in the clade have previously been reported to produce antimicrobial compounds (Zucchi et al., 2012, Semedo et al., 2004).
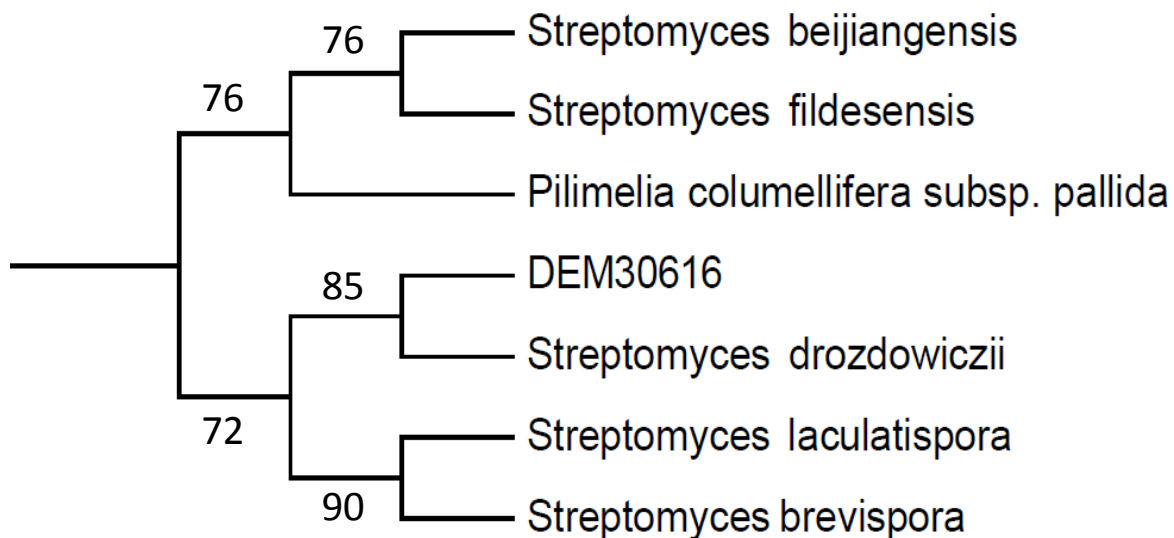
Figure 5.6. Phylogenetic subtree for a selected set of taxa calculated using Mega v6.06 from complete 16S rRNA sequences using the (Saitou and Nei, 1987) neighbour-joining method, illustrating the taxonomic position of DEM30616 relative to species found most similar by an EzTaxon search. Percentages at the nodes represent the levels of bootstrap support (n=1000).

5.2.5   Active compound purification

5.2.5.1 Ethyl acetate extraction

In preliminary solvent extraction experiments with ethyl acetate the active compound remained in the aqueous phase (figure 5.7), therefore this purification step was omitted in the future, with reverse phase chromatography used instead to crudely purify the active compound.
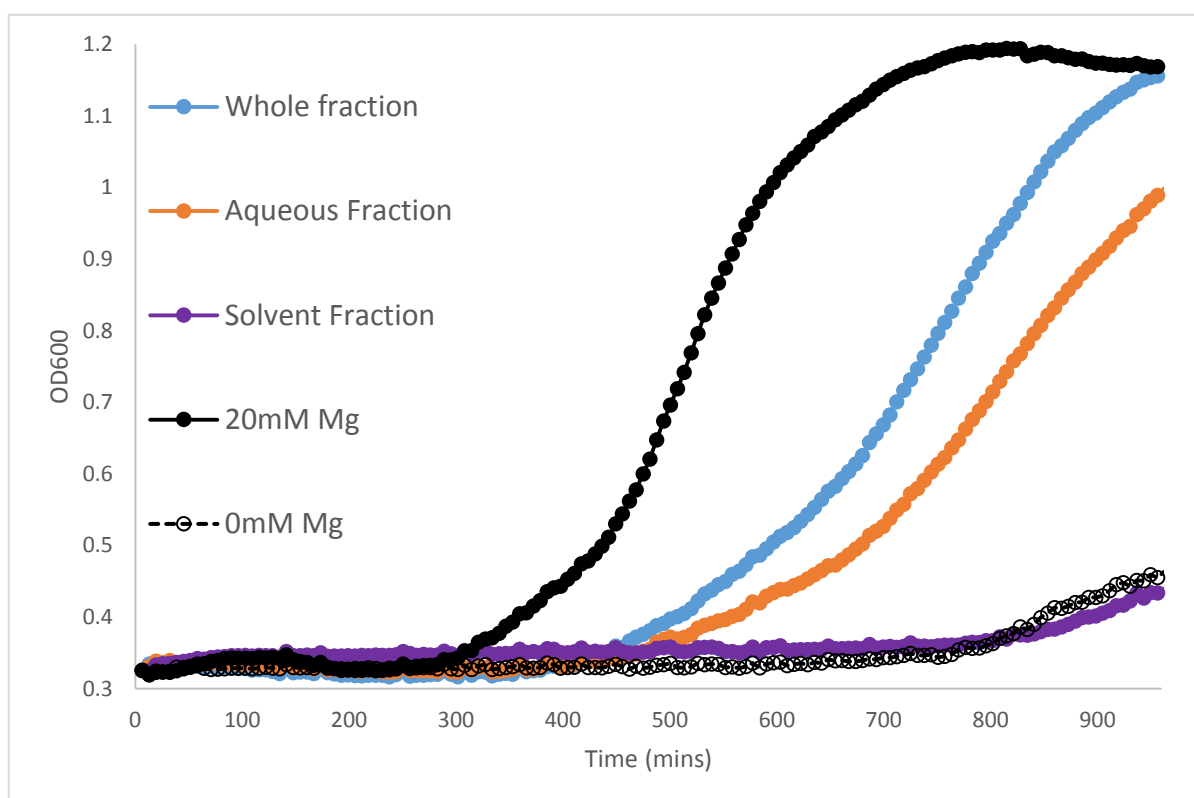
Figure 5.7. The aqueous and solvent fractions from an ethyl acetate extraction tested against *Δmbl* (JB84). 10 μl of each fraction was added to a total volume of 200 μl. Graph is illustrative of the results of two purifications each with two biological replicates and 8 technical replicates. 20 mM MgCl$_2$ was used as the positive control; no supplementation was the negative.

5.2.5.2 Reverse phase chromatography

An aliquot (30-50 ml) of filtered supernatant was loaded onto a C18 30 g silica SNAP Biotage column and eluted with methanol (325 ml; 13 CV) at a flow rate of 25 ml/min with a fraction size of 10 ml. Methanol in the fractions was removed using a centrifugal evaporator under pressure (40 mBar, 1725 rpm). After removal of the solvent, fractions were tested in the established assay. Elution of the active material was bimodal in distribution across the fractions, with peaks in activity around fractions 15 and 23. The positions of the fractions with greatest activity varied between purification, but the bimodal distribution remained constant. In addition the first peak was usually sharper, with only a single fraction exhibiting activity, whereas the second group of active fractions tended to show a peak then a gradual decline (figure 5.8). For clarity, the first active compound will be referred to as DEM30616-A, and the second as DEM30616-B.
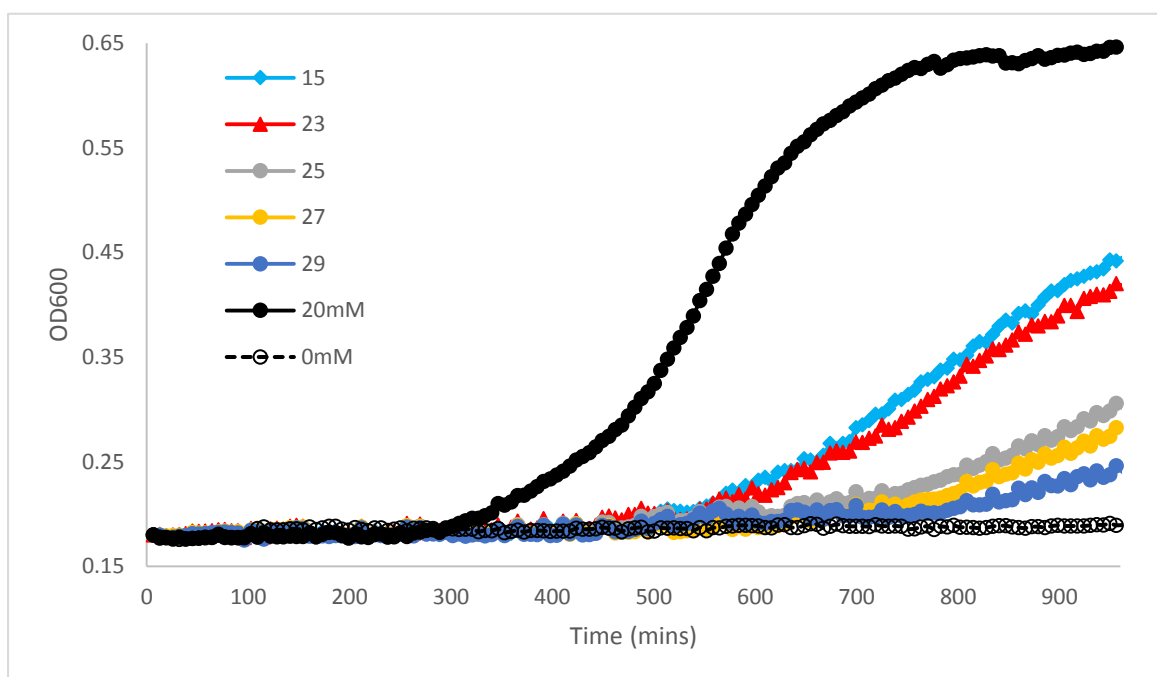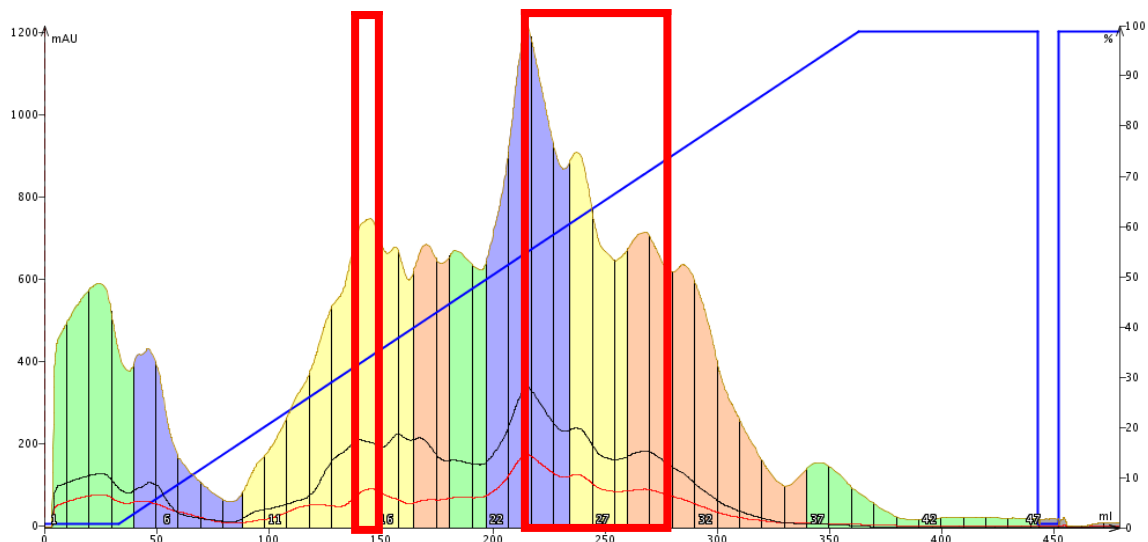
Figure 5.8. Absorbance of the fractions during reverse-phase chromatography from a gradient of 0-100% methanol. Red rectangles indicate the fractions that contained active material. Different colours represent theoretical compounds annotated by the computer software. Graph representative of two biological replicates, each with eight technical replicates. Fractions that contained no active material were indistinguishable from the negative control and were omitted for clarity.

5.2.5.3 HPLC separations of DEM30616-A and DEM30616-B

To further purify the compounds the active fractions were run on an Agilent 1260 Infinity HPLC system. The fractions were loaded onto an Agilent Phenomenex column (150x4.50 mm; 4 μm) attached to an integrated pre-column. A 200μl sample of each active fraction was run on a linear gradient from 0-100% over 45 minutes (H_2O (0.1% formic acid): acetonitrile (0.1% formic acid)) at a flow rate of 1 ml/min with UV/vis detection at 254 nm, and were collected every 25 seconds. Acetonitrile was removed using a centrifugal evaporator under pressure. After removal of the solvent the fractions were tested against Δ*mbl* in the assay. Unfortunately, despite several repeats, HPLC separation of DEM30616-A yielded only low level, albeit reproducible activity, in a single fraction (figure 5.9A). In contrast, two of the HPLC fractions of DEM30616-B retained the majority of their activity following purification (figure 5.9B).
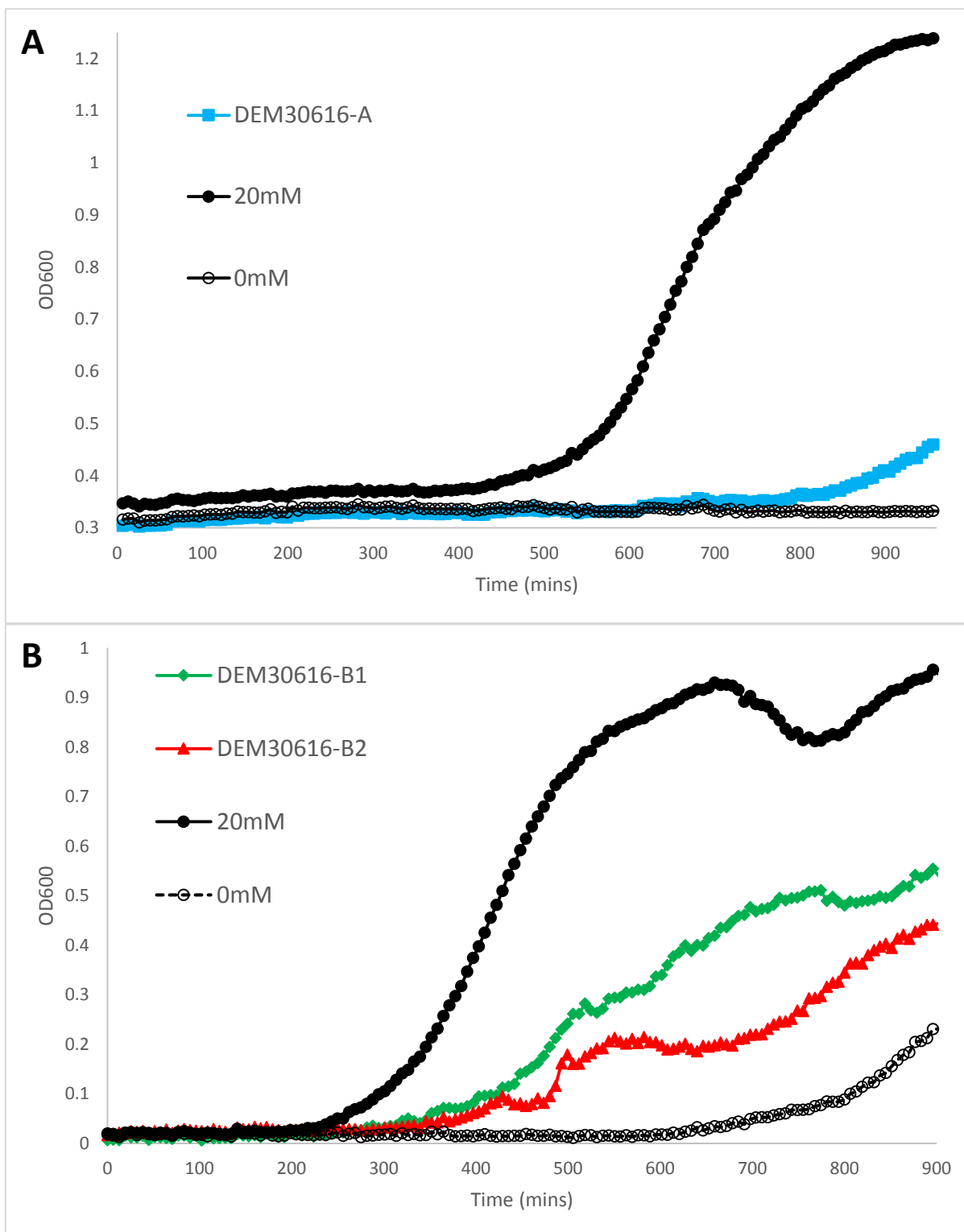
Figure 5.9. HPLC separation of the Biotage fraction 15 (A) and fraction 23 (B) yield active material with varying levels of activity. The two compounds purified from fraction 23 eluted 60 seconds apart. Graphs representative of two biological replicates with a minimum of four technical replicates. Fractions that contained no active material were indistinguishable from the negative control and were omitted for clarity.

5.2.6 Mass spectroscopy identifies DEM30616-A of the compounds as Coelichelin

As reported previously, the activity seen in the semi-pure fraction was being lost following HPLC purification. Despite the activity being very low, it could be reproduced, suggesting that the fraction contained the compound of interest. Analysis by HPLC, revealed the fraction was suitable for analysis by mass spectroscopy (figure 5.10). The main peak in the mass spectral trace, at 566 Da, was used to search the dictionary of natural products. The search returned several possible compounds, one of which was the siderophore, coelichelin. This identity was confirmed by comparison of the MS/MS fragmentation pattern of the isolated compound to the fragmentation pattern of coelichelin as these were largely identical.
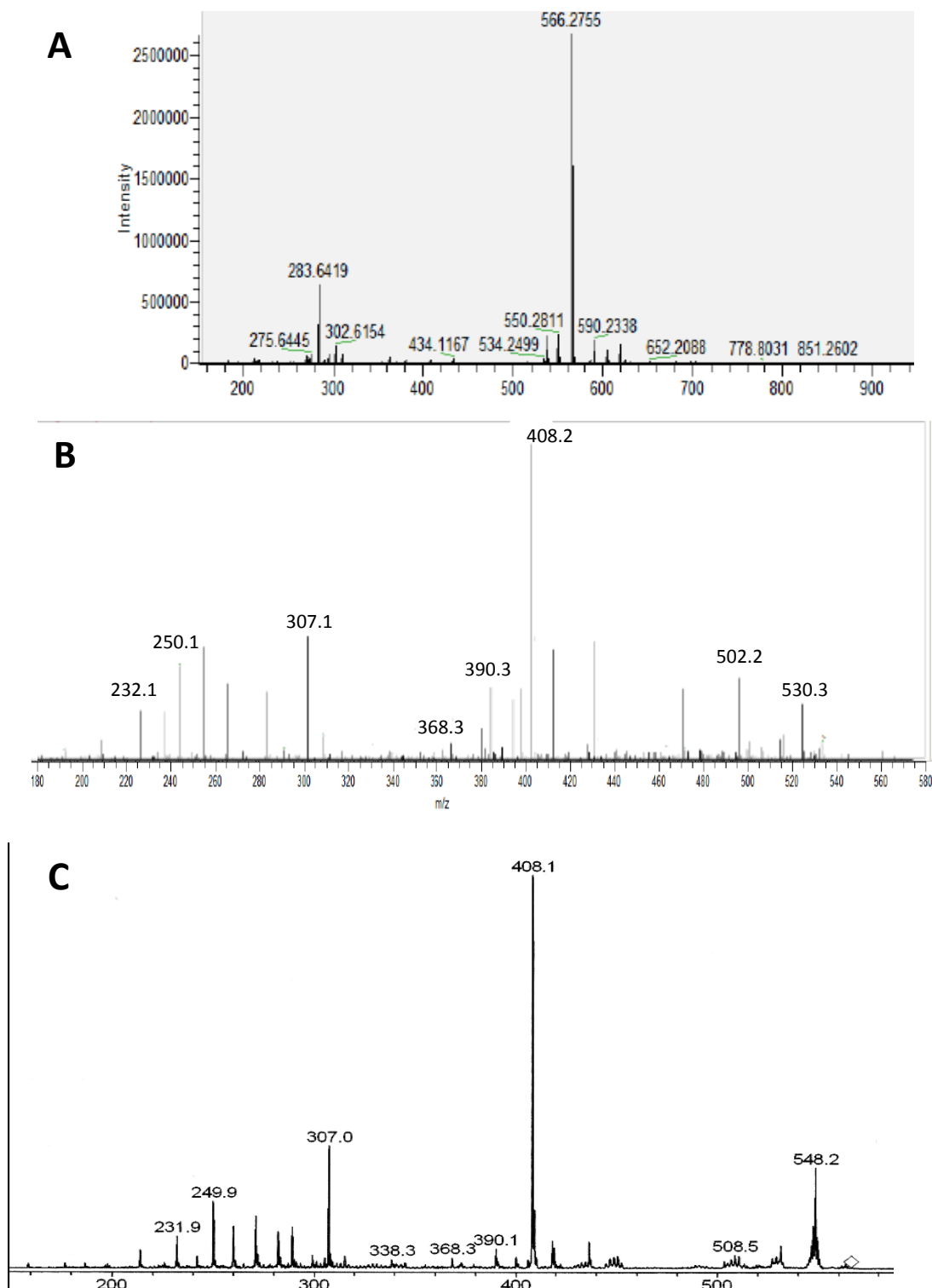
Figure 5.10. MS of the active compound purified present in DEM30616-A (A). MS/MS analysis of the mass at 566 (B). MS/MS data of the fragmentation of the mass at 566 is very similar to that reported previously of desferricoelichelin (C) (Zucchi et al., 2012). MS was performed by Joe Gray.

5.2.7 Sequencing and analysis of the DEM30616 genome reveals the presence of a homologue of the *cch* cluster of *Streptomyces coelicolor*

Coelichelin was identified in one of the first genome mining screens in the *Streptomyces* model organism, *S. coelicolor* (Zucchi et al., 2012, Challis and Ravel, 2000). This work identified coelichelin as a siderophore with a tri-hydroxamate structure (figure 5.11.A). That a siderophore could have an effect on LtaS was somewhat surprising. However, it has been shown that another naturally derived siderophore with the same backbone, foroxymithine (figure 5.11.B), is able to act as an inhibitor of the angiotensin I converting enzyme (ACE) by chelating the zinc. It has since been demonstrated that coelichelin is also able to act as an ACE inhibitor, presumably by a similar function (Challis, 2014).

To probe DEM30616 further and identify potential biosynthetic clusters, the genome was sequenced on the MiSeq platform. Unfortunately, the coverage from the sequencing was too low for *de novo* assembly, however it was possible to assemble the DEM30616 genome against the *S. coelicolor* A3(2) reference genome. A complete *cch* cluster, responsible for coelichelin synthesis in *S. coelicolor,* could be identified in DEM30616 with a roughly 85% level of similarity.
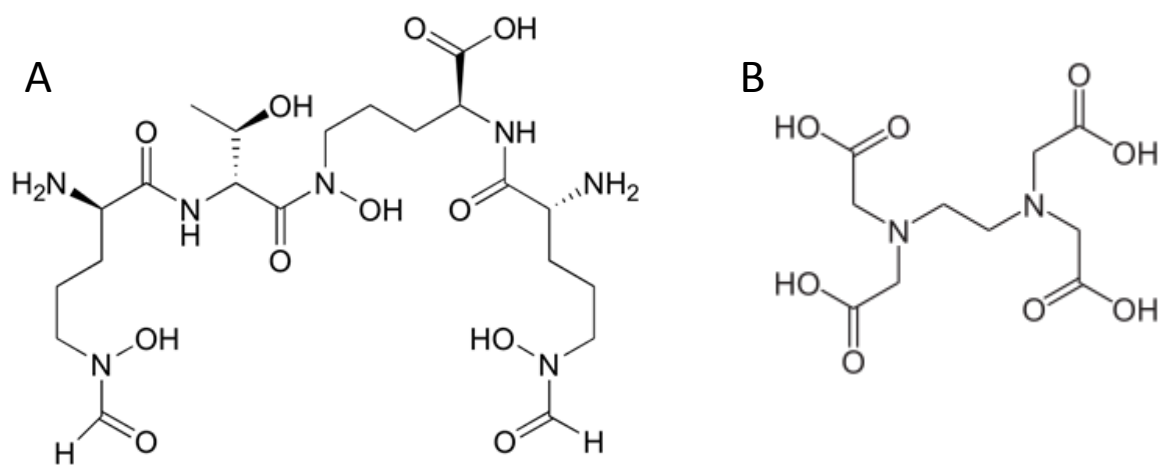
Figure 5.11. The structure of coelichelin (A) and its analogue foroxymithine (B).

5.2.8 Foroxymithine, a compound with a similar backbone to coelichelin has no restorative effect on Δ*mbl*

Coelichelin is not commercially available, though compounds with similar tri-hydroxamate structures are. One of these is foroxymithine. With a similar tri-hydroxamate structure, it was conceivable that foroxymithine could have similar inhibitory effect on LtaS as coelichelin appears to have. A range of foroxymithine concentrations were tested, but no restorative effect on the growth of the Δ*mbl* strain was observed (data not shown).

5.2.9 A sensitivity to iron could explain the effect of coelichelin on Δ*mbl*

As an alternative way to investigate the possible role of a siderophore in alleviating the magnesium dependence of Δ*mbl*, strains 168CA and Δ*mbl* (supplemented with 20 mM MgCl$_2$) were treated with a range of concentrations of FeCl$_3$. Surprisingly, the Δ*mbl* strain was significantly more sensitive to increased iron concentration than the wild type strain (figure 5.12). This suggests that the results seen with coelichelin may be a result of reduced iron toxicity on the Δ*mbl* strain, rather than a reduction in the magnesium dependence/inhibition of LtaS.
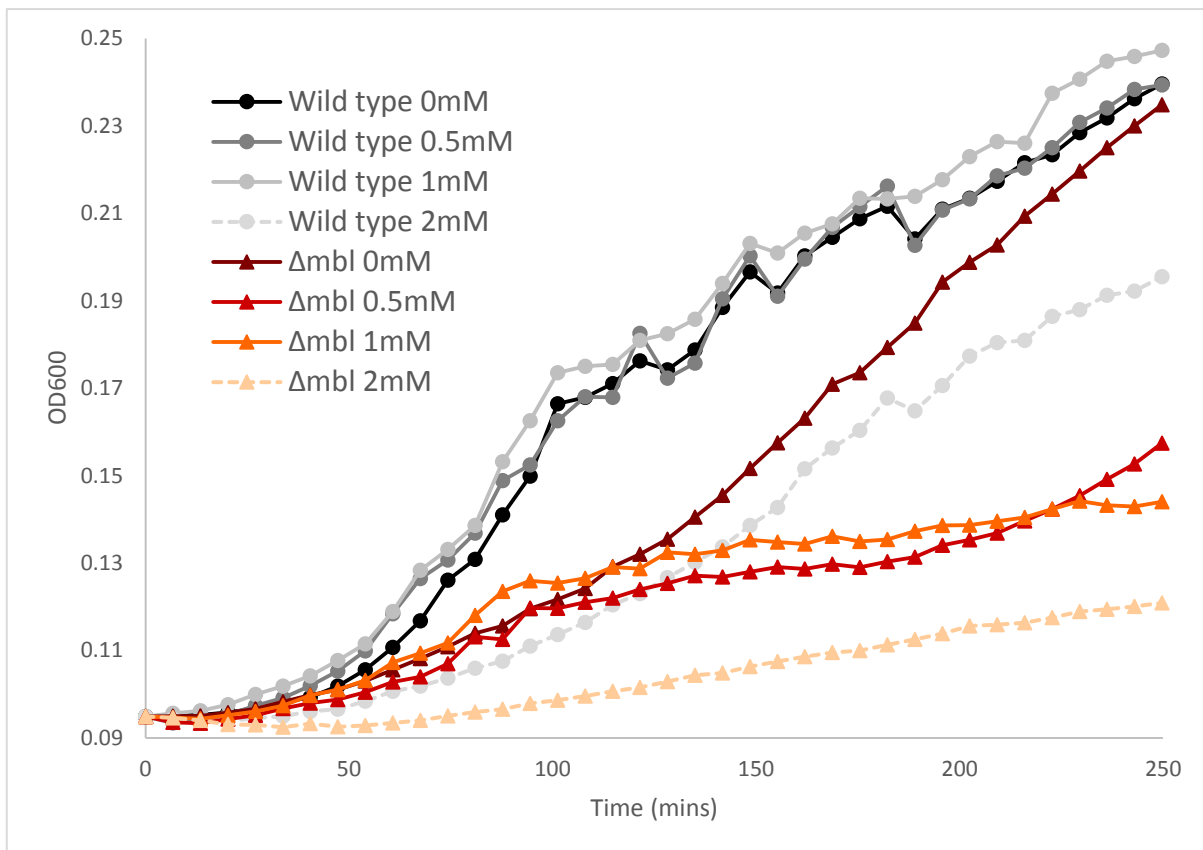
Figure 5.12. Growth of the wild type (168CA) and *Δmbl* (JB84) strains in the presence of varying concentrations of FeCl$_3$. To sustain *Δmbl* growth, cultures were supplemented with 20 mM Mg^{2+}.

5.2.10 DEM30616-B may be an ester with structural homology to the glycolipid anchor of LTA

Further purification of the DEM30616-B peak by preparative HPLC yielded two fractions with strong, reproducible activity in the established assay. Both fractions were sent for mass spectroscopy. In both cases the identification was less straightforward than that of coelichelin, with a number of possible compounds sharing the same mass. Several of these compounds could be disregarded, as the UV/vis traces for the two purified active compounds indicated a low level of conjugation; therefore, candidates with a high level of conjugation could be ignored. The identity of the compounds was investigated by the heuristic filtering of the mass spectroscopy peaks (Semedo et al., 2004). From the data obtained it is possible to determine the possible elemental formulae that adhere to the LEWIS and SENIOR chemical rules (Miessler and Tarr, 2011, Senior, 1951). In brief, these rules filter against formulae that are unlikely to exist or would be highly unstable in nature. The chemical formula can be further probed by examination of the relative abundance of the different isotopes in the compounds of interest. Finally, the fragmentation peaks obtained from the mass spectroscopy (figure 5.13) were screened against the predicted fragmentation patterns of compounds contained in the dictionary of natural products. Combined use of these techniques suggested the possible identity of one of the compounds as an ester of a fatty acid, hexanoic acid, and a sugar, β-D-xylopyranosyl-(1→6)-β-D-glucopyranosyl. The identity of the second compound from the HPLC separation could be another sugar: 3',4',5,7-Tetrahydroxyflavone; 7-O-[α-L-Rhamnopyranosylamino-(1→6)-6-deoxy-β-D-glucopyranoside].

A DAD1 C, Sig=254,4 Ref=360,100 (JAMES\2014-11-28 A2 - C11 90.D)

B DAD1 C, Sig=254,4 Ref=360,100 (JAMES\2014-11-28 A2 - D11 91.D)
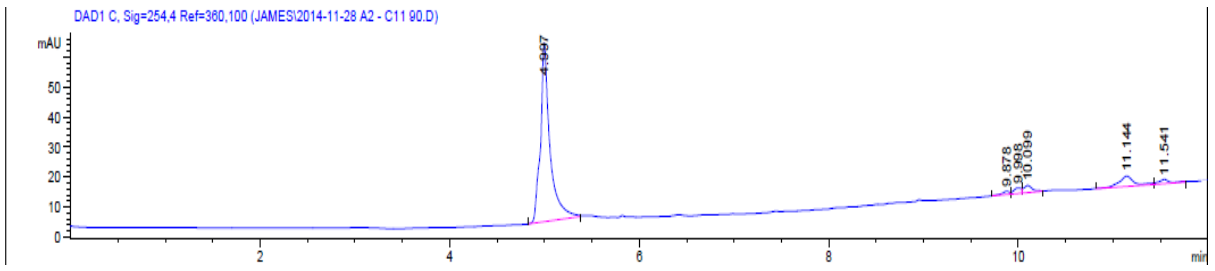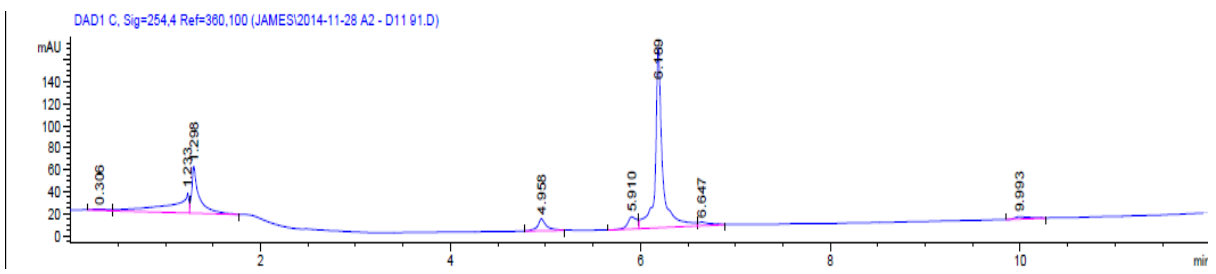
C
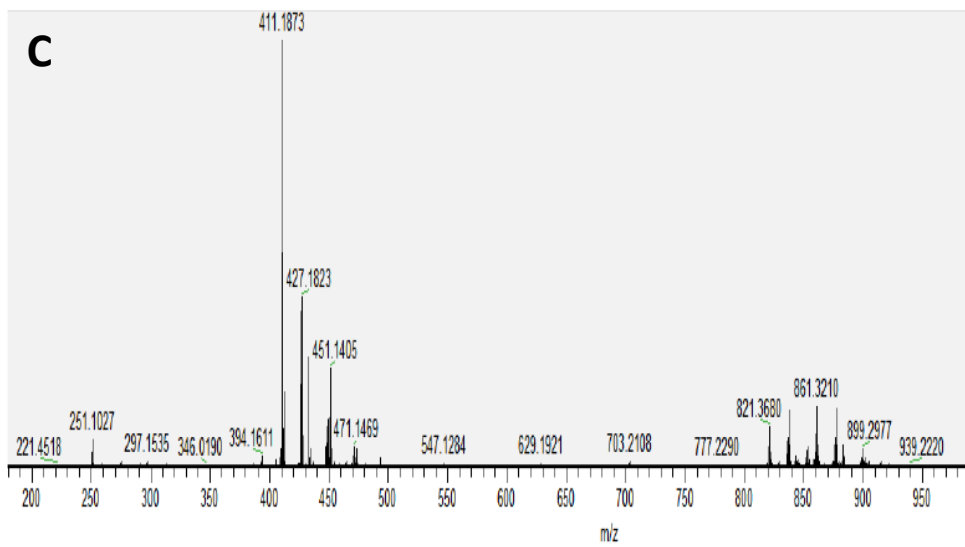
D
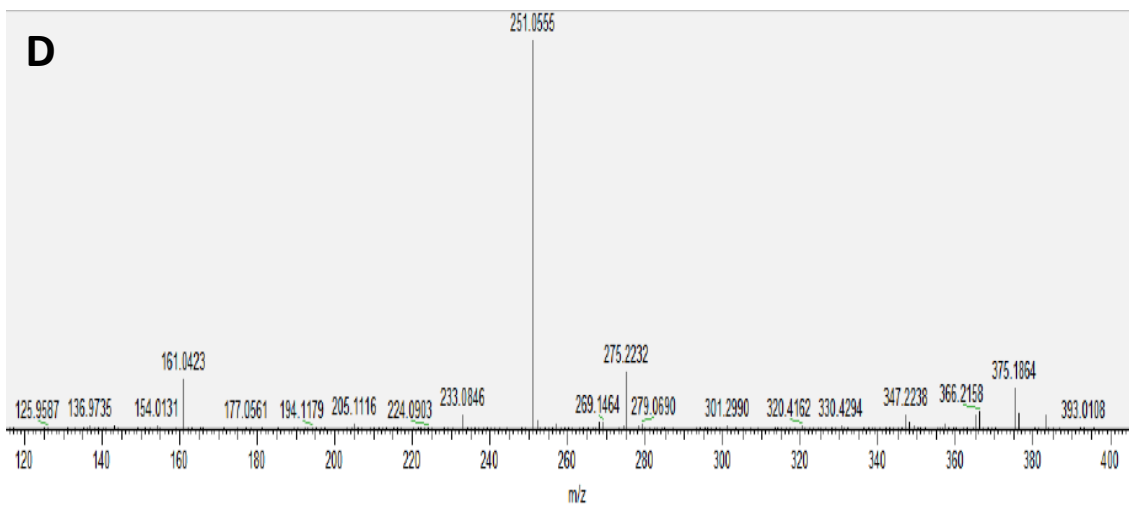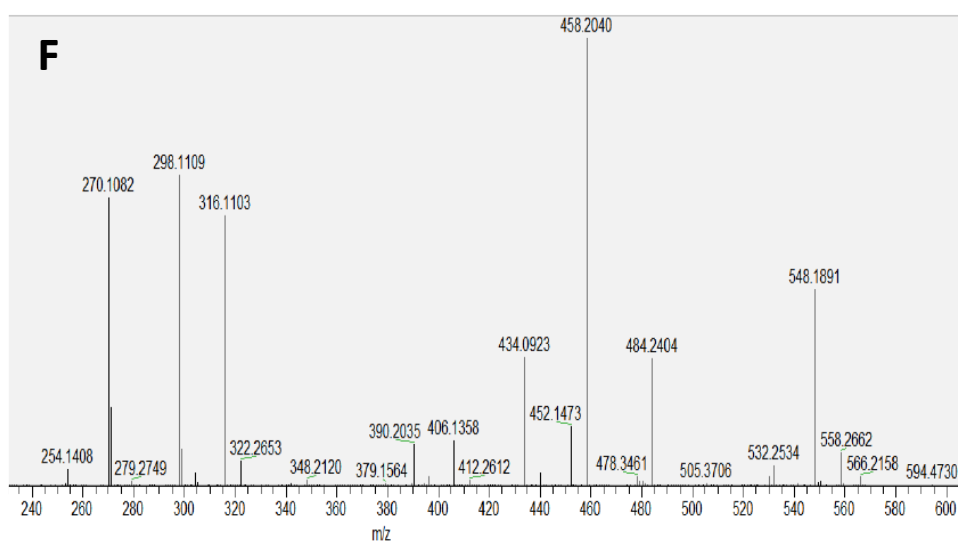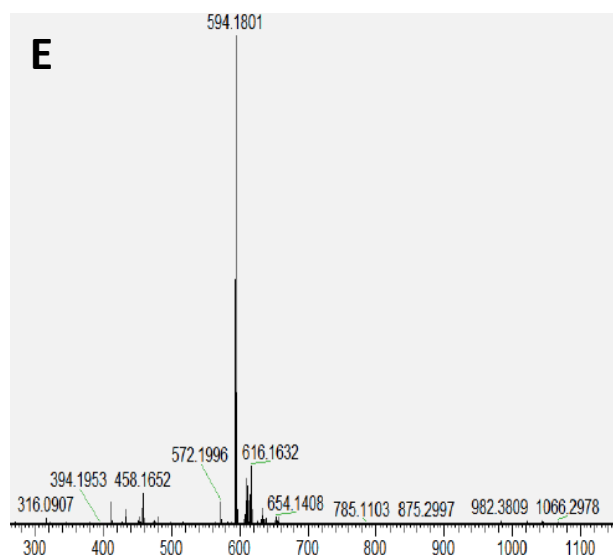
Figure 5.13. Purification of the active compound(s) from the fractions containing the second peak of activity following reverse phase chromatography. HPLC profiles of the fractions in wells C11 (A) and D11 (B). MS of the compounds present in fraction C11 (C) and fraction D11 (E). MS/MS fragmentation of the dominant peaks of C11; 411 (D) and D11; 594 (F). HPLC and mass spectroscopy were performed as described in materials and methods. Mass spectroscopy was performed by Dr. Joe Gray.

To validate the presence of the compounds a fresh culture of DEM30616 was grown and the supernatant harvested. Using the same extraction and purification steps (reverse phase chromatography and HPLC) as described previously, it was possible to isolate a single fraction that had activity in the Δ*mbl* assay. Identity of the compound was confirmed to be DEM30616-B via mass spectroscopy. The second compound was not recovered.

The structure of the first compound was of particular interest as it appears not dissimilar from the structure of the glycolipid anchor to which the glycerol phosphate (Gro-P) subunits are attached to by the LtaS enzyme (figure 5.14). In principle, the compound might work either by directly inhibiting LtaS or by being incorporated into LTA in such a way as to render it non-functional.

Anecdotally, the compound appears highly stable, with little-to-no loss of activity over time (3+ months) when stored at -20°C. Further, neither repeated cycles of freeze-thaw nor overnight storage at room temperature appeared to affect the activity of the compound in the Δ*mbl* recovery assay.

A

B
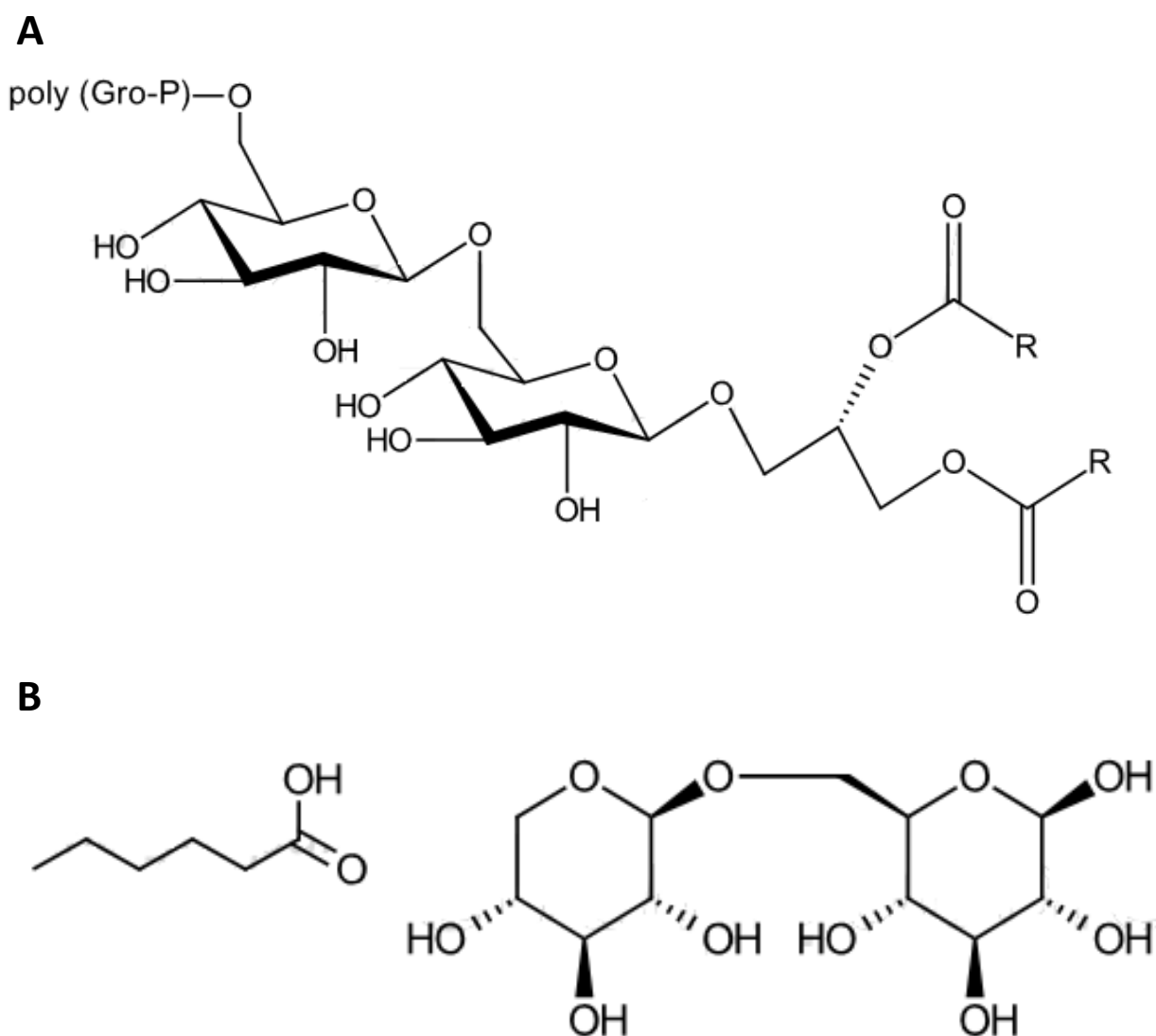
Figure 5.14. Chemical structure of the diacyl-glycerol (DAG) subunit of LTA (A) and the predicted structure of the active compound (B). The hexanoic acid is displayed adjacent to the sugar residues as the oxygen it is bound to is unknown.

5.2.11 The compounds do not work by inducing suppressor mutations in the assay strain

It was possible that the compounds in the screen were promoting the development of suppressor mutations that enable the Δ*mbl* strain to grow independent of magnesium. To examine this issue, at the completion of the growth assay, the cells from the wells treated with 20 mM Mg^{2+} and the compound were used to inoculate fresh media +/- 20 mM $MgCl_2$ to an OD_{600}=0.05 and were grown for 2 hours at 37°C. The cells from both wells remained dependent on the presence of high levels of magnesium for healthy growth; removal of magnesium rendered the cells sick (figure 5.15). This showed that the Δ*mbl* cells treated with the compound remained dependent on magnesium in the absence of the compound.
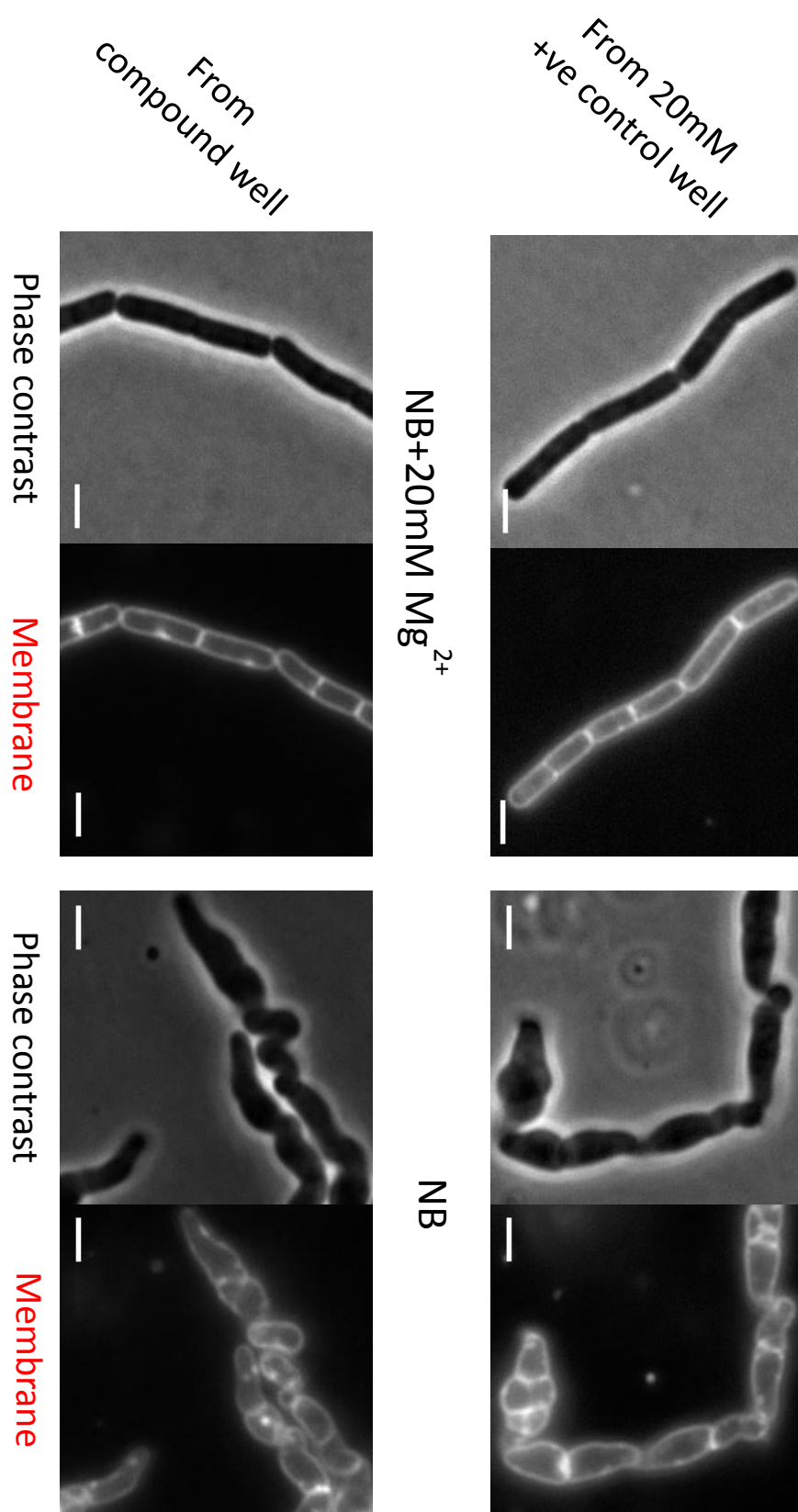
Figure 5.15. Δ*mbl* (JB84) cells remain dependent on magnesium following growth with the compound. Cells were grown for 16 hours in the established assay. At the end point cells from the test wells and the positive control wells were diluted to OD_{600}=0.05 in fresh media +/- 20mM $MgCl_2$ and were grown for two hours at 37°C. Scale bar = 3 μm

5.2.12 Treatment with the compound restores the morphology of Δ*mbl* cells

As described previously, in the absence of magnesium Δ*mbl* cells are very sick, becoming fat with a twisted morphology. In the presence of magnesium, the disturbances to morphology are largely alleviated, though the cells remain smaller than the wild type (Schirner et al., 2009). When *ltaS* is disrupted in a Δ*mbl* background growth is restored to that of the wild type (Schirner et al., 2009). Therefore, examination of the morphology of the Δ*mbl* cells treated with the DEM30616-B compound might provide insights into the effect the compound has on cells. In agreement with Jones et al. 2001, figure 5.16.B demonstrates that Δ*mbl* cells grown in the presence of magnesium, whilst viable, form shorter, fatter cells. In contrast, the Δ*mbl* cells grown without magnesium supplementation are very sick, with gross morphological changes (figure 5.16.C). Whilst the micrographs depict growth, such clusters of cells were infrequently found. Interestingly, the morphology of the Δ*mbl* cells treated with the DEM30616-B compound appeared to take on a more wild type morphology. The alleviation of the growth defects was limited to the early- and mid-exponential phases. These observations supported the notion that the compound targets LtaS. As growth continued the cells treated with compound became progressively sicker, resulting in aberrant cell shapes and lysis. This drop in fitness may have arisen as a result of the compound irreversibly binding to its target, being metabolised or otherwise being exhausted.

t550

t716

t960

A   Δ*mbl* + compound

B   Δ*mbl* + 20mM Mg^{2+}

C   Δ*mbl* - no addition

Phase contrast   Membrane
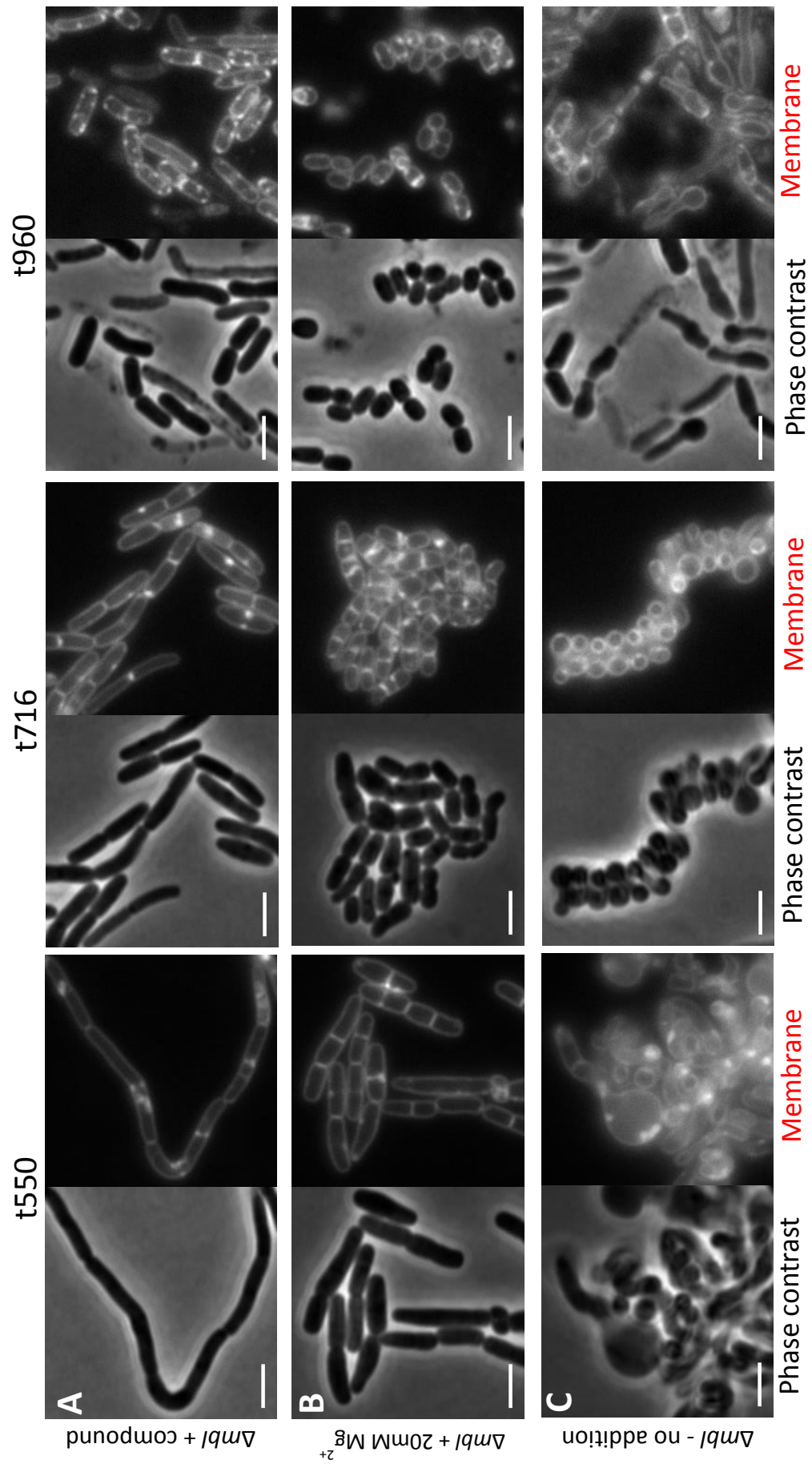
Figure 5.16. Morphology of Δ*mbl* (JB84) cells at various time points when grown with the DEM30616-B compound (A), with 20mM MgCl$_2$ (B) or grown in just nutrient broth (C). Membranes were visualised by staining with FM5-95. Scale bar = 3 µm

5.2.13 Treatment with the compound slightly impairs the growth of wild type 168CA but renders it exquisitely sensitive to Mn^{2+}

One of the phenotypes reported for the $\Delta ltaS$ mutant of *B. subtilis* is a high degree of sensitivity to the cation Mn^{2+} (Schirner et al., 2009). As an additional test as to whether DEM30616-B targets LtaS, the *B. subtilis* wild-type strain was treated with the compound, in the presence or absence of added 0.05 mM Mn^{2+}. Strikingly, the combination of Mn^{2+} and compound completely abolished growth of the wild type strain (figure 5.17), again consistent with the notion that the compound acts on LtaS.
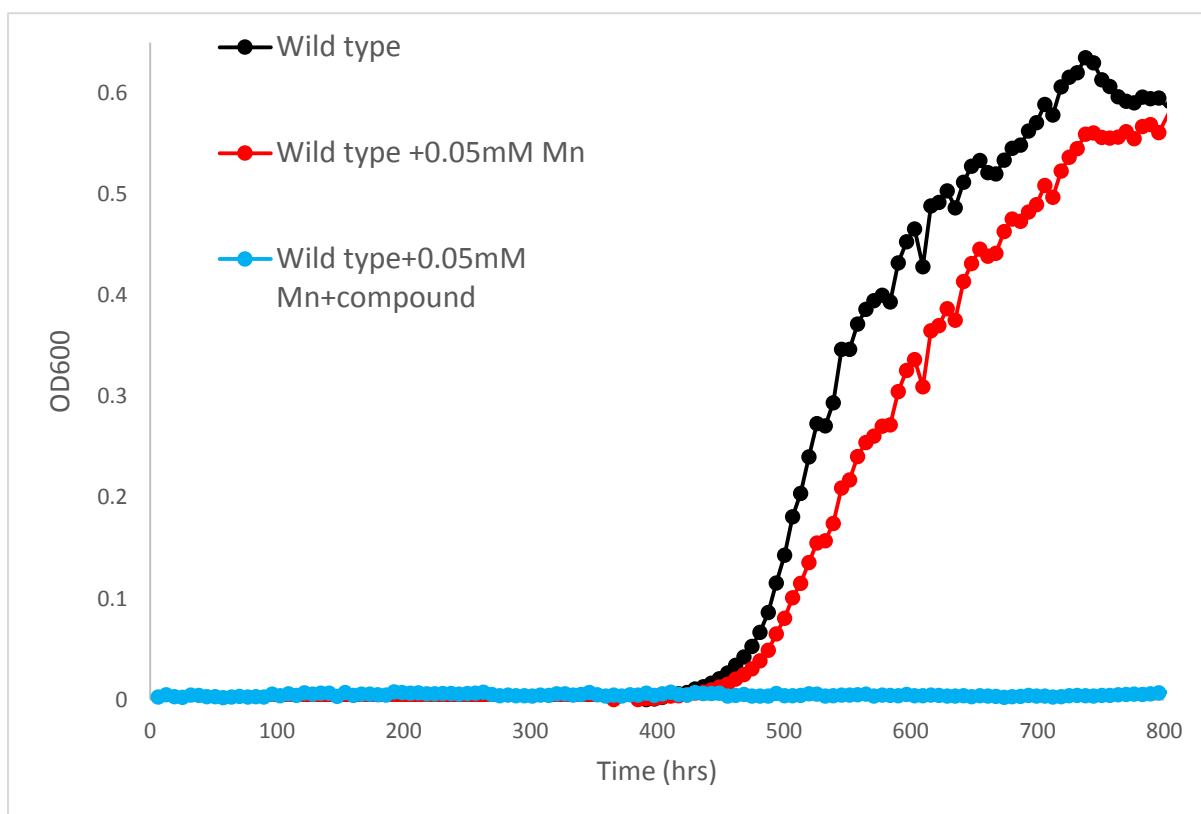
Figure 5.17. Treatment with the compound DEM30616-B abolishes the ability of the wild type (168CA) to grow in the presence of 0.05mM Mn^{2+}. Cells were diluted 10^{-4} in nutrient broth and grown for 20 hours in a plate reader at 37°C.

5.2.14 The compound has a minimal effect on growth of a Δ*ltaS* mutant

If the compound worked by inhibiting LtaS it was anticipated that treatment of a Δ*ltaS* strain with the compound would give no further growth inhibition beyond that already induced by the loss of LtaS. A Δ*ltaS* strain, along with strains bearing deletions of two of the paralogues, Δ*yqgS* and Δ*yfnI,* were treated with 10 µl of DEM30616-B. Growth of both the "minor" paralogues was substantially affected by presence of the compound, whereas growth of the Δ*ltaS* strain was more or less unaffected (figure 5.18). Note that the Δ*ltaS* strain used in this work was significantly slower growing than the wild type strain (168CA). This is in contrast with the earlier work that reports little difference when *ltaS* is deleted in *B. subtilis* (Schirner, 2009).
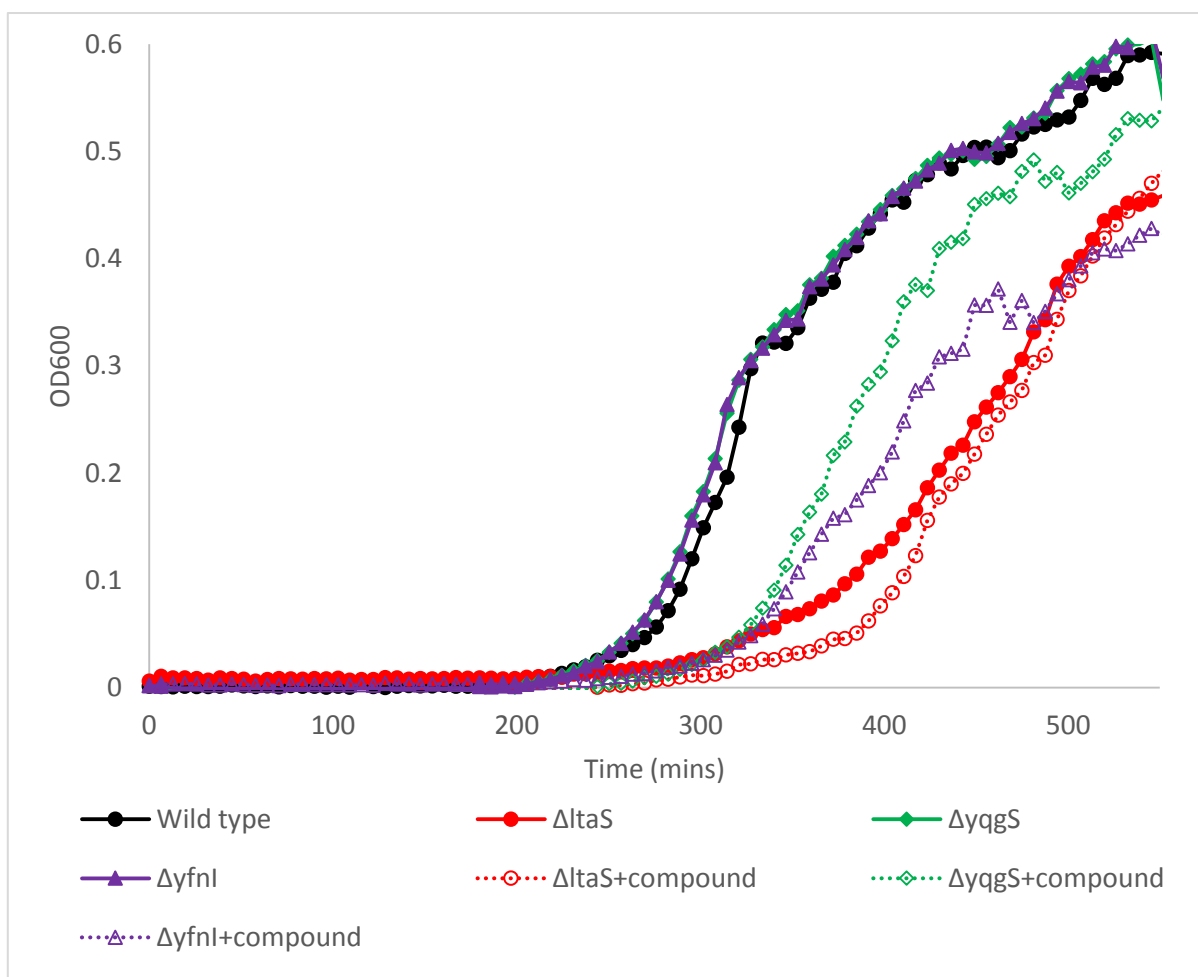
Figure 5.18. Growth of Δ*ltaS* (JB25), Δ*yqgS* (JB27), Δ*yfnI* (JB24) and the wild type (168CA) in the presence and absence of compound DEM30616-B. Growth was significantly reduced in the strains with a functional copy of the primary synthase, LtaS, whereas the Δ*ltaS* strain was largely unaffected. All the strains were diluted 10^{-4} and grown in LB at 37°C.

5.2.15 The compound has a bacteriostatic effect on the growth of *Staphylococcus aureus*

Unexpectedly, preliminary investigations using the filtered extract from DEM30616 cultures improved the growth of *S. aureus* over that of the untreated cells (figure 5.19.A). However, treatment of *S. aureus* with the purified DEM30616-B compound revealed that the compound significantly slowed the growth of cells (figure 5.19.B). Examination of the morphology of the cells treated with the compound by microscopy did not reveal any morphological changes (figure 5.19.D). This is in contrast to the results of depletion studies, which demonstrated that LtaS is essential for proper envelope assembly (Grundling and Schneewind, 2007b).

An earlier study had found that *S. aureus* Δ*ltaS* mutants were viable when grown at 30°C, but not at 37°C (Oku et al., 2009). This temperature sensitivity was used previously to identify potential small molecule inhibitors of LtaS (Richter et al., 2013). When *S. aureus* was grown with the DEM30616-B compound at 30°C, a reduction in the growth rate was observed, but no clear temperature dependence could be seen (figure 5.19.C). The reason for this discrepancy remains unknown.
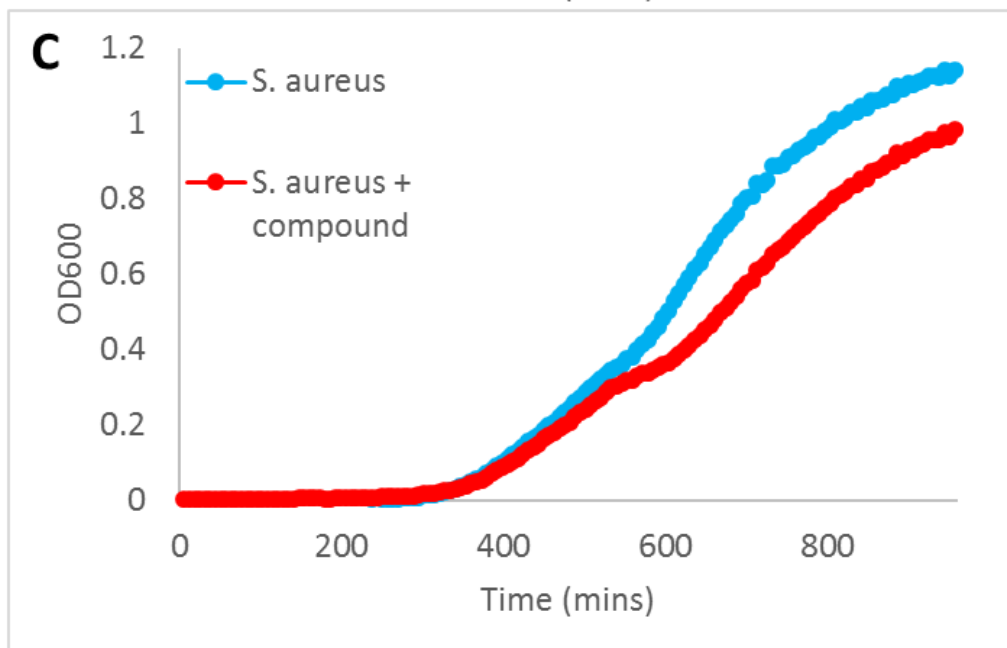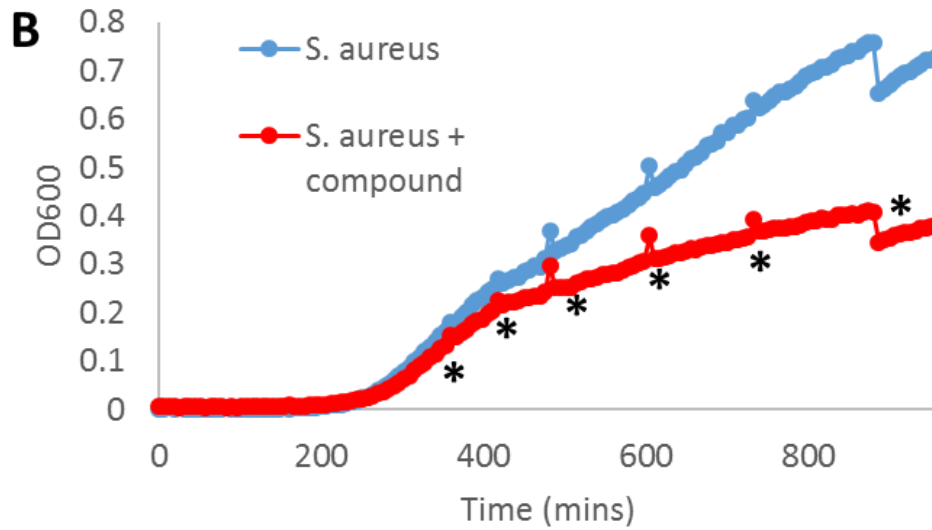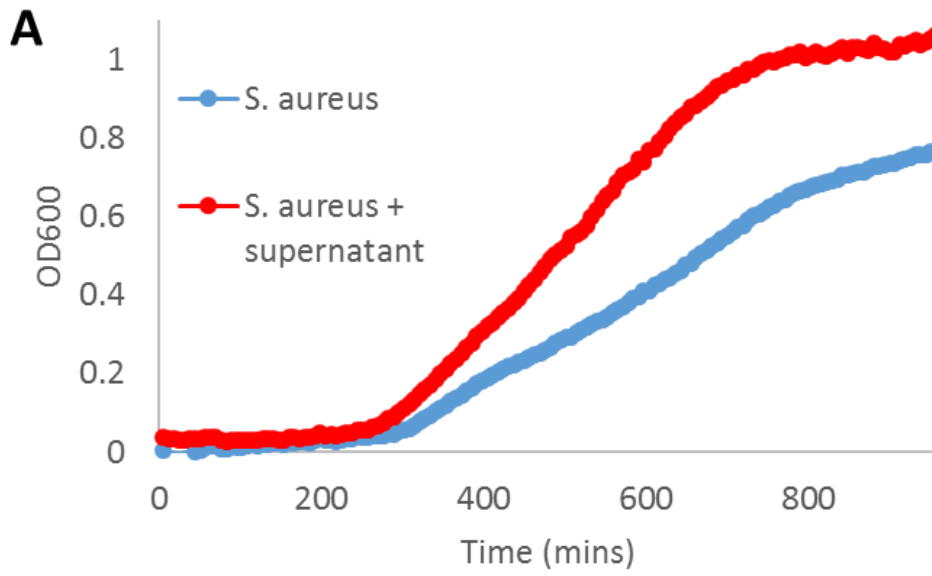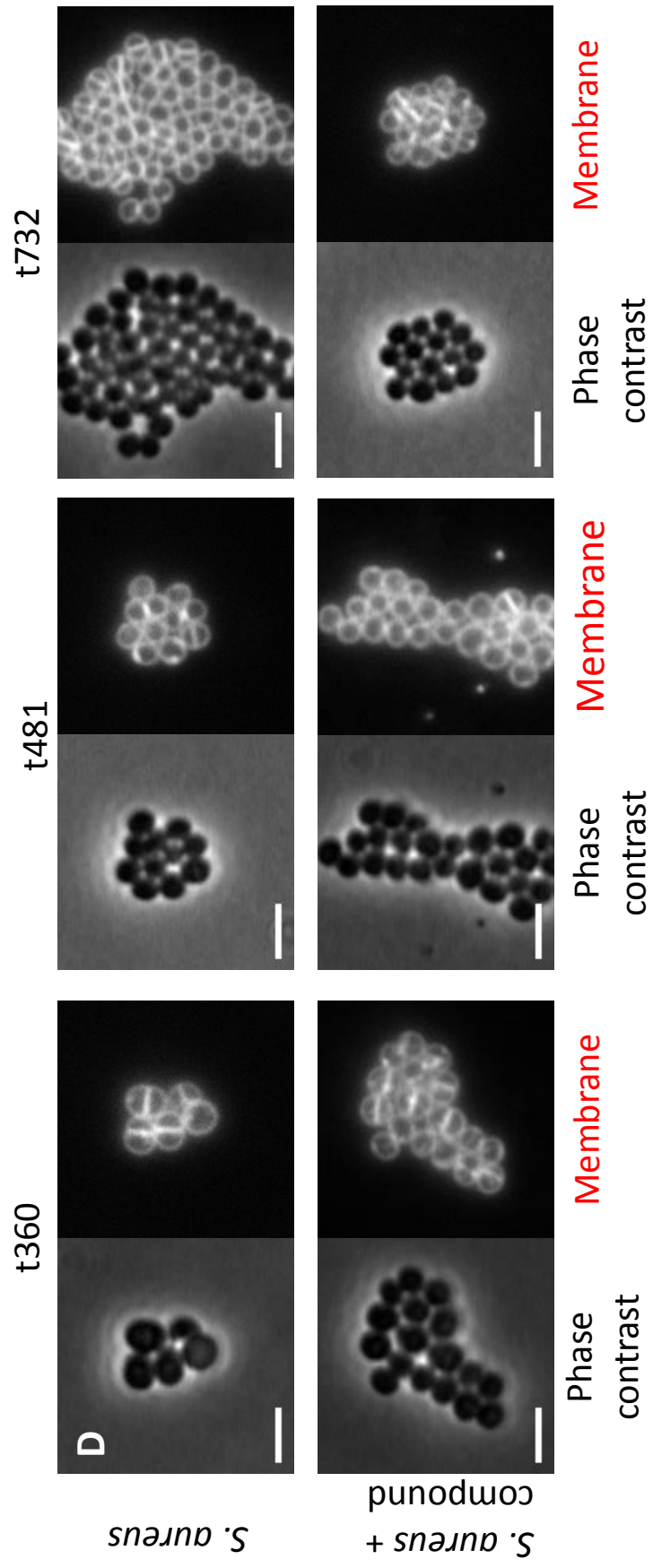
Figure 5.19. The effect of the compound on *Staphylococcus aureus.* **A).** Treatment with the filtered supernatant from DEM30616 improves the growth of *S. aureus* (RN4220). **B).** Growth rate of *S. aureus* (RN4220) is reduced in the presence of the compound. Cells were diluted 10^{-4} in nutrient broth and grown at 37°C in a plate reader. * indicates time points at which the experiment was paused and 5 µl removed for microscopy. **C). D).** Microscopy of *S. aureus* in the presence or absence of the compound at a selection of the time points illustrated by a * in **(A)**. Membrane was stained with FM5-95 dye.

5.2.16 Scaling up of production for compound purification

To purify more of the active DEM30616-B compound was grown until dense in 500 ml GYM before being fed into a bioreactor containing 16 L fresh GYM. Dissolved oxygen, rpm and temperature were monitored and controlled during the growth. The pH was followed. 15 ml samples were taken twice daily for six days. The bioreactor used did not have the equipment necessary to monitor glucose levels during growth. Instead, these were measured after the conclusion of the growth from the samples taken.

The presence of the compound was checked in the established assay on the fifth day. In contrast to the earlier work carried out at a smaller volume in which the greatest activity was observed on day 6, the activity peaked after four days of growth (figure 5.20.D). The production of the compound appeared to correlate with the entry into stationary phase (figure 5.20.A) and a drop in pH (figure 5.20.C). The drop in glucose levels appeared to be a function of the growth and entry into stationary phase (figure 5.20.B).
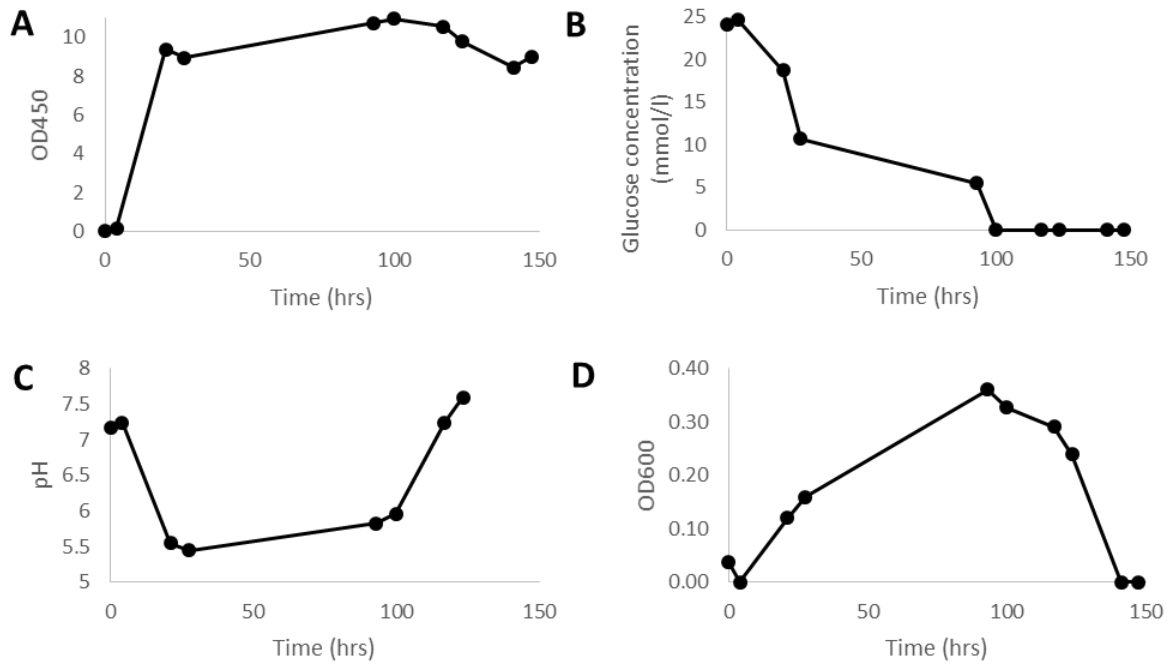
Figure 5.20. Changes in optical density (A), glucose concentration (B), pH (C) and activity of the supernatant in the Δ*mbl* assay (D) during growth of DEM30616 in a bioreactor. Activity of the supernatant represents growth of Δ*mbl* after 650 minutes in the assay blanked against the negative control (no addition of Mg^{2+}). Growth of DEM30616 in the bioreactor was performed by Ryan Sweet of Demuris ltd.

5.3 Discussion

As a result of the frequent use and misuse of antibiotics, levels of resistance in the human microbiome are increasing inexorably. For *S. aureus*, drug resistance in the form of MRSA is associated with elevated levels of mortality and morbidity. With the transfer of vancomycin from the *enterococci* to *S. aureus* (Weigel et al., 2003), followed by the development of linezolid and daptomycin resistance (Arbeit et al., 2004, Stevens et al., 2002) there is a high demand for novel antibiotics targeting *S. aureus*. In addition, LTA has been implicated as playing an important role in the pathogenesis of other important Gram-positive pathogens such as *Listeria monocytogenes* (Abachin et al., 2002). In both of *S. aureus* and *L. monocytogenes*, lipoteichoic acid is essential for robust growth (Webb et al., 2009, Grundling and Schneewind, 2007b), rendering it an attractive target for new antibiotics.

In this work, we propose and validate a new screening method for the discovery of novel antimicrobial compounds. Much of the natural product screening of the past thirty years has been hindered by the repeated isolation of known antibiotic classes (Baltz, 2008). Pre-existing methods for identifying antibiotics hinge on the ability of the compound to kill bacteria. Different screening methods may use reporter strains (Czarny et al., 2014) or differential killing (Richter et al., 2013), but ultimately they still seek compounds that kill the bacteria in the screen, and thus run the risk of repeated isolation of known compounds. What makes the screen used in this investigation different is that it identifies natural products that *improve* the growth of the assay strain. This therefore eliminates the possibility of identifying known compounds. In addition, because of the selectivity of the screening, there is greater confidence that the compound is indeed acting on LtaS.

Of course, such a screen, hinging as it does on LtaS being essential for the growth of species such as *S. aureus*, but also that its loss is a suppressor for the Δ*mbl* phenotype of *B. subtilis,* does mean that the method cannot be widely applied in the search for novel antibiotics. It therefore is more suited for the development of compounds for academic uses. Many genes when deleted sicken the cell and promote the development of suppressor mutations. Unfortunately, it is unlikely that many of these suppressor mutations are in turn essential for the growth and development of the bacterial cell as

ltaS is. However, the suppressor mutations themselves are often of interest in the understanding of bacterial physiology. Development of compounds targeting the gene products of the suppressors may help improve research into these pathways.

Due to the limited quantity of active material at the time of writing it was not possible to carry out experiments to more definitively confirm the activity of the compound against LtaS. Upon acquisition of more active material it would be hoped to expand upon the indirect evidence presented in this investigation by demonstrating via immunoblotting that treatment with the compound will disrupt LTA synthesis in a heterologous host (Grundling and Schneewind, 2007b, Richter et al., 2013). In addition, a greater quantity of the compound will allow for the complete identification of the compound DEM30616-B by H_1-NMR or X-ray crystallography. The current hypothetical structure of DEM30616-B allows us to make predictions about its mechanisms of action. The compound, an ester of a fatty acid and a sugar group, resembles the structure of the DAG subunit onto which the LtaS molecule attaches the poly Gro-P chain. It could therefore be hypothesised that the compound is occupying the active site of the LtaS enzyme. Alternatively, it is possible that the compound acts as a substrate during LTA synthesis, but that the resulting molecule is non-functional. Of course, such theories remain entirely speculative until the structure of the compound is solved. In turn, it may even be possible to co-crystallise the compound with the catalytic head group of LtaS.

The compound identified in this work is not the first to be found to potentially inhibit the function of LtaS. That accolade belongs to the small molecule identified in the work of (Richter et al., 2013). However, the DEM30616-B compound would be the first isolated from a natural source. In addition, the earlier small molecule the use of the small molecule previously identified is of limited medical use due to the instability of the molecule. It is hoped that the compound identified in this work is more stable.

The current evidence suggests that the compound DEM30616-B is targeting LTA synthesis. It does remain possible that the compound is actually targeting another process, as several suppressor mutants were identified in the study that inspired this work (Schirner et al., 2009). In such an event, the compound may lose its medical relevance, but will remain of interest as ultimately, it enables the growth of *mbl* mutants in conditions that are not normally permissive. Whilst our knowledge of *mbl* and the

actin-like cytoskeleton is improving, it remains a conflicted field (Errington, 2015). Use of the compound may enable more light to be shed on this intriguing protein. Whilst not of direct relevance to the scope of this work, it was of some interest that a sensitivity to iron was observed in the Δ*mbl* background, particularly as such a sensitivity to iron has not been previously reported. As this was beyond the remit of the work, it was not pursued further.

6. Summary and general discussion

6.1 L-form growth in low osmolarities can be facilitated by the loss of MreB

A long standing question regarding L-form biology is their natural relevance. L-forms have been studied extensively in a laboratory setting in which high levels of osmoprotectant must be maintained to ensure continued survival. This contrasts with reports in which L-form-like bodies have been observed in association with plant and animal tissues. In such conditions, the continued survival of L-forms would not be expected, resulting in the massive lysis of the cells. The historical literature reported that L-forms could be adapted to low osmolarities, but the characterisation of these L-forms was very limited due to the lack of effective techniques at that time. Work by (Leaver et al., 2009) established a reproducible method for generating L-forms derived from the Gram positive model organism *Bacillus subtilis*. Inspired by this work, the decision was made to revisit the issue of the survival of L-forms in low osmolarities.

In chapter 3, a variety of different techniques to adapt L-forms to low osmolarities were trialled, with the development of a novel adaptation method enabling the generation of L-forms that were able to grow and survive in conditions containing minimal concentrations of sucrose or salt. Whole genome sequencing of these strains revealed a number of mutations. Whilst the most exciting mutation, an in-frame deletion in *mreB*, was explored in chapter 4 as a proof of principle the involvement of a deletion of *scoC* in allowing L-forms to grow in low osmolarities was confirmed. ScoC is a transcriptional repressor that is involved in several processes, among which is the repression of the Opp polypeptide transport system. It has previously been demonstrated that the Opp system is involved in the osmotic stress response, via the import of proline rich peptides (Zaprasis et al., 2013). As MreB became the primary focus of this work, the role of *scoC* was not further explored in this thesis. However, it provides an interesting avenue for any further research in this area as the expectation would be that to survive in low osmolarities L-forms would need to deplete their pools of compatible solutes, not increase them.

The effects of *mreB* mutations on the ability of L-forms to grow in low osmolarities was investigated at length in chapter 4. The 60bp in-frame deletion identified in two of the osmo-resistant L-form mutants were initially considered to represent a gain or loss of function. However, this was not the case and the mutation was in all likelihood, resulting

in an unstable protein. Consistent with this result, rigorous testing revealed that Δ*mreB* strains were able to grow in low osmolarities, though far less reliably than the original mutant strains. This discrepancy was likely an effect of the secondary mutations present in the mutant strains. Remarkably, it was demonstrated that L-forms carrying either the partial deletion or a complete deletion of *mreB* were able to survive in not just minimal levels of osmoprotection, but in the complete absence of supplemented osmoprotection.

As the work stands, it is not possible to assign a clear role to *mreB* in the L-form state. It could have been speculated that MreB forms filaments that interact with the membrane and thus restrict the membrane reacting to an increase in turgor. However, the current view is that MreB forms filaments that are not as extensive as once thought. Recent work has demonstrated that the formation of these filaments is dependent on the presence of lipid II, a compound that should be absent in the L-form strain used. It is therefore presumed that under the conditions present in the L-forms the MreB would be existing as cytoplasmic monomers (Schirner et al., 2015). It had also been previously demonstrated that MreB helps to organise the membrane of the cell, with loss of the three MreB homologues resulting in an increase in membrane fluidity (Strahl et al., 2014). As membrane fluidity had been previously been implicated in L-form survival in low osmolarities (Harold, 1964, Montgomerie et al., 1973) it was hypothesised that a change in fluidity was in effect here. This proved not to be the case, as the test results showed no difference in the membrane fluidity between any of the strains tested. Changes in the membrane profile have been observed, though it is not currently known if this is a cause or effect of the loss of a major membrane associated protein.

Although it was not possible within the time frame of this investigation to understand the effect the loss of MreB is having on the L-form cells, this work has nevertheless suggested additional roles for this important protein. Traditionally, MreB has only been associated with the control and regulation of peptidoglycan synthesis, though it has been implicated in the regulation of the membrane. Discovery that the loss of MreB contributes to a phenotype in a cell lacking peptidoglycan was therefore an exciting and unexpected result. It strongly suggests the existence of functions outside those

associated with directing cell wall synthesis. As yet these functions are unknown and mere speculation.

In the future, it may prove possible to utilise the techniques and results generated in this work to explore the potential roles L-forms may play in infections of both plants and animals. In the past, much of the research into these processes have compromised of case studies and have been unable to prove a direct causation between L-forms and the various disease associations suspected. In part, the research into this area has been stymied by the inability of L-forms to grow robustly in plant or animal tissues or in the media associated with these tissues. The research presented in this thesis may enable these problems to be addressed in a robust and reproducible manner.

6.2 Use of a novel screening method to identify an inhibitor of LtaS

In chapter 5, a potential inhibitor of LtaS identified through a novel screening protocol from a unique collection of actinomycetes was verified and purified. The compound was produced by a novel *Streptomyces* strain, strain DEM30616, which has minimal relatedness to any known antibiotic producing strains. Identification of a compound validates both the screening method and the belief that actinomycetes still represent a vast reservoir of potential antimicrobial products. The active compound was isolated and purified, with the results of the mass spectroscopy allowing the compound to be tentatively identified as an ester of fatty acid and a sugar group. Interestingly, this structure mimics that of the DAG subunit that anchors the poly gro-P chain of LTA into the cell membrane. This structure enabled the prediction of a mechanism of action. The most likely proposal is that the compound replaces DAG within the active site, preventing the formation of LTA. Another possibility is that the compound is incorporated into LTA, replacing DAG, but that the resulting LTA molecule is somehow unable to perform its normal functions. Such predictions assume that the isolated compound is indeed inhibiting the formation of LTA. The evidence presented in chapter 5 is compelling, though the tests performed constitute an indirect measure of LtaS inhibition.

Ongoing work is primarily focussed on the scaling up of the production of the active compound from the strain DEM30616. By acquiring a greater quantity of the compound

it will enable the identification of the compound; this will likely be carried out either by H_1-NMR or by crystallisation. As the crystal structure of the catalytic domain of LtaS has already been solved (Schirner et al., 2009), it may be possible to predict the compound binding site and the accompanying mechanism of action.

Acquisition of a greater quantity of the compound will also allow for more experiments to be performed to confirm that the compound acts by inhibiting the formation of LTA. The work demonstrated in this thesis has indicated indirectly through a number of different techniques that the compound is inhibiting the production of LTA. Further experiments could involve the examination of the effect of the compound on the sporulation of *B. subtilis*; it has been demonstrated previously that a *B. subtilis* Δ*ltaS* Δ*yqgS* double mutant is defective in sporulation (Schirner et al., 2009). However, the gold standard will be the direct observation of the loss of LTA in bacteria treated with the compound. Such a method has been previously described, with levels of LTA or WTA able to be monitored by immunoblotting. In brief, this method involves the expression of the lipoteichoic acid synthetic pathway in a heterologous host that does not normally produce LTA, such as *E. coli* (Richter et al., 2013, Grundling and Schneewind, 2007b).

In addition, a pure compound will enable for the quantitation of the dosage dependence for *S. aureus* and *B. subtilis* growth. As it stands, the dosage dependence reported in this work is qualitative, with doses used measured relative to each other. On a grander scheme, with the assumption that action against LtaS is confirmed, it will be of interest to examine the effect the compound may play against Gram positive pathogens in animal infection models. In the event that the compound is not suitable for clinical application the compound may well prove useful for academic use. Treatment with an LtaS inhibitor will prove useful for transient depletion of LTA, or to study LTA function in species in which the synthetic enzyme has not been identified.

In the somewhat unlikely event that the compound is shown not to have a role in the inhibition of LtaS, it will still enable the exploration the bacterial cytoskeleton. No matter what the actual target of the compound is, it certainly alleviates the magnesium dependence exhibited by Δ*mbl* strains. It could therefore be considered that the compound could enable further study into the function of the cytoskeleton.

7. References

ABACHIN, E., POYART, C., PELLEGRINI, E., MILOHANIC, E., FIEDLER, F., BERCHE, P. & TRIEU-CUOT, P. 2002. Formation of D-alanyl-lipoteichoic acid is required for adhesion and virulence of Listeria monocytogenes. *Mol Microbiol,* 43**,** 1-14.

ABHAYAWARDHANE, Y. & STEWART, G. C. 1995. Bacillus subtilis possesses a second determinant with extensive sequence similarity to the Escherichia coli mreB morphogene. *J Bacteriol,* 177**,** 765-73.

ADAMS, D. W. & ERRINGTON, J. 2009. Bacterial cell division: assembly, maintenance and disassembly of the Z ring. *Nat Rev Microbiol,* 7**,** 642-53.

ALOYSIUS, S. K. D. & PATON, A. M. 1984. Artificially Induced Symbiotic Associations of L-Form Bacteria and Plants. *Journal of Applied Bacteriology,* 56**,** 465-477.

AMIJEE, F., ALLAN, E. J., WATERHOUSE, R. N., GLOVER, L. A. & PATON, A. M. 1992. Nonpathogenic Association of L-Form Bacteria (Pseudomonas-Syringae Pv Phaseolicola) with Bean-Plants (Phaseolus-Vulgaris L) and Its Potential for Biocontrol of Halo Blight Disease. *Biocontrol Science and Technology,* 2**,** 203-214.

ARAKAWA, T. & TIMASHEFF, S. N. 1985. The stabilization of proteins by osmolytes. *Biophys J,* 47**,** 411-4.

ARBEIT, R. D., MAKI, D., TALLY, F. P., CAMPANARO, E., EISENSTEIN, B. I., DAPTOMYCIN & INVESTIGATORS 2004. The safety and efficacy of daptomycin for the treatment of complicated skin and skin-structure infections. *Clin Infect Dis,* 38**,** 1673-81.

ARCHIBALD, A. R., ARMSTRONG, J. J., BADDILEY, J. & HAY, J. B. 1961. Teichoic acids and the structure of bacterial walls. *Nature,* 191**,** 570-2.

ATILANO, M. L., PEREIRA, P. M., YATES, J., REED, P., VEIGA, H., PINHO, M. G. & FILIPE, S. R. 2010. Teichoic acids are temporal and spatial regulators of peptidoglycan cross-linking in Staphylococcus aureus. *Proc Natl Acad Sci U S A,* 107**,** 18991-6.

AUSMEES, N., KUHN, J. R. & JACOBS-WAGNER, C. 2003. The bacterial cytoskeleton: an intermediate filament-like function in cell shape. *Cell,* 115**,** 705-13.

BALTZ, R. H. 2008. Renaissance in antibacterial discovery from actinomycetes. *Curr Opin Pharmacol,* 8**,** 557-63.

BARAK, I., MUCHOVA, K., WILKINSON, A. J., O'TOOLE, P. J. & PAVLENDOVA, N. 2008. Lipid spirals in Bacillus subtilis and their role in cell division. *Mol Microbiol,* 68**,** 1315-27.

BARRETEAU, H., KOVAC, A., BONIFACE, A., SOVA, M., GOBEC, S. & BLANOT, D. 2008. Cytoplasmic steps of peptidoglycan biosynthesis. *FEMS Microbiol Rev,* 32**,** 168-207.

BATIZA, A. F., KUO, M. M., YOSHIMURA, K. & KUNG, C. 2002. Gating the bacterial mechanosensitive channel MscL invivo. *Proc Natl Acad Sci U S A,* 99**,** 5643-8.

BAUR, S., RAUTENBERG, M., FAULSTICH, M., GRAU, T., SEVERIN, Y., UNGER, C., HOFFMANN, W. H., RUDEL, T., AUTENRIETH, I. B. & WEIDENMAIER, C. 2014. A nasal epithelial receptor for Staphylococcus aureus WTA governs adhesion to epithelial cells and modulates nasal colonization. *PLoS Pathog,* 10**,** e1004089.

BERDY, J. 2012. Thoughts and facts about antibiotics: where we are now and where we are heading. *J Antibiot (Tokyo),* 65**,** 385-95.

BERRIER, C., BESNARD, M., AJOUZ, B., COULOMBE, A. & GHAZI, A. 1996. Multiple mechanosensitive ion channels from Escherichia coli, activated at different thresholds of applied pressure. *J Membr Biol,* 151**,** 175-87.

BERTSCHE, U., YANG, S. J., KUEHNER, D., WANNER, S., MISHRA, N. N., ROTH, T., NEGA, M., SCHNEIDER, A., MAYER, C., GRAU, T., BAYER, A. S. & WEIDENMAIER, C. 2013.

Increased cell wall teichoic acid production and D-alanylation are common phenotypes among daptomycin-resistant methicillin-resistant Staphylococcus aureus (MRSA) clinical isolates. *PLoS One,* 8**,** e67398.

BHAVSAR, A. P., BEVERIDGE, T. J. & BROWN, E. D. 2001. Precise deletion of tagD and controlled depletion of its product, glycerol 3-phosphate cytidylyltransferase, leads to irregular morphology and lysis of Bacillus subtilis grown at physiological temperature. *J Bacteriol,* 183**,** 6688-93.

BHAVSAR, A. P., ERDMAN, L. K., SCHERTZER, J. W. & BROWN, E. D. 2004. Teichoic acid is an essential polymer in Bacillus subtilis that is functionally distinct from teichuronic acid. *J Bacteriol,* 186**,** 7865-73.

BIEMANS-OLDEHINKEL, E., MAHMOOD, N. A. & POOLMAN, B. 2006. A sensor for intracellular ionic strength. *Proc Natl Acad Sci U S A,* 103**,** 10624-9.

BILLINGS, G., OUZOUNOV, N., URSELL, T., DESMARAIS, S. M., SHAEVITZ, J., GITAI, Z. & HUANG, K. C. 2014. De novo morphogenesis in L-forms via geometric control of cell growth. *Mol Microbiol,* 93**,** 883-96.

BISICCHIA, P., NOONE, D., LIOLIOU, E., HOWELL, A., QUIGLEY, S., JENSEN, T., JARMER, H. & DEVINE, K. M. 2007. The essential YycFG two-component system controls cell wall metabolism in Bacillus subtilis. *Mol Microbiol,* 65**,** 180-200.

BISTER, B., BISCHOFF, D., STROBELE, M., RIEDLINGER, J., REICKE, A., WOLTER, F., BULL, A. T., ZAHNER, H., FIEDLER, H. P. & SUSSMUTH, R. D. 2004. Abyssomicin C-A polycyclic antibiotic from a marine Verrucosispora strain as an inhibitor of the p-aminobenzoic acid/tetrahydrofolate biosynthesis pathway. *Angew Chem Int Ed Engl,* 43**,** 2574-6.

BISWAS, R., MARTINEZ, R. E., GOHRING, N., SCHLAG, M., JOSTEN, M., XIA, G., HEGLER, F., GEKELER, C., GLESKE, A. K., GOTZ, F., SAHL, H. G., KAPPLER, A. & PESCHEL, A. 2012. Proton-binding capacity of Staphylococcus aureus wall teichoic acid and its role in controlling autolysin activity. *PLoS One,* 7**,** e41415.

BOCH, J., KEMPF, B. & BREMER, E. 1994. Osmoregulation in Bacillus subtilis: synthesis of the osmoprotectant glycine betaine from exogenously provided choline. *J Bacteriol,* 176**,** 5364-71.

BOCH, J., KEMPF, B., SCHMID, R. & BREMER, E. 1996. Synthesis of the osmoprotectant glycine betaine in Bacillus subtilis: characterization of the gbsAB genes. *J Bacteriol,* 178**,** 5121-9.

BOOTH, I. R. & BLOUNT, P. 2012. The MscS and MscL families of mechanosensitive channels act as microbial emergency release valves. *J Bacteriol,* 194**,** 4802-9.

BOUCHER, H. W., TALBOT, G. H., BRADLEY, J. S., EDWARDS, J. E., GILBERT, D., RICE, L. B., SCHELD, M., SPELLBERG, B. & BARTLETT, J. 2009. Bad bugs, no drugs: no ESKAPE! An update from the Infectious Diseases Society of America. *Clin Infect Dis,* 48**,** 1-12.

BRIERS, Y., STAUBLI, T., SCHMID, M. C., WAGNER, M., SCHUPPLER, M. & LOESSNER, M. J. 2012. Intracellular vesicles as reproduction elements in cell wall-deficient L-form bacteria. *PLoS One,* 7**,** e38514.

BROWN, S., SANTA MARIA, J. P., JR. & WALKER, S. 2013. Wall teichoic acids of gram-positive bacteria. *Annu Rev Microbiol,* 67**,** 313-36.

BUDIN, I., DEBNATH, A. & SZOSTAK, J. W. 2012. Concentration-driven growth of model protocell membranes. *J Am Chem Soc,* 134**,** 20812-9.

CANE, D. E., WALSH, C. T. & KHOSLA, C. 1998. Harnessing the biosynthetic code: combinations, permutations, and mutations. *Science,* 282**,** 63-8.

CARBALLIDO-LOPEZ, R. 2006. The bacterial actin-like cytoskeleton. *Microbiol Mol Biol Rev,* 70**,** 888-909.

CARBALLIDO-LOPEZ, R., FORMSTONE, A., LI, Y., EHRLICH, S. D., NOIROT, P. & ERRINGTON, J. 2006. Actin homolog MreBH governs cell morphogenesis by localization of the cell wall hydrolase LytE. *Dev Cell,* 11**,** 399-409.

CHALLIS, G. L. 2014. *RE: Personal Communication.* Type to J, E.

CHALLIS, G. L. & RAVEL, J. 2000. Coelichelin, a new peptide siderophore encoded by the Streptomyces coelicolor genome: structure prediction from the sequence of its non-ribosomal peptide synthetase. *FEMS Microbiol Lett,* 187**,** 111-4.

CHANG, S. & COHEN, S. N. 1979. High frequency transformation of Bacillus subtilis protoplasts by plasmid DNA. *Mol Gen Genet,* 168**,** 111-5.

CHEN, Y., CAO, S., CHAI, Y., CLARDY, J., KOLTER, R., GUO, J. H. & LOSICK, R. 2012. A Bacillus subtilis sensor kinase involved in triggering biofilm formation on the roots of tomato plants. *Molecular Microbiology,* 85**,** 418-430.

CHOI, K. H., HEATH, R. J. & ROCK, C. O. 2000. beta-ketoacyl-acyl carrier protein synthase III (FabH) is a determining factor in branched-chain fatty acid biosynthesis. *J Bacteriol,* 182**,** 365-70.

COLLINS, L. V., KRISTIAN, S. A., WEIDENMAIER, C., FAIGLE, M., VAN KESSEL, K. P., VAN STRIJP, J. A., GOTZ, F., NEUMEISTER, B. & PESCHEL, A. 2002. Staphylococcus aureus strains lacking D-alanine modifications of teichoic acids are highly susceptible to human neutrophil killing and are virulence attenuated in mice. *J Infect Dis,* 186**,** 214-9.

CORNELL, R. B. & TANEVA, S. G. 2006. Amphipathic helices as mediators of the membrane interaction of amphitropic proteins, and as modulators of bilayer physical properties. *Curr Protein Pept Sci,* 7**,** 539-52.

CORRIGAN, R. M., ABBOTT, J. C., BURHENNE, H., KAEVER, V. & GRUNDLING, A. 2011. c-di-AMP is a new second messenger in Staphylococcus aureus with a role in controlling cell size and envelope stress. *PLoS Pathog,* 7**,** e1002217.

CRONAN, J. E., JR. & WALDROP, G. L. 2002. Multi-subunit acetyl-CoA carboxylases. *Prog Lipid Res,* 41**,** 407-35.

CRUICKSHANK, C. C., MINCHIN, R. F., LE DAIN, A. C. & MARTINAC, B. 1997. Estimation of the pore size of the large-conductance mechanosensitive ion channel of Escherichia coli. *Biophys J,* 73**,** 1925-31.

CZARNY, T. L., PERRI, A. L., FRENCH, S. & BROWN, E. D. 2014. Discovery of novel cell wall-active compounds using P ywaC, a sensitive reporter of cell wall stress, in the model gram-positive bacterium Bacillus subtilis. *Antimicrob Agents Chemother,* 58**,** 3261-9.

D'ELIA, M. A., MILLAR, K. E., BEVERIDGE, T. J. & BROWN, E. D. 2006a. Wall teichoic acid polymers are dispensable for cell viability in Bacillus subtilis. *J Bacteriol,* 188**,** 8313-8316.

D'ELIA, M. A., PEREIRA, M. P., CHUNG, Y. S., ZHAO, W. J., CHAU, A., KENNEY, T. J., SULAVIK, M. C., BLACK, T. A. & BROWN, E. D. 2006b. Lesions in teichoic acid biosynthesis in Staphylococcus aureus lead to a lethal gain of function in the otherwise dispensable pathway. *J Bacteriol,* 188**,** 4183-4189.

DA COSTA, M. S., SANTOS, H. & GALINSKI, E. A. 1998. An overview of the role and diversity of compatible solutes in Bacteria and Archaea. *Adv Biochem Eng Biotechnol,* 61**,** 117-53.

DANIEL, R. A. & ERRINGTON, J. 2003. Control of cell morphogenesis in bacteria: two distinct ways to make a rod-shaped cell. *Cell,* 113**,** 767-76.

DAVIS, N. K. & CHATER, K. F. 1990. Spore colour in Streptomyces coelicolor A3(2) involves the developmentally regulated synthesis of a compound biosynthetically related to polyketide antibiotics. *Mol Microbiol,* 4**,** 1679-91.

DE AZAVEDO, J. C., FOSTER, T. J., HARTIGAN, P. J., ARBUTHNOTT, J. P., O'REILLY, M., KREISWIRTH, B. N. & NOVICK, R. P. 1985. Expression of the cloned toxic shock syndrome toxin 1 gene (tst) in vivo with a rabbit uterine model. *Infect Immun,* 50**,** 304-9.

DEAMER, D. W. & BRAMHALL, J. 1986. Permeability of lipid bilayers to water and ionic solutes. *Chem Phys Lipids,* 40**,** 167-88.

DEFEU SOUFO, H. J. & GRAUMANN, P. L. 2004. Dynamic movement of actin-like proteins within bacterial cells. *EMBO Rep,* 5**,** 789-94.

DEFEU SOUFO, H. J. & GRAUMANN, P. L. 2005. Bacillus subtilis actin-like protein MreB influences the positioning of the replication machinery and requires membrane proteins MreC/D and other actin-like proteins for proper localization. *BMC Cell Biol,* 6**,** 10.

DEFEU SOUFO, H. J. & GRAUMANN, P. L. 2006. Dynamic localization and interaction with other Bacillus subtilis actin-like proteins are important for the function of MreB. *Mol Microbiol,* 62**,** 1340-56.

DIENES, L. & SHARP, J. T. 1956. The role of high electrolyte concentration in the production and growth of L forms of bacteria. *J Bacteriol,* 71**,** 208-13.

DIMINIC, J., STARCEVIC, A., LISFI, M., BARANASIC, D., GACESA, R., HRANUELI, D., LONG, P. F., CULLUM, J. & ZUCKO, J. 2014. Evolutionary concepts in natural products discovery: what actinomycetes have taught us. *J Ind Microbiol Biotechnol,* 41**,** 211-7.

DMITRIEV, B. A., EHLERS, S. & RIETSCHEL, E. T. 1999. Layered murein revisited: a fundamentally new concept of bacterial cell wall structure, biogenesis and function. *Med Microbiol Immunol,* 187**,** 173-81.

DMITRIEV, B. A., TOUKACH, F. V., SCHAPER, K. J., HOLST, O., RIETSCHEL, E. T. & EHLERS, S. 2003. Tertiary structure of bacterial murein: the scaffold model. *J Bacteriol,* 185**,** 3458-68.

DOMINGUE, G. J. 2010. Demystifying pleomorphic forms in persistence and expression of disease: Are they bacteria, and is peptidoglycan the solution? *Discov Med,* 10**,** 234-46.

DOMINGUE, G. J., SR. & WOODY, H. B. 1997. Bacterial persistence and expression of disease. *Clin Microbiol Rev,* 10**,** 320-44.

DOMINGUEZ-CUEVAS, P., MERCIER, R., LEAVER, M., KAWAI, Y. & ERRINGTON, J. 2012. The rod to L-form transition of Bacillus subtilis is limited by a requirement for the protoplast to escape from the cell wall sacculus. *Molecular Microbiology,* 83**,** 52-66.

DOMINGUEZ-CUEVAS, P., PORCELLI, I., DANIEL, R. A. & ERRINGTON, J. 2013. Differentiated roles for MreB-actin isologues and autolytic enzymes in Bacillus subtilis morphogenesis. *Mol Microbiol,* 89**,** 1084-98.

DOMINGUEZ-ESCOBAR, J., CHASTANET, A., CREVENNA, A. H., FROMION, V., WEDLICH-SOLDNER, R. & CARBALLIDO-LOPEZ, R. 2011. Processive movement of MreB-associated cell wall biosynthetic complexes in bacteria. *Science,* 333**,** 225-8.

EHLERT, K. & HOLTJE, J. V. 1996. Role of precursor translocation in coordination of murein and phospholipid synthesis in Escherichia coli. *J Bacteriol,* 178**,** 6766-71.

ERRINGTON, J. 2013. L-form bacteria, cell walls and the origins of life. *Open Biol,* 3**,** 120143.

ERRINGTON, J. 2015. Bacterial morphogenesis and the enigmatic MreB helix. *Nat Rev Microbiol,* 13**,** 241-8.

ERRINGTON J, S. K. 2009. *METHOD FOR IDENTIFYING INHIBITORS OF LIPOTEICHOIC ACID SYNTHASE*. PCT/GB2009/002824.

ERTEL, A., MARANGONI, A. G., MARSH, J., HALLETT, F. R. & WOOD, J. M. 1993. Mechanical properties of vesicles. I. Coordinated analysis of osmotic swelling and lysis. *Biophys J,* 64**,** 426-34.

FARHA, M. A., KOTEVA, K., GALE, R. T., SEWELL, E. W., WRIGHT, G. D. & BROWN, E. D. 2014. Designing analogs of ticlopidine, a wall teichoic acid inhibitor, to avoid formation of its oxidative metabolites. *Bioorg Med Chem Lett,* 24**,** 905-10.

FARHA, M. A., LEUNG, A., SEWELL, E. W., D'ELIA, M. A., ALLISON, S. E., EJIM, L., PEREIRA, P. M., PINHO, M. G., WRIGHT, G. D. & BROWN, E. D. 2013. Inhibition of WTA synthesis blocks the cooperative action of PBPs and sensitizes MRSA to beta-lactams. *ACS Chem Biol,* 8**,** 226-33.

FAY, A. & DWORKIN, J. 2009. Bacillus subtilis homologs of MviN (MurJ), the putative Escherichia coli lipid II flippase, are not essential for growth. *J Bacteriol,* 191**,** 6020-8.

FEDTKE, I., GOTZ, F. & PESCHEL, A. 2004. Bacterial evasion of innate host defenses--the Staphylococcus aureus lesson. *Int J Med Microbiol,* 294**,** 189-94.

FERGUSON, C. M. J., BOOTH, N. A. & ALLAN, E. J. 2000. An ELISA for the detection of Bacillus subtilis L-form bacteria confirms their symbiosis in strawberry. *Lett Appl Microbiol,* 31**,** 390-394.

FETTIPLACE, R. & HAYDON, D. A. 1980. Water permeability of lipid membranes. *Physiol Rev,* 60**,** 510-50.

FISCHER, W. 1988. Physiology of lipoteichoic acids in bacteria. *Adv Microb Physiol,* 29**,** 233-302.

FISHOV, I. & NORRIS, V. 2012. Membrane heterogeneity created by transertion is a global regulator in bacteria. *Curr Opin Microbiol,* 15**,** 724-30.

FITTIPALDI, N., SEKIZAKI, T., TAKAMATSU, D., HAREL, J., DOMINGUEZ-PUNARO MDE, L., VON AULOCK, S., DRAING, C., MAROIS, C., KOBISCH, M. & GOTTSCHALK, M. 2008. D-alanylation of lipoteichoic acid contributes to the virulence of Streptococcus suis. *Infect Immun,* 76**,** 3587-94.

FLARDH, K. 2010. Cell polarity and the control of apical growth in Streptomyces. *Curr Opin Microbiol,* 13**,** 758-65.

FORMSTONE, A., CARBALLIDO-LOPEZ, R., NOIROT, P., ERRINGTON, J. & SCHEFFERS, D. J. 2008. Localization and interactions of teichoic acid synthetic enzymes in Bacillus subtilis. *J Bacteriol,* 190**,** 1812-21.

FORMSTONE, A. & ERRINGTON, J. 2005. A magnesium-dependent mreB null mutant: implications for the role of mreB in Bacillus subtilis. *Mol Microbiol,* 55**,** 1646-57.

FUJISAKI, S., HARA, H., NISHIMURA, Y., HORIUCHI, K. & NISHINO, T. 1990. Cloning and nucleotide sequence of the ispA gene responsible for farnesyl diphosphate synthase activity in Escherichia coli. *J Biochem,* 108**,** 995-1000.

FUJITA, Y., MATSUOKA, H. & HIROOKA, K. 2007. Regulation of fatty acid metabolism in bacteria. *Mol Microbiol,* 66**,** 829-39.

GANCHEV, D. N., HASPER, H. E., BREUKINK, E. & DE KRUIJFF, B. 2006. Size and orientation of the lipid II headgroup as revealed by AFM imaging. *Biochemistry,* 45**,** 6195-202.

GARCIA-SAEZ, A. J., CHIANTIA, S. & SCHWILLE, P. 2007. Effect of line tension on the lateral organization of lipid membranes. *J Biol Chem,* 282**,** 33537-44.

GARNER, E. C., BERNARD, R., WANG, W., ZHUANG, X., RUDNER, D. Z. & MITCHISON, T. 2011. Coupled, circumferential motions of the cell wall synthesis machinery and MreB filaments in B. subtilis. *Science,* 333**,** 222-5.

GARTNER, D., GEISSENDORFER, M. & HILLEN, W. 1988. Expression of the Bacillus subtilis xyl operon is repressed at the level of transcription and is induced by xylose. *J Bacteriol,* 170**,** 3102-9.

GILL, R. L., JR., CASTAING, J. P., HSIN, J., TAN, I. S., WANG, X., HUANG, K. C., TIAN, F. & RAMAMURTHI, K. S. 2015. Structural basis for the geometry-driven localization of a small protein. *Proc Natl Acad Sci U S A,* 112**,** E1908-15.

GILPIN, R. W. & PATTERSON, S. K. 1976. Adaptation of a stable L-form of Bacillus subtilis to minimal salts medium without osmotic stabilizers. *J Bacteriol,* 125**,** 845-9.

GILPIN, R. W., YOUNG, F. E. & CHATTERJEE, A. N. 1973. Characterization of a stable L-form of Bacillus subtilis 168. *J Bacteriol,* 113**,** 486-99.

GLASER, P., SHARPE, M. E., RAETHER, B., PEREGO, M., OHLSEN, K. & ERRINGTON, J. 1997. Dynamic, mitotic-like behavior of a bacterial protein required for accurate chromosome partitioning. *Genes Dev,* 11**,** 1160-8.

GLOVER, W. A., YANG, Y. & ZHANG, Y. 2009. Insights into the molecular basis of L-form formation and survival in Escherichia coli. *PLoS One,* 4**,** e7316.

GOEHRING, N. W. & BECKWITH, J. 2005. Diverse paths to midcell: assembly of the bacterial cell division machinery. *Curr Biol,* 15**,** R514-26.

GOMEZ-ESCRIBANO, J. P., CASTRO, J. F., RAZMILIC, V., CHANDRA, G., ANDREWS, B., ASENJO, J. A. & BIBB, M. J. 2015. The Streptomyces leeuwenhoekii genome: de novo sequencing and assembly in single contigs of the chromosome, circular plasmid pSLE1 and linear plasmid pSLE2. *BMC Genomics,* 16**,** 485.

GROSS, M., CRAMTON, S. E., GOTZ, F. & PESCHEL, A. 2001. Key role of teichoic acid net charge in Staphylococcus aureus colonization of artificial surfaces. *Infect Immun,* 69**,** 3423-6.

GRUNDLING, A. & SCHNEEWIND, O. 2007a. Genes required for glycolipid synthesis and lipoteichoic acid anchoring in Staphylococcus aureus. *J Bacteriol,* 189**,** 2521-2530.

GRUNDLING, A. & SCHNEEWIND, O. 2007b. Synthesis of glycerol phosphate lipoteichoic acid in Staphylococcus aureus. *Proc Natl Acad Sci U S A,* 104**,** 8478-8483.

GRUNDY, F. J. & HENKIN, T. M. 1992. Characterization of the Bacillus subtilis rpsD regulatory target site. *J Bacteriol,* 174**,** 6763-70.

GUST, B., CHALLIS, G. L., FOWLER, K., KIESER, T. & CHATER, K. F. 2003. PCR-targeted Streptomyces gene replacement identifies a protein domain needed for biosynthesis of the sesquiterpene soil odor geosmin. *Proc Natl Acad Sci U S A,* 100**,** 1541-6.

HANCOCK, I. C., WISEMAN, G. & BADDILEY, J. 1976. Biosynthesis of the unit that links teichoic acid to the bacterial wall: inhibition by tunicamycin. *FEBS Lett,* 69**,** 75-80.

HANCZYC, M. M., FUJIKAWA, S. M. & SZOSTAK, J. W. 2003. Experimental models of primitive cellular compartments: encapsulation, growth, and division. *Science,* 302**,** 618-22.

HAROLD, F. M. 1964. Stabilization of Streptococcus Faecalis Protoplasts by Spermine. *J Bacteriol,* 88**,** 1416-20.

HARZ, H., BURGDORF, K. & HOLTJE, J. V. 1990. Isolation and separation of the glycan strands from murein of Escherichia coli by reversed-phase high-performance liquid chromatography. *Anal Biochem,* 190**,** 120-8.

HASHIMOTO, M., OOIWA, S. & SEKIGUCHI, J. 2012. Synthetic lethality of the lytE cwlO genotype in Bacillus subtilis is caused by lack of D,L-endopeptidase activity at the lateral cell wall. *J Bacteriol,* 194**,** 796-803.

HEATH, R. J., SU, N., MURPHY, C. K. & ROCK, C. O. 2000. The enoyl-[acyl-carrier-protein] reductases FabI and FabL from Bacillus subtilis. *J Biol Chem,* 275**,** 40128-33.

HEPTINSTALL, S., ARCHIBALD, A. R. & BADDILEY, J. 1970. Teichoic Acids and Membrane Function in Bacteria. *Nature,* 225**,** 519-&.

HOLLAND, L. M., CONLON, B. & O'GARA, J. P. 2011. Mutation of tagO reveals an essential role for wall teichoic acids in Staphylococcus epidermidis biofilm development. *Microbiology,* 157**,** 408-18.

HOLTJE, J. V. 1998. Growth of the stress-bearing and shape-maintaining murein sacculus of Escherichia coli. *Microbiol Mol Biol Rev,* 62**,** 181-203.

HUANG, K. C., MUKHOPADHYAY, R. & WINGREEN, N. S. 2006. A curvature-mediated mechanism for localization of lipids to bacterial poles. *PLoS Comput Biol,* 2**,** e151.

HUBSCHER, J., LUTHY, L., BERGER-BACHI, B. & STUTZMANN MEIER, P. 2008. Phylogenetic distribution and membrane topology of the LytR-CpsA-Psr protein family. *BMC Genomics,* 9**,** 617.

IFTIME, D., KULIK, A., HARTNER, T., ROHRER, S., NIEDERMEYER, T. H., STEGMANN, E., WEBER, T. & WOHLLEBEN, W. 2015. Identification and activation of novel biosynthetic gene clusters by genome mining in the kirromycin producer Streptomyces collinus Tu 365. *J Ind Microbiol Biotechnol*.

IKEDA, H., ISHIKAWA, J., HANAMOTO, A., SHINOSE, M., KIKUCHI, H., SHIBA, T., SAKAKI, Y., HATTORI, M. & OMURA, S. 2003. Complete genome sequence and comparative analysis of the industrial microorganism Streptomyces avermitilis. *Nat Biotechnol,* 21**,** 526-31.

ITAYA, M., KONDO, K. & TANAKA, T. 1989. A neomycin resistance gene cassette selectable in a single copy state in the Bacillus subtilis chromosome. *Nucleic Acids Res,* 17**,** 4410.

JAHN, N., BRANTL, S. & STRAHL, H. 2015. Against the mainstream: the membrane-associated type I toxin BsrG from Bacillus subtilis interferes with cell envelope biosynthesis without increasing membrane permeability. *Mol Microbiol,* 98**,** 651-66.

JANAS, T., CHOJNACKI, T., SWIEZEWSKA, E. & JANAS, T. 1994. The effect of undecaprenol on bilayer lipid membranes. *Acta Biochim Pol,* 41**,** 351-8.

JENKE-KODAMA, H., BORNER, T. & DITTMANN, E. 2006. Natural biocombinatorics in the polyketide synthase genes of the actinobacterium Streptomyces avermitilis. *PLoS Comput Biol,* 2**,** e132.

JONES, L. J., CARBALLIDO-LOPEZ, R. & ERRINGTON, J. 2001. Control of cell shape in bacteria: helical, actin-like filaments in Bacillus subtilis. *Cell,* 104**,** 913-22.

KABACK, H. R., DUNTEN, R., FRILLINGOS, S., VENKATESAN, P., KWAW, I., ZHANG, W. & ERMOLOVA, N. 2007. Site-directed alkylation and the alternating access model for LacY. *Proc Natl Acad Sci U S A,* 104**,** 491-4.

KAWAI, Y., ASAI, K. & ERRINGTON, J. 2009. Partial functional redundancy of MreB isoforms, MreB, Mbl and MreBH, in cell morphogenesis of Bacillus subtilis. *Mol Microbiol,* 73**,** 719-31.

KAWAI, Y., MARLES-WRIGHT, J., CLEVERLEY, R. M., EMMINS, R., ISHIKAWA, S., KUWANO, M., HEINZ, N., BUI, N. K., HOYLAND, C. N., OGASAWARA, N., LEWIS, R. J., VOLLMER, W., DANIEL, R. A. & ERRINGTON, J. 2011. A widespread family of bacterial cell wall assembly proteins. *Embo Journal,* 30**,** 4931-4941.

KAWAI, Y., MERCIER, R., WU, L. J., DOMINGUEZ-CUEVAS, P., OSHIMA, T. & ERRINGTON, J. 2015. Cell growth of wall-free L-form bacteria is limited by oxidative damage. *Curr Biol,* 25**,** 1613-8.

KINGSTON, A. W., LIAO, X. & HELMANN, J. D. 2013. Contributions of the sigma(W) , sigma(M) and sigma(X) regulons to the lantibiotic resistome of Bacillus subtilis. *Mol Microbiol,* 90**,** 502-18.

KITANI, S., MIYAMOTO, K. T., TAKAMATSU, S., HERAWATI, E., IGUCHI, H., NISHITOMI, K., UCHIDA, M., NAGAMITSU, T., OMURA, S., IKEDA, H. & NIHIRA, T. 2011. Avenolide, a Streptomyces hormone controlling antibiotic production in Streptomyces avermitilis. *Proc Natl Acad Sci U S A,* 108**,** 16410-5.

KLIENEBERGER, E. 1935. The natural occurrence of pleuropneumonia-like organisms in apparent symbiosis with Streptobacillus moniliformis and other bacteria. *J. Pathol. Bacteriol.,* 40**,** 93-105.

KOBAYASHI, K., EHRLICH, S. D., ALBERTINI, A., AMATI, G., ANDERSEN, K. K., ARNAUD, M., ASAI, K., ASHIKAGA, S., AYMERICH, S., BESSIERES, P., BOLAND, F., BRIGNELL, S. C., BRON, S., BUNAI, K., CHAPUIS, J., CHRISTIANSEN, L. C., DANCHIN, A., DEBARBOUILLE, M., DERVYN, E., DEUERLING, E., DEVINE, K., DEVINE, S. K., DREESEN, O., ERRINGTON, J., FILLINGER, S., FOSTER, S. J., FUJITA, Y., GALIZZI, A., GARDAN, R., ESCHEVINS, C., FUKUSHIMA, T., HAGA, K., HARWOOD, C. R., HECKER, M., HOSOYA, D., HULLO, M. F., KAKESHITA, H., KARAMATA, D., KASAHARA, Y., KAWAMURA, F., KOGA, K., KOSKI, P., KUWANA, R., IMAMURA, D., ISHIMARU, M., ISHIKAWA, S., ISHIO, I., LE COQ, D., MASSON, A., MAUEL, C., MEIMA, R., MELLADO, R. P., MOIR, A., MORIYA, S., NAGAKAWA, E., NANAMIYA, H., NAKAI, S., NYGAARD, P., OGURA, M., OHANAN, T., O'REILLY, M., O'ROURKE, M., PRAGAI, Z., POOLEY, H. M., RAPOPORT, G., RAWLINS, J. P., RIVAS, L. A., RIVOLTA, C., SADAIE, A., SADAIE, Y., SARVAS, M., SATO, T., SAXILD, H. H., SCANLAN, E., SCHUMANN, W., SEEGERS, J. F., SEKIGUCHI, J., SEKOWSKA, A., SEROR, S. J., SIMON, M., STRAGIER, P., STUDER, R., TAKAMATSU, H., TANAKA, T., TAKEUCHI, M., THOMAIDES, H. B., VAGNER, V., VAN DIJL, J. M., WATABE, K., WIPAT, A., YAMAMOTO, H., YAMAMOTO, M., YAMAMOTO, Y., YAMANE, K., YATA, K., YOSHIDA, K., YOSHIKAWA, H., ZUBER, U. & OGASAWARA, N. 2003. Essential Bacillus subtilis genes. *Proc Natl Acad Sci U S A,* 100**,** 4678-83.

KOIDE, A., PEREGO, M. & HOCH, J. A. 1999. ScoC regulates peptide transport and sporulation initiation in Bacillus subtilis. *J Bacteriol,* 181**,** 4114-7.

KOMAKI, H., ICHIKAWA, N., HOSOYAMA, A., FUJITA, N. & IGARASHI, Y. 2015. Draft genome sequence of marine-derived Streptomyces sp. TP-A0598, a producer of anti-MRSA antibiotic lydicamycins. *Stand Genomic Sci,* 10**,** 58.

KOVACS, M., HALFMANN, A., FEDTKE, I., HEINTZ, M., PESCHEL, A., VOLLMER, W., HAKENBECK, R. & BRUCKNER, R. 2006. A functional dlt operon, encoding proteins required for incorporation of d-alanine in teichoic acids in gram-positive bacteria, confers resistance to cationic antimicrobial peptides in Streptococcus pneumoniae. *J Bacteriol,* 188**,** 5797-805.

KRISTIAN, S. A., LAUTH, X., NIZET, V., GOETZ, F., NEUMEISTER, B., PESCHEL, A. & LANDMANN, R. 2003. Alanylation of teichoic acids protects Staphylococcus aureus against Toll-like receptor 2-dependent host defense in a mouse tissue cage infection model. *J Infect Dis,* 188**,** 414-23.

KUNST, F., OGASAWARA, N., MOSZER, I., ALBERTINI, A. M., ALLONI, G., AZEVEDO, V., BERTERO, M. G., BESSIERES, P., BOLOTIN, A., BORCHERT, S., BORRISS, R., BOURSIER, L., BRANS, A., BRAUN, M., BRIGNELL, S. C., BRON, S., BROUILLET, S., BRUSCHI, C. V., CALDWELL, B., CAPUANO, V., CARTER, N. M., CHOI, S. K., CODANI, J. J., CONNERTON, I. F., DANCHIN, A. & ET AL. 1997. The complete genome sequence of the gram-positive bacterium Bacillus subtilis. *Nature,* 390**,** 249-56.

LAGES, M. C., BEILHARZ, K., MORALES ANGELES, D., VEENING, J. W. & SCHEFFERS, D. J. 2013. The localization of key Bacillus subtilis penicillin binding proteins during cell growth is determined by substrate availability. *Environ Microbiol,* 15**,** 3272-81.

LAHLALI, R., PENG, G., GOSSEN, B. D., MCGREGOR, L., YU, F. Q., HYNES, R. K., HWANG, S. F., MCDONALD, M. R. & BOYETCHKO, S. M. 2013. Evidence that the biofungicide Serenade (Bacillus subtilis) suppresses clubroot on canola via antibiosis and induced host resistance. *Phytopathology,* 103**,** 245-54.

LAN, G., DANIELS, B. R., DOBROWSKY, T. M., WIRTZ, D. & SUN, S. X. 2009. Condensation of FtsZ filaments can drive bacterial cell division. *Proc Natl Acad Sci U S A,* 106**,** 121-6.

LANTOS, P. M., AUWAERTER, P. G. & WORMSER, G. P. 2014. A systematic review of Borrelia burgdorferi morphologic variants does not support a role in chronic Lyme disease. *Clin Infect Dis,* 58**,** 663-71.

LASKARIS, P., TOLBA, S., CALVO-BADO, L. & WELLINGTON, E. M. 2010. Coevolution of antibiotic production and counter-resistance in soil bacteria. *Environ Microbiol,* 12**,** 783-96.

LAUTRU, S., DEETH, R. J., BAILEY, L. M. & CHALLIS, G. L. 2005. Discovery of a new peptide natural product by Streptomyces coelicolor genome mining. *Nat Chem Biol,* 1**,** 265-9.

LEAVER, M., DOMINGUEZ-CUEVAS, P., COXHEAD, J. M., DANIEL, R. A. & ERRINGTON, J. 2009. Life without a wall or division machine in Bacillus subtilis. *Nature,* 457**,** 849-853.

LEE, A. G. 2004. How lipids affect the activities of integral membrane proteins. *Biochim Biophys Acta,* 1666**,** 62-87.

LEE, K., CAMPBELL, J., SWOBODA, J. G., CUNY, G. D. & WALKER, S. 2010. Development of improved inhibitors of wall teichoic acid biosynthesis with potent activity against Staphylococcus aureus. *Bioorg Med Chem Lett,* 20**,** 1767-70.

LEEUWENHOEK, A. V. 1695. *Arcana naturae detecta*.

LENARCIC, R., HALBEDEL, S., VISSER, L., SHAW, M., WU, L. J., ERRINGTON, J., MARENDUZZO, D. & HAMOEN, L. W. 2009. Localisation of DivIVA by targeting to negatively curved membranes. *EMBO J,* 28**,** 2272-82.

LEON, O. & PANOS, C. 1976. Adaptation of an osmotically fragile L-form of Streptococcus pyogenes to physiological osmotic conditions and its ability to destroy human heart cells in tissue culture. *Infect Immun,* 13**,** 252-62.

LEVINA, N., TOTEMEYER, S., STOKES, N. R., LOUIS, P., JONES, M. A. & BOOTH, I. R. 1999. Protection of Escherichia coli cells against extreme turgor by activation of MscS and MscL mechanosensitive channels: identification of genes required for MscS activity. *EMBO J,* 18**,** 1730-7.

LI, Y., FLOROVA, G. & REYNOLDS, K. A. 2005. Alteration of the fatty acid profile of Streptomyces coelicolor by replacement of the initiation enzyme 3-ketoacyl acyl carrier protein synthase III (FabH). *J Bacteriol,* 187**,** 3795-9.

LIN, S., HANSON, R. E. & CRONAN, J. E. 2010. Biotin synthesis begins by hijacking the fatty acid synthetic pathway. *Nat Chem Biol,* 6**,** 682-8.

LOMBO, F., VELASCO, A., CASTRO, A., DE LA CALLE, F., BRANA, A. F., SANCHEZ-PUELLES, J. M., MENDEZ, C. & SALAS, J. A. 2006. Deciphering the biosynthesis pathway of the antitumor thiocoraline from a marine actinomycete and its expression in two streptomyces species. *Chembiochem,* 7**,** 366-76.

LOPEZ, D. & KOLTER, R. 2010. Functional microdomains in bacterial membranes. *Genes Dev,* 24**,** 1893-902.

MADIGAN, M. T., MADIGAN, M. T. & BROCK, T. D. 2009. *Brock biology of microorganisms,* San Francisco, CA, Pearson/Benjamin Cummings.

MAGER, J. 1959. The stabilizing effect of spermine and related polyamines and bacterial protoplasts. *Biochim Biophys Acta,* 36**,** 529-31.

MAUCK, J. & GLASER, L. 1972. On the mode of in vivo assembly of the cell wall of Bacillus subtilis. *J Biol Chem,* 247**,** 1180-7.

MAURER, J. A. & DOUGHERTY, D. A. 2001. A high-throughput screen for MscL channel activity and mutational phenotyping. *Biochim Biophys Acta,* 1514**,** 165-9.

MBAMALA, E. C., BEN-SHAUL, A. & MAY, S. 2005. Domain formation induced by the adsorption of charged proteins on mixed lipid membranes. *Biophys J,* 88**,** 1702-14.

MEESKE, A. J., SHAM, L. T., KIMSEY, H., KOO, B. M., GROSS, C. A., BERNHARDT, T. G. & RUDNER, D. Z. 2015. MurJ and a novel lipid II flippase are required for cell wall biogenesis in Bacillus subtilis. *Proc Natl Acad Sci U S A,* 112**,** 6437-42.

MEIER, E. L. & GOLEY, E. D. 2014. Form and function of the bacterial cytokinetic ring. *Curr Opin Cell Biol,* 26**,** 19-27.

MENICHETTI, F. 2005. Current and emerging serious Gram-positive infections. *Clin Microbiol Infect,* 11 Suppl 3**,** 22-8.

MERCIER, R., DOMINGUEZ-CUEVAS, P. & ERRINGTON, J. 2012. Crucial role for membrane fluidity in proliferation of primitive cells. *Cell Rep,* 1**,** 417-23.

MERCIER, R., KAWAI, Y. & ERRINGTON, J. 2013. Excess membrane synthesis drives a primitive mode of cell proliferation. *Cell,* 152**,** 997-1007.

MERCIER, R., KAWAI, Y. & ERRINGTON, J. 2014. General principles for the formation and proliferation of a wall-free (L-form) state in bacteria. *Elife,* 3.

MEROUEH, S. O., BENCZE, K. Z., HESEK, D., LEE, M., FISHER, J. F., STEMMLER, T. L. & MOBASHERY, S. 2006. Three-dimensional structure of the bacterial cell wall peptidoglycan. *Proc Natl Acad Sci U S A,* 103**,** 4404-9.

MIESSLER, G. L. & TARR, D. A. 2011. *Inorganic chemistry,* Upper Saddle River, NJ, Pearson Prentice Hall.

MILEYKOVSKAYA, E. & DOWHAN, W. 2009. Cardiolipin membrane domains in prokaryotes and eukaryotes. *Biochim Biophys Acta,* 1788**,** 2084-91.

MONTGOMERIE, J. Z., KALAMANSON, G. M., HUBERT, E. G. & GUZE, L. B. 1972. Osmotic Stability and Sodium and Potassium Content of L-Forms of Streptococcus Faecalis. *Journal of Bacteriology,* 110**,** 624-&.

MONTGOMERIE, J. Z., KALMANSON, G. M. & GUZE, L. B. 1973. Fatty acid composition of L-forms of Streptococcus faecalis cultured at different osmolalities. *J Bacteriol,* 115**,** 73-5.

MORATH, S., GEYER, A. & HARTUNG, T. 2001. Structure-function relationship of cytokine induction by lipoteichoic acid from Staphylococcus aureus. *J Exp Med,* 193**,** 393-7.

MORIKAWA, M. 2006. Beneficial biofilm formation by industrial bacteria Bacillus subtilis and related species. *Journal of Bioscience and Bioengineering,* 101**,** 1-8.

MORIMOTO, T., LOH, P. C., HIRAI, T., ASAI, K., KOBAYASHI, K., MORIYA, S. & OGASAWARA, N. 2002. Six GTP-binding proteins of the Era/Obg family are essential for cell growth in Bacillus subtilis. *Microbiology,* 148**,** 3539-52.

MUCHOVA, K., CHROMIKOVA, Z. & BARAK, I. 2013. Control of Bacillus subtilis cell shape by RodZ. *Environ Microbiol,* 15**,** 3259-71.

MURPHY, K., TRAVERS, P., WALPORT, M. & JANEWAY, C. 2008. *Janeway's immunobiology,* New York, Garland Science.

MURRAY, H., FERREIRA, H. & ERRINGTON, J. 2006. The bacterial chromosome segregation protein Spo0J spreads along DNA from parS nucleation sites. *Mol Microbiol,* 61**,** 1352-61.

MURRAY, T., POPHAM, D. L. & SETLOW, P. 1998. Bacillus subtilis cells lacking penicillin-binding protein 1 require increased levels of divalent cations for growth. *J Bacteriol,* 180**,** 4555-63.

NAGORSKA, K., BIKOWSKI, M. & OBUCHOWSKJI, M. 2007. Multicellular behaviour and production of a wide variety of toxic substances support usage of Bacillus subtilis as a powerful biocontrol agent. *Acta Biochimica Polonica,* 54**,** 495-508.

NAISMITH, J. H. & BOOTH, I. R. 2012. Bacterial mechanosensitive channels--MscS: evolution's solution to creating sensitivity in function. *Annu Rev Biophys,* 41**,** 157-77.

NEEDHAM, D. & NUNN, R. S. 1990. Elastic deformation and failure of lipid bilayer membranes containing cholesterol. *Biophys J,* 58**,** 997-1009.

NEILANDS, J. B. 1995. Siderophores: structure and function of microbial iron transport compounds. *J Biol Chem,* 270**,** 26723-6.

NEUHAUS, F. C. & BADDILEY, J. 2003. A continuum of anionic charge: structures and functions of D-alanyl-teichoic acids in gram-positive bacteria. *Microbiol Mol Biol Rev,* 67**,** 686-723.

NISHIBORI, A., KUSAKA, J., HARA, H., UMEDA, M. & MATSUMOTO, K. 2005. Phosphatidylethanolamine domains and localization of phospholipid synthases in Bacillus subtilis membranes. *J Bacteriol,* 187**,** 2163-74.

NOUAILLE, S., COMMISSAIRE, J., GRATADOUX, J. J., RAVN, P., BOLOTIN, A., GRUSS, A., LE LOIR, Y. & LANGELLA, P. 2004. Influence of lipoteichoic acid D-alanylation on protein secretion in Lactococcus lactis as revealed by random mutagenesis. *Appl Environ Microbiol,* 70**,** 1600-7.

OGLECKA, K., RANGAMANI, P., LIEDBERG, B., KRAUT, R. S. & PARIKH, A. N. 2014. Oscillatory phase separation in giant lipid vesicles induced by transmembrane osmotic differentials. *Elife,* 3**,** e03695.

OKORO, C. K., BROWN, R., JONES, A. L., ANDREWS, B. A., ASENJO, J. A., GOODFELLOW, M. & BULL, A. T. 2009. Diversity of culturable actinomycetes in hyper-arid soils of the Atacama Desert, Chile. *Antonie Van Leeuwenhoek,* 95**,** 121-33.

OKU, Y., KUROKAWA, K., MATSUO, M., YAMADA, S., LEE, B. L. & SEKIMIZU, K. 2009. Pleiotropic roles of polyglycerolphosphate synthase of lipoteichoic acid in growth of Staphylococcus aureus cells. *J Bacteriol,* 191**,** 141-51.

OLSHAUSEN, P. V., DEFEU SOUFO, H. J., WICKER, K., HEINTZMANN, R., GRAUMANN, P. L. & ROHRBACH, A. 2013. Superresolution imaging of dynamic MreB filaments in B. subtilis--a multiple-motor-driven transport? *Biophys J,* 105**,** 1171-81.

ONODA, T., OSHIMA, A., NAKANO, S. & MATSUNO, A. 1987. Morphology, growth and reversion in a stable L-form of Escherichia coli K12. *J Gen Microbiol,* 133**,** 527-34.

OSAWA, M., ANDERSON, D. E. & ERICKSON, H. P. 2008. Reconstitution of contractile FtsZ rings in liposomes. *Science,* 320**,** 792-4.

OU, X., BLOUNT, P., HOFFMAN, R. J. & KUNG, C. 1998. One face of a transmembrane helix is crucial in mechanosensitive channel gating. *Proc Natl Acad Sci U S A,* 95**,** 11471-5.

PARASASSI, T., DE STASIO, G., D'UBALDO, A. & GRATTON, E. 1990. Phase fluctuation in phospholipid membranes revealed by Laurdan fluorescence. *Biophys J,* 57**,** 1179-86.

PARSONS, J. B. & ROCK, C. O. 2013. Bacterial lipids: metabolism and membrane homeostasis. *Prog Lipid Res,* 52**,** 249-76.

PATHOM-AREE, W., STACH, J. E., WARD, A. C., HORIKOSHI, K., BULL, A. T. & GOODFELLOW, M. 2006. Diversity of actinomycetes isolated from Challenger Deep sediment (10,898 m) from the Mariana Trench. *Extremophiles,* 10**,** 181-9.

PATON, A. M. & INNES, C. M. J. 1991. Methods for the Establishment of Intracellular Associations of L-Forms with Higher-Plants. *Journal of Applied Bacteriology,* 71**,** 59-64.

PAYNE, D. J., GWYNN, M. N., HOLMES, D. J. & POMPLIANO, D. L. 2007. Drugs for bad bugs: confronting the challenges of antibacterial discovery. *Nat Rev Drug Discov,* 6**,** 29-40.

PENN, J., LI, X., WHITING, A., LATIF, M., GIBSON, T., SILVA, C. J., BRIAN, P., DAVIES, J., MIAO, V., WRIGLEY, S. K. & BALTZ, R. H. 2006. Heterologous production of daptomycin in Streptomyces lividans. *J Ind Microbiol Biotechnol,* 33**,** 121-8.

PERRY, A. M., TON-THAT, H., MAZMANIAN, S. K. & SCHNEEWIND, O. 2002. Anchoring of surface proteins to the cell wall of Staphylococcus aureus. III. Lipid II is an in vivo peptidoglycan substrate for sortase-catalyzed surface protein anchoring. *J Biol Chem,* 277**,** 16241-8.

PROJAN, S. J. & SHLAES, D. M. 2004. Antibacterial drug discovery: is it all downhill from here? *Clin Microbiol Infect,* 10 Suppl 4**,** 18-22.

RAMAMURTHI, K. S., LECUYER, S., STONE, H. A. & LOSICK, R. 2009. Geometric cue for protein localization in a bacterium. *Science,* 323**,** 1354-7.

REIMOLD, C., DEFEU SOUFO, H. J., DEMPWOLFF, F. & GRAUMANN, P. L. 2013. Motion of variable-length MreB filaments at the bacterial cell membrane influences cell morphology. *Mol Biol Cell,* 24**,** 2340-9.

REUTER, M., HAYWARD, N. J., BLACK, S. S., MILLER, S., DRYDEN, D. T. & BOOTH, I. R. 2014. Mechanosensitive channels and bacterial cell wall integrity: does life end with a bang or a whimper? *J R Soc Interface,* 11**,** 20130850.

RHEE, H. J., KIM, E. J. & LEE, J. K. 2007. Physiological polyamines: simple primordial stress molecules. *J Cell Mol Med,* 11**,** 685-703.

RICHTER, S. G., ELLI, D., KIM, H. K., HENDRICKX, A. P., SORG, J. A., SCHNEEWIND, O. & MISSIAKAS, D. 2013. Small molecule inhibitor of lipoteichoic acid synthesis is an antibiotic for Gram-positive bacteria. *Proc Natl Acad Sci U S A,* 110**,** 3531-6.

ROJAS, E., THERIOT, J. A. & HUANG, K. C. 2014. Response of Escherichia coli growth rate to osmotic shock. *Proc Natl Acad Sci U S A,* 111**,** 7807-12.

ROMANTSOV, T., HELBIG, S., CULHAM, D. E., GILL, C., STALKER, L. & WOOD, J. M. 2007. Cardiolipin promotes polar localization of osmosensory transporter ProP in Escherichia coli. *Mol Microbiol,* 64**,** 1455-65.

ROWLAND, S. L., WADSWORTH, K. D., ROBSON, S. A., ROBICHON, C., BECKWITH, J. & KING, G. F. 2010. Evidence from artificial septal targeting and site-directed mutagenesis that residues in the extracytoplasmic beta domain of DivIB mediate its interaction with the divisomal transpeptidase PBP 2B. *J Bacteriol,* 192**,** 6116-25.

RUBENHAGEN, R., MORBACH, S. & KRAMER, R. 2001. The osmoreactive betaine carrier BetP from Corynebacterium glutamicum is a sensor for cytoplasmic K+. *EMBO J,* 20**,** 5412-20.

RUIZ, N. 2008. Bioinformatics identification of MurJ (MviN) as the peptidoglycan lipid II flippase in Escherichia coli. *Proc Natl Acad Sci U S A,* 105**,** 15553-7.

RUZIN, A., SEVERIN, A., RITACCO, F., TABEI, K., SINGH, G., BRADFORD, P. A., SIEGEL, M. M., PROJAN, S. J. & SHLAES, D. M. 2002. Further evidence that a cell wall precursor [C(55)-MurNAc-(peptide)-GlcNAc] serves as an acceptor in a sorting reaction. *J Bacteriol,* 184**,** 2141-7.

SAITOU, N. & NEI, M. 1987. The neighbor-joining method: a new method for reconstructing phylogenetic trees. *Mol Biol Evol,* 4**,** 406-25.

SALJE, J., VAN DEN ENT, F., DE BOER, P. & LOWE, J. 2011. Direct membrane binding by bacterial actin MreB. *Mol Cell,* 43**,** 478-87.

SANDRE, O., MOREAUX, L. & BROCHARD-WYART, F. 1999. Dynamics of transient pores in stretched vesicles. *Proc Natl Acad Sci U S A,* 96**,** 10591-6.

SCHEFFERS, D. J. & PINHO, M. G. 2005. Bacterial cell wall synthesis: new insights from localization studies. *Microbiol Mol Biol Rev,* 69**,** 585-607.

SCHEFFERS, D. J. & TOL, M. B. 2015. LipidII: Just Another Brick in the Wall? *PLoS Pathog,* 11**,** e1005213.

SCHIRNER, K. 2009. *Cell Morphogenesis of Bacillus subtilis: Roles of Actin Homologues and Lipoteichoic Acid Synthases.* Doctor of Philosophy, Newcastle University.

SCHIRNER, K. & ERRINGTON, J. 2009. The cell wall regulator {sigma}I specifically suppresses the lethal phenotype of mbl mutants in Bacillus subtilis. *J Bacteriol,* 191**,** 1404-13.

SCHIRNER, K., EUN, Y. J., DION, M., LUO, Y., HELMANN, J. D., GARNER, E. C. & WALKER, S. 2015. Lipid-linked cell wall precursors regulate membrane association of bacterial actin MreB. *Nat Chem Biol,* 11**,** 38-45.

SCHIRNER, K., MARLES-WRIGHT, J., LEWIS, R. J. & ERRINGTON, J. 2009. Distinct and essential morphogenic functions for wall- and lipo-teichoic acids in Bacillus subtilis. *Embo Journal,* 28**,** 830-842.

SCHNEIDER, C. A., RASBAND, W. S. & ELICEIRI, K. W. 2012. NIH Image to ImageJ: 25 years of image analysis. *Nat Methods,* 9**,** 671-5.

SCHUMANN, U., EDWARDS, M. D., RASMUSSEN, T., BARTLETT, W., VAN WEST, P. & BOOTH, I. R. 2010. YbdG in Escherichia coli is a threshold-setting mechanosensitive channel with MscM activity. *Proc Natl Acad Sci U S A,* 107**,** 12664-9.

SEMEDO, L. T., GOMES, R. C., LINHARES, A. A., DUARTE, G. F., NASCIMENTO, R. P., ROSADO, A. S., MARGIS-PINHEIRO, M., MARGIS, R., SILVA, K. R., ALVIANO, C. S., MANFIO, G. P., SOARES, R. M., LINHARES, L. F. & COELHO, R. R. 2004. Streptomyces drozdowiczii sp. nov., a novel cellulolytic streptomycete from soil in Brazil. *Int J Syst Evol Microbiol,* 54**,** 1323-8.

SENIOR, J. K. 1951. Partitions and their representative graphs. *American Journal of Mathematics,* 73**,** 663-689.

SEWELL, E. W. & BROWN, E. D. 2014. Taking aim at wall teichoic acid synthesis: new biology and new leads for antibiotics. *J Antibiot (Tokyo),* 67**,** 43-51.

SINGER, S. J. & NICOLSON, G. L. 1972. The fluid mosaic model of the structure of cell membranes. *Science,* 175**,** 720-31.

SMITH, T. J., BLACKMAN, S. A. & FOSTER, S. J. 2000. Autolysins of Bacillus subtilis: multiple enzymes with multiple functions. *Microbiology,* 146 (Pt 2)**,** 249-62.

STEVENS, D. L., HERR, D., LAMPIRIS, H., HUNT, J. L., BATTS, D. H. & HAFKIN, B. 2002. Linezolid versus vancomycin for the treatment of methicillin-resistant Staphylococcus aureus infections. *Clin Infect Dis,* 34**,** 1481-90.

STEWART, G. C. 2005. Taking shape: control of bacterial cell wall biosynthesis. *Mol Microbiol,* 57**,** 1177-81.

STRAHL, H., BURMANN, F. & HAMOEN, L. W. 2014. The actin homologue MreB organizes the bacterial cell membrane. *Nat Commun,* 5**,** 3442.

STRAHL, H. & HAMOEN, L. W. 2010. Membrane potential is important for bacterial cell division. *Proc Natl Acad Sci U S A,* 107**,** 12281-6.

SUKHAREV, S. 2002. Purification of the small mechanosensitive channel of Escherichia coli (MscS): the subunit structure, conduction, and gating characteristics in liposomes. *Biophys J,* 83**,** 290-8.

SUKHAREV, S. I., SIGURDSON, W. J., KUNG, C. & SACHS, F. 1999. Energetic and spatial parameters for gating of the bacterial large conductance mechanosensitive channel, MscL. *J Gen Physiol,* 113**,** 525-40.

SVETINA, S. 2009. Vesicle budding and the origin of cellular life. *Chemphyschem,* 10**,** 2769-76.

SWOBODA, J. G., MEREDITH, T. C., CAMPBELL, J., BROWN, S., SUZUKI, T., BOLLENBACH, T., MALHOWSKI, A. J., KISHONY, R., GILMORE, M. S. & WALKER, S. 2009. Discovery of a small molecule that blocks wall teichoic acid biosynthesis in Staphylococcus aureus. *ACS Chem Biol,* 4**,** 875-83.

TOOMEY, R. E. & WAKIL, S. J. 1966. Studies on the mechanism of fatty acid synthesis. XV. Preparation and general properties of beta-ketoacyl acyl carrier protein reductase from Escherichia coli. *Biochim Biophys Acta,* 116**,** 189-97.

TSATSKIS, Y., KHAMBATI, J., DOBSON, M., BOGDANOV, M., DOWHAN, W. & WOOD, J. M. 2005. The osmotic activation of transporter ProP is tuned by both its C-terminal coiled-coil and osmotically induced changes in phospholipid composition. *J Biol Chem,* 280**,** 41387-94.

TURNER, R. D., VOLLMER, W. & FOSTER, S. J. 2014. Different walls for rods and balls: the diversity of peptidoglycan. *Mol Microbiol,* 91**,** 862-74.

TYPAS, A., BANZHAF, M., GROSS, C. A. & VOLLMER, W. 2012. From the regulation of peptidoglycan synthesis to bacterial growth and morphology. *Nature Reviews Microbiology,* 10**,** 123-36.

URSELL, T. S., NGUYEN, J., MONDS, R. D., COLAVIN, A., BILLINGS, G., OUZOUNOV, N., GITAI, Z., SHAEVITZ, J. W. & HUANG, K. C. 2014. Rod-like bacterial shape is maintained by feedback between cell curvature and cytoskeletal localization. *Proc Natl Acad Sci U S A,* 111**,** E1025-34.

VAGNER, V., DERVYN, E. & EHRLICH, S. D. 1998. A vector for systematic gene inactivation in Bacillus subtilis. *Microbiology,* 144 (Pt 11)**,** 3097-104.

VAN DEN ENT, F., AMOS, L. A. & LOWE, J. 2001. Prokaryotic origin of the actin cytoskeleton. *Nature,* 413**,** 39-44.

VAN DEN ENT, F., IZORE, T., BHARAT, T. A., JOHNSON, C. M. & LOWE, J. 2014. Bacterial actin MreB forms antiparallel double filaments. *Elife,* 3**,** e02634.

VAN DEN ENT, F., JOHNSON, C. M., PERSONS, L., DE BOER, P. & LOWE, J. 2010. Bacterial actin MreB assembles in complex with cell shape protein RodZ. *EMBO J,* 29**,** 1081-90.

VAN DEN ENT, F., LEAVER, M., BENDEZU, F., ERRINGTON, J., DE BOER, P. & LOWE, J. 2006. Dimeric structure of the cell shape protein MreC and its functional implications. *Mol Microbiol,* 62**,** 1631-42.

VAN OOIJ, C. & LOSICK, R. 2003. Subcellular localization of a small sporulation protein in Bacillus subtilis. *J Bacteriol,* 185**,** 1391-8.

VAN TEEFFELEN, S., WANG, S., FURCHTGOTT, L., HUANG, K. C., WINGREEN, N. S., SHAEVITZ, J. W. & GITAI, Z. 2011. The bacterial actin MreB rotates, and rotation depends on cell-wall assembly. *Proc Natl Acad Sci U S A,* 108**,** 15822-7.

VOLLMER, W. & BERTSCHE, U. 2008. Murein (peptidoglycan) structure, architecture and biosynthesis in Escherichia coli. *Biochim Biophys Acta,* 1778**,** 1714-34.

VOLLMER, W., BLANOT, D. & DE PEDRO, M. A. 2008. Peptidoglycan structure and architecture. *FEMS Microbiol Rev,* 32**,** 149-67.

VOLLMER, W. & HOLTJE, J. V. 2004. The architecture of the murein (peptidoglycan) in gram-negative bacteria: vertical scaffold or horizontal layer(s)? *J Bacteriol,* 186**,** 5978-87.

WACHI, M., DOI, M., TAMAKI, S., PARK, W., NAKAJIMA-IIJIMA, S. & MATSUHASHI, M. 1987. Mutant isolation and molecular cloning of mre genes, which determine cell shape, sensitivity to mecillinam, and amount of penicillin-binding proteins in Escherichia coli. *J Bacteriol,* 169**,** 4935-40.

WAKSMAN, S. A. & SCHATZ, A. 1943. Strain Specificity and Production of Antibiotic Substances. *Proc Natl Acad Sci U S A,* 29**,** 74-9.

WALDE, P., COSENTINO, K., ENGEL, H. & STANO, P. 2010. Giant vesicles: preparations and applications. *Chembiochem,* 11**,** 848-65.

WALKER, R., FERGUSON, C. M., BOOTH, N. A. & ALLAN, E. J. 2002. The symbiosis of Bacillus subtilis L-forms with Chinese cabbage seedlings inhibits conidial germination of Botrytis cinerea. *Lett Appl Microbiol,* 34**,** 42-5.

WANG, W., BLACK, S. S., EDWARDS, M. D., MILLER, S., MORRISON, E. L., BARTLETT, W., DONG, C., NAISMITH, J. H. & BOOTH, I. R. 2008. The structure of an open form of an E. coli mechanosensitive channel at 3.45 A resolution. *Science,* 321**,** 1179-83.

WARD, J. B., JR. & ZAHLER, S. A. 1973. Genetic studies of leucine biosynthesis in Bacillus subtilis. *J Bacteriol,* 116**,** 719-26.

WATERHOUSE, R. N., BUHARIWALLA, H., BOURN, D., RATTRAY, E. J. & GLOVER, L. A. 1996. CCD detection of lux-marked Pseudomonas syringae pv phaseolicola L-forms associated with Chinese cabbage and the resulting disease protection against Xanthomonas campestris. *Lett Appl Microbiol,* 22**,** 262-266.

WEBB, A. J., KARATSA-DODGSON, M. & GRUNDLING, A. 2009. Two-enzyme systems for glycolipid and polyglycerolphosphate lipoteichoic acid synthesis in Listeria monocytogenes. *Mol Microbiol,* 74**,** 299-314.

WEIDENMAIER, C., KOKAI-KUN, J. F., KRISTIAN, S. A., CHANTURIYA, T., KALBACHER, H., GROSS, M., NICHOLSON, G., NEUMEISTER, B., MOND, J. J. & PESCHEL, A. 2004. Role of teichoic acids in Staphylococcus aureus nasal colonization, a major risk factor in nosocomial infections. *Nat Med,* 10**,** 243-5.

WEIGEL, L. M., CLEWELL, D. B., GILL, S. R., CLARK, N. C., MCDOUGAL, L. K., FLANNAGAN, S. E., KOLONAY, J. F., SHETTY, J., KILLGORE, G. E. & TENOVER, F. C. 2003. Genetic analysis of a high-level vancomycin-resistant isolate of Staphylococcus aureus. *Science,* 302**,** 1569-71.

WHATMORE, A. M., CHUDEK, J. A. & REED, R. H. 1990. The effects of osmotic upshock on the intracellular solute pools of Bacillus subtilis. *J Gen Microbiol,* 136**,** 2527-35.

WILLIAMS, R. E. 1963. L FORMS OF STAPHYLOCOCCUS AUREUS. *J Gen Microbiol,* 33**,** 325-34.

WOBSER, D., ALI, L., GROHMANN, E., HUEBNER, J. & SAKINC, T. 2014. A novel role for D-alanylation of lipoteichoic acid of enterococcus faecalis in urinary tract infection. *PLoS One,* 9**,** e107827.

WOOD, J. M. 1999. Osmosensing by bacteria: signals and membrane-based sensors. *Microbiol Mol Biol Rev,* 63**,** 230-62.

WOOD, J. M. 2011. Bacterial osmoregulation: a paradigm for the study of cellular homeostasis. *Annu Rev Microbiol,* 65**,** 215-38.

WOOD, J. M. 2015. Bacterial responses to osmotic challenges. *J Gen Physiol,* 145**,** 381-8.

WOOLRIDGE, D. P., VAZQUEZ-LASLOP, N., MARKHAM, P. N., CHEVALIER, M. S., GERNER, E. W. & NEYFAKH, A. A. 1997. Efflux of the natural polyamine spermidine facilitated by the Bacillus subtilis multidrug transporter Blt. *J Biol Chem,* 272**,** 8864-6.

WORMANN, M. E., CORRIGAN, R. M., SIMPSON, P. J., MATTHEWS, S. J. & GRUNDLING, A. 2011. Enzymatic activities and functional interdependencies of Bacillus subtilis lipoteichoic acid synthesis enzymes. *Molecular Microbiology,* 79**,** 566-583.

WU, L. J. & ERRINGTON, J. 1998. Use of asymmetric cell division and spoIIIE mutants to probe chromosome orientation and organization in Bacillus subtilis. *Mol Microbiol,* 27**,** 777-86.

XIE, J., BOGDANOV, M., HEACOCK, P. & DOWHAN, W. 2006. Phosphatidylethanolamine and monoglucosyldiacylglycerol are interchangeable in supporting topogenesis and function of the polytopic membrane protein lactose permease. *J Biol Chem,* 281**,** 19172-8.

YAO, X., JERICHO, M., PINK, D. & BEVERIDGE, T. 1999. Thickness and elasticity of gram-negative murein sacculi measured by atomic force microscopy. *J Bacteriol,* 181**,** 6865-75.

YOSHIDA, M., KASHIWAGI, K., SHIGEMASA, A., TANIGUCHI, S., YAMAMOTO, K., MAKINOSHIMA, H., ISHIHAMA, A. & IGARASHI, K. 2004. A unifying model for the role of polyamines in bacterial cell growth, the polyamine modulon. *J Biol Chem,* 279**,** 46008-13.

ZAPRASIS, A., BRILL, J., THURING, M., WUNSCHE, G., HEUN, M., BARZANTNY, H., HOFFMANN, T. & BREMER, E. 2013. Osmoprotection of Bacillus subtilis through import and proteolysis of proline-containing peptides. *Appl Environ Microbiol,* 79**,** 576-87.

ZEIGLER, D. R., PRAGAI, Z., RODRIGUEZ, S., CHEVREUX, B., MUFFLER, A., ALBERT, T., BAI, R., WYSS, M. & PERKINS, J. B. 2008. The origins of 168, W23, and other Bacillus subtilis legacy strains. *J Bacteriol,* 190**,** 6983-95.

ZHANG, W., CAMPBELL, H. A., KING, S. C. & DOWHAN, W. 2005. Phospholipids as determinants of membrane protein topology. Phosphatidylethanolamine is required for the proper topological organization of the gamma-aminobutyric acid permease (GabP) of Escherichia coli. *J Biol Chem,* 280**,** 26032-8.

ZHANG, Y. Q., LIU, H. Y., CHEN, J., YUAN, L. J., SUN, W., ZHANG, L. X., ZHANG, Y. Q., YU, L. Y. & LI, W. J. 2010. Diversity of culturable actinobacteria from Qinghai-Tibet plateau, China. *Antonie Van Leeuwenhoek,* 98**,** 213-23.

ZHU, T. F. & SZOSTAK, J. W. 2009. Coupled growth and division of model protocell membranes. *J Am Chem Soc,* 131**,** 5705-13.

ZUCCHI, T. D., KIM, B. Y., KSHETRIMAYUM, J. D., WEON, H. Y., KWON, S. W. & GOODFELLOW, M. 2012. Streptomyces brevispora sp. nov. and Streptomyces laculatispora sp. nov., actinomycetes isolated from soil. *Int J Syst Evol Microbiol,* 62**,** 478-83.

ZUCKO, J., LONG, P. F., HRANUELI, D. & CULLUM, J. 2012. Horizontal gene transfer and gene conversion drive evolution of modular polyketide synthases. *J Ind Microbiol Biotechnol,* 39**,** 1541-7.

Appendices

Appendix 1. Solutions and buffers

Name	Composition
Blocking buffer	5% milk powder in PBS
	0.1% Tween20

CAA (casamino acids)	20% casamino acids
DNA loading dye	0.04% bromphenol blue in 50% glycerol
Ferric ammonium citrate	2.2mg/ml Ferric ammonium citrate
RF1	100 mM RbCl
	50 mM potassium acetate
	10 mM $CaCl_2$
	15% glycerol
RF2	10 mM MOPS
	10 mM $RbCl_2$
	75 mM $CaCl_2$
	15% glycerol
SMM (Spizizen minimal medium)	1.4% K_2HPO_4
	0.2% $(NH_4)_2SO_4$
	0.6% KH_2PO_4
	0.2% sodium citrate
	0.02% $MgSO_4$
Solution E	40% D-glucose
Solution F	1 M $MgSO_4$
Solution H	50 mM $MnSO_4$
SSC	0.15 M NaCl
	0.01M sodium tricitrate
	Adjust to pH 7.0

Staining solution A	60g $(NH_4)_2SO_4$ final conc. 8%
	15ml phosphoric acid 85% (final conc. 1.6%)
Staining solution B	1.6% Coomassie brilliant blue (G)
50x TAE buffer	2 M Tris pH 8.0
	50 mM acetic acid
	100 mM EDTA
TE buffer	10 mM Tris pH 8.0
	1 mM EDTA
Transfer buffer (for semi-dry transfer)	3 g Tris
	14.4 g glycine
	150 ml methanol
	Fill up to 1 L with dH_2O

Appendix 2. Growth media

Name	Composition
Competence medium	10 ml SMM
	0.125 ml solution E
	0.1 ml tryptophan solution
	0.06 ml solution F
	0.01 ml CAA
	0.005 ml ferric ammonium citrate
GYM medium	4 g glucose
	4 g yeast extract
	10 g malt extract
	Adjust pH to 7, fill up to 1 L with dH_2O; autoclave
LB medium	10 g Tryptone
	5 g Yeast extract
	10 g NaCl
	Adjust pH to 7, fill up to 1 L with dH_2O; autoclave
MSM	365 g sucrose
	4.64 g $MgCl_2$
	8.13 g maleic acid
	Adjust pH to 7, fill up to 1 L with dH_2O; autoclave
Nutrient agar	28 g Oxoid Nutrient agar
	fill up to 1 L with dH_2O; autoclave

Nutrient broth	13 g Oxoid Nutrient broth
	fill up to 1 L with dH$_2$O; autoclave
PAB medium	17.5 g Oxoid antibiotic medium no. 3
	fill up to 1 L with dH$_2$O; autoclave
Starvation medium	10 ml SMM
	0.125 ml solution E
	0.06 ml solution F

Appendix 3. Oligonucleotides

Name	Sequence (5'-3')	Construction
oJB33	AATTTAATTTCCGCGGGCATCATCGGAGGAGCAG	pJB1
oJB34	AAGGGAATTTGGATCCGAGCCTTGCTAAGCTGAGCC	pJB1
oJB35	AAGGGAATTTAAGCTTCCGTATGACCTGAATATTAATG	pJB1
oJB36	AAGGGAATTCTCGAGCGACGAATTGTCGGAAG	pJB1
oJB43	AACCCAAGAGCTCTGAATTCGCGGCCGCAGATC	JB158
oJB44	GCCGCGAACCAGGGAATGAGAATAGTGAATGG	JB158
oJB50	AACAGAACCGAGCTCCCGGCAGCGGTTAACTGG	JB140
oJB51	AACCCAAGGATCCATCAGCTGGCACCTTCC	JB140
oJB63	CCACCCAGGATCCCGACAGCGGAATTGACTCAAGC	
oJB64	GAAGAAAGGGAATTCGCGGGCAGTGAGCGCAACG	
oJB77	CCAACCCGAATTCCCTTTCGTCGCAATGGTTTGTG	pJB2
oJB78	CCAACCCGGATCCCTTTATCGACATCATGAAGC	pJB2
oJB84	CGCGATTAAAATGGAAATCGGATCTGCAG	pJB3/pJB4
oJB85	CGATTTCCATTTTAATCGCGTCATCCATCTC	pJB3/pJB4
LENm1	GCGTGTTTATTTGCCGC	JB158
LENm2	TCGTAGTCTAGAGTGTTACAAATATCCTTTTTCC	JB158
LENm3	TCGTAGTCTAGAATTTGTAACACTTTTTTTTCGTCGAATTAAGC	JB158
LENm4	CATAGCCCTGCAAAACCA	JB158

Oligonucleotides used for verification of mutations identified in the whole genome sequencing are not listed. They were typically designed approximately 25-50bp each side of the predicted mutation.

Appendix 4. Table of mutations

LR2								
Region	Type	Reference	Allele	Zygosity	Count	Coverage	Frequency	Gene
165749	Deletion	C	-	Homozygous	105	107	98.130841	
165751	Deletion	C	-	Homozygous	104	104	100	
165825^165826	Insertion	-	C	Homozygous	94	99	94.949495	
166037^166038	Insertion	-	T	Homozygous	75	80	93.75	
166344	Deletion	G	-	Homozygous	52	52	100	
557865^557866	Insertion	-	T	Homozygous	45	48	93.75	
608214^608215	Insertion	-	A	Homozygous	31	37	83.783784	
961817	SNV	G	A	Homozygous	111	111	100	ssuB
1317152^1317153	Insertion	-	GT	Homozygous	105	105	100	
1317153^1317154	Insertion	-	T	Homozygous	100	104	96.153846	
1372773	SNV	C	A	Homozygous	39	41	95.121951	
1581413	SNV	T	C	Homozygous	81	85	95.294118	mraW
1581669	SNV	A	G	Homozygous	78	78	100	ftsL
1581749	SNV	G	C	Homozygous	72	74	97.297297	ftsL
1582629	SNV	A	G	Homozygous	65	68	95.588235	pbpB
1582646	SNV	C	A	Homozygous	77	78	98.717949	pbpB
1582727	SNV	C	G	Homozygous	73	73	100	pbpB
1584096..1584097	MNV	AA	GG	Homozygous	41	41	100	pbpB
1584099..1584101	MNV	AAG	TCC	Homozygous	41	41	100	
1586307	SNV	A	C	Homozygous	28	30	93.333333	
1586533	SNV	A	G	Homozygous	92	92	100	murE
1867634	SNV	G	A	Homozygous	77	78	98.717949	
1891914	SNV	C	G	Heterozygous	22	71	30.985915	xylA
1891914	SNV	C	C	Heterozygous	48	71	67.605634	xylA
2097080^2097081	Insertion	-	A	Homozygous	48	56	85.714286	
2271424	SNV	T	C	Homozygous	113	116	97.413793	uvrX
2271505	SNV	C	T	Homozygous	114	114	100	uvrX
2271523	SNV	A	C	Homozygous	92	95	96.842105	uvrX
2480646..2480647	MNV	TA	AT	Homozygous	125	125	100	
2480654	Deletion	T	-	Homozygous	124	126	98.412698	

2480667	Deletion	T	-	Homozygous	128	128	100	
2526904	Deletion	T	-	Homozygous	111	114	97.368421	xseB
2579550..2579551	MNV	TC	GT	Heterozygous	18	52	34.615385	pstA
2579550..2579551	MNV	TC	TC	Heterozygous	34	52	65.384615	pstA
2579554	SNV	C	T	Heterozygous	11	48	22.916667	pstA
2579554	SNV	C	C	Heterozygous	35	48	72.916667	pstA
2579564..2579569	MNV	TGGCGC	AAAAAA	Heterozygous	15	61	24.590164	pstA
2579564..2579569	MNV	TGGCGC	TGGCGC	Heterozygous	44	61	72.131148	pstA
2581726^2581727	Insertion	-	T	Homozygous	99	106	93.396226	
3010782	SNV	G	A	Homozygous	85	86	98.837209	ytkK
3178443	SNV	T	C	Homozygous	31	32	96.875	rrnB-16S
3391676	SNV	A	G	Homozygous	82	84	97.619048	gerAA
3391685	SNV	T	C	Homozygous	78	80	97.5	gerAA
3770058^3770059	Insertion	-	A	Homozygous	66	75	88	
3935823	Deletion	T	-	Homozygous	78	79	98.734177	
4005693	SNV	A	C	Homozygous	59	61	96.721311	
4095811	SNV	C	T	Homozygous	84	88	95.454545	yxbD
4155390^4155391	Insertion	-	A	Homozygous	114	115	99.130435	
4189058	Deletion	A	-	Heterozygous	65	173	37.572254	
4189058	SNV	A	A	Heterozygous	104	173	60.115607	
4189063^4189064	Insertion	-	A	Heterozygous	60	176	34.090909	
4189063^4189064	Insertion	-	-	Heterozygous	114	176	64.772727	
4189071	SNV	T	A	Heterozygous	57	159	35.849057	
4189071	SNV	T	T	Heterozygous	99	159	62.264151	
4189087	SNV	C	T	Heterozygous	62	151	41.059603	
4189087	SNV	C	C	Heterozygous	82	151	54.304636	
4189100	SNV	C	T	Heterozygous	56	144	38.888889	tetL
4189100	SNV	C	C	Heterozygous	82	144	56.944444	tetL
4189102	SNV	T	A	Heterozygous	55	152	36.184211	tetL
4189102	SNV	T	T	Heterozygous	94	152	61.842105	tetL
4189127	SNV	T	A	Heterozygous	37	128	28.90625	tetL
4189127	SNV	T	T	Heterozygous	91	128	71.09375	tetL
4189135^4189136	Insertion	-	A	Heterozygous	33	126	26.190476	tetL
4189135^4189136	Insertion	-	-	Heterozygous	92	126	73.015873	tetL
4189139^4189140	Insertion	-	CA	Heterozygous	28	120	23.333333	tetL
4189139^4189140	Insertion	-	-	Heterozygous	92	120	76.666667	tetL

4189141^4189142	Insertion	-	ATTC	Heterozygous	28	118	23.728814	tetL
4189141^4189142	Insertion	-	-	Heterozygous	90	118	76.271186	tetL
4189145	SNV	G	A	Heterozygous	27	101	26.732673	tetL
4189145	SNV	G	G	Heterozygous	71	101	70.29703	tetL

M1								
Region	Type	Reference	Allele	Zygosity	Count	Coverage	Frequency	Gene
14808	SNV	A	C	Heterozygous	86	210	40.95238	rrnO-5S
14808	SNV	A	A	Heterozygous	124	210	59.04762	rrnO-5S
96240	SNV	G	A	Heterozygous	166	569	29.17399	
96240	SNV	G	G	Heterozygous	402	569	70.65026	
372434..372435	MNV	GT	CG	Heterozygous	150	517	29.01354	nucA
372434..372435	MNV	GT	GT	Heterozygous	367	517	70.98646	nucA
522503..522504	Replacement	AA	T	Heterozygous	142	449	31.62584	rsbW
522503..522504	MNV	AA	AA	Heterozygous	307	449	68.37416	rsbW
1075057	SNV	C	A	Homozygous	95	95	100	trpP
1075060^1075061	Insertion	-	G	Homozygous	120	120	100	trpP
1075064	SNV	A	C	Homozygous	147	147	100	trpP
1075066	SNV	A	T	Homozygous	158	158	100	trpP
1104996	Deletion	C	-	Homozygous	254	255	99.60784	aprE
1104999^1105000	Insertion	-	A	Homozygous	229	230	99.56522	aprE
1523004	Deletion	T	-	Heterozygous	192	484	39.66942	adeC
1523004	SNV	T	T	Heterozygous	292	484	60.33058	adeC
1523007	Deletion	C	-	Heterozygous	192	487	39.42505	adeC
1523007	SNV	C	C	Heterozygous	295	487	60.57495	adeC
1765777	SNV	C	A	Heterozygous	357	603	59.20398	
1765777	SNV	C	C	Heterozygous	246	603	40.79602	
1891754	SNV	A	G	Heterozygous	144	568	25.35211	
1891754	SNV	A	A	Heterozygous	424	568	74.64789	
1891785	SNV	C	T	Heterozygous	214	663	32.27753	
1891785	SNV	C	C	Heterozygous	449	663	67.72247	
1891794	SNV	A	T	Heterozygous	215	661	32.52648	
1891794	SNV	A	A	Heterozygous	446	661	67.47352	
1891801	SNV	G	T	Heterozygous	237	696	34.05172	
1891801	SNV	G	G	Heterozygous	459	696	65.94828	
1891821..1891823	MNV	AAA	GGG	Heterozygous	147	665	22.10526	
1891821..1891823	MNV	AAA	AAA	Heterozygous	518	665	77.89474	

Region	Type	Reference	Allele	Zygosity	Count	Coverage	Frequency	Gene
2722642	SNV	T	G	Heterozygous	165	459	35.94771	yrdQ
2722642	SNV	T	T	Heterozygous	294	459	64.05229	yrdQ
2722646	SNV	G	A	Heterozygous	201	491	40.93686	
2722646	SNV	G	G	Heterozygous	289	491	58.85947	
2722649	SNV	A	C	Heterozygous	215	497	43.25956	
2722649	SNV	A	A	Heterozygous	282	497	56.74044	
2722663^2722664	Insertion	-	T	Heterozygous	222	508	43.70079	
2722663^2722664	Insertion	-	-	Heterozygous	286	508	56.29921	
2988777	SNV	A	G	Heterozygous	331	594	55.72391	accD
2988777	SNV	A	A	Heterozygous	263	594	44.27609	accD
3422547..3422548	MNV	AC	GG	Heterozygous	217	547	39.67093	yvgJ
3422547..3422548	MNV	AC	AC	Heterozygous	329	547	60.14625	yvgJ
4084771^4084772	Insertion	-	A	Heterozygous	178	451	39.46785	
4084771^4084772	Insertion	-	-	Heterozygous	273	451	60.53215	

JB114								
Region	Type	Reference	Allele	Zygosity	Count	Coverage	Frequency	Gene
96240	SNV	G	A	Heterozygous	62	211	29.38389	
96240	SNV	G	G	Heterozygous	149	211	70.61611	
372434..372435	MNV	GT	CG	Heterozygous	49	191	25.65445	nucA
372434..372435	MNV	GT	GT	Heterozygous	142	191	74.34555	nucA
1349537^1349538	Insertion	-	CA	Homozygous	94	94	100	pit
1523004	Deletion	T	-	Heterozygous	64	134	47.76119	adeC
1523004	SNV	T	T	Heterozygous	70	134	52.23881	adeC
1523007	Deletion	C	-	Heterozygous	64	139	46.04317	adeC
1523007	SNV	C	C	Heterozygous	75	139	53.95683	adeC
1765777	SNV	C	A	Heterozygous	114	233	48.92704	
1765777	SNV	C	C	Heterozygous	119	233	51.07296	
1891754	SNV	A	G	Heterozygous	60	240	25	
1891754	SNV	A	A	Heterozygous	180	240	75	
1891785	SNV	C	T	Heterozygous	101	306	33.00654	
1891785	SNV	C	C	Heterozygous	205	306	66.99346	
1891794	SNV	A	T	Heterozygous	92	293	31.39932	
1891794	SNV	A	A	Heterozygous	201	293	68.60068	
1891801	SNV	G	T	Heterozygous	91	278	32.73381	
1891801	SNV	G	G	Heterozygous	187	278	67.26619	
1891822..1891823	MNV	AA	GG	Heterozygous	49	222	22.07207	

1891822..1891823	MNV	AA	AA	Heterozygous	173	222	77.92793	
2722642	SNV	T	G	Heterozygous	75	124	60.48387	yrdQ
2722642	SNV	T	T	Heterozygous	49	124	39.51613	yrdQ
2722646	SNV	G	A	Heterozygous	86	134	64.1791	
2722646	SNV	G	G	Heterozygous	48	134	35.8209	
2722649	SNV	A	C	Heterozygous	94	140	67.14286	
2722649	SNV	A	A	Heterozygous	46	140	32.85714	
2722663^2722664	Insertion	-	T	Heterozygous	95	139	68.34532	
2722663^2722664	Insertion	-	-	Heterozygous	44	139	31.65468	
2814260..2814273	Deletion	GAATGCGGCCGACG	-	Homozygous	98	98	100	yrvM
2861122..2861181	Deletion	TTCAGCCGTACGGTCACCGATCATCAGATTGTACGTTTTTCTGATGTAGTTGATAATCGC	-	Heterozygous	65	83	78.31325	mreB
2861122..2861181	MNV	TTCAGCCGTACGGTCACCGATCATCAGATTGTACGTTTTTCTGATGTAGTTGATAATCGC	TTCAGCCGTACGGTCACCGATCATCAGATTGTACGTTTTTCTGATGTAGTTGATAATCGC	Heterozygous	18	83	21.68675	mreB
2988777	SNV	A	G	Heterozygous	84	174	48.27586	accD
2988777	SNV	A	A	Heterozygous	90	174	51.72414	accD
3056567^3056568	Insertion	-	T	Homozygous	104	104	100	ytzB
3422547..3422548	MNV	AC	GG	Heterozygous	83	198	41.91919	yvgJ
3422547..3422548	MNV	AC	AC	Heterozygous	115	198	58.08081	yvgJ
3624985	SNV	C	A	Homozygous	105	105	100	ftsE
4084771^4084772	Insertion	-	A	Heterozygous	128	279	45.87814	
4084771^4084772	Insertion	-	-	Heterozygous	151	279	54.12186	

JB115								
Region	Type	Reference	Allele	Zygosity	Count	Coverage	Frequency	Gene
125099	SNV	C	A	Homozygous	528	532	99.24812	rpoB
171331	SNV	T	G	Heterozygous	130	304	42.76316	
171331	SNV	T	T	Heterozygous	174	304	57.23684	
2072630	SNV	T	G	Heterozygous	90	218	41.2844	yobL
2072630	SNV	T	T	Heterozygous	126	218	57.79817	yobL
2072633	SNV	T	A	Heterozygous	90	210	42.85714	yobL
2072633	SNV	T	T	Heterozygous	120	210	57.14286	yobL
2072636	SNV	A	G	Heterozygous	88	200	44	yobL
2072636	SNV	A	A	Heterozygous	112	200	56	yobL
2072639	SNV	G	A	Heterozygous	86	190	45.26316	yobL
2072639	SNV	G	G	Heterozygous	104	190	54.73684	yobL
2072645	SNV	A	G	Heterozygous	88	198	44.44444	yobL
2072645	SNV	A	A	Heterozygous	110	198	55.55556	yobL
2072648	SNV	A	T	Heterozygous	78	170	45.88235	yobL
2072648	SNV	A	A	Heterozygous	92	170	54.11765	yobL
2072651	SNV	T	C	Heterozygous	80	186	43.01075	yobL
2072651	SNV	T	T	Heterozygous	106	186	56.98925	yobL
2072669	SNV	A	G	Heterozygous	40	132	30.30303	yobL
2072669	SNV	A	A	Heterozygous	92	132	69.69697	yobL
2276476	SNV	A	T	Heterozygous	60	170	35.29412	yokI
2276476	SNV	A	A	Heterozygous	110	170	64.70588	yokI
2861115..2861174	Deletion	TAATCGCTTCAGCCGTACGGTCACCGATCATCAGATTGTACGTTTTTCTGATGTAGTTGA	-	Homozygous	378	378	100	mreB
3056567^3056568	Insertion	-	T	Homozygous	332	336	98.80952	ytzB
3812832^3812833	Insertion	-	C	Homozygous	270	274	98.54015	rpoE
4187758..4187759	MNV	TG	AT	Heterozygous	142	568	25	tetB
4187758..4187759	MNV	TG	TG	Heterozygous	426	568	75	tetB
4188346	SNV	G	T	Heterozygous	138	510	27.05882	tetB
4188346	SNV	G	G	Heterozygous	368	510	72.15686	tetB
4188623	SNV	C	T	Heterozygous	106	466	22.74678	tetB
4188623	SNV	C	C	Heterozygous	358	466	76.82403	tetB
4189141^4189142	Insertion	-	A	Heterozygous	58	280	20.71429	tetL

JB116								
Region	Type	Reference	Allele	Zygosity	Count	Coverage	Frequency	Gene
502452	SNV	G	C	Homozygous	81	83	97.59036	ydbI
1070342	SNV	A	T	Heterozygous	17	44	38.63636	
1070342	SNV	A	A	Heterozygous	27	44	61.36364	
2530296	Deletion	T	-	Homozygous	59	60	98.33333	yqhY
2579550	SNV	T	G	Heterozygous	6	17	35.29412	pstA
2579550	SNV	T	T	Heterozygous	10	17	58.82353	pstA
4188023	SNV	A	T	Heterozygous	33	143	23.07692	tetB
4188023	SNV	A	A	Heterozygous	107	143	74.82517	tetB
4188041	SNV	G	A	Heterozygous	33	135	24.44444	tetB
4188041	SNV	G	G	Heterozygous	99	135	73.33333	tetB
4188077	SNV	A	G	Heterozygous	29	130	22.30769	tetB
4188077	SNV	A	A	Heterozygous	98	130	75.38462	tetB
4188089	SNV	C	A	Heterozygous	32	135	23.7037	tetB

JB117								
Region	Type	Reference	Allele	Zygosity	Count	Coverage	Frequency	Gene
96240	SNV	G	A	Heterozygous	65	191	34.03141	
96240	SNV	G	G	Heterozygous	126	191	65.96859	
372434..372435	MNV	GT	CG	Heterozygous	49	180	27.22222	nucA
372434..372435	MNV	GT	GT	Heterozygous	131	180	72.77778	nucA
1523004	Deletion	T	-	Heterozygous	93	168	55.35714	adeC
1523004	SNV	T	T	Heterozygous	75	168	44.64286	adeC
1523007	Deletion	C	-	Heterozygous	93	168	55.35714	adeC
1523007	SNV	C	C	Heterozygous	75	168	44.64286	adeC
1731572	Deletion	A	-	Homozygous	102	102	100	
1765777	SNV	C	A	Heterozygous	166	275	60.36364	
1765777	SNV	C	C	Heterozygous	109	275	39.63636	
1891785	SNV	C	T	Heterozygous	114	372	30.64516	
1891785	SNV	C	C	Heterozygous	258	372	69.35484	
1891794	SNV	A	T	Heterozygous	112	376	29.78723	
1891794	SNV	A	A	Heterozygous	264	376	70.21277	
1891801	SNV	G	T	Heterozygous	119	371	32.07547	
1891801	SNV	G	G	Heterozygous	252	371	67.92453	
2456435	Deletion	T	-	Homozygous	87	88	98.86364	ansA
2530296	Deletion	T	-	Homozygous	88	88	100	yqhY
2722642	SNV	T	G	Heterozygous	96	210	45.71429	yrdQ
2722642	SNV	T	T	Heterozygous	114	210	54.28571	yrdQ
2722646	SNV	G	A	Heterozygous	112	230	48.69565	
2722646	SNV	G	G	Heterozygous	118	230	51.30435	
2722649	SNV	A	C	Heterozygous	118	243	48.55967	
2722649	SNV	A	A	Heterozygous	125	243	51.44033	

Region	Type	Reference	Allele	Zygosity	Count	Coverage	Frequency	Gene
2722663^2722664	Insertion	-	T	Heterozygous	125	232	53.87931	
2722663^2722664	Insertion	-	-	Heterozygous	107	232	46.12069	
2988777	SNV	A	G	Heterozygous	84	185	45.40541	accD
2988777	SNV	A	A	Heterozygous	100	185	54.05405	accD
3315400..3315489	Deletion	AGCCGAGGCGTTTGCTGAAGCTGATGTCCTCGTCTGTAATTTGGGAGATCCCCTTTACTTTGACGTCTTCCAGATCCACGTTCATCGAGA	-	Heterozygous	77	101	76.23762	hom
3315400..3315489	MNV	AGCCGAGGCGTTTGCTGAAGCTGATGTCCTCGTCTGTAATTTGGGAGATCCCCTTTACTTTGACGTCTTCCAGATCCACGTTCATCGAGA	AGCCGAGGCGTTTGCTGAAGCTGATGTCCTCGTCTGTAATTTGGGAGATCCCCTTTACTTTGACGTCTTCCAGATCCACGTTCATCGAGA	Heterozygous	24	101	23.76238	hom
3422547..3422548	MNV	AC	GG	Heterozygous	83	216	38.42593	yvgJ
3422547..3422548	MNV	AC	AC	Heterozygous	132	216	61.11111	yvgJ
4084771^4084772	Insertion	-	A	Heterozygous	134	295	45.42373	
4084771^4084772	Insertion	-	-	Heterozygous	161	295	54.57627	

JB118								
Region	Type	Reference	Allele	Zygosity	Count	Coverage	Frequency	Gene
96240	SNV	G	A	Heterozygous	67	194	34.53608	
96240	SNV	G	G	Heterozygous	127	194	65.46392	
372434..372435	MNV	GT	CG	Heterozygous	59	175	33.71429	nucA
372434..372435	MNV	GT	GT	Heterozygous	116	175	66.28571	nucA
1523004	Deletion	T	-	Heterozygous	71	172	41.27907	adeC
1523004	SNV	T	T	Heterozygous	101	172	58.72093	adeC
1523007	Deletion	C	-	Heterozygous	71	168	42.2619	adeC

Region	Type	Reference	Allele	Zygosity	Count	Coverage	Frequency	Gene
1523007	SNV	C	C	Heterozygous	97	168	57.7381	adeC
1765777	SNV	C	A	Heterozygous	189	299	63.2107	
1765777	SNV	C	C	Heterozygous	110	299	36.7893	
1891754	SNV	A	G	Heterozygous	62	281	22.06406	
1891754	SNV	A	A	Heterozygous	219	281	77.93594	
1891785	SNV	C	T	Heterozygous	122	362	33.70166	
1891785	SNV	C	C	Heterozygous	240	362	66.29834	
1891794	SNV	A	T	Heterozygous	116	374	31.01604	
1891794	SNV	A	A	Heterozygous	258	374	68.98396	
1891801	SNV	G	T	Heterozygous	123	384	32.03125	
1891801	SNV	G	G	Heterozygous	261	384	67.96875	
2456435	Deletion	T	-	Homozygous	94	94	100	ansA
2530296	Deletion	T	-	Homozygous	83	83	100	yqhY
2722642	SNV	T	G	Heterozygous	114	203	56.15764	yrdQ
2722642	SNV	T	T	Heterozygous	89	203	43.84236	yrdQ
2722646	SNV	G	A	Heterozygous	125	224	55.80357	
2722646	SNV	G	G	Heterozygous	99	224	44.19643	
2722649	SNV	A	C	Heterozygous	136	231	58.87446	
2722649	SNV	A	A	Heterozygous	95	231	41.12554	
2722663^2722664	Insertion	-	T	Heterozygous	139	228	60.96491	
2722663^2722664	Insertion	-	-	Heterozygous	89	228	39.03509	
2988777	SNV	A	G	Heterozygous	132	223	59.19283	accD
2988777	SNV	A	A	Heterozygous	91	223	40.80717	accD
3422547..3422548	MNV	AC	GG	Heterozygous	84	228	36.84211	yvgJ
3422547..3422548	MNV	AC	AC	Heterozygous	144	228	63.15789	yvgJ
4084771^4084772	Insertion	-	A	Heterozygous	173	314	55.09554	
4084771^4084772	Insertion	-	-	Heterozygous	141	314	44.90446	

JB119								
Region	Type	Reference	Allele	Zygosity	Count	Coverage	Frequency	Gene
2456435	Deletion	T	-	Homozygous	115	116	99.13793	ansA
2530296	Deletion	T	-	Homozygous	131	131	100	yqhY

JB120								
Region	Type	Reference	Allele	Zygosity	Count	Coverage	Frequency	Gene
96240	SNV	G	A	Heterozygous	49	184	26.63043	
96240	SNV	G	G	Heterozygous	135	184	73.36957	
372434..372435	MNV	GT	CG	Heterozygous	47	177	26.55367	nucA
372434..372435	MNV	GT	GT	Heterozygous	130	177	73.44633	nucA

Region	Type	Reference	Allele	Zygosity	Count	Coverage	Frequency	Gene
490580	SNV	G	T	Heterozygous	36	119	30.2521	
490580	SNV	G	G	Heterozygous	80	119	67.22689	
1523004	Deletion	T	-	Heterozygous	93	176	52.84091	adeC
1523004	SNV	T	T	Heterozygous	83	176	47.15909	adeC
1523007	Deletion	C	-	Heterozygous	92	177	51.9774	adeC
1523007	SNV	C	C	Heterozygous	85	177	48.0226	adeC
1765777	SNV	C	A	Heterozygous	114	215	53.02326	
1765777	SNV	C	C	Heterozygous	101	215	46.97674	
1891785	SNV	C	T	Heterozygous	103	350	29.42857	
1891785	SNV	C	C	Heterozygous	247	350	70.57143	
1891794	SNV	A	T	Heterozygous	94	320	29.375	
1891794	SNV	A	A	Heterozygous	226	320	70.625	
1891801	SNV	G	T	Heterozygous	96	329	29.17933	
1891801	SNV	G	G	Heterozygous	233	329	70.82067	
2456435	Deletion	T	-	Homozygous	97	97	100	ansA
2530296	Deletion	T	-	Homozygous	80	80	100	yqhY
2722642	SNV	T	G	Heterozygous	91	195	46.66667	yrdQ
2722642	SNV	T	T	Heterozygous	104	195	53.33333	yrdQ
2722646	SNV	G	A	Heterozygous	105	216	48.61111	
2722646	SNV	G	G	Heterozygous	110	216	50.92593	
2722649	SNV	A	C	Heterozygous	111	217	51.15207	
2722649	SNV	A	A	Heterozygous	106	217	48.84793	
2722663^2722664	Insertion	-	T	Heterozygous	112	225	49.77778	
2722663^2722664	Insertion	-	-	Heterozygous	113	225	50.22222	
2797830	SNV	T	G	Homozygous	100	100	100	yrzL
2988777	SNV	A	G	Heterozygous	117	214	54.6729	accD
2988777	SNV	A	A	Heterozygous	97	214	45.3271	accD
3422547..3422548	MNV	AC	GG	Heterozygous	88	201	43.78109	yvgJ
3422547..3422548	MNV	AC	AC	Heterozygous	113	201	56.21891	yvgJ
4084771^4084772	Insertion	-	A	Heterozygous	132	297	44.44444	
4084771^4084772	Insertion	-	-	Heterozygous	165	297	55.55556	

JB121								
Region	Type	Reference	Allele	Zygosity	Count	Coverage	Frequency	Gene
96240	SNV	G	A	Heterozygous	48	155	30.96774	
96240	SNV	G	G	Heterozygous	106	155	68.3871	
118116	SNV	G	A	Homozygous	123	124	99.19355	nusG
171331	SNV	T	G	Heterozygous	35	142	24.64789	
171331	SNV	T	T	Heterozygous	107	142	75.35211	
372434..372435	MNV	GT	CG	Heterozygous	77	195	39.48718	nucA

372434..37 2435	MNV	GT	GT	Heterozygous	117	195	60	nucA
490580	SNV	G	T	Heterozygous	23	101	22.77228	
490580	SNV	G	G	Heterozygous	76	101	75.24752	
1523004	Deletion	T	-	Heterozygous	79	181	43.64641	adeC
1523004	SNV	T	T	Heterozygous	102	181	56.35359	adeC
1523007	Deletion	C	-	Heterozygous	79	182	43.40659	adeC
1523007	SNV	C	C	Heterozygous	103	182	56.59341	adeC
1765777	SNV	C	A	Heterozygous	133	229	58.0786	
1765777	SNV	C	C	Heterozygous	96	229	41.9214	
1891754	SNV	A	G	Heterozygous	72	219	32.87671	
1891754	SNV	A	A	Heterozygous	147	219	67.12329	
1891785	SNV	C	T	Heterozygous	99	268	36.9403	
1891785	SNV	C	C	Heterozygous	169	268	63.0597	
1891794	SNV	A	T	Heterozygous	97	268	36.19403	
1891794	SNV	A	A	Heterozygous	171	268	63.80597	
1891801	SNV	G	T	Heterozygous	104	274	37.9562	
1891801	SNV	G	G	Heterozygous	170	274	62.0438	
1891821..1 891823	MNV	AAA	GGG	Heterozygous	63	248	25.40323	
1891821..1 891823	MNV	AAA	AAA	Heterozygous	185	248	74.59677	
1987120	SNV	G	C	Heterozygous	78	103	75.72816	ppsB
1987120	SNV	G	G	Heterozygous	25	103	24.27184	ppsB
2456435	Deletion	T	-	Homozygous	89	90	98.88889	ansA
2530296	Deletion	T	-	Homozygous	106	107	99.06542	yqhY
2722642	SNV	T	G	Heterozygous	72	179	40.22346	yrdQ
2722642	SNV	T	T	Heterozygous	107	179	59.77654	yrdQ
2722646	SNV	G	A	Heterozygous	80	190	42.10526	
2722646	SNV	G	G	Heterozygous	110	190	57.89474	
2722649	SNV	A	C	Heterozygous	83	187	44.38503	
2722649	SNV	A	A	Heterozygous	104	187	55.61497	
2722663^2 722664	Insertion	-	T	Heterozygous	89	167	53.29341	
2722663^2 722664	Insertion	-	-	Heterozygous	78	167	46.70659	
2988777	SNV	A	G	Heterozygous	138	237	58.22785	accD
2988777	SNV	A	A	Heterozygous	98	237	41.35021	accD
3422547..3 422548	MNV	AC	GG	Heterozygous	75	185	40.54054	yvgJ
3422547..3 422548	MNV	AC	AC	Heterozygous	110	185	59.45946	yvgJ
4084771^4 084772	Insertion	-	A	Heterozygous	46	121	38.01653	
4084771^4 084772	Insertion	-	-	Heterozygous	75	121	61.98347	

JB122								
Region	Type	Reference	Allele	Zygosity	Count	Coverage	Frequency	Gene
96240	SNV	G	A	Heterozygous	51	196	26.02041	
96240	SNV	G	G	Heterozygous	145	196	73.97959	
372434..372435	MNV	GT	CG	Heterozygous	55	188	29.25532	nucA
372434..372435	MNV	GT	GT	Heterozygous	133	188	70.74468	nucA
490580	SNV	G	T	Heterozygous	33	138	23.91304	
490580	SNV	G	G	Heterozygous	103	138	74.63768	
1523004	Deletion	T	-	Heterozygous	86	162	53.08642	adeC
1523004	SNV	T	T	Heterozygous	76	162	46.91358	adeC
1523007	Deletion	C	-	Heterozygous	88	163	53.98773	adeC
1523007	SNV	C	C	Heterozygous	75	163	46.01227	adeC
1765777	SNV	C	A	Heterozygous	173	272	63.60294	
1765777	SNV	C	C	Heterozygous	99	272	36.39706	
1891754	SNV	A	G	Heterozygous	67	258	25.96899	
1891754	SNV	A	A	Heterozygous	191	258	74.03101	
1891785	SNV	C	T	Heterozygous	111	331	33.53474	
1891785	SNV	C	C	Heterozygous	220	331	66.46526	
1891794	SNV	A	T	Heterozygous	105	337	31.15727	
1891794	SNV	A	A	Heterozygous	232	337	68.84273	
1891801	SNV	G	T	Heterozygous	101	334	30.23952	
1891801	SNV	G	G	Heterozygous	233	334	69.76048	
2427538	SNV	C	G	Homozygous	82	82	100	ypzK
2456435	Deletion	T	-	Homozygous	86	86	100	ansA
2530296	Deletion	T	-	Homozygous	92	93	98.92473	yqhY
2722642	SNV	T	G	Heterozygous	81	173	46.82081	yrdQ
2722642	SNV	T	T	Heterozygous	92	173	53.17919	yrdQ
2722646	SNV	G	A	Heterozygous	105	196	53.57143	
2722646	SNV	G	G	Heterozygous	91	196	46.42857	
2722649	SNV	A	C	Heterozygous	109	201	54.22886	
2722649	SNV	A	A	Heterozygous	92	201	45.77114	
2722663^2722664	Insertion	-	T	Heterozygous	113	188	60.10638	
2722663^2722664	Insertion	-	-	Heterozygous	75	188	39.89362	
2797830	SNV	T	G	Homozygous	106	106	100	yrzL
2988777	SNV	A	G	Heterozygous	100	185	54.05405	accD
2988777	SNV	A	A	Heterozygous	85	185	45.94595	accD
3422547..3422548	MNV	AC	GG	Heterozygous	81	214	37.85047	yvgJ
3422547..3422548	MNV	AC	AC	Heterozygous	133	214	62.14953	yvgJ
4084771^4084772	Insertion	-	A	Heterozygous	127	285	44.5614	
4084771^4084772	Insertion	-	-	Heterozygous	158	285	55.4386	

JB125								
Region	Type	Reference	Allele	Zygosity	Count	Coverage	Frequency	Gene
2456435	Deletion	T	-	Homozygous	94	96	97.91667	ansA
2530296	Deletion	T	-	Homozygous	85	85	100	yqhY
2579550	SNV	T	G	Heterozygous	7	32	21.875	pstA
2579550	SNV	T	T	Heterozygous	22	32	68.75	pstA
2797830	SNV	T	G	Homozygous	87	88	98.86364	yrzL
4189139^4189140	Insertion	-	A	Heterozygous	22	98	22.44898	tetL

JB126								
Region	Type	Reference	Allele	Zygosity	Count	Coverage	Frequency	Gene
176141	SNV	T	C	Homozygous	14	14	100	rrnG-23S
176143	Deletion	T	-	Homozygous	16	17	94.11765	
176185^176186	Insertion	-	C	Homozygous	20	21	95.2381	
2456435	Deletion	T	-	Homozygous	46	46	100	ansA
2530296	Deletion	T	-	Homozygous	56	57	98.24561	yqhY
2579556	SNV	A	T	Heterozygous	7	18	38.88889	pstA
2579556	SNV	A	A	Heterozygous	11	18	61.11111	pstA
2579560..2579561	MNV	GC	TG	Heterozygous	7	20	35	pstA
2579560..2579561	MNV	GC	GC	Heterozygous	13	20	65	pstA
2579564..2579568	MNV	TGGCG	AAAAA	Heterozygous	8	23	34.78261	pstA
2579564..2579568	MNV	TGGCG	TGGCG	Heterozygous	15	23	65.21739	pstA